

INVESTIGATION OF ELEMENTAL ANALYSIS USING
NEUTRON-CAPTURE GAMMA RAY SPECTRA

by

John N. Hamawi

B.Sc., Haile Sellassie I University
(Ethiopia, 1962)

S.M., Massachusetts Institute of Technology
(Cambridge, Mass., 1964)

Nucl. Eng., Massachusetts Institute of Technology
(Cambridge, Mass., 1966)

Submitted in Partial Fulfillment
of the Requirements for the
Degree of Doctor of
Philosophy
at the
Massachusetts Institute of Technology
September 1969

Signature of Author

Department of Nuclear Engineering
August 18, 1969

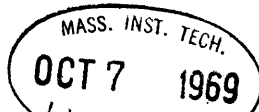
Certified by

Thesis Supervisor

Accepted by

Chairman, Departmental Committee
on Graduate Students

Archives



INVESTIGATION OF ELEMENTAL ANALYSIS USING
NEUTRON-CAPTURE GAMMA RAY SPECTRA

John N. Hamawi

Submitted to the Department of Nuclear Engineering,
Massachusetts Institute of Technology, on August 18, 1969
in partial fulfillment of the requirements for the degree
of Doctor of Philosophy.

ABSTRACT

This thesis evaluated the potential of neutron-capture gamma rays in elemental analysis. A large portion of the work was devoted to the development of a method for the analysis of weak peaks in gamma ray spectra. This was based on equations developed for the standard deviation in the measurement of the various peak parameters, consideration being also given to the reduction in the statistical fluctuations obtained by smoothing the data with the use of Fourier transforms. Two methods of peak area determination were considered and their relative effectiveness examined. An equation was then derived for the minimum weight of an element needed for reliable quantitative analysis. The equations were verified using both real and pseudo-experimental data constructed with the use of a computer.

Experiments were carried out using the MIT Reactor with samples positioned (a) in a high neutron flux next to the reactor tank (2×10^{13} n/sq.cm sec), and (b) in an external neutron beam facility of relatively lower but well thermalized flux (2×10^8 n/sq.cm sec). Capture gamma ray spectra were obtained with a three-crystal system capable of operating in the free mode, the Compton suppression mode and as a pair spectrometer. The results were used to examine the relative analytical sensitivity of the internal and external sample arrangements and the various gamma detection modes.

The minimum measurable weights of 75 elements were evaluated for a stainless steel sample. For these computations use was made of the listing of capture gamma ray spectra recently established by the MIT gamma spectroscopy group. In a majority of the cases the detection limits range between 0.1 percent and 10 percent. Equations were developed for extending the results to different samples and different experimental arrangements.

Thesis Supervisor: Prof. Norman C. Rasmussen
Title: Professor of Nuclear Engineering

ACKNOWLEDGEMENTS

It is with great pleasure that acknowledgement is hereby made of all the friends and associates who have shown interest in this thesis and who, in one way or another, have assisted towards its completion. My particular gratitude and appreciation are extended to my supervisor, Professor Norman C. Rasmussen, whose helpful criticism, encouraging comments and continuous supervision are in a large measure responsible for the success of this research. Further thanks are extended to Professor Franklyn Clikeman for his many helpful suggestions and for acting as thesis reader.

During the course of this thesis I became indebted to my colleagues Thomas L. Harper and Roberto Yoshiyuti Hukai for their participation with me in interesting and stimulating discussions on a number of topics associated with this work. A special word of thanks is also extended to the members of the Reactor Operations Office and the Radiation Protection Office of the MITR who took part in the sample handling operations associated with the internal sample measurements.

It is a pleasure also to acknowledge the U.S. Bureau of Mines for the financial support of the contract under which part of this thesis was done.

TABLE OF CONTENTS

	<u>Page</u>
ABSTRACT	2
ACKNOWLEDGEMENTS	3
TABLE OF CONTENTS	4
LIST OF FIGURES	7
LIST OF TABLES	10
I. INTRODUCTION	12
II. CAPTURE GAMMA VERSUS ORDINARY ACTIVATION ANALYSIS	20
2.1 Introduction	20
2.2 Theoretical Sensitivities	20
2.3 The Minimum Measurable Weight	28
III. METHOD OF DATA ANALYSIS	30
3.1 Introduction	30
3.2 GAMANL	32
3.3 Method of Linear Background fit	33
3.4 Method of Peak Area Determination	39
3.4.1 Area Equations	41
3.4.2 Errors	46
3.5 Limiting Values for Peak Areas	50
3.6 Equation for the Minimum Measurable Weight	56
IV. EXPERIMENTAL EQUIPMENT	62
4.1 Introduction	62
4.2 Description of the Experimental Facilities	62
4.2.1 The Internal-Sample Facility	63
4.2.2 The External-Sample Facility	69

	<u>Page</u>
4.3 The Gamma Ray Spectrometer	73
V. RELATIVE SENSITIVITY OF THE VARIOUS EXPERIMENTAL ARRANGEMENTS	82
5.1 Introduction	82
5.2 Internal versus External	82
5.3 Relative Sensitivity of the Gamma Detection Modes	86
5.3.1 The Stainless Steel Sample	87
5.3.2 Characteristic Features of the Gamma Ray Spectra	90
5.3.3 Relative Effectiveness of the Detection Modes	96
VI. A TEST ON THE EQUATION FOR THE MINIMUM WEIGHT	107
6.1 Introduction	107
6.2 The Method	107
6.3 Analysis of the Pair Spectrum	108
6.4 Manganese Peaks in the Spectrum	127
VII. THE MINIMUM MEASURABLE WEIGHTS OF THE ELEMENTS	136
7.1 Introduction	136
7.2 Minimum Measurable Weights of the Elements in Stainless Steel	137
7.3 Development of the Extrapolation Equations	146
VIII. SUMMARY AND CONCLUSIONS	166
APPENDIX I. EFFECTS OF SMOOTHING ON SPECTRAL DATA	170
A1.1 Method of Smoothing	170
A1.2 Smoothing Filter Function	172
A1.3 Degree of Smoothing	174
A1.4 Effects of Smoothing on the Peak Parameters	181

	<u>Page</u>
APPENDIX II PEAK WIDTHS AND METHOD OF LEAST-SQUARES FIT	188
A2.1 Reasons for the Fit	188
A2.2 Doppler Broadening	189
A2.3 The Least-Squares Fit	193
A2.4 Application	196
APPENDIX III ERROR EQUATIONS	202
A3.1 The Error Equations	202
A3.2 Applications	209
APPENDIX IV PROMINENT CAPTURE GAMMA RAYS OF THE ELEMENTS AND THEIR MINIMUM MEASURABLE WEIGHTS IN STAINLESS STEEL	230
APPENDIX V COMPUTER CODES	265
REFERENCES	307

LIST OF FIGURES

		<u>Page</u>
Fig. 1.1	Neutron-induced gamma rays	13
Fig. 1.2	Various experimental arrangements for prompt activation analysis	14
Fig. 3.1	Typical neutron-capture gamma ray spectrum (Internal facility, Al-6061 sample 1.62 g)	31
Fig. 3.2	A graphical presentation of the method for linear background fit	37
Fig. 3.3	Histogram of a typical spectral peak (n = 12 in this case)	42
Fig. 3.4	Ratio of errors in the two methods of peak area determination	48
Fig. 3.5	The Gaussian area percent error for various values of h and B	49
Fig. 3.6	An illustration of the three peak-area limiting levels	55
Fig. 4.1	A plan view of the internal neutron beam facility and gamma spectrometer	64
Fig. 4.2	Details of the internal beam collimator and end plug	66
Fig. 4.3a	Photograph of sample holder and remote handling tool, disengaged; central disc is a stainless steel sample, 0.5-inch in diameter	68
Fig. 4.3b	Sample holder and tool engaged together, ready for mounting	68
Fig. 4.4a	Top view of MIT Reactor and 4THL irradiation facility (from Ref. [H8])	71
Fig. 4.4b	Front view of the 4THL irradiation facility and the Ge(Li) capture gamma spectrometer [H8]	72
Fig. 4.5	The liqui-nitrogen 'snout' dewar, fully withdrawn. The Ge(Li) crystal is located at the tip of the dewar	74

Fig. 4.6	A general view of the three-crystal spectrometer set up for internal-sample measurements	74
Fig. 4.7	Absolute efficiency of the spectrometer operated in the Compton suppression mode	77
Fig. 4.8	Absolute efficiency of the pair spectrometer	79
Fig. 5.1	Stainless steel spectrum obtained with the internal-sample facility (3.5g)	84
Fig. 5.2	Orientation of the stainless steel sample with respect to the neutron beam and the Ge(Li) detector (sample weight 78.83 grams)	89
Fig. 5.3	The free-mode stainless steel spectrum (flux x time = 1.32×10^{13} n/sq.cm)	91
Fig. 5.4	The Compton suppression stainless steel spectrum (flux x time = 1.33×10^{12} n/sq.cm)	92
Fig. 5.5	The stainless-steel pair spectrum (flux x time = 1.94×10^{13} n/sq.cm)	93
Fig. 5.6	Ratio of the minimum detectable weights by the different gamma-detection modes	100
Fig. 6.1	Linearity correction curve	118
Fig. 7.1	Shape of background continuum in Compton suppression spectra	156
Fig. 7.2	Shape of background continuum in pair spectra	157
Fig. A1.1	Fourier transforms of two 4096-channel gamma ray spectra	173
Fig. A1.2	Section of noise spectrum and typical smoothed data for light and heavy smoothing	176
Fig. A1.3	Frequency distribution of grouped data in the raw and smoothed noise spectra	177
Fig. A1.4	The error reduction factor r for various combinations of the filter parameters ω_m and σ_m	179

		<u>Page</u>
Fig. A1.5	Fourier transform of a pure-noise spectrum	180
Fig. A1.6	Oscillations introduced by the filter functions shown in Fig. A1.7 for heavy smoothing	186
Fig. A1.7	Filter functions used in obtaining the oscillations shown in Fig. A1.6; all filters have $r = 1.9$ except filter (d) which is for normal smoothing in this case	187
Fig. A2.1	Fitting the energy-width data to various polynomials by the method of least squares	200
Fig. A2.2	Confidence interval in the three fits shown in Fig. A2.1	201
Fig. A3.1	Three of the one hundred pseudo-experimental peaks produced by the code ARTSPEC (Note that the y-scale does not start from zero)	210

LIST OF TABLES

<u>Table</u>		<u>Page</u>
II(1)	Sensitivities in Elemental Analysis	22
II(2)	Ratio of Minimum Detectable Weights Ordinary versus Prompt Capture Gamma Analysis	24
III(1)	Typical Peak Parameters Corresponding to the Three Peak Area Limiting Levels	54
IV(1)	Compton Suppression Efficiency and Transmission factors for Various Absorbers	76
IV(2)	Pair Spectrometer Efficiency and Transmission Factors for Various Absorbers	78
V(1)	Elemental Composition of the SS-303 Sample	88
V(2)	Gamma Ray Transmission Factors Through 0.45 cm of Fe	90
V(3)	Background Data and Minimum Weight Ratios for the Free Mode and Compton Suppression Systems	99
V(4)	Background Data and Minimum Weight Ratios for the Free Mode System and the Pair Spectrometer	102
V(5)	Background Data, Efficiency, Width and Minimum Weight Ratios for the Compton Suppression System and the Pair Spectrometer	105
VI(1)	Part of GAMANL Output SS-303 Pair Spectrum	109
VI(2)	Part of WTANAL Output Analysis of SS-303 Sample	121
VI(3)	Expected and Actual Peak Areas from Manganese in SS-303 Sample and Corresponding Peak Area Limiting Levels	129
VII(1)	Limits for Quantitative Determination for Manganese	139
VII(2)	Limits for Quantitative Determination Compton Suppression	142

	<u>Page</u>
VII(3) Limits for Quantitative Determination Pair Spectrometer	144
VII(4) Limits for Quantitative Determination Grouped Data	147
VII(5) Experimental Data Employed in the Evalua- tion of the f_{CS} and f_{PS} Coefficients	152
VII(6) b(E) Distribution in Compton Suppression Spectra	158
VII(7) b(E - 1022) Distribution in Pair Spectro- meter Spectra	162
AI(1) Effect of Various Smoothing Filter Functions on the Spectral Peak Parameters (Statistical Analysis based on 100 Pseudo-experimental Peaks	183
AII(1) Doppler Broadening Contribution to Peak Width	192
AII(2) POLYFIT Output Results of Least-Squares Fit	198
AIII(1) Part of GAMANL Output for the Analysis of the 100 Artificial Peaks	211
AIII(2) Statistical Analysis Applied to the 100 Pseudo-Experimental Peaks	214
AIII(3) Pertinent Information Associated with the Three Aluminum Runs	217
AIII(4) Comparison of the Three Aluminum Runs, Pair Spectrometer, Internal Sample	218
AIV(1) Compton Spectrometer Limits for Quantitative Determination	232
AIV(2) Pair Spectrometer Limits for Quantitative Determination	242
AIV(3) Twelve of the Most Prominent Capture Gamma Rays of 75 Elements Listed in Terms of Increasing Gamma Ray Energy	256

Chapter I

INTRODUCTION

Conventional neutron activation analysis has been shown to have good analytical sensitivity for many elements. It has found its place in all the physical sciences and has been widely employed in a non-destructive manner in the analysis of samples containing elements at trace levels and higher concentrations [G1, L1, L2, P1, W1]. In this method, the elemental composition of a sample is determined through the analysis of the gamma ray spectra of the radionuclides formed within the sample by neutron capture. As such, the method is applicable only if the product nucleus is (a) radioactive, (b) is formed in reasonable amounts, and (c) has a half-life that is neither too long to produce sufficient activity nor too short for measurement. Evidently a number of elements throughout the periodic table are not susceptible to this type of analysis.

Another approach to elemental analysis that still uses the neutron as the bombarding particle but does not rely on the radionuclear properties of the product nuclei is what is often referred to as prompt activation analysis. In this case, as is shown in Figures 1.1 and 1.2, one examines (a) the prompt gamma rays resulting from fast neutron inelastic scattering or (b) the prompt gamma rays associated with thermal neutron capture. And since all nuclei have unique neutron inelastic scattering and absorption cross sections, any element may now be identified and its concentration in a given

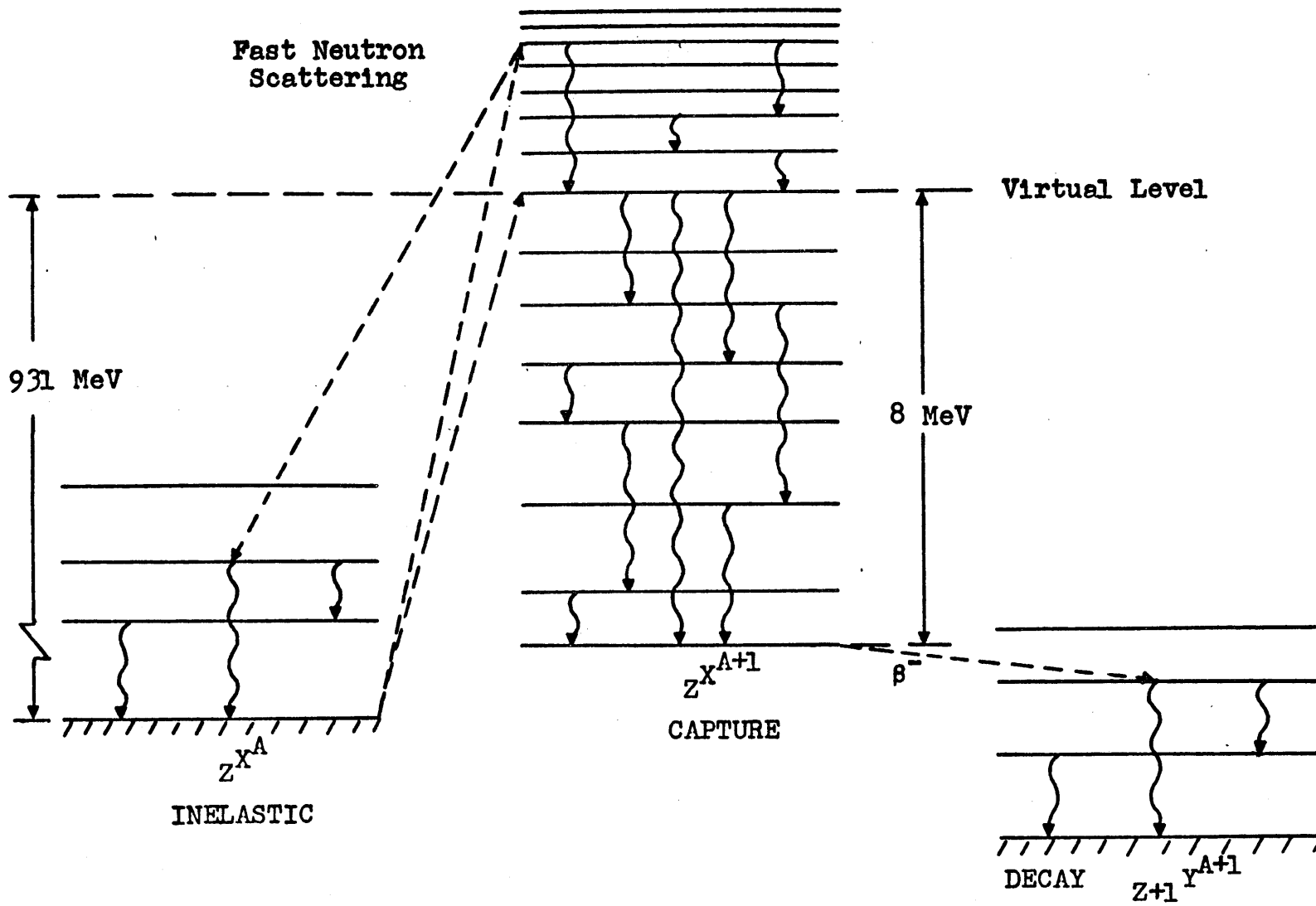


Fig. 1.1 Neutron induced gamma rays

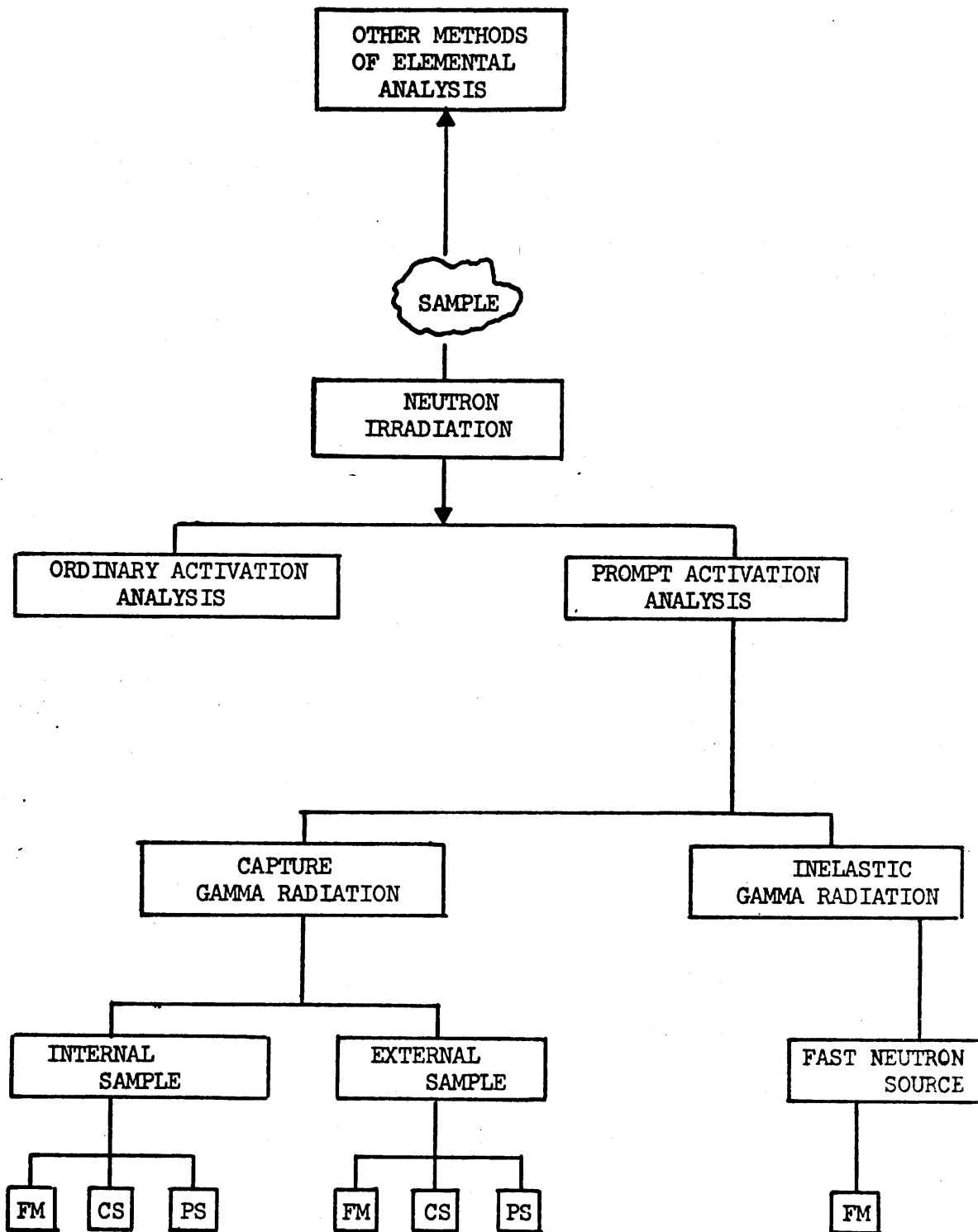


Fig. 1.2 Various experimental arrangements for prompt activation analysis.

sample determined.

The method of prompt activation analysis thus offers a number of reactions that are not available to the analysis based on delayed gamma radiations. Nevertheless, the measurement and utilization of prompt gamma rays has been hindered mainly by the complex nature of the spectra. The low resolution (tens of keV) NaI(Tl) scintillations detectors, which are invariably used in ordinary activation analysis, strongly restricts the usefulness of these detectors in prompt activation analysis. The recent development, however, of large (approximately 50 c.c.) lithium-drifted germanium detectors, with resolutions of a few keV, offers the possibility of using this technique in a number of new applications [Tl, El, Ml, P2, S2, O2].

The desire to apply these detectors to the development of prompt activation analysis was one of the primary motivations for the work performed under the supervision and guidance of Prof. Norman C. Rasmussen at MIT by a number of researchers. The work on thermal neutron capture includes the design and construction of a Ge(Li) pair spectrometer and an external neutron beam facility by J. N. Hanson [H2] and V. J. Orphan [O1], and the acquisition and computer analysis of the neutron-capture gamma ray spectra of 75 elements by Y. Fukai [R2] and T. Inouye [I2]. The data and the technique have been applied to the analysis of coal samples of varying ash content. The results were very encouraging and provided a preliminary measure of the potential of capture gamma analysis [R3].

The work on neutron inelastic scattering is still under way and has involved the construction of a facility utilizing Pu-Be neutrons, and the acquisition of prompt gamma-ray data for a number of elements by D. P. Simonson [S4] and B. Hui [H6]. The work reported in this thesis is aimed at establishing the potential of neutron-capture gamma rays as an analytical tool in elemental analysis.

Most of the reported experimental investigations of prompt gamma rays have been to study nuclear energy levels (e.g. I. V. Groshev et al. [G4], O. I. Sumbaev et al. [S1], P. Van Assche et al. [V1], G. A. Bartholomew et al. [B1], K. J. Wetzel [W3], etc.). As a result the literature on elemental analysis by neutron capture gamma ray spectroscopy is not plentiful, most of the work being moreover restricted to the determination of elements that do not satisfy the requirements of ordinary activation analysis. B. W. Garbrah and J. E. Whitley [G3] report the determination of boron in steel using a 2x2" NaI(Tl) crystal. Feasibility studies on the utilization of neutron inelastic scattering and neutron capture for the analysis of coal and iron ore samples are reported by T. C. Martin et al. [M2] and R. F. Stewart et al. [S3]. Certain estimates for the minimum detectable weights of Ca, Ni, and Dy using a Ge(Li) spectrometer and an internal-sample arrangement were published by S. E. Arnell et al. [A1]. R. C. Greenwood [G5] has applied the method to the analysis of meteorite and terrestrial-type rock samples. Biological samples were studied by D. Comar [C6], and A. Elkady [E3] reports the use of capture

gammas for the identification of gold in mixtures. A design of an apparatus for the measurement of trace elements is reported by S. M. Lombard et al. [L5] together with results for boron and cadmium.

Apparently the potentialities of capture gamma rays for elemental analysis are for the most part unexplored. Some semi-empirical results on the sensitivity of capture gamma analysis are reported by T. L. Isenhour and G. H. Morrison [11], and R. C. Greenwood and J. Reed [G2], and later W. G. Lussie and J. L. Brownlee, Jr. [L3], point out that this technique may play an important role in elemental and isotopic analyses. An assessment of capture gamma analysis is presented by B. W. Garbrah et al. [G7]; these authors report that the accuracy attainable in the analysis of practical samples is strongly dependent on the extent of matrix interferences and that the sensitivity of the technique is limited by the absorption cross section of the element of interest.

It is the objective of this thesis then to study the potential of neutron capture gamma rays in elemental analysis, the emphasis being on the development of general equations which can be used to predict the sensitivity of the measurement for any element in a given sample.

In Chapter II the reported theoretical sensitivities of capture gamma and ordinary activation analysis are discussed and their relative effectiveness considered. In Chapter III is presented the derivation of the equations for the minimum number of counts in a given spectrum needed for reliable

quantitative analysis, and for the corresponding minimum elemental weight. The remaining chapters are devoted to the experimental measurements required to obtain the empirical information needed for the application of the equations developed in Chapter III.

Neutron-capture gamma ray spectra were obtained at the MIT Reactor with the samples positioned (a) in a high neutron flux next to the reactor tank (internal sample), and (b) in an external neutron beam facility of relatively lower but well thermalized flux, also characterized by lower background radiation and better geometry. The gamma-ray three crystal spectrometer, consisting of a 30 c.c. coaxial Ge(Li) detector surrounded by two NaI(Tl) crystals and including a 4096-channel analyser, was operated in the free mode (FM), the Compton suppression mode (CS), and as a pair spectrometer (PS). In Fig. 1.2 are shown the various possible combinations of source-sample position and gamma detection mode. Analysis of the results in the internal and external facilities will indicate which set up and which detection mode are more efficient.

The possibility of using a fast neutron radioactive source for the production of neutron-capture gamma ray spectra (O. A. Wasson et al. [W2], and R. F. Stewart [S3]), with the neutrons thermalizing within the sample itself if the sample is large enough or in a convenient moderator, was not considered.

To investigate the potential limits of detection offered by neutron-capture gamma ray analysis it will also be necessary to use the listing of gamma ray spectra recently established

by the MIT gamma spectroscopy group [R2]. The peaks recognized in the spectra of 75 elements have been listed by the author in increasing order of energy so as to facilitate the qualitative analysis [H7]. The peak intensities have been expressed in a new set of units so that they can be incorporated directly in the quantitative determination. In actual practice a large number of the capture gamma rays of each element can be used for elemental analysis in order to reduce the error in the measurements. In this work, where interest lies in the determination of the sensitivity limits, the emphasis will be on that prominent gamma ray of each element whose corresponding peak area in a given spectrum can be measured with the least error.

Chapter II

CAPTURE GAMMA VERSUS ORDINARY ACTIVATION ANALYSIS

2.1 Introduction

As noted in the introduction, the application of capture gamma analysis requires spectrometers of high resolution and high efficiency because of the complexity of the gamma ray spectra. The recent development of Ge(Li) detectors has provided a means of overcoming this difficulty and it is now of interest to explore theoretically the effectiveness of this new method of elemental analysis with respect to that of ordinary activation. The following section is devoted to this.

2.2 Theoretical Sensitivities

Another reason that capture gamma analysis has not received as much attention as ordinary activation analysis is that in practice the latter may be used to detect amounts that are several orders of magnitude smaller.

Consider a neutron irradiation facility specified by a neutron flux ϕ and a gamma ray spectrometer characterized by a solid angle Ω and a counting efficiency ϵ . The minimum weight of an element of natural composition that may be detected in such a system is given by

$$m = 4\pi C / [\phi \Omega \epsilon I (1 - e^{-\lambda T_1}) e^{-\lambda T_d}] \quad (2.1)$$

for the case of ordinary activation analysis, and by

$$m = 4\pi C / [\phi \Omega \epsilon I] \quad (2.2)$$

when the analysis is based on capture gamma rays. In these equations C represents a set of minimal count rates which, where applicable, are specified with respect to the irradiation time T_1 and the half-lives $T_{\frac{1}{2}}$ of the radionuclides. T_d is the decay time after irradiation and λ the decay constant. I is defined as the number of photons of specified energy emitted per gram of element of natural composition per incident thermal neutron/sq. cm. The most intense decay and capture gamma rays of each element may be used for its identification.

Isenhour and Morrison [11] have applied the above equations to the evaluation of the sensitivities for the detection of 63 elements by ordinary activation and capture gamma analysis. They assumed unit neutron flux, unit solid angle, 100 percent counting efficiency, and zero decay time. They also employed Buchanan's criteria of one-hour irradiation for the count rates C which are

$$\begin{array}{ll}
 C = 1000 \text{ counts per minute for} & T_{\frac{1}{2}} < 1 \text{ min} \\
 C = 100 \text{ counts per minute for} & 1 \text{ min} < T_{\frac{1}{2}} < 1 \text{ hour} \\
 C = 10 \text{ counts per minute for} & T_{\frac{1}{2}} > 1 \text{ hour}
 \end{array}$$

For the capture gamma rays C was set equal to 10 cpm. In addition, the calculations were based on the most intense gamma rays of the elements.

The results of these authors, which are summarized in Table II(1), indicate that in almost all cases capture gamma analysis is inherently more sensitive. However, the high

TABLE II(1)

SENSITIVITIES IN ELEMENTAL ANALYSIS

SENSITIVITY Grams *	ORDINARY ACTIVATION ANALYSIS Elements	PROMPT CAPTURE GAMMA ANALYSIS Elements
$10^{-6} - 10^{-5}$	Fe	
$10^{-7} - 10^{-6}$	S, Se	
$10^{-8} - 10^{-7}$	Cd, Cr, Nd, Si, Sn, Zr	
$10^{-9} - 10^{-8}$	Ce, Cu, F, Gd, K, Mg, Mo, Ni, Ta, Te, Ti, Zn	Bi, Sn
$10^{-10} - 10^{-9}$	Ba, Cl, Hg, Pr, Pt, Sb, Sc, Tm	C, F, Nb
$10^{-11} - 10^{-10}$	Ag, Al, As, Br, Ca, Er, Ga, Hf, I, Ir, La, Na, Nb, Re, Sm, Sr, W	Al, As, Au, Ba, Be, Br, Ce, Ga, Mg, Pr, Sb, Si, Sr, Tl, Zn, Zr
$10^{-12} - 10^{-11}$	Au, Co, Cs, Eu, Ho, Mn, Rh, V	Ag, Ca, Cr, Cs, Cu, Fe, I, K, La, Mn, Mo, Na, Ni, P, Pt, Re, Rh, S, Se, Te, V, W
$10^{-13} - 10^{-12}$	In	Co, Ho, In, Ir, Nd, Sc, Ta, Ti, Tm
$10^{-14} - 10^{-13}$	Dy	Cl, Er, H, Hf, Hg
$10^{-15} - 10^{-14}$		Cd, Dy, Eu, Sm
$10^{-16} - 10^{-15}$		B, Gd

* For a neutron flux of 10^{13} n/cm² sec, and a 100 percent detection efficiency.

background radiation associated with experiments involving the detection of capture gamma rays dictates that the sample to detector distance be appreciable so that adequate detector shielding can be provided against the undesirable background radiation. Also, in order to avoid exposing the detector to the direct neutron and gamma beams from the neutron source, it is necessary in some instances to place the samples away from the source center, and hence at relatively lower neutron fluxes. As a result, and with reference to equation (2.2), the relatively lower neutron fluxes and smaller solid angles increase considerably the minimum weight of an element that can be detected by this technique.

The ratio R_m of the minimum detectable weights of each element by the two methods analysed by Isenhour and Morrison (ordinary versus capture gamma) are shown in Table II(2) for two different values of G , where

$$G = \frac{(\phi \Omega \epsilon) \text{ associated with capture gamma anal.}}{(\phi \Omega \epsilon) \text{ associated with ordinary activation}} \quad (2.3)$$

Note that for the practically unattainable case of $G = 1$ ordinary activation analysis is more sensitive for only Au and Nb. For the more realistic value of $G = 10^{-5}$, however, it prevails for approximately 75 percent of the cases. (Note that other elements not considered by Isenhour and Morrison that are not suitable for ordinary activation analysis are He, Li, N, O, Pb and Y).

A further disadvantage of capture gamma analysis is that

TABLE II(2)

RATIO OF MINIMUM DETECTABLE WEIGHTS
ORDINARY VERSUS PROMPT CAPTURE GAMMA ANALYSIS

Ratio R_m $G = 1$ *	E L E M E N T S	Ratio R_m $G = 10^{-5}$ #
infinite	B, Be, Bi, C, H, P, Tl,	infinite
$10^7 - 10^8$	Cd, Gd	$10^2 - 10^3$
$10^6 - 10^7$	Fe, Nd	$10^1 - 10^2$
$10^5 - 10^6$	S, Se	$10^0 - 10^1$
$10^4 - 10^5$	Cl, Cr, Hg, Sm, Ta, Ti	$10^{-1} - 10^0$
$10^3 - 10^4$	Cu, Er, Eu, K, Mo, Ni, Sc, Si, Te, Tm, Zr	$10^{-2} - 10^{-1}$
$10^2 - 10^3$	Ag, Ce, Hf, I, Mg, Pt, Zn	$10^{-3} - 10^{-2}$
$10^1 - 10^2$	Ba, Ca, Co, Dy, F, Ga, Ho, Ir, La, Na, Pr, Re, Sb, Sn, W	$10^{-4} - 10^{-3}$
$10^0 - 10^1$	Al, As, Br, Cs, In, Mn, Rh, Sr, V	$10^{-5} - 10^{-4}$
$10^{-1} - 10^0$	Au, Nb	$10^{-6} - 10^{-5}$

* Conditions: Same neutron flux available for both methods
Same detection efficiency (including geometry) in both cases.

Conditions: The product of neutron flux and detection efficiency available for ordinary activation is 10^7 times larger than that for prompt capture gamma analysis.

the already complex gamma ray spectra are complicated even more by the following processes:

- (a) Undesirable neutron and gamma radiation reaching the detector directly from the neutron source and by scattering off the sample and its holder
- (b) Undesirable gamma radiation emanating from the sample holder and other structural material as a result of neutron bombardment
- (c) Undesirable gamma radiation originating in the sample but reaching the detector via Compton scattering, and
- (d) delayed gamma rays.

In the case of a collimated neutron beam effects (a), (b) and (c) may be eliminated by recording four spectra as suggested by Hammermesh and Hummel [H4]:

1. Sample in the neutron beam
2. Sample in beam, but with thermal neutrons removed from the beam by suitable absorber
3. Sample removed from the beam, with absorber still in position
4. Both sample and absorber removed from the beam.

The gamma spectrum of interest is then obtained by subtracting spectra according to

$$1 - 2 + 3 - 4.$$

Such a procedure is not practical and is still liable to error because of possible spectral shifts resulting from variations in the electronics and also of possible fluctuations in the

beam intensity. Delayed gamma rays are still a problem; these may be reduced by modulating the neutron beam and gating the logic unit of the analyser in phase with the neutron bursts (Isenhour et al. [11]).

In summary then, elemental analysis based on neutron capture gamma rays is characterized by complex gamma ray spectra and is insensitive in the trace-level domain for most elements because of the restrictions mentioned above. Not to be overlooked, however, are certain definite advantages in its favour. In cases where interest lies in the quantitative determination of the main constituents of materials, as on certain production lines for instance [S3], capture gamma analysis appears best suited when coupled with a suitably thermalized neutron source. The following reasons apply:

- (a) Radioactive neutron sources are economical, reliable, readily available and capable of unattended continuous operation
- (b) The experimental arrangement for such an on-line analysis is extremely simple and does not involve the complexities and inconveniences associated with nuclear reactors and accelerators
- (c) No flux monitoring is necessary
- (d) The gamma rays are prompt and may be analysed without delay and, unlike ordinary activation analysis, a single run is sufficient for the identification of all the elemental constituents
- (e) In view of the high penetrability of neutrons and

the low attenuation of high energy gamma rays, very large samples may be used, a procedure which eliminates sampling errors that ordinary activation analysis is often faced with.

Other fields of science and technology where prompt capture gamma analysis can find extensive application include in-field geological surveying and oceanology [M3], lunar and planetary explorations [C1], [G2(b)], etc. The usefulness of capture gamma analysis, therefore, should not be thought of as limited to that special group of elements mentioned earlier. And as the intensities of readily available radioactive neutron sources will soon surpass 10^{10} n/sec, the method is likely to become tremendously attractive. (W. C. Reining [R1] gives the following data on a Cf^{252} fission neutron source: 11 curies, 5×10^{10} n/sec yield, approximately 20, 000 dollars for the radionuclide, 2.9 rad/hour gamma dose at 1 meter, 0.8 watts of heat generation, 2.65 years of half-life, and less than 1 cm^3 volume. The softer neutron spectrum of such a source, as compared to the (α,n) sources, makes it particularly attractive for capture gamma measurements.).

In concluding this section it must be mentioned that many authors, such as Isenhour and Morrison [I1], R. C. Greenwood and J. Reed [G2] and H. R. Lukens [L2], have correctly considered capture gamma analysis as simply a technique complementary to the far more effective ordinary activation analysis.

2.3 The Minimum Measurable Weight

Evaluation of the potentialities of capture gamma analysis is thus of prime importance. It must be emphasized here that the results of Isenhour and Morrison on the calculated sensitivities are inadequate for this purpose and must be used only as guide lines because they can lead to erroneous results in actual experiments. For instance, the calculations were based on the most intense gamma rays of the elements which, in view of the energy dependence of the gamma detection efficiency of the spectrometer, do not necessarily correspond to the strongest peaks visible in the spectra. Moreover, the sensitivities were based on the arbitrarily chosen minimal counts rates C for possible detection of the gamma rays irrespective of the amplitude of the continuum background on which the gamma peaks are located. In fact more counts are needed to identify a peak if the peak is sitting on a high background and it is to appear above the statistical fluctuations of the latter. And finally no mention is made of the errors associated with the calculated sensitivities. The subsequent work is aimed at overcoming the above deficiencies.

If we rewrite equation (2.2) for the minimum measurable weight by capture gamma analysis as

$$m = 4\pi A_{\min} / [\phi \Omega \epsilon I t] \quad (2.4)$$

where t is the counting time and $A_{\min} = C t$, it is evident that the values of m we seek to establish depend directly on the minimum number of counts A_{\min} that can be used satisfacto-

rily for quantitative determination. It is thus necessary to establish a method for determining A_{\min} and as A_{\min} is itself a function of background, it is important to know what this continuum background radiation is over the whole spectrum and how it varies with different experimental arrangements and different gamma detection modes.

In the chapter that follows an equation for A_{\min} will be derived. This will be based on an improved method for the measurement of small peaks in gamma ray spectra. The energy dependence of the background continuum will be considered in later chapters.

Chapter III

METHOD OF DATA ANALYSIS

3.1 Introduction

When a sample is placed in a neutron flux and the resulting prompt capture gamma radiation is detected and analysed by means of a Ge(Li) spectrometer, there results a gamma spectrum that usually includes some 100-200 peaks ranging in energy from 200 keV to 10 MeV with typical fwhm (full-width at half maxima) of the order of 6 to 12 keV. The actual experimental arrangements for obtaining such spectra, of which a typical example is shown in Fig. 3.1, will be described in the chapters that follow. For the present let us assume that we are faced with the problem of establishing the energies and intensities of the peaks that appear in one such spectrum. Once these are measured, the characteristic gamma rays of any element can be used to identify its presence in the sample and the areas of the corresponding photopeaks can be used to establish its concentration.

In the section that follows there is presented a short description of the computer code that was developed by the gamma spectroscopy group for the analysis of these complex spectra. Sections 3.3 and 3.4 are devoted to the description of those functions of the program developed or modified by the author, and to the presentation of the error equations associated with the measurement of the photopeak areas. Since the equation for the minimum detectable area that we seek to establish is directly related to the error equations, a large

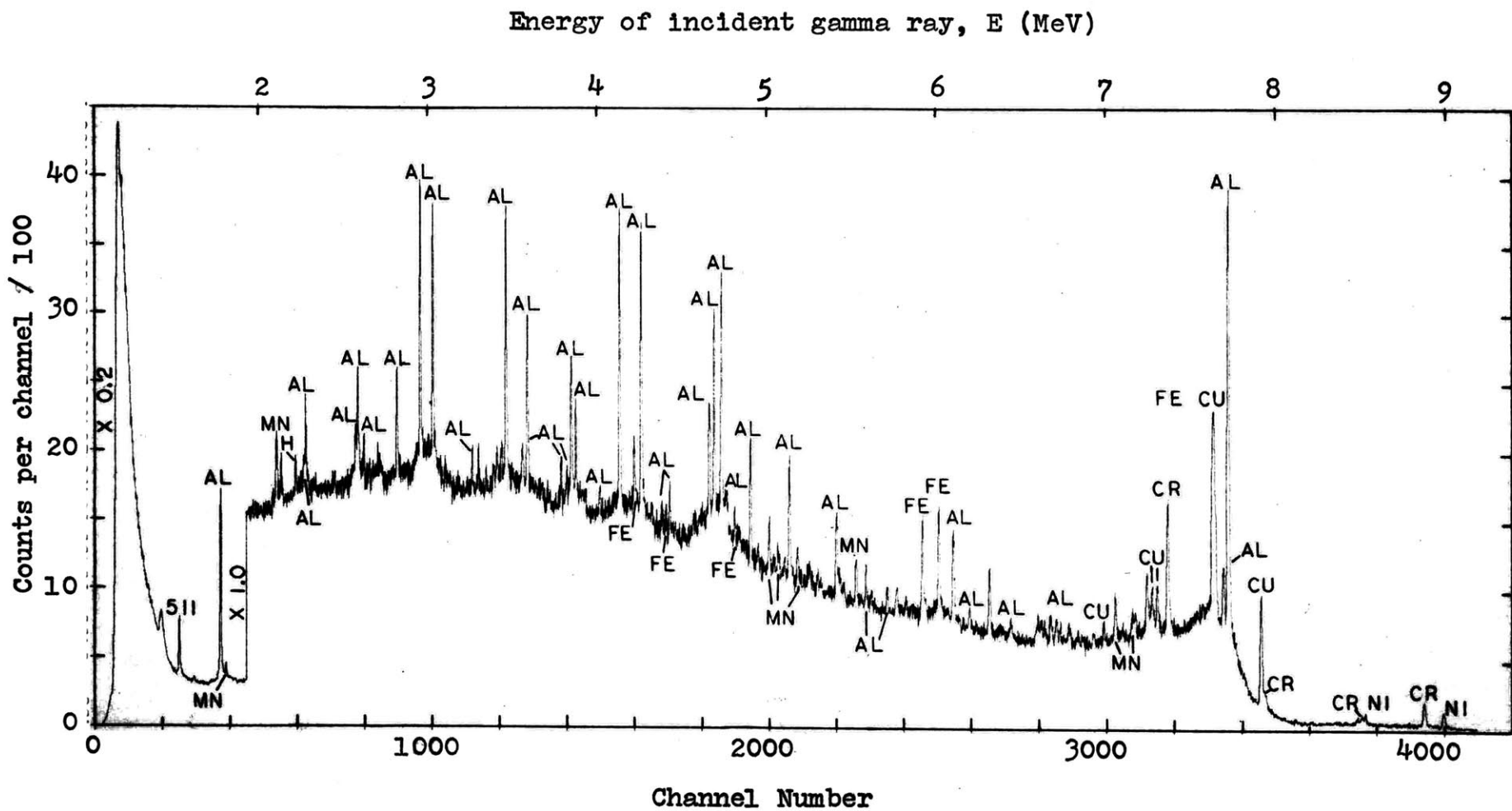


Fig. 3.1 Typical neutron-capture gamma ray spectrum
(Internal facility, Al-6061 sample, 1.62 g)

part of this chapter is devoted to the latter. In section 3.5 are developed three equations on peak area limiting values (or levels) which must be consulted in deciding whether a weak peak in a given spectrum should be labelled as 'good for reliable quantitative determination', or 'good only for qualitative analysis', or simply 'unreliable'. And finally in the last section appears the derivation of the equation for the minimum weight of an element needed for reliable quantitative determination.

3.2 GAMANL

GAMANL is a computer program applying Fourier transforms to the analysis of gamma ray spectra and is the result of a long series of manhour units. It is a code that smooths the data and automatically identifies all the peaks in complex spectra and determines all their geometrical parameters. The original version of the program was developed by T. Inouye [I2(a)]. Modifications and improvements were subsequently made by T. Harper [H8] and the author. The author's main contributions include the development of (a) an improved method of linear background fit for separating the photopeaks from the underlying continuum, (b) an improvement in the analysis of multiplets, (c) a new approach to peak area determination and (d) the development of equations for the errors in the measured peak parameters. A description of the program was published recently ([H1], [I2(b)]).

The program is written in the Fortran IV language for the MIT IBM 360/65 computer and performs the following

operations in about 75 seconds of computation time:

- (a) Smooths the data by employing Fourier transforms; this reduces the random fluctuations without affecting the spectral resolution
- (b) Fits a linear background under the peaks using one to five point averaging at the minima, special criteria being applied for the identification of partially resolved multiplets
- (c) Improves the spectral resolution by using the same Fourier transform with different constants (optional)
- (d) Identifies the maxima of all the peaks by employing certain slope criteria and calculates the energies (within 1 to 2 keV) using two energy standards correcting also for system non-linearity by making use of special input data
- (e) Calculates the height, the height to background ratio, the fwhm, the least-squares fitted fwhm representative of the whole spectrum, and the area of the peaks (by two methods) together with an estimate for the standard deviation in its measurement, and
- (f) Calculates the intensity of the gamma rays by correcting the areas for detector efficiency.

A typical output of this program is shown in section 6.3

3.3 Method of Linear Background Fit

The most important step in the analysis of a given spectrum is the separation of the photopeaks from the underlying continuum. This background is caused (a) by the

continuous gamma spectrum associated with the neutron source and (b) by those gamma rays of originally discrete energy which reach the detector via Compton scattering or which deposit only part of their energy within the sensitive volume of the detector.

In our analysis such a continuum is represented over small subranges of the spectrum by a linear function that connects specially chosen minima in the smoothed data. The smoothing operation which is applied to the raw data prior to this step eliminates most of the random fluctuations and thus makes the identification of all the minima possible. One is faced, however, with the problem of identifying from among these minima those whose recorded counts are due only to the continuous background and do not include any contributions from nearby peaks; that is, care must be taken for the identification of multiplets.

Several criteria have been employed in the past with varying success for choosing the correct minima for this linear background fit. In the original version of the program a condition was placed on the slope of the line between two adjacent minima M_0 and M_1 . The second minimum was accepted or rejected according to whether the absolute value of the slope of the line was smaller or larger than a specified critical value. In mathematical terms, the condition for accepting channel M_1 as a minimum is

$$\left| H(M_1) - H(M_0) \right| < C' (M_1 - M_0) \quad (3.1)$$

where $H(MO)$ and $H(ML)$ are the counts in channels MO and ML , channel MO being itself a minimum satisfying the same condition. This procedure requires that the value of the constant C' be small if multiplets are to be identified and large if the continuous background is increasing or decreasing rapidly. In practice only one value can be specified for C' and therefore the method is liable to serious errors. C' was set at about 20 to 30.

Another approach [H8] sets the criterion at

$$H(ML) - H(MO) < C'' \sqrt{H(MO)} \quad (3.2)$$

Here again the constant C'' (approximately 2 or 3) must be small for the identification of multiplets and large for cases of rapid increases in the continuous background. Satisfactory results can be expected in most cases.

The linear background fit presently used in GAMANL has been developed by the author. Its method of operation may be understood with reference to Fig. 3.2. Assume at first that the method to be described below has already been applied to the low-number channels and that channel MO is accepted as a true minimum; i.e. the number of counts recorded in channel MO is due entirely to the continuous background radiation. Because of the statistical fluctuations in the data, the value of the minimum is obtained by averaging the counts in the channels neighbouring MO according to

$$\bar{H}(MO) = \sum_{j=-p}^{j=p} a_j H(MO+j) \quad \Bigg/ \quad \sum_{j=-p}^{j=p} a_j \quad (3.3)$$

where

$$a_j = 1 \quad \text{if} \quad |H(MO+j) - H(MO)| \leq q \sqrt{H(MO)}$$

and $a_j = 0$ in all other cases.

$H(MO+j)$ is the number of counts recorded in channel $(MO+j)$. Note that a maximum of $2p+1$ channels are considered in the averaging. For our spectra, in which typical peaks occupy 10 to 15 channels, p was set equal to 2 and q was arbitrarily set equal to 1. In cases where the amplifier settings are so chosen that the peak signals are stored in a larger or smaller number of channels, the value of p can be adjusted accordingly.

The next potential minimum in Fig. 3.2 is in channel $M1$. For this to be accepted as a valid minimum the next two higher minima $M2$ and $M3$ must satisfy the following conditions:

(a) for $H(M1) > \bar{H}(MO)$

$$\begin{aligned} (1) \quad |H^*(M2) - H(M2)| &\leq C \sqrt{(M2 - M1) \times H(M2)} \\ (2) \quad |H^*(M3) - H(M3)| &\leq C \sqrt{(M3 - M1) \times H(M3)} \end{aligned} \quad (3.4)$$

or

(b) for $H(M1) < \bar{H}(MO)$

$$(1) \quad H^*(M2) - H(M2) \leq C \sqrt{(M2 - M1) \times H(M2)} \quad (3.5)$$

$H(M2)$ and $H(M3)$ are the number of counts in the minima in channels $M2$ and $M3$, and $H^*(M2)$ and $H^*(M3)$ are the counts these channels would have had they been located along the straight line joining $\bar{H}(MO)$ to $H(M1)$. The right-hand side

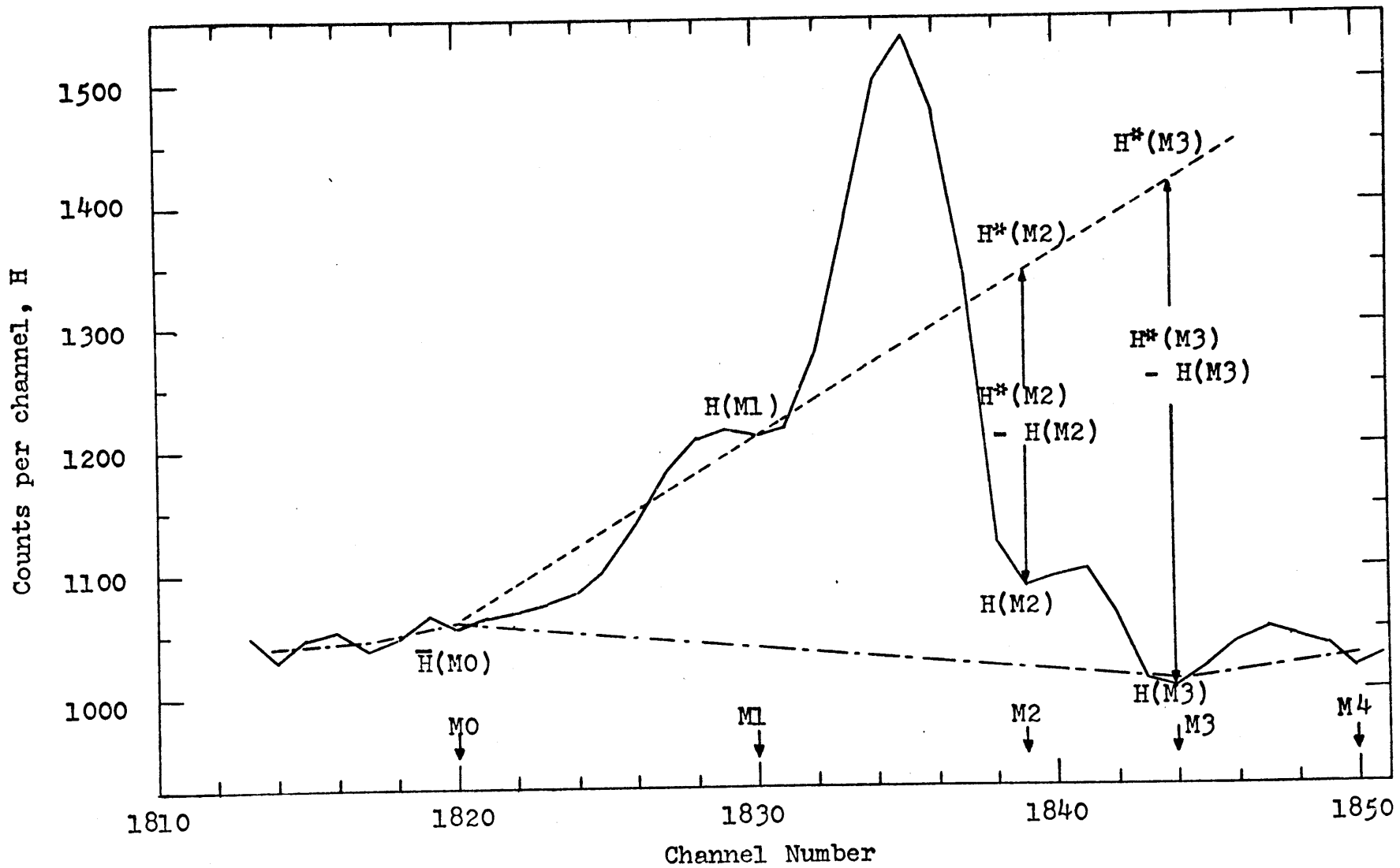


Fig. 3.2 A graphical presentation of the method for linear background fit

of these equations were chosen arbitrarily; the square-root sign represents a measure of the statistical fluctuations in the counts. The constant C was set equal to 1.2 in this work. Condition a(2) was specially added for the definite identification of triplets since condition a(1) might not be sufficient for this purpose. The sets of conditions may be extended further for the identification of higher order multiplets by introducing similar expressions for M⁴, M⁵, etc.

If channel M₁ does not meet the requirements for a valid minimum, as is the case in Fig. 3.2, the point is ignored and a similar analysis is carried out using points M₀, M₂, M₃ and M₄. Due to the limitations of our program to analyze high-order multiplets, this procedure is stopped if five consecutive minima do not satisfy the conditions.

In Appendix V is presented the latest form of the computer code (subroutine) written to perform the above operations. It differs in a number of points from the one published in [H(1)] in view of certain important changes that were made recently.

This method of linear background fit has the following advantages:

- (a) The chosen minima are more representative of the true background because of the point averaging
- (b) Identification of the multiplets is rendered more effective by applying the criteria not to the minimum that must be accepted or rejected but to the next minima higher, and

- (c) Sharp rates of change in the continuum background do not influence its effectiveness since the analysis does not depend on the slope of the baseline to be drawn.

For comparison note that in Fig. 3.2 both points M1 and M2 satisfy the conditions set by equation (3.1) and are therefore used in the first method of background fit described above. Similarly, in the second fit technique, point M2 satisfies equation (3.2) and is therefore accepted as a true minimum.

Choosing the correct background fit is indeed the most important step in the analysis of the data. Once this is accomplished it is only a simple matter to obtain the values for the various peak parameters. The methods of peak area determination, which is of particular importance in this work, are presented in the section that follows.

3.4 Methods of Peak Area Determination

What has prompted the work on peak area measurement is the fact that the proposed methods of area calculation available in the literature are either liable to large errors or are too complex and time consuming to warrant their use in our analysis. In particular, the method of straight sums (Covell [C2]), whereby the area is obtained by summing the counts in the channels forming the peak and subtracting the underlying continuum, does in fact require a point by point plot of the whole spectrum for the sake of certifying that the 'computer-chosen' peaks are not deformed in any way.

For example, if point M1 in Fig. 3.2 were a mere 10 counts (or approximately 1 percent) larger there would be no minimum at M1 and the triplet would have been 'thought of' by the computer as a doublet. And it is fairly often that small unresolved peaks are located at the wings of larger ones.

Again, in some other proposed methods, where the peak distribution is assumed to be Gaussian (C. L. Carnahan [C3]) the standard deviation of the Gaussian is assumed to be known a priori thus rendering the results of an analysis questionable in cases of slight voltage shifts in the electronics which change the apparent energy resolution.

Finally, there is the more precise method of least-squares fitting the spectral data to a Gaussian function superimposed on a linear background. It has been reported by a number of authors such as Graber and Watson [G6], Daddi and D'Angelo [D1], Helmer et al. [H3], Liuzzi and Pasternack [L4], and Trombka and Schmadebeck [T2]. The iterative procedure employed in this analysis, which inevitably leads to long computation times, constitutes its main drawback. In our analysis, where the accuracy is limited mostly by the efficiency calibration of the spectrometer this expense is not warranted.

The method of area evaluation that is proposed in section 3.4.1 assumes that the peak area distributions are characterized by a Gaussian with an energy-dependent fwhm obtained by least-squares fitting the fwhm of the strongest peaks in the actual data. As will ^{be} shown later, the resulting reduction

in the error of the areas makes this method more attractive than that of the straight-sums, the latter being more accurate only for very strong non-deformed peaks. Moreover, because of the smoothing process we apply to the data before we attempt to analyze them, the accuracy with which the peak parameters can be determined is comparable to that resulting from the more elaborate procedures mentioned above.

3.4.1 Area Equations

Two methods of area calculation are presented in this section. The first is the method of straight-sums as employed in the original version of the GAMANL code. The second method was developed by the author and has been added to this code.

With reference to Fig. 3.3 the area under the peak according to the straight-sums approach is

$$A_S = \sum_{k=1}^{n-1} H_k - \frac{n-1}{2} (\bar{H}_0 + \bar{H}_n) \quad (3.6)$$

where n is the number of intervals occupied by the peak and \bar{H}_0 and \bar{H}_n are the peak minima evaluated by equation (3.3).

In the second method, the peak distributions are assumed to be Gaussian having a peak height h and an area given by

$$A_G = 1.0645 \psi \bar{w} h \quad (3.7)$$

Here ψ is a correction factor to account for the deviation of the data points from a true Gaussian distribution; it is determined experimentally for each spectrum and usually has a value of approximately 1.02. \bar{w} represents the full-width

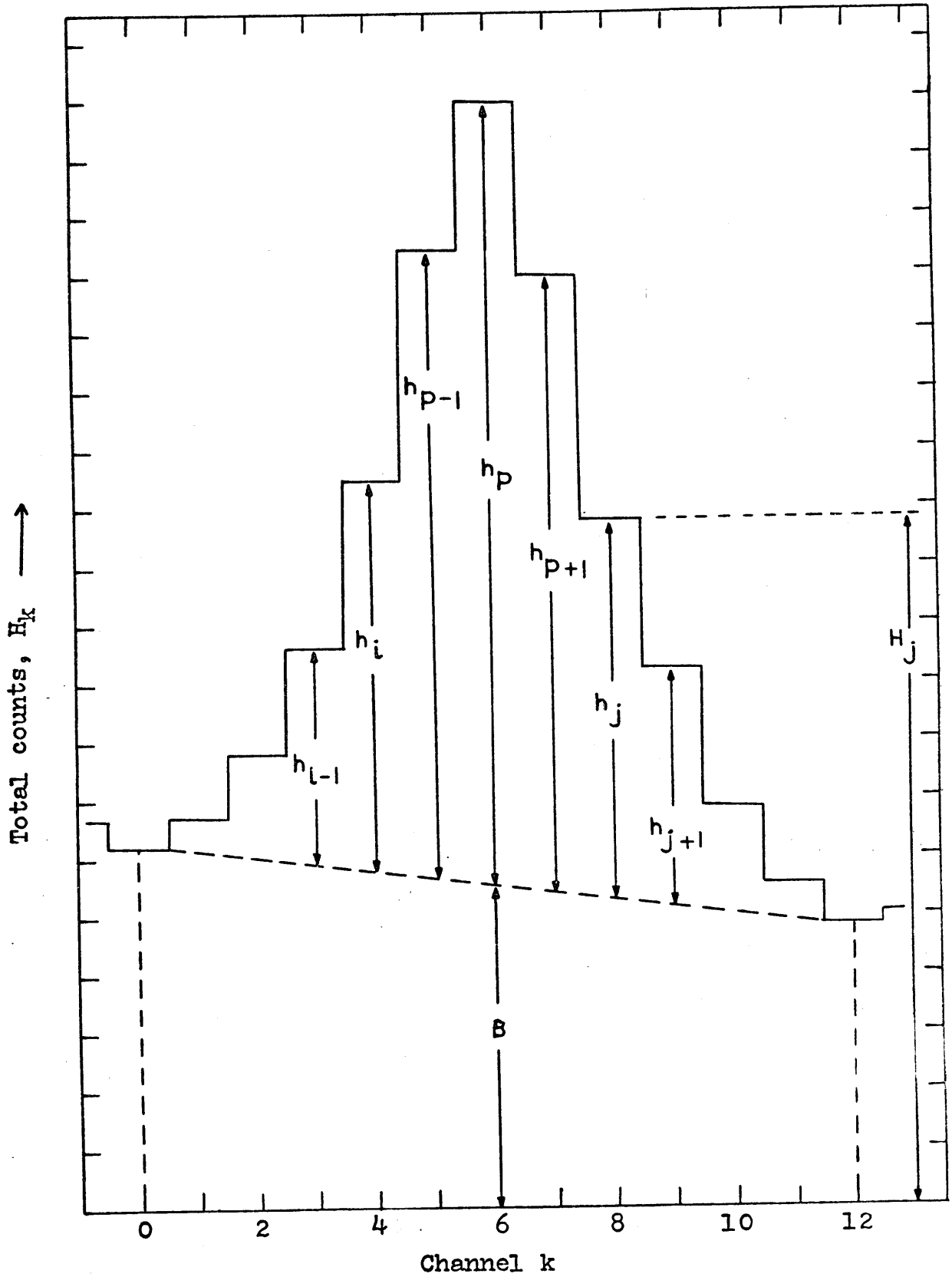


Fig. 3.3 Histogram of a typical spectral peak
($n = 12$ in this case)

at half maximum of a peak (or peak width as it will often be referred to) at energy E determined by least-squares fitting the properly weighted widths and energies of the strongest peaks in the spectrum to a smooth function. The algebra associated with this procedure is presented in Appendix II together with sample results.

Note that data spread over the whole spectrum is used to evaluate ψ and \bar{w} , and as this is done routinely for each spectrum, slight distortions or voltage shifts that occur are accounted for. The advantage of the method lies in the reduction of the error in the peak width, the fitted value of the width at any particular position in the spectrum being more accurate than that obtainable from any one single peak at the same position.

It must be pointed out here that the idea of using one single curve to represent the variation of peak width with energy is not physically correct since some of the gamma rays in the fit are liable to be Doppler broadened if they are emitted while the nucleus is still recoiling from the emission of other gamma rays in the same cascade. As shown in Appendix II, ^{11}B lines can be broadened by as much as 1.5 keV but, in general, typical values are in the vicinity of 0.1 keV. The actual error in the measured widths in our case is in general larger than this and therefore the effect is not expected to affect the fit in any significant way. Moreover, in the application of gamma spectroscopy to elemental analysis one usually compares the unknown sample

to a standard and hence systematic errors in the fit, if any, cancel out.

In our method of analysis the actual peak width is obtained by assuming linear interpolation between the channels whose count is just above and just below the peak half maxima. With reference to Fig. 3.3 the width is

$$w = j - i + \frac{h_i - (h/2)}{h_i - h_{i-1}} + \frac{h_j - (h/2)}{h_j - h_{j+1}} \quad (3.8)$$

As noted earlier, h is the peak height and is determined by a second order interpolation applied to the three highest points in the peak after the background continuum has been subtracted. Denoting these three points by h_{p-1} , h_p and h_{p+1} the peak height equation takes the form

$$h = h_p (1 + \alpha) \quad (3.9)$$

where

$$\alpha = \frac{(h_{p+1} - h_{p-1})^2}{8h_p(2h_p - h_{p-1} - h_{p+1})} \quad (3.10)$$

For the case of multiplets, consider one consisting of m peaks whose maxima are located at positions c_j , $j = 1, 2, 3, \dots, m$. The number of counts h'_j registered at these maxima have contributions from all the peaks in the multiplet according to

$$h'_j = \sum_{i=1}^m h_i \exp \left[- \frac{(c_j - c_i)^2}{2\sigma^2} \right] \quad (3.11)$$

where σ is the standard deviation of the Gaussian peaks and

is related to the width by $\sigma = \bar{w} / (2 \times 1.1774)$.

h_1 are the true number of counts corresponding to each peak individually and may be obtained by solving the above simultaneous equations.

The peak area corresponding to each peak in the multiplet is obtained, in the Gaussian approach, by using these h_1 values in equation (3.7). In the straight-sums approach, on the other hand, the total area in the multiplet, $(A_S)_t$ is normally apportioned to the m peaks according to the equation

$$(A_S)_j = [(A_S)_t h_j] / \sum_{i=1}^m h_i \quad (3.12)$$

Note that for the analysis of multiplets both methods of area determination must rely on the resolution of the system at that particular position in the spectrum, the multiplet itself being unsuitable for supplying such information. In the original version of the program (GAMANL) the system resolution was approximated by a linear function whose parameters were dictated by the values of the fwhm of the two energy calibration lines in the spectrum. In its present form the code uses the least-squares-fitted width for these computations.

For non-deformed peaks, both methods of area determination must give comparable results. In practice the relative values of the areas obtained by the two techniques are used as a measure of confidence.

3.4.2 Errors

In order to investigate which of the two methods of peak area determination is more reliable, it is necessary to compare the error equations associated with each of these two techniques. The development of these equations, as well as the errors incurred in the measurement of the other peak parameters, are presented in Appendix III. It suffices for the moment to note that the standard deviation (which will often be referred to as the error) in the straight-sums area A_S is given by

$$\sigma(A_S) = \sqrt{A_S + (3\bar{w} - 1)[1 + (3\bar{w} - 1)^2/2r^2] B} \quad (3.13)$$

where $B = (H_0 + H_n)/2$ and is the average background value underneath the peak. r represents the reduction in the statistical fluctuations of the data by the smoothing process and has a value of 1.34 for the filter function that was often used in this work; more information on r appears in Appendix I.

In the Gaussian approach the standard deviation in the area is given by

$$\sigma(A_G) = A_G \sqrt{[(1 + \alpha)/hr]^2 (h + 1.5B) + s^2/\bar{w}^2} \quad (3.14)$$

where the first term represents the relative standard deviation in the peak height h , and s accounts for the error in the fitted width \bar{w} resulting from the least-squares operation (see equation (A2.16)).

The above equations, whose derivation was based on a

number of assumptions, were tested using both real and pseudo-experimental data. Details may be found in Appendix III.

In order to afford a comparison between the two methods of peak area determination (s/\bar{w}) is equation (3.14) was assumed to have the empirical value of approximately 0.02 for those peaks which, because of the weighting procedure described in Appendix II, do not have any significant influence on the fit; it is smaller for more intense peaks. A typical fwhm of 4 channels was used. The results of the comparison are presented in Fig. 3.4 for a number of values for the background continuum B in terms of the ratio of the two errors defined as

$$R_{\sigma} = [\sigma(A_G) / \sigma(A_S)]$$

Values for R_{σ} larger than unity indicate that the standard deviation in the area determined by the Gaussian approach is relatively larger and that therefore the method of straight-sums should be preferred. R_{σ} values less than unity shift the preference to the Gaussian approach.

The actual percent error in A_G is shown in Fig. 3.5. Note that for $[\sigma(A_G)/A_G] = 15$ percent the corresponding relative error in the straight-sums area, $[\sigma(A_S)/A_S]$, will range from $(15/0.7) = 21$ percent to $(15/0.58) = 26$ percent for B values ranging from 25 to infinity. The significance of this is noteworthy since, according to the peak area limiting values (or levels) developed in the following section, only areas with less than 20 percent error can be employed

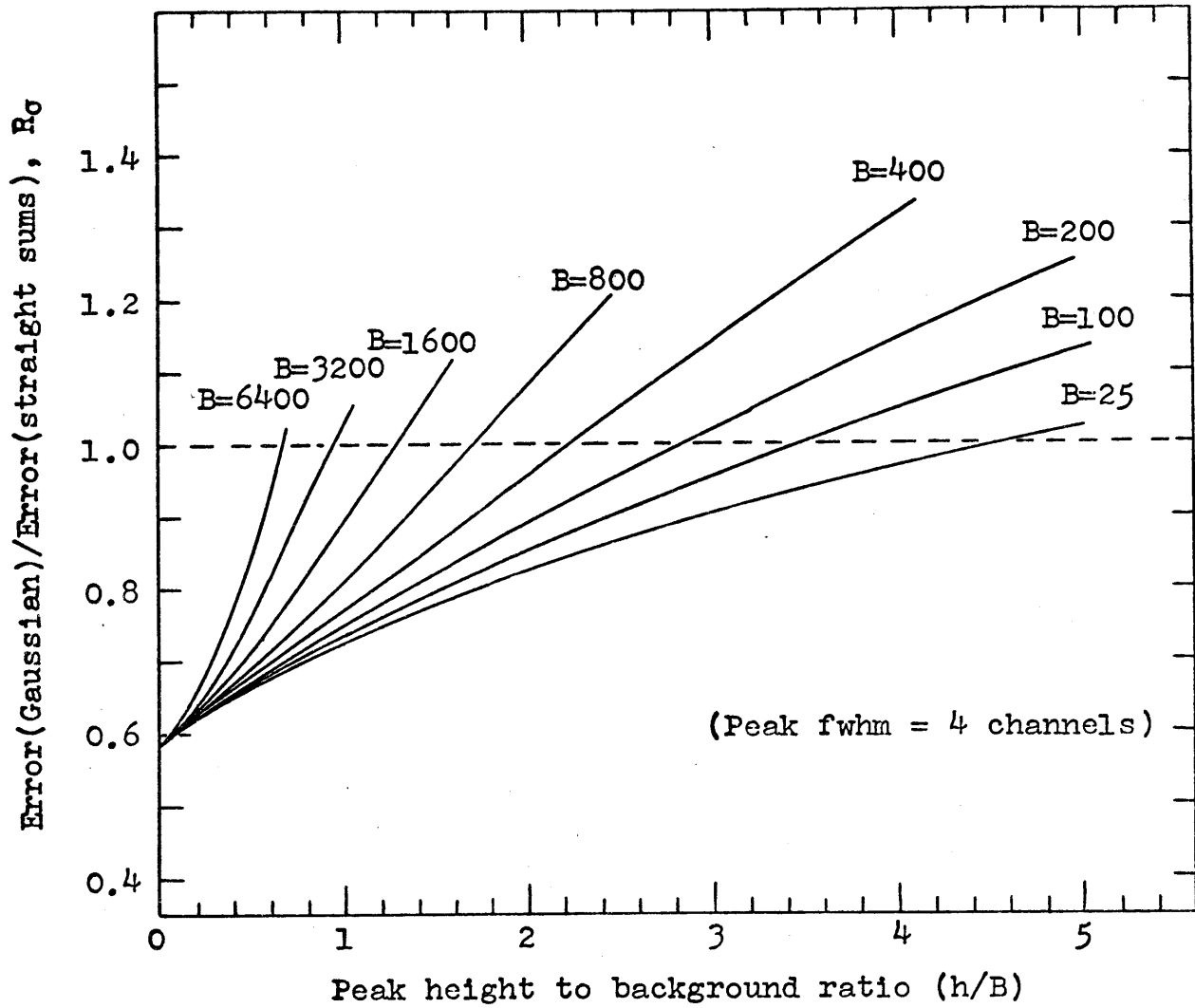


Fig. 3.4 Ratio of the errors in the two methods of peak area determination

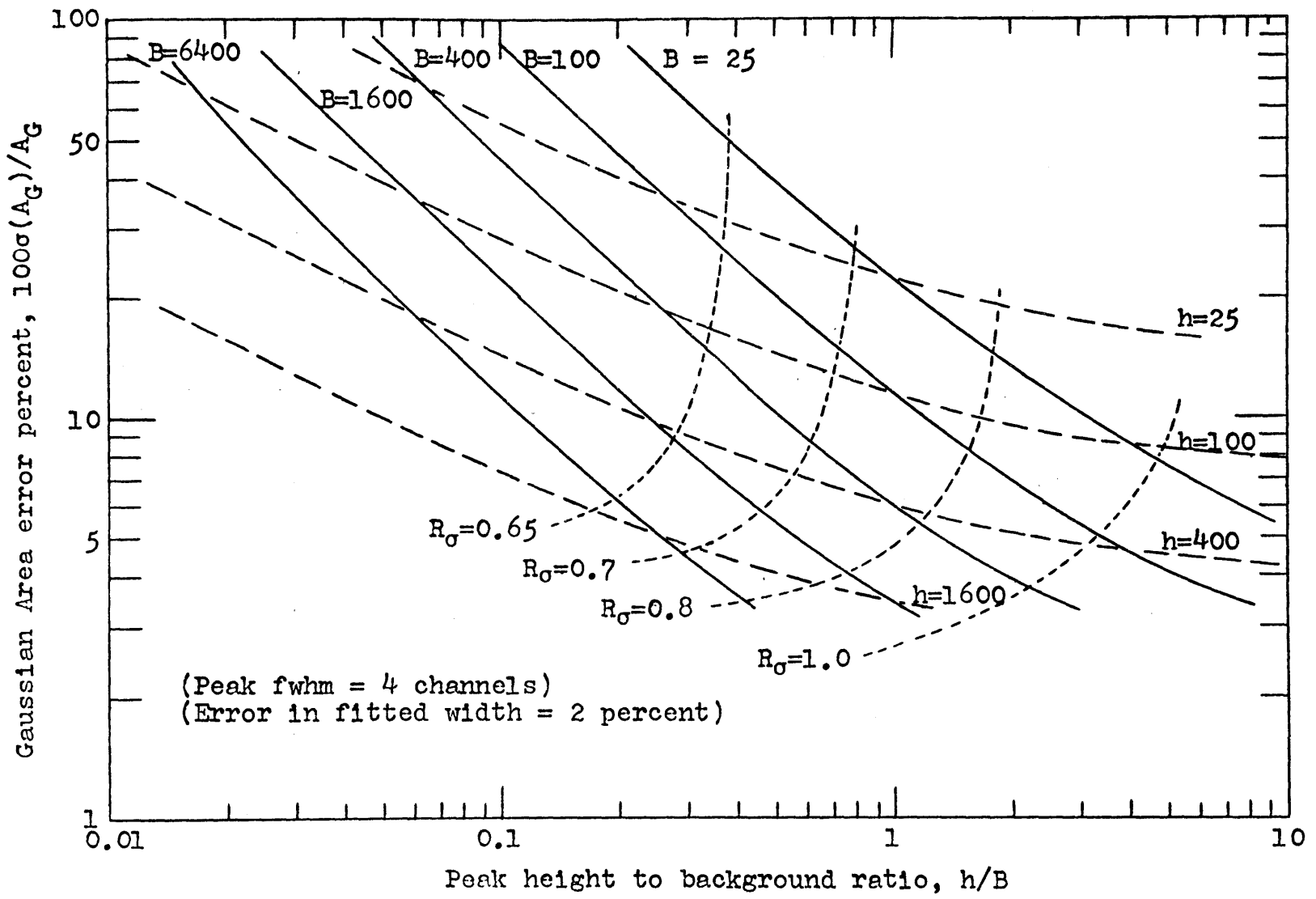


Fig. 3.5 The Gaussian area percent error for various values of h and B

reliably for quantitative determination.

It is seen from Fig. 3.4 that the straight-sums approach must be preferred only for strong peaks with large (h/B) values. However, such peaks constitute only a small fraction of the spectrum. In addition, this method of peak area determination cannot account for small unresolved peaks located at the wings of larger ones and, moreover, it must rely on the fitted width for the evaluation of the number of counts corresponding to each peak in a multiplet. These observations, coupled together with the interest in this work in the measurement of small peaks, have convinced the author that, as far as elemental analysis using both standard and unknown samples is concerned, the Gaussian method is to be preferred. In fact the method may be applied without any restrictions to cases that are not subject to Doppler broadening effects.

As a final validation of the above remarks there is presented in Appendix III a comparison between three aluminum spectra obtained under similar experimental conditions. It may be observed there that there is better agreement between corresponding Gaussian areas than between areas obtained by the method of straight sums.

3.5 Limiting Values for Peak Areas

The error equations presented above, which were based on a number of assumptions and empirically determined constants, are only simple estimates of the standard deviation in the measured parameters. If these are assumed to be

known exactly, a confidence interval specified by k_1 can be set on the value of any parameter y according to

$$y - k_1 \sigma(y) < y < y + k_1 \sigma(y) \quad (3.15)$$

For confidence intervals of 50, 68.3, 90 and 99.46 percent k_1 has the values of 0.6745, 1.000, 1.645 and 3.00 respectively. Thus, for example, there is a 90 percent probability that y is within the interval

$$y - 1.645 \sigma(y) < y < y + 1.645 \sigma(y) .$$

Proceeding further, if the limit y_{\min} for quantitative determination of y is set equal to $k_2 k_1 \sigma(y)$, then y will lie in the interval

$$k_2 k_1 \sigma(y) - k_1 \sigma(y) < y < k_2 k_1 \sigma(y) + k_2 k_1 \sigma(y) \quad (3.16)$$

or

$$y_{\min} = k_2 k_1 \sigma(y_{\min}) \pm k_1 \sigma(y_{\min})$$

k_2 is related to the desired error in the measurement, this being equal to $(100/k_2)$ percent. For $k_1 = 1.00$ and $k_2 = 5$ there is, for instance, a 68.3 percent probability that the error in y_{\min} will be 20 percent. This is equivalent to a 99.46 percent probability that the same value of y_{\min} (which is $5 \sigma(y_{\min})$ in this case) will have an error of 60 percent, k_1 and k_2 now having the values of 3 and $(5/3)$.

In the particular case of the minimum area A_{\min} which can be used satisfactorily for quantitative analysis, equations (3.14) and (3.16) give, by using A_{\min} in place of y_{\min} ,

$$A_{\min} = [1.0645k_1k_2\psi\bar{w}(1+\alpha)/r]\sqrt{(A_{\min}/1.0645\psi\bar{w}) + 1.5B} \quad (3.17)$$

The relatively small error in the fitted width was neglected. Solving for A_{\min} there results

$$A_{\min} = [1.0644\psi\bar{w}(1+\alpha)^2k_1^2k_2^2/(2r^2)]\left\{1 + \sqrt{6B[r/(k_1k_2(1+\alpha))]^2 + 1}\right\} \quad (3.18)$$

The expression "limit for quantitative determination" was borrowed from an article by L. A. Currie [C4] who has re-examined the question of signal detection and signal extraction in analytical and nuclear chemistry in view of the occurrence in the literature of numerous, inconsistent and limited definitions of detection limits. Currie defines three limiting levels: (a) the net signal level (instrument response) above which an 'observed' signal may be reliably recognized as 'detected'; (b) the 'true' net signal level which may be a priori expected to lead to detection, and (c) the level at which the measurement precision will be satisfactory for quantitative determination.

Following Currie's approach, the critical level in the area measurement corresponds to

$$A_{\text{crit}} = [1.0645\psi\bar{w}k_0(1+\alpha)/r]\sqrt{1.5B} \quad (3.19)$$

The detection limit, which is so defined that it is always greater than zero, is equivalent to

$$A_{\text{det}} = [1.0645k_0\psi\bar{w}(1+\alpha)/r]\{[k_0(1+\alpha)/r] + 2\sqrt{1.5B}\} \quad (3.20)$$

Assuming that risks of 5 percent are acceptable, the constant

k_0 takes on the value 1.645; this is the value recommended by Currie. His final expression for the determination level is similar to equation (3.18) derived above but with only one constant standing for the product $k_1 k_2$.

Analysis of spectra associated with this research has shown that satisfactory results can be expected for $k_1 = 1$ and $k_2 = 5$. Using these values in the above three equations, together with $\alpha = 0.02$ (see Appendix III), $\psi = 1.02$ and $r = 1.34$ there results

$$A_{\text{crit}} = 1.67 \bar{w} \sqrt{B} \quad (3.21)$$

$$A_{\text{det}} = 1.71 \bar{w} [1 + 1.95\sqrt{B}] \quad (3.22)$$

$$A_{\text{min}} = 7.91 \bar{w} [1 + \sqrt{1 + 0.41 B}] \quad (3.23)$$

Typical values of the peak parameters corresponding to these three limiting levels are given in Table III(1). A fwhm of 4 channels was assumed for all cases. A graphical presentation, which is representative of all the cases considered, is shown in Fig. 3.6.

From Table III(1) it can be established that for the particular filter function used ($r = 1.34$) and any value of the fwhm

- (a) Peak areas with error larger than 60 percent fall below the critical level
- (b) Peak areas with error larger than 30 percent constitute unreliable detection
- (c) Peaks areas whose error lies in the range of

TABLE III(1)

TYPICAL PEAK PARAMETERS CORRESPONDING TO THE
THREE PEAK AREA LIMITING LEVELS

	PARAMETER	B = 100	B = 800	B = 1600	B = 6400
CRITICAL LEVEL	A_{crit}	66.8	188.9	267.2	534.4
	h	15.4	43.5	61.6	123.0
	h/\sqrt{B}	1.54	1.54	1.54	1.54
	$\sigma(A) \%$	63.8	61.9	61.5	61.2
DETECTION LEVEL	A_{det}	140.4	384.5	541.0	1075.
	h	32.3	88.5	124.6	247.5
	h/\sqrt{B}	3.23	3.13	3.12	3.09
	$\sigma(A) \%$	32.0	31.0	30.9	30.7
DETERMINATION LEVEL	A_{min}	236.7	605.5	842.6	1652.
	h	54.5	139.4	194.0	380.6
	h/\sqrt{B}	5.45	4.93	4.85	4.76
	$\sigma(A) \%$	20.0	20.0	20.0	20.0

In all cases the full width at half maximum was set
equal to 4 channels.

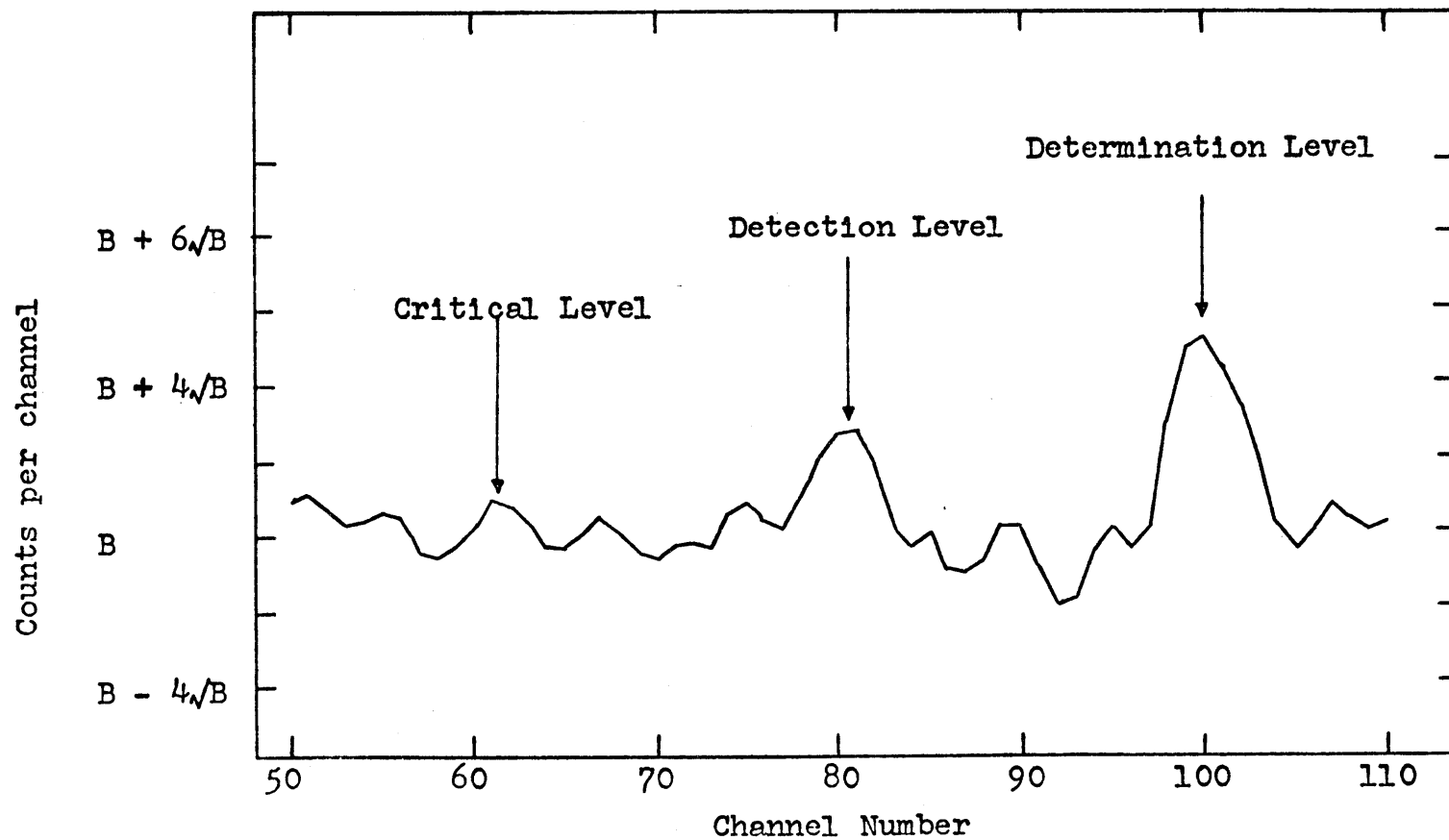


Fig. 3.6 An illustration of the three peak-area limiting levels

20 to 30 percent should be restricted to qualitative analysis only, and

- (d) Peak areas with less than 20 percent error can be reliably employed for quantitative determination.

In all three cases, the (h/\sqrt{B}) values are approximately constant, irrespective of the amplitude of the continuum background. The heights of the peaks corresponding to the critical, the detection and the determination levels are approximately $1.5\sqrt{B}$, $3\sqrt{B}$ and $5\sqrt{B}$.

Note that the limiting levels are a function of the system resolution. Consider, for instance, the peak-area critical level for two cases characterized by widths \bar{w}_a and \bar{w}_b . The background values, accumulated under otherwise identical experimental conditions, will be B_a and B_b , where $B_a = (\bar{w}_b/\bar{w}_a) B_b$. Therefore $A_{crit,a} = \sqrt{(\bar{w}_a/\bar{w}_b)} A_{crit,b}$. This is because in our method of background evaluation the background data are computed with the same accuracy irrespective of the number of channels occupied by typical peaks. In fact the limiting levels would be the same if the number of points used to evaluate the average background (equation (3.3)) were adjusted with respect to the system resolution and amplifier settings.

3.6 Equation for the Minimum Measurable Weight

The minimum measurable weight of an element in a given sample is obtained by combining equations (2.4) and (3.18). With $\alpha = 1.02$, $k_1 = 1$, $k_2 = 5$, and introducing the total mass of the sample M and the energy-channel conversion factor

C (keV/channel), there results

$$\frac{m}{M} = \frac{[13.8\bar{w}(E-511y)/(Cr^2)] \left\{ 1 + \sqrt{1 + 0.23Cr^2B(E-511y)} \right\}}{M \phi t \epsilon I (\Omega / 4\pi)} \quad (3.24)$$

where the peak width $\bar{w}(E - 511y)$ is now in units of keV and the background $B(E - 511y)$ is in (counts/keV).

Interpretation of this equation is as follows. Consider a sample of mass M irradiated for a time t by a thermal neutron flux ϕ in a gamma²-detection facility having a fractional solid angle $(\Omega / 4\pi)$ and an energy-dependent efficiency ϵ . The gamma rays that reach the detector, both directly and indirectly via Compton scattering, give rise to a continuum background spectrum on which are superimposed a number of discrete peaks. At the end of the irradiation the value of this continuum background at energy E is $B(E)$. Suppose next that one of the sample constituents emits upon neutron capture a number of gamma rays one of which has an energy E and an intensity I (photons/gram n/cm²). If this gamma ray is sufficiently intense there will appear in the spectrum at energy $E - 511y$ keV, with $y = 0, 1$ and 2 , a peak of width $\bar{w}(E - 511y)$ keV whose count content, or peak area, will depend, among other parameters, on the concentration of the constituent in the sample. (The value $y = 0$ corresponds to the full-energy peak; $y = 1$ and $y = 2$ represent the single- and double-escape peaks in which case one or both of the two 511 positron annihilation rays escape the detector). If this peak area is exactly equal to the numerator in equation (3.24) then, by

definition, m denotes the minimum measurable weight of the sample constituent in question that can be determined with a 20 percent standard deviation when the analysis is based on its characteristic gamma ray of energy E . Note that this error reflects only the expected error in the peak area determination due to the statistical fluctuations in the count in each channel in the spectrum. No error has been assumed in the parameters in equation (3.24) and it is expected that these errors will cancel out when, in actual practice, the unknown sample is compared to a standard.

For each characteristic gamma ray of this sample constituent there corresponds a given minimum weight m . The most sensitive gamma ray for elemental analysis is then that for which m is least. Note that this does not necessarily correspond to the most intense gamma ray of the element in question since this may coincide with an unfavourably high background and/or a relatively low detection efficiency.

Equation (3.24) gives the minimum weight requirement for elemental analysis based on the measurement of a single gamma ray. In actual practice use should be made of all the gamma rays of each element observed in the spectrum.

Application of this equation requires, among other things, values for the energies and intensities of the gamma rays. A compilation of this data was published recently by our laboratory for 75 elements [R2]. As an additional aid to elemental analysis, the energies and intensities of all the capture gamma rays of these elements have been ordered by the

author in terms of increasing energy and were published in a separate report [H7]. A similar list which includes only the strongest gamma rays of each element (up to a maximum of 12) is presented in Appendix IV.

The peak intensities reported in reference [R2] are in units of photons per 100 neutron captures. These have been expressed in reference [H7] in terms of number of photons emitted per gram of element of natural composition per incident neutron/cm², using the equation

$$I = [0.6023 \sigma i / (100 A)] \quad (3.25)$$

where σ is the thermal neutron absorption cross section (barns), i is the gamma ray intensity in photons per 100 neutron captures, and A is the atomic weight of the element. In this set of units the intensities may be thought of as an index of the relative analytical sensitivity of the elements. In addition, interference effects may be resolved with less effort since the relative significance of gamma rays originating from different elements may be evaluated directly using these intensities. In what follows use will be made of both sets of intensity units.

The equation for the minimum measurable weight is also seen to be a function of other important parameters. Note in particular that improvements in the system resolution and reduction in the background continuum without equally affecting the peak counts lead to a decrease in the minimum peak area needed for measurement and therefore to an improvement in the

sensitivity of the method for elemental analysis. System resolution depends on the quality of the detector and associated electronics; it is for the most part limited by the state of the existing technology. The continuum background, on the other hand, depends on the design of the experimental set up and on the techniques employed in reducing the undesirable radiation.

Reduction in the minimum weight requirement can also be accomplished by an increase in the count rate of the system. Such an increase can be obtained, for instance, by increasing the sample weight, the effective solid angle, the neutron flux and/or by improving the gamma detection efficiency. To this end, consider two cases characterized by count rates c and c' and let us evaluate the ratio, R , for the minimum weight concentration required for analysis in each case. With reference to equation (3.24), the unity terms in the curly brackets may be neglected, as a first approximation, when compared to the term involving the background continuum. Since the count rate also depends directly on the sample weight, the solid angle, the neutron flux and the detection efficiency, the ratio R can be approximated by the equation

$$R = \frac{\frac{m}{M}}{\frac{m'}{M'}} = \frac{M' \phi \Omega \epsilon \sqrt{B} (E-511y)}{M \phi \Omega \epsilon \sqrt{B'} (E-511y)} = \frac{c' \sqrt{B} (E-511y)}{c \sqrt{B'} (E-511y)} \quad (3.26)$$

The counting time was assumed equal in both cases. This can be simplified further by noting that the background continuum is a direct function of the count rate. The result is

$$R = \sqrt{(c'/c)} .$$

Thus, if the neutron flux, for instance, is increased by a factor q , the minimum weight of an element required for analysis will be reduced by a factor of approximately \sqrt{q} . Note that from the results of Isenhour and Morrison [11] discussed in Chapter II, an improvement in the system sensitivity by a factor of q would have been anticipated. This is because these authors made the assumption that the same number of counts are needed to identify and analyze a peak irrespective of the amplitude of the background continuum on which the peak is located.

Application of the minimum weight equation is straightforward if all the parameters on the right-hand side of equation (3.24) are known. The actual facilities used to obtain the necessary empirical information are considered in the chapter that follows. A test on the validity of the equation and its application for the determination of the minimum measurable weights of the elements are given in Chapters VI and VII.

Chapter IV

EXPERIMENTAL EQUIPMENT

4.1 Introduction

The techniques and procedures used in this work for extracting reliable information from weak peaks in gamma ray spectra were presented in the previous chapter and its associated appendices. The advantages of smoothing the data were demonstrated together with the precautions which must be taken in applying the smoothing. Methods of background subtraction and peak area determination were also discussed. Also developed was an equation for the minimum measurable quantity of an element in a given sample that can be detected by neutron-capture gamma ray spectroscopy. In this chapter consideration will be given to the actual experimental facilities required to obtain the empirical information needed for the application of this equation.

4.2 Description of the Experimental Facilities

In experiments involving the measurement and utilization of gamma rays from thermal neutron capture, two alternative geometrical arrangements of neutron source, target sample, and detector are available. In the first case one may extract a thermal neutron beam from a reactor, absorb the neutrons in the sample of interest, and study the resulting capture gamma rays with a detector located close to the sample. The other possibility is to locate the sample in a high neutron flux region of the reactor and view the capture gamma rays from

a considerable distance with a detector located outside the reactor.

At the start of this work it was not entirely clear which of these two geometrical arrangements would be more effective for elemental analysis. As a result data were taken using both alternatives. The facilities employed in these measurements, which will be referred to as the internal and external sample facilities, are described in the sections that follow.

4.2.1 The Internal-Sample Facility

A plan view of the internal facility and its orientation relative to the MIT reactor is shown in Fig. 4.1. Its basic features include the 4THL through port, neutron and gamma collimation and shielding, a sample holder, and a three-crystal spectrometer.

The through port is a 4 1/2 - inch i.d. tube tangent to the reactor tank on the thermal column side. The port centerline is 16 inches below the centerline of the fuel. The part of the port inside the thermal shield is embedded in graphite; the rest of it is in heavy concrete. Because of multiple scattering in the graphite the neutrons strike the sample from essentially all directions. At the sample position, close to the reactor tank, and for 5-MW reactor power, the neutron flux is approximately 1.9×10^{13} n/cm² sec and the cadmium ratio is about 9. At the same position the gamma dose is 1.3×10^8 R/hr. Nuclear heating of the uncooled facility leads to an ambient temperature of about 350°C (MITR Reference Manual).

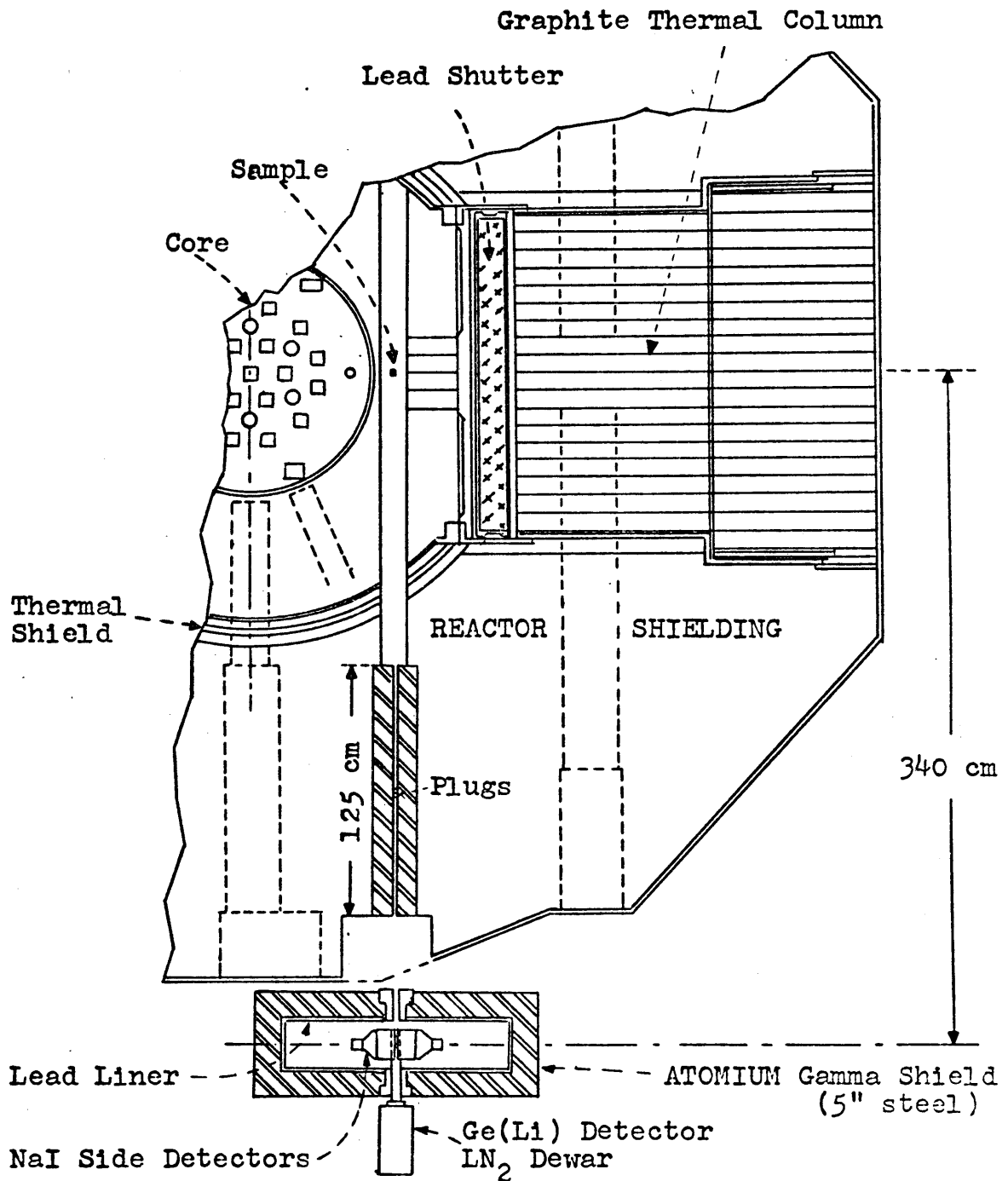


Fig. 4.1 A plan view of the internal neutron beam facility and gamma spectrometer

Capture gamma rays from the sample are first collimated inside the through port so as to reduce the flux of neutrons and scattered gamma radiation escaping the reactor. Details of the internal collimation are shown in Fig. 4.2. It consists of a stainless steel tube (SS304, 0.75-inch o.d., 1/16-inch wall, 22.25 inches long) placed in the central hole of the main port plug. The tip of the tube carries a 1 1/8 - inch polyethelene plug for neutron scattering and thermalization, a 1 1/4 - inch LiF plug for neutron absorption and a 1/2 inch lead plug for low energy gamma attenuation.

Final collimation of the gamma beam was accomplished with an external collimator in front of the Ge(Li) detector. With a sample-to-detector distance equal to 134 inches (340 cm), a 3/8-inch collimator gave a fractional solid angle of 4.9×10^{-7} . The collimation was such that the walls of the through port were not viewed by the detector. The effective area viewed by the detector was a circle of about 1 inch diameter. The actual samples used were only 1/2 inch in diameter.

To reduce the gamma radiation resulting from neutron capture at the other end of the port (port 4TH3), a special tip consisting of aluminium, boral and lead was placed at the front of the port's main plug (see Fig. 4.2). The boral lining, also not viewed by the detector, served the purpose of reducing the number of scattered neutrons that reached the lead block. Lead was chosen because of its simple two-gamma

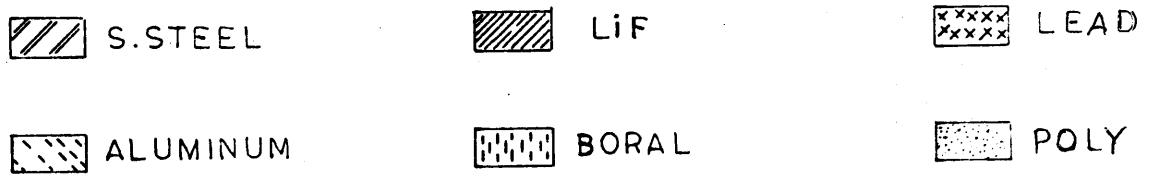
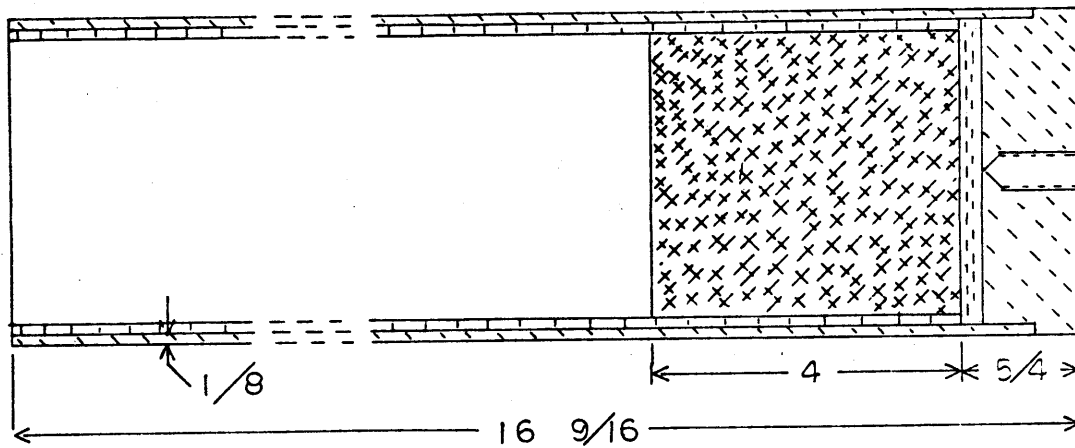
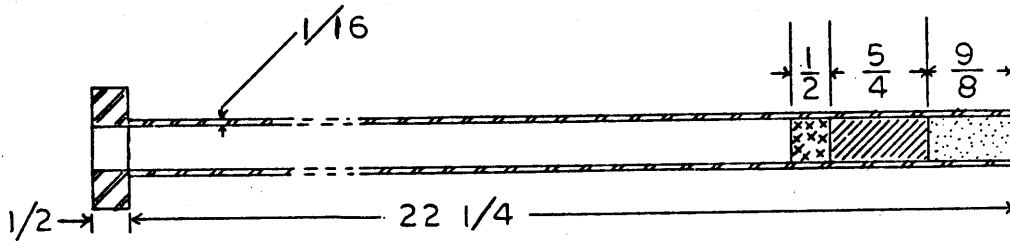


Fig. 4.2 Details of the internal beam collimator and end plug

capture spectrum.

An external beam shutter, consisting of a 2-inch masonite block followed by 4 inches of lead, could be rolled across the beam whenever the system was not in use. Additional overall shielding was provided by an 8-inch wall erected behind the spectrometer. With no sample, the gamma dose in the beam was about 80 mr/hr, most of it being due to low-energy scattered radiation. With typical samples in position the gamma dose was approximately 10 to 20 times higher and could be reduced to nominal values by placing additional lead absorbers in the beam and/or by placing the sample at other points along the through tube, away from the high-flux central position.

Samples were fastened at the center of special sample holders and inserted for irradiation with a remote-handling tool using the end of the port opposite the spectrometer. Photographs of the tool and the sample holder, which were specially designed for use with solid samples, are shown in Fig. 4.3. The handling tool is 12 feet long; its method of operation may be inferred from the photograph and will not be described here. The holders were cylinders 2 1/2 inches long, 4 3/8 inches o.d. with about 5/16-inch wall. Al-1100 was used in the construction. A large fraction of the sides of the holder were machined out to reduce the amount of material irradiated. Typical holders weighed approximately 90 grams. These holders have the disadvantage of becoming highly radioactive. However, they do not introduce any neutron or

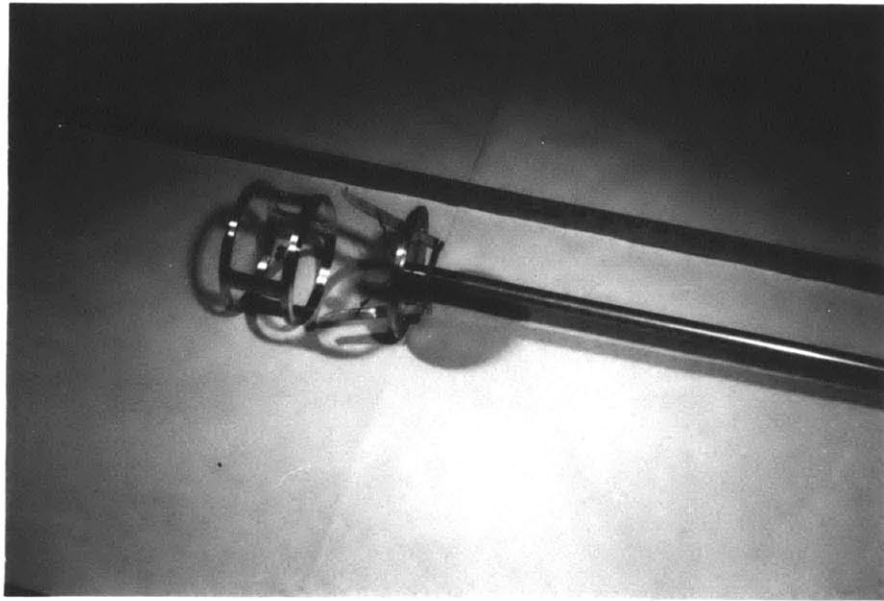


Fig. 4.3(a) Photograph of sample holder and remote handling tool, disengaged; central disc is a stainless steel sample, $\frac{1}{2}$ -inch in diameter.

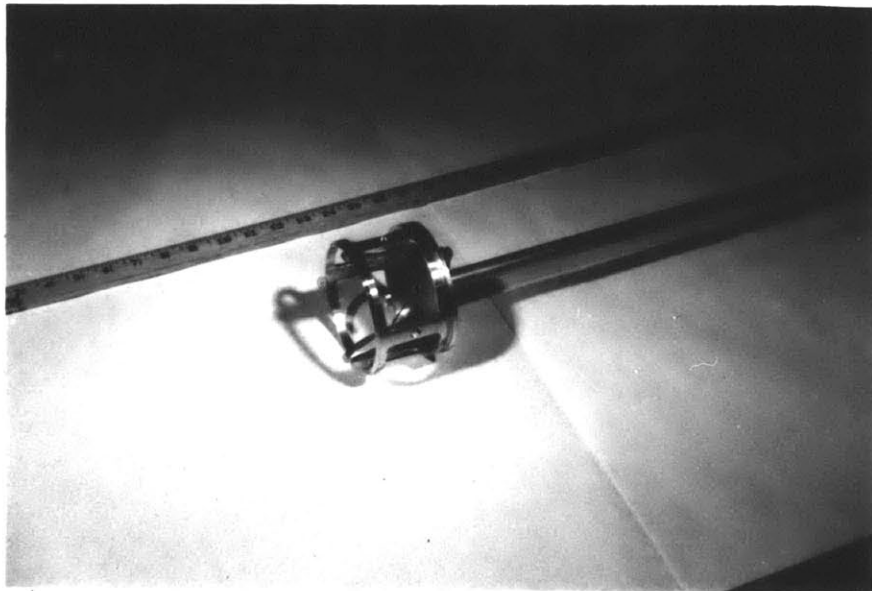


Fig. 4.3(b) Sample holder and tool engaged together, ready for mounting.

gamma scattered radiations in the beam viewed by the detector as would be the case, for instance, with a sample embedded in a graphite block.

Insertions and removals of samples were performed remotely with little radiation hazard to the three or four persons involved in the operation. A complete sample change required approximately 15 minutes with most of the time needed for the removal and repositioning of the heavy steel plug at the port entrance. The port could not be opened during reactor operation because of the prohibitively high radiation levels. Sample changing was thus limited to one per week and was performed a minimum of 18 hours after reactor shutdown. Upon removal from the reactor, the holders and samples had activities of approximately 50 mr/hr at 1 meter mostly due to the copper activity in the aluminum holder. Consequently, sample holders were limited to only one irradiation.

The advantages and disadvantages of this facility as compared to the external set up will be discussed in Chapter V. Other internal-sample systems with rather different characteristics have been described by Motz and Journey [M5], G. E. Thomas et al. [T3], and S. E. Arnell et al. [A1].

4.2.2 The External-Sample Facility

This facility was constructed by T. Harper as a part of the research for his doctoral thesis on capture gamma measurements. In this section will be presented a short description of the set up, the emphasis being on information pertinent to understanding the results presented in the following chapters.

Complete details may be found in reference [H8].

A plan view of this external facility and gamma spectrometer is shown in Fig. 4.4(a). It is a permanent facility which uses the 4TH1 tangential through port formerly used for the internal sample measurements. Included is the companion facility constructed by Y. Hukai for lattice fuel rod irradiation studies [H9].

Neutrons from the reactor core are scattered by a graphite plug and form the 4TH1 neutron beam. The beam diameter is reduced to 3 1/2 inches by a steel collimator. A lead plug placed inside the collimator reduces the gamma flux impinging on the sample and then scattering into the detector without degrading the neutron flux excessively. In this geometry the samples receive a well-thermalized flux (Cd ratio about 80) of approximately 1.8×10^8 n/cm² sec. The flux may be monitored by placing gold foils on the aluminum sample holder.

A front view of the facility indicating the vertical gamma ray path from the sample to the spectrometer is shown in Fig. 4.4(b). The sample to detector distance is about 39 inches and the effective solid angle can be adjusted by placing collimators between the sample and the detector. For the 1/2, 3/4 and 1 inch collimators available the corresponding fractional solid angles are 1.59×10^{-5} , 3.17×10^{-5} and 4.15×10^{-5} respectively. A 1 1/2 inch masonite block was placed in the gamma beam so as to reduce the number of neutrons reaching the Ge(Li) detector.

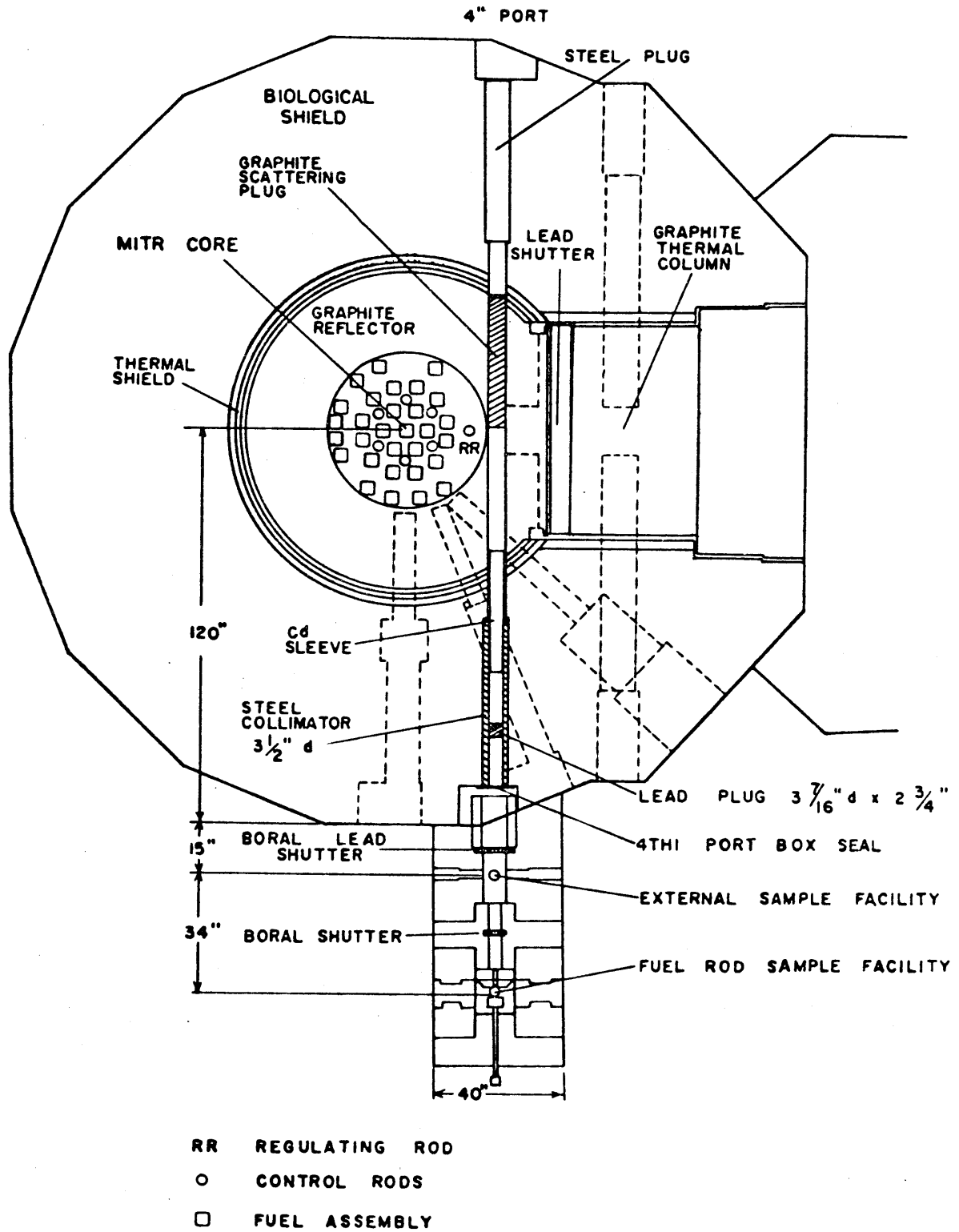


Fig. 4.4(a) Top view of the MIT Reactor and the 4TH irradiation facility (from Ref. [H8])

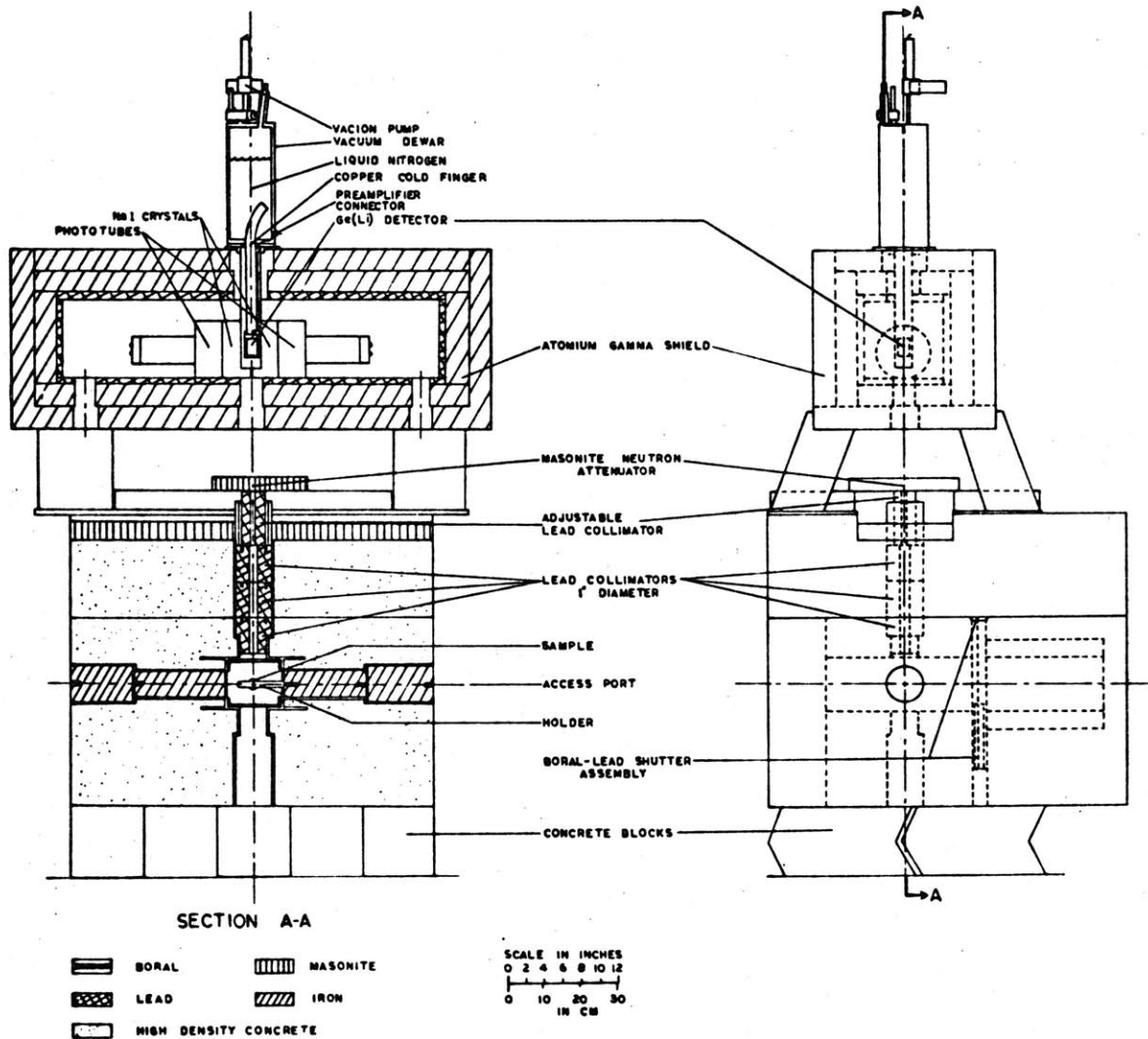


Fig. 4.4(b) Front view of the 4THL irradiation facility and the Ge(Li) capture gamma spectrometer [H8]

4.3 The Gamma-Ray Spectrometer

The spectrometer used in this work consists of a 30 c.c. coaxial Ge(Li) detector (No. 45) placed between two NaI crystals 6 inches in diameter and 3 inches thick. As shown in Fig. 4.4b the crystals are positioned inside a gamma shield of 5 inches of steel plus $3/4$ inch lead. The shield was built by Atomium Corporation and has been described by J. N. Hanson [H2]. A photograph of the liquid-nitrogen 'snout' dewar, with the Ge(Li) detector located in the tip, is shown in Fig. 4.5 together with the $3/8$ and 1 inch collimators.

In view of the three-crystal combination, the spectrometer is capable of operation in (a) the direct or free mode, (b) in the Compton suppression mode at low energies (200 keV to 2500 keV), and (c) as a pair spectrometer at high energies (greater than approximately 1500 keV).

In the free mode all signals above the discrimination level produced in the Ge(Li) detector are amplified, analyzed and recorded. For operation as a Compton or Pair spectrometer, on the other hand, use is also made of the signals from the NaI(Tl) crystals. In the Compton mode, when a pulse from either NaI(Tl) detector is in time coincidence with a pulse from the Ge(Li) detector, the signal from the Ge(Li) detector is not analysed. This arrangement results in a reduction of the Compton background since a large fraction of the Compton events occurring in the germanium are rejected if the scattered gammas are detected by either NaI(Tl). In the

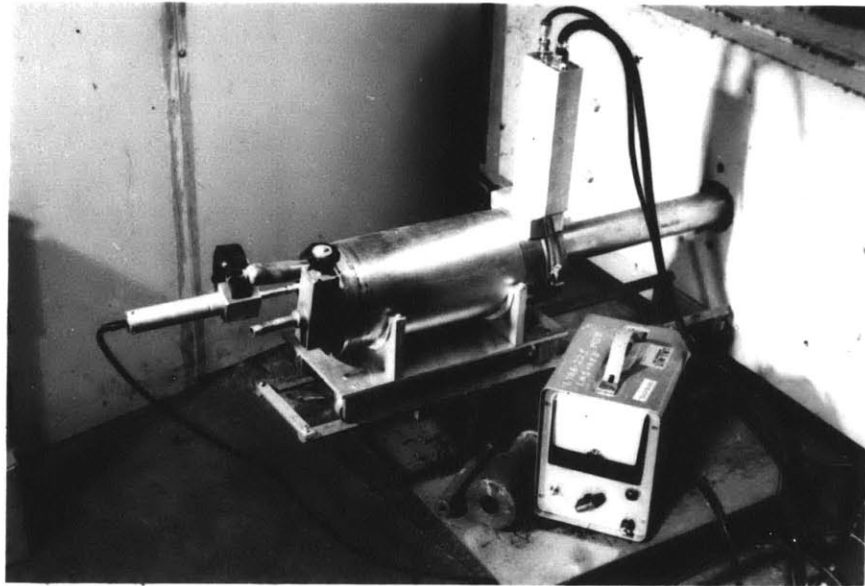


Fig. 4.5 The liquid-nitrogen 'snout' dewar, fully withdrawn. The Ge(Li) crystal is located at the tip of the dewar.

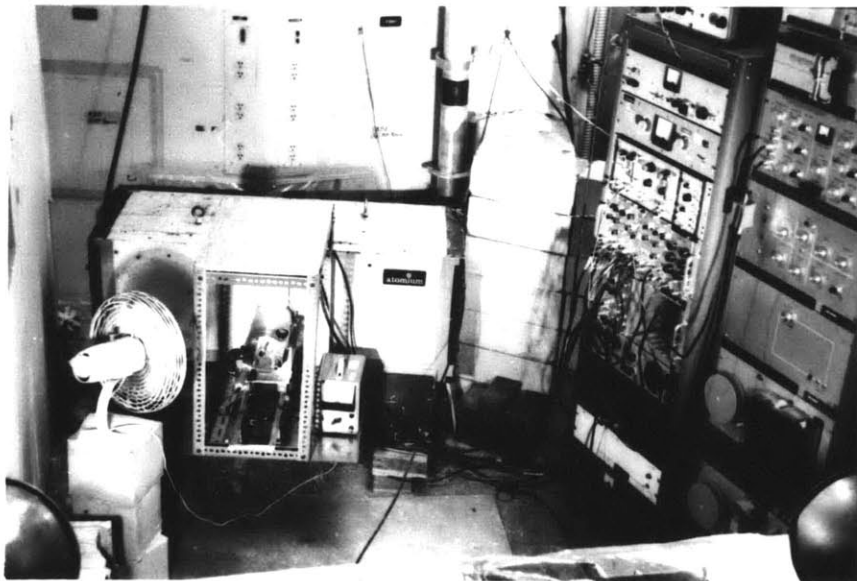


Fig. 4.6 A general view of the three-crystal spectrometer set up for internal-sample measurements.

pair mode of operation a signal from the Ge(Li) detector is recorded only when it is in coincidence with 0.511 MeV signals from each of the NaI(Tl) crystals. This arrangement yields a spectrum in which only double-escape peaks appear, full-energy peaks, single-escape peaks and Compton background being rejected.

The reader is referred to references [O1] and [H8] for complete details of the electronics associated with the spectrometer. It is noteworthy that use of a 4096-channel Nuclear Data Analyser (Model 161F) allowed the high-energy capture spectrum (1.5 to 9 MeV) of most elements to be obtained in a single run while still maintaining 6 or 7 channels per peak. The internal sample data were taken with the electronic system described by Orphan [O1]; a photograph of the spectrometer and the electronics as set up for these measurements is shown in Fig. 4.6. The system described by Harper [H8] was used for the external sample experiments. This includes a number of changes and improvements over that described by Orphan, such as the incorporation of a new pre-amplifier and amplifier set. In both cases the overall energy resolution of the system varied from about 8 keV at low energies to approximately 12 keV at high energy (9 MeV).

The intrinsic gamma detection efficiencies of the system in the Compton suppression mode and as a pair spectrometer are given in the second columns of Tables IV(1) and IV(2) and are shown in Figs. 4.7 and 4.8. The Compton suppression efficiency represents the probability for the total absorption

TABLE IV(1)

COMPTON SUPPRESSION EFFICIENCY AND TRANSMISSION
FACTORS FOR VARIOUS ABSORBERS

Energy <u>E(keV)</u>	Efficiency <u>€</u>	Transmission Factors			
		<u>5/8" LiF</u>	<u>17/16" Poly</u>	<u>1" Lead</u>	<u>1½" Masonite</u>
200	.110	.793	.693	0.0	.515
400	.055	.801	.751	.0025	.591
600	.035	.810	.785	.0375	.632
800	.025	.818	.809	.090	.665
1000	.020	.825	.826	.139	.700
1200	.016	.833	.840	.182	.721
1400	.014	.840	.851	.214	.736
1600	.012	.848	.860	.236	.751
1800	.010	.855	.868	.255	.765
2000	.0088	.861	.875	.268	.775
2200	.0078	.868	.882	.276	.783
2400	.0069	.874	.887	.283	.795
2600	.0059	.880	.891	.289	.807
2800	.0052	.886	.895	.294	.815
3000	.0045	.891	.899	.297	.822
3200	.0038	.896	.902	.298	.828
3400	.0034	.902	.905	.299	.834
3600	.0031	.907	.908	.299	.838
3800	.0025	.911	.910	.298	.844
4000	.0023	.916	.912	.298	.848

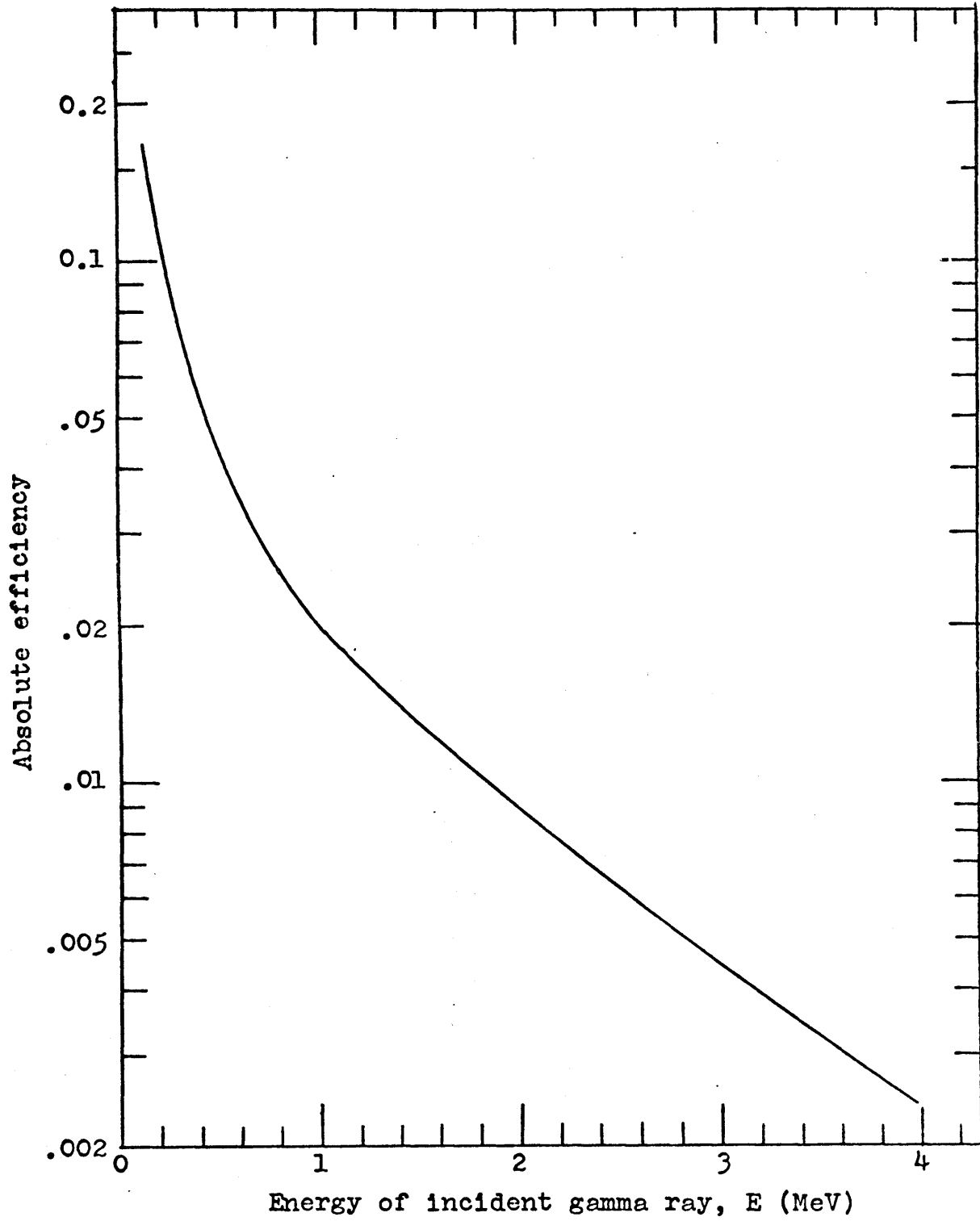


Fig. 4.7 Absolute efficiency of the spectrometer operated in the Compton suppression mode

TABLE IV(2)

PAIR SPECTROMETER EFFICIENCY AND TRANSMISSION
FACTORS FOR VARIOUS ABSORBERS

Energy keV	Efficiency $\times 10^4$	Transmission Factors			
		5/8" LiF	17/16" Poly	1" Lead	1½" Masonite
1000	0.0	.825	.826	.139	.700
1500	0.78	.844	.856	.229	.736
2000	2.5	.861	.875	.268	.775
2500	4.5	.877	.886	.282	.798
3000	6.5	.891	.899	.297	.822
3500	8.4	.904	.906	.297	.834
4000	9.7	.916	.912	.298	.847
4500	10.5	.926	.917	.296	.855
5000	10.4	.934	.922	.293	.862
5500	10.2	.941	.925	.289	.867
6000	9.7	.947	.928	.285	.871
6500	9.0	.951	.931	.281	.875
7000	8.1	.954	.933	.276	.879
7500	7.2	.956	.935	.271	.882
8000	6.4	.956	.937	.267	.885
8500	5.6	.955	.938	.261	.887
9000	4.6	.952	.940	.256	.889
9500	3.5	.948	.941	.250	.890
10000	2.3	.942	.943	.244	.892

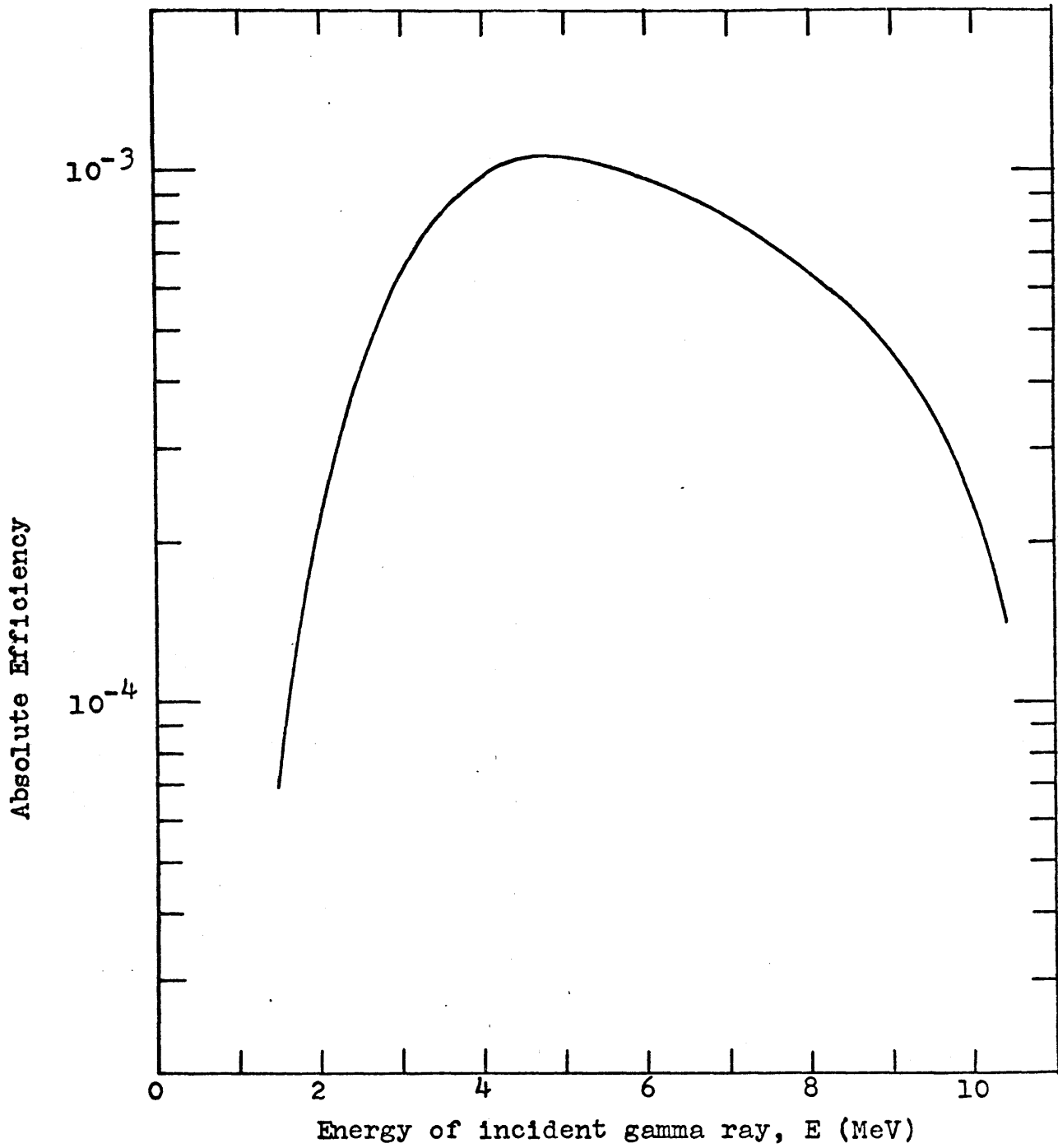


Fig. 4.8 Absolute efficiency of the pair spectrometer

of the gamma ray energy within the sensitive volume of the Ge(Li) detector. For operation as a pair spectrometer, on the other hand, the efficiency includes (a) the probability of having a pair event within the sensitive volume of the Ge(Li) detector, (b) the probability that the electron and positron pair will not escape from the Ge(Li) detector, (c) the probability that the energetic electron and positron will not lose any energy by bremsstrahlung which escapes the Ge(Li) detector, and (d) the probability that both 511-keV photons resulting from the positron annihilation within the Ge(Li) detector will escape from the Ge(Li) detector and be totally absorbed by the NaI(Tl) crystals.

For operation in the free mode, the energy response of a Ge(Li) detector makes it desirable to have two efficiency curves, one for the full-energy peak and one for the double-escape peak. For the 30 cm³ detector employed in this work, the detection efficiency of the full energy peak is most useful in the energy region below 3 MeV. Above this energy the increasing pair production cross section makes it advantageous to use the efficiency of the double-escape peak. The efficiency values for total energy absorption in the free mode are identical to those presented for operation of the spectrometer with Compton suppression. For the double-escape peak, on the other hand, the efficiency may be obtained by multiplying the pair spectrometer values by a constant factor. This factor, which represents the inverse of the probability that both 511-keV gamma rays will escape from the Ge(Li)

detector and be totally absorbed by the NaI(Tl) crystals, is equal to 7.0 for the spectrometer in question; it is independent of energy.

It is usual practice to include in the efficiency curves corrections for the attenuation of the gamma rays by absorbers placed permanently between the sample and the detector. Because of the different absorbers used in the two facilities the efficiency values reported here do not include any such corrections. Instead, transmission factors for the absorbers used in this work are presented in Tables IV(1) and IV(2) for various gamma ray energies.

Analytical sensitivity can be affected both by the design of the experimental set up and by the gamma detection techniques employed. The relative sensitivities of the various experimental arrangements are examined in the following chapter.

Chapter V
RELATIVE SENSITIVITY OF THE VARIOUS
EXPERIMENTAL ARRANGEMENTS

5.1 Introduction

This chapter presents the operating characteristics of the internal and external facilities and the various gamma detection modes. The facilities will be examined and conclusions will be reached as to which of the two arrangements is more sensitive and more suitable for elemental analysis. This will be followed by an evaluation of the relative sensitivity of the various options available for the accumulation of the gamma ray spectra. A stainless steel sample will be used for an example.

5.2 Internal versus External

In this section we will examine the two experimental facilities described in Chapter IV and determine which is more effective for elemental analysis. Consideration will be given to the ratio of the minimum weight concentrations of an element that can be measured in a given sample by using these two alternative geometrical arrangements.

Experimental data have shown that, in both cases, scattered gamma radiation originating from the reactor core is of sufficiently low energy and intensity such that it does not interfere with the high energy capture gamma spectra. Also, in the facilities described, the gamma rays resulting from neutron capture in the structural material surrounding the

sample and the detectors contribute, in most cases, only a small fraction of the background continuum. As a result, the background continuum observed in the two facilities has the same general shape. This can be verified, for instance, by examining the pair spectrometer data shown in Figs. 5.1 and 5.5 for two stainless steel samples.

To a first approximation, therefore, the ratio of the minimum weight requirements in each case is given by equation (3.26). Substituting the maximum values available for the neutron fluxes, the solid angles and the efficiencies, the ratio R reduces to

$$R(\text{int/ext}) = \frac{(m_{\text{int}}/M_{\text{int}})}{(m_{\text{ext}}/M_{\text{ext}})} = (1/33) \sqrt{[M_{\text{ext}}/M_{\text{int}}]}$$

Thus one sees that for a sample of given size the internal sample system can be used to measure elemental concentrations that are approximately 33 times less than those required by the other geometry. The main advantage of the internal facility is thus its sensitivity. Its inherent drawbacks are also worth noting. Some of these are listed below:

- (a) Sample heating by nuclear events might become serious. The ambient temperature is about 350°C but samples such as boron may become several hundred degrees hotter because of the energy released in the (n,α) reaction and the total deposition of the alpha energy within the sample. Some type of cooling is necessary to permit more freedom in the choice of sample materials.

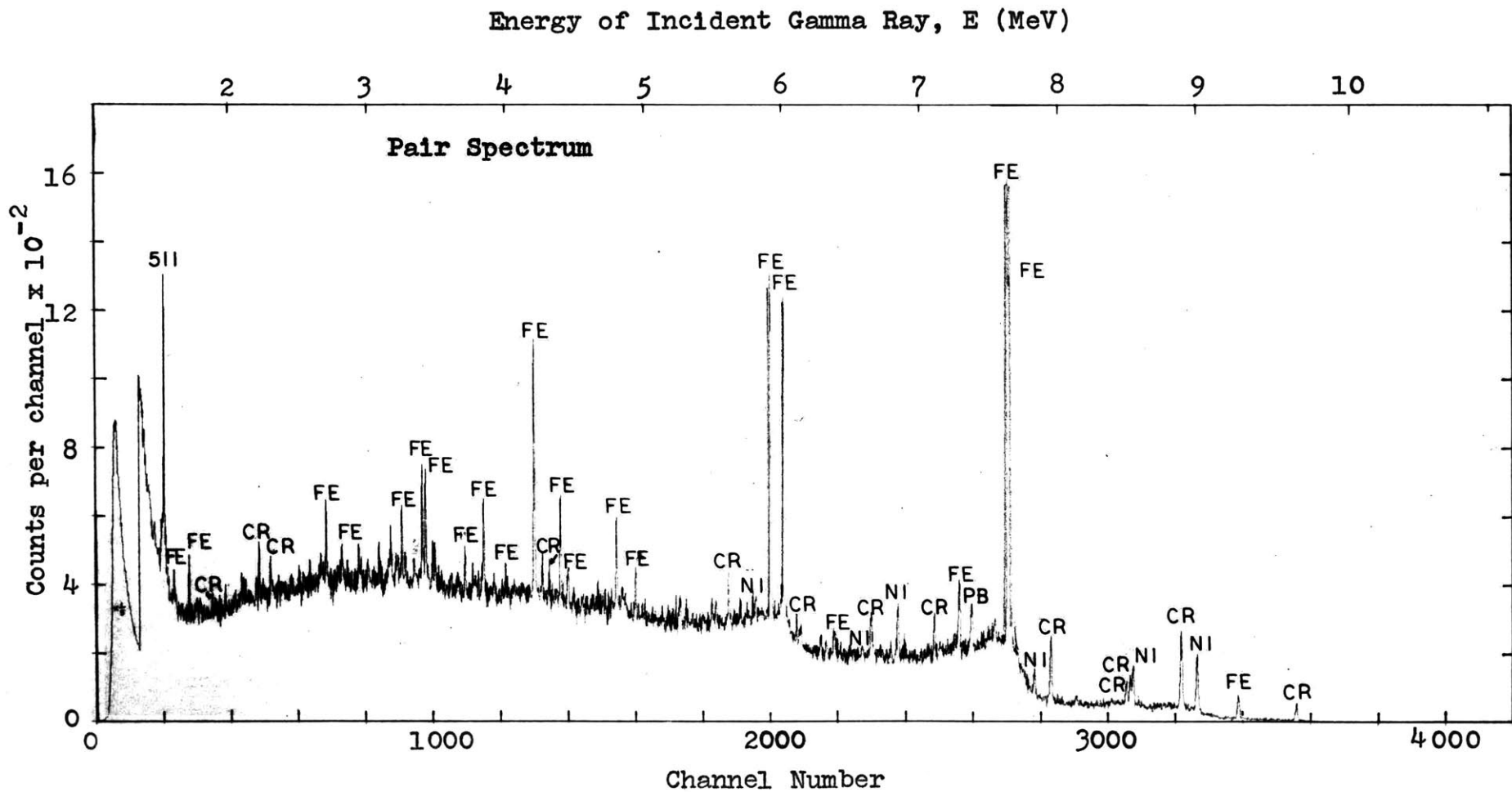


Fig. 5.1 Stainless steel spectrum obtained with the internal-sample facility (3.5 g)

- (b) The neutron spectrum has a low Cd ratio (about 9) and therefore the gamma ray production cross sections available from measurements utilizing well-thermalized neutron beams might not be directly applicable for elemental analysis. Use of a standard eliminates this difficulty.
- (c) Samples become highly radioactive and difficult to handle.

The internal facility used in this work had also the following additional disadvantages:

- (d) Sample-changing procedures were inconvenient and had to be done during reactor shut down. This limited the irradiation to one sample per week.
- (e) Flux monitoring using the normal foil activation procedure was impossible since the foils would have been irradiated from reactor start up to reactor shut down while capture gamma spectra were normally accumulated for only a fraction of this time.

These limitations are not necessarily applicable to all internal-sample systems since such facilities might include provisions for sample and foil handling with the reactor in operation.

Internal-sample facilities, therefore, are not convenient to use for elemental analysis. However, the high count rate available with such arrangements makes them suitable for studies involving reactions with low cross sections or samples which

are available only in small quantities, such as separated isotopes. Their geometrical arrangement also makes them suitable for studying the gamma ray spectra resulting from neutron capture in gases.

The main advantages of the external facility include the convenient sample changing and flux monitoring procedures and the low-level activities of the irradiated samples. Its main drawback is that ^{it} is less sensitive than the alternative internal arrangement.

Experiments have shown that the high sensitivity of the internal facility could not be used advantageously since the detector could not tolerate the very intense gamma ray beam impinging on it. In fact, the maximum counting rate that our present system can accommodate without a significant deterioration in the energy resolution due to multiple pulse effects can be attained in most cases by using the external facility together with properly chosen sample weights and solid angles. Thus for samples available in sizes of roughly 30 grams or greater use of the internal arrangement is not advantageous. As a result the internal-sample experiments were discontinued. In the section that follows consideration will be given to data obtained with the external system; systems of this type have been used in many cases for analytical applications ([G7], [G2], [II], [3] and present work).

5.3 Relative Sensitivity of the Gamma Detection Modes

In the foregoing section the advantages and drawbacks of the internal and external sample facilities were examined and

conclusions were reached as to which is more sensitive and more suitable for elemental analysis. Analytical sensitivity can also be affected by the method employed for the detection of the gamma rays. The degree by which the various detection modes influence the sensitivity is examined in this section. The conclusions will be based on the analysis of gamma ray spectra obtained from the irradiation of a stainless steel sample. The properties of the sample are discussed first. This is followed by a description of the characteristics of the gamma ray spectra and the evaluation of the relative sensitivity of the three detection modes.

5.3.1 The Stainless Steel Sample

The sample, type SS-303, cylindrical in shape, had a diameter of 3.81 cm, a height of 0.904 cm, and a volume of 10.31 cm^3 and weighed 78.825 grams. From the elemental composition of the sample supplied by its manufacturer it was possible to evaluate the fraction of neutrons captured by each of the sample constituents. These results are presented in Table V(1). The accuracy of these data was not evaluated since the error in the reported composition of the sample was not available. The macroscopic capture cross section of the sample, Σ_a , is $(2.641/10.31) = 0.256 \text{ cm}^{-1}$.

The orientation of the sample with respect to the neutron beam and the gamma ray detector is shown in Fig. 5.2. Flux depression in the sample was approximated by the equation

$$\text{flux depression} = 1 - \exp(-\Sigma_a x) .$$

TABLE V(1)

ELEMENTAL COMPOSITION OF THE SS-303 SAMPLE

Element	Weight Percent	Weight in Sample	Density (g/cm ³)	$\sum_a V$ cm ²	Percent Captures
Fe	69.12	54.48	7.87	1.539	58.28
Cr	18.25	14.39	7.19	0.517	19.57
Ni	9.35	7.37	8.90	0.348	13.17
Mn	1.68	1.32	7.43	0.193	7.31
Si	0.50	0.39	2.33	0.0014	0.051
Mo	0.36	0.28	10.2	0.0048	0.182
S	0.275	0.217	2.07	0.0021	0.079
Cu	0.29	0.229	8.96	0.0083	0.316
Co	0.09	0.071	8.8	0.0277	1.05
C	0.056	0.044	1.60	0.000008	0.0003
P	0.034	0.027	1.82	0.0001	0.0038
Total				2.641	

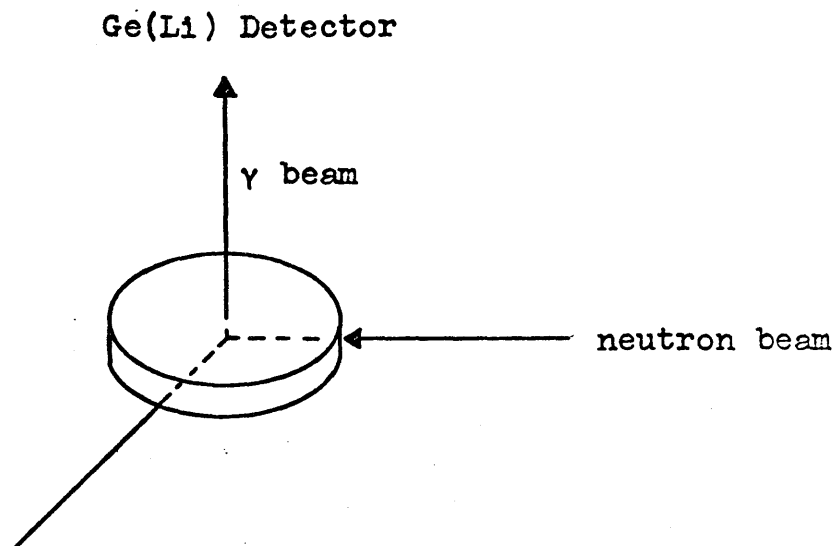


Fig. 5.2 Orientation of the stainless steel sample with respect to the neutron beam and the Ge(Li) detector

Here x is the distance through the sample that will yield the average neutron attenuation. In this approximation it was set equal to half the sample diameter.

Gamma self-shielding was accounted for by assuming that the gamma rays had to travel, on the average, through half the thickness of the sample. At high energies the fraction of gamma rays transmitted by the sample was 0.89. At low energies, in which case the attenuation coefficients vary significantly with energy, the transmission factors were evaluated for a number of energies and are listed in Table V(2). In these calculations the sample was approximated to be pure Fe with a density equal to that of the stainless steel. In this way it was possible to use the mass-attenuation coefficients for Fe available in the literature.

Table V(2)

GAMMA RAY TRANSMISSION FACTORS THROUGH 0.45 cm OF Fe

<u>E</u>	<u>T</u>	<u>E</u>	<u>T</u>	<u>E</u>	<u>T</u>
0.2	0.623	1.6	0.854	3.0	0.884
0.4	0.729	1.8	0.861	3.2	0.886
0.6	0.770	2.0	0.865	3.4	0.888
0.8	0.796	2.2	0.869	3.6	0.890
1.0	0.815	2.4	0.873	3.8	0.892
1.2	0.831	2.6	0.876	4.0	0.893
1.4	0.844	2.8	0.880		

E is the energy of the gamma ray, in MeV

T is the transmission factor

5.3.2 Characteristic Features of the Gamma Ray Spectra

In Figs 5.3, 5.4 and 5.5 are shown the three gamma ray spectra obtained by operating the system in the free mode, the Compton suppression mode, and as a pair spectrometer. Several characteristic features of the spectra are worth noting. We will consider each spectrum separately.

In the free mode spectrum, typical features such as full-energy peaks, single-escape peaks, and double-escape peaks are readily visible. At low energies the spectrum is dominated by full-energy peaks. The double-escape peaks, which carry a double-bar sign for identification, dominate at high energies. Single-escape peaks, with only one bar, are visible only in a few cases. Other features such as various edges

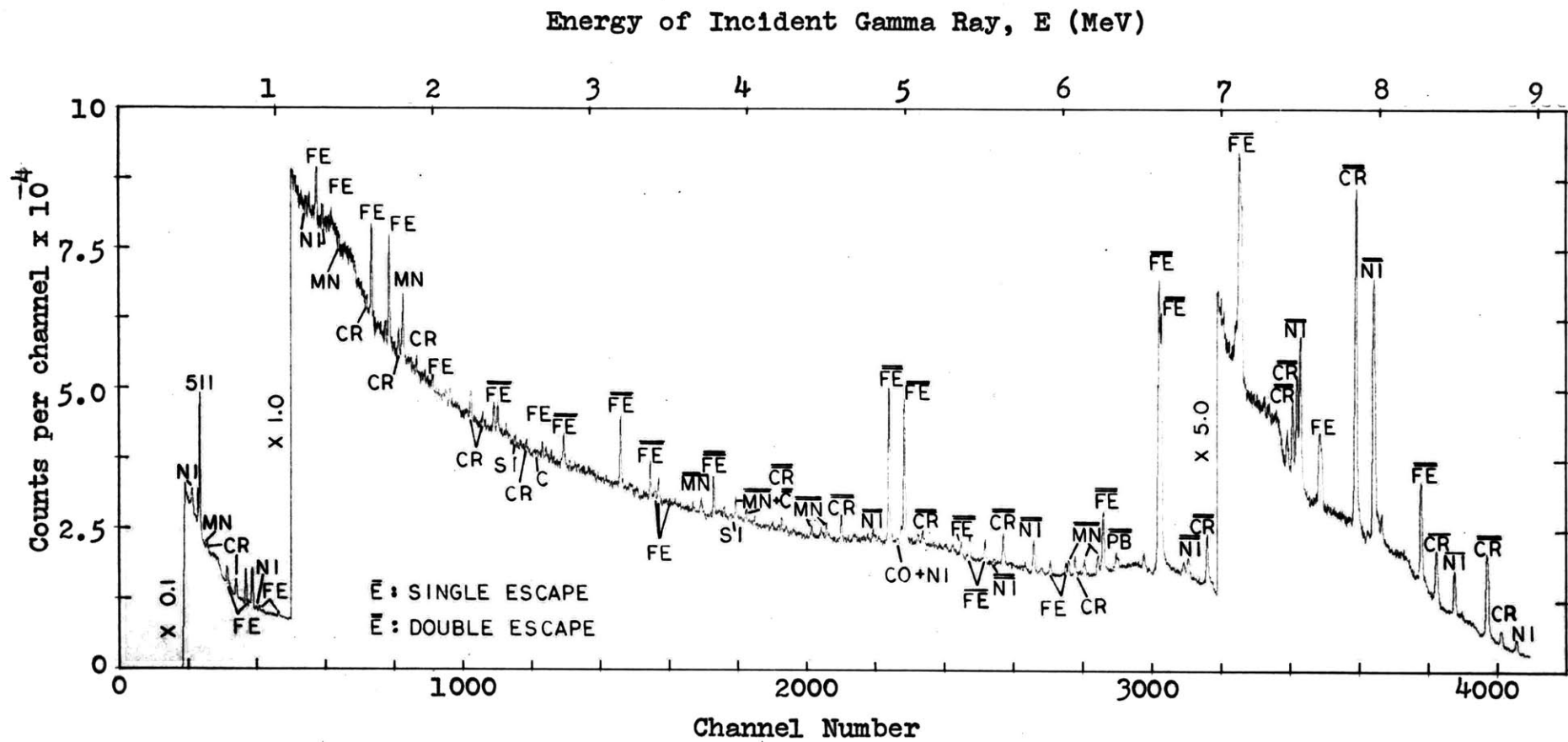


Fig. 5.3 The free-mode stainless steel spectrum
 (flux \times time = 1.32×10^{13} n/cm²)

Energy of Incident Gamma Ray, E (MeV)

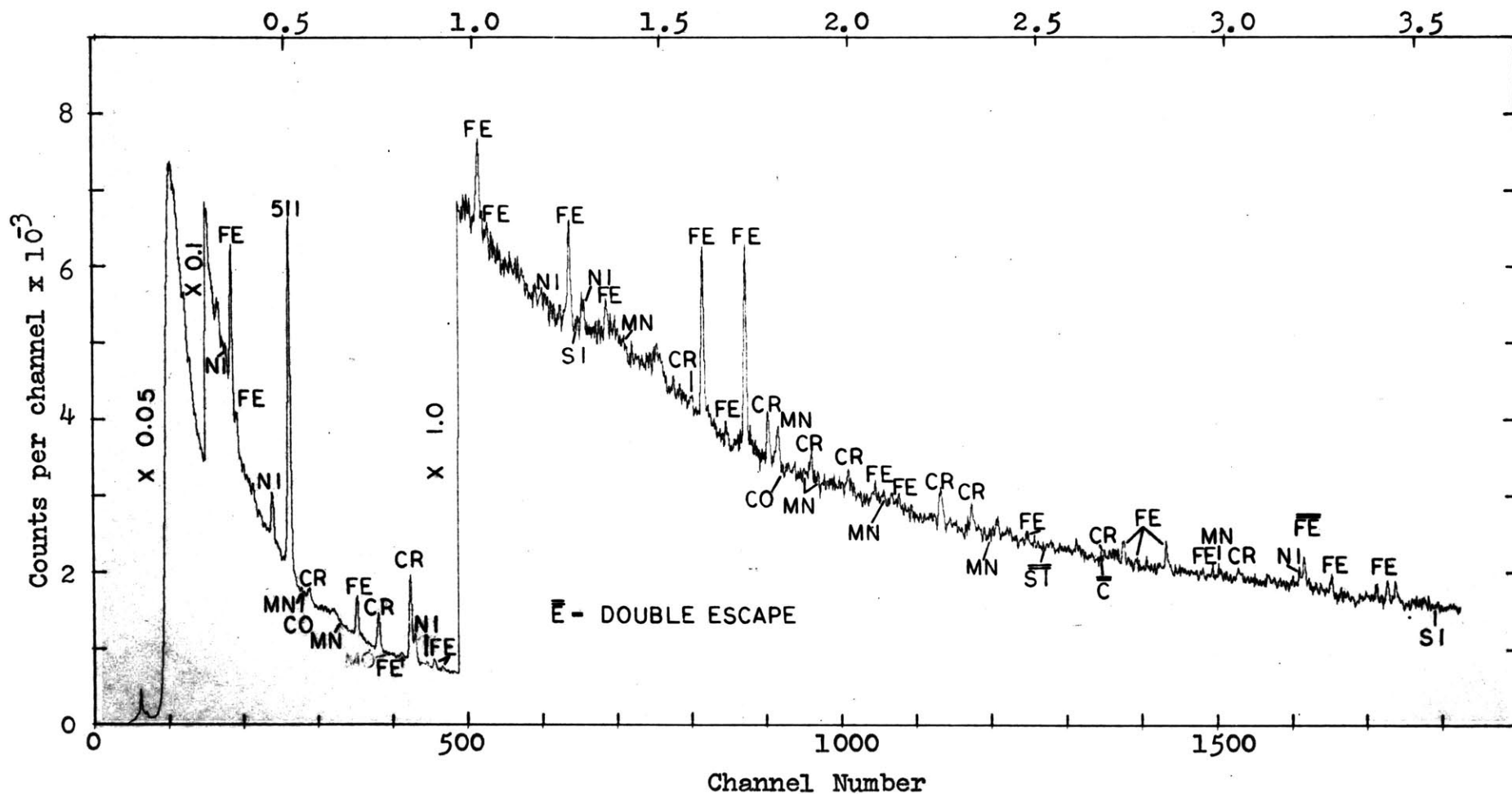


Fig. 5.4 The Compton-suppression stainless steel spectrum (flux×time=1.33×10¹²n/cm²)

Energy of Incident Gamma Ray, E (MeV)

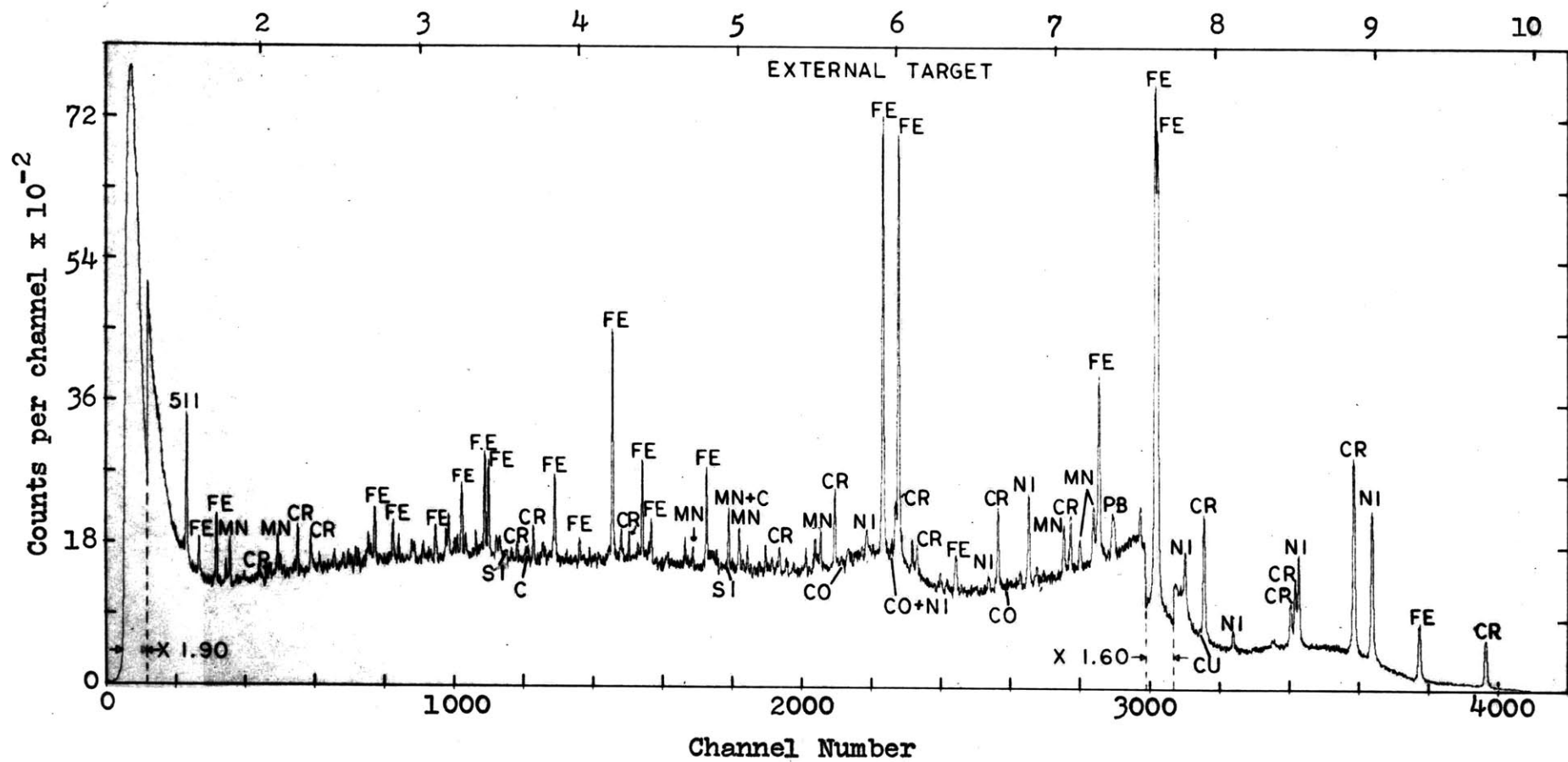


Fig. 5.5 The stainless steel pair spectrum
(flux x time = 1.94×10^{13} n/cm²)

formed by Compton scattering of the incident gamma rays are also visible. The multichannel analyser (MCA) count rate was 2345 counts per second and data were accumulated for 1020 minutes. The high-energy section of the spectrum appears to be particularly interesting for elemental analysis.

In the Compton suppression mode, Fig. 5.4, the spectrum is the result of data accumulated for 120 minutes at an MCA count rate of 1630 counts per second. The lower count rate in this case, as compared to the free mode value, is due to the reduction in the background continuum attained by operating the spectrometer with Compton suppression. Note that the reduction in the background is not uniform over the whole spectrum; it is a function varying slowly with energy and will be discussed in the section that follows. Also worth noting in the spectrum is the presence of double-escape peaks. For double-escape peaks to be present in the Compton suppression mode the annihilation radiation must not deposit any energy in the NaI(Tl) crystals. This occurs whenever the 511-keV photons are absorbed by the structural material existing between the Ge(Li) detector and the NaI(Tl) crystals or whenever these rays escape from the system completely. Therefore, Compton suppression spectra must always be carefully examined for the presence of double-escape peaks. The intensity of such peaks is considerably reduced by the anti-coincidence mantle and as a result identification of their origin is more difficult. One way to identify double escape peaks in Compton suppression spectra is to compare

the energy difference between various peaks to the value of 1022 keV.

The pair spectrum in Fig. 5.5 represents a 1360-minute irradiation at an MCA count rate of 65 counts per second. Comparison of this spectrum with that obtained by operating the system in the free mode shows that the pair spectrometer eliminates the full-energy peak and the single-escape peak and results in a considerable background suppression. The spectrum consists only of double-escape peaks and therefore complexities and ambiguities in its interpretation are considerably reduced. The presence of the 511-keV photopeak is the only exception to this and is discussed below.

The triple-coincidence requirement for detecting annihilation photons is satisfied by chance or by one of a number of real processes that can be postulated. One such process involves the following steps:

(a) Compton scattering of a high-energy gamma ray by one of the NaI(Tl) crystals with the deposition there of 400 to 600 keV of energy which satisfies the requirement for triple coincidence

(b) the absorption of the scattered gamma ray by a pair production event in the structural material surrounding the Ge(Li) detector or within its dead layer

(c) the absorption of one of the positron annihilation rays by the Ge(Li) detector and the absorption of the other annihilation ray by the second NaI(Tl) crystal.

The energies of the double-escape peaks in the pair

spectrometer are increased by 1022 keV so that they correspond to the energy of the incident gamma rays. As a result the 511 annihilation line, which was assigned the value of $511 + 1022 = 1533$ keV was originally identified as an intense Fe background line since it appeared in all measurements with the pair spectrometer [O1]. The origin of this 1533 line was previously pointed out in reference [R2].

5.3.3 Relative Effectiveness of the Detection Modes

At this point the question arises as to which of these gamma detection modes is most efficient for elemental analysis. For low energy measurements one is faced with the problem of choosing between the free mode and Compton suppression. For high energy applications the alternatives include operation of the system in the free mode or as a pair spectrometer. And in the intermediate energy range it is possible to perform an analysis by operating the system in any one of the three modes described.

In evaluating the relative sensitivity of the detection modes, extensive use will be made of equation (3.24) for the minimum measurable weight. The energy-channel conversion factor C required for the application of this equation was assigned the value of 2 keV/channel for all cases; taken in the usual order, the actual spectra had 2.184, 1.977 and 2.189 keV/channel. The peak area correction factor ψ which accounts for the deviation of the spectral data from a true Gaussian distribution was set equal to 1.02. In addition, all spectra were subjected to the same degree of smoothing represented

by the reduction factor $r = 1.34$. The system resolution was assumed to be the same in all cases and was set equal to that obtained for the pair spectrum. The width-energy relation obtained by applying the least-squares fit to 46 peaks in the spectrum is given by

$$\bar{w}(E - 1022) = 9.46 - 0.919E \times 10^{-3} + 0.196E^2 \times 10^{-6} \quad (5.1a)$$

where $\bar{w}(E - 1022)$ is the fwhm (in keV) of the double-escape peak of a gamma ray of energy E (keV). The corresponding fwhm of the full-energy peak is

$$w(E) = 8.726 - 0.518E \times 10^{-3} + 0.196E^2 \times 10^{-6} . \quad (5.1b)$$

In order to afford a realistic comparison it was also necessary to reduce the data in all three runs to the same flux time value. Since the three sets of data were accumulated at different times and there appeared to be differences in the orientation of the sample with respect to the neutron beam, the flux time products were evaluated from the analysis of the spectra. In this procedure the flux time values were adjusted such that the calculated intensities of the various intense gamma rays in the individual spectra agreed well with the intensities reported in reference [R2]. The results obtained for the three cases are:

<u>System</u>	<u>Flux time value</u>
Free Mode	$1.32 \times 10^{13} \text{ n/cm}^2$
Compton suppres.	$1.33 \times 10^{12} \text{ n/cm}^2$
Pair Spectrom.	$1.94 \times 10^{13} \text{ n/cm}^2$

Note that these values include neutron flux depression and corrections for fraction of sample seen. The fractional solid angle associated with these flux time values was 1.59×10^{-5} in all cases. The free mode and Compton suppression data were thus multiplied by 1.47 and 14.6, respectively, in order to normalize them to those obtained with the pair spectrometer.

The advantages of using the spectrometer in the Compton suppression mode rather than in the free mode are evident. Since the background continuum can be suppressed without affecting the detection efficiency, it is clear from equation (3.24) that a reduction in the continuum by a factor q will improve the sensitivity of the system for elemental analysis by approximately \sqrt{q} . The actual improvement that can be attained with our system is shown in Table V(3) and Fig. 5.6(a). It is given in terms of the ratio of the minimum measurable weights required by the Compton suppression and free mode systems when the analysis is based on the same gamma ray in both cases. From equation (3.24), with $r = 1.34$ and $C = 2$ keV/channel, this ratio is

$$R(\text{CS}/\text{FM}) = \frac{m_{\text{CS}}}{m_{\text{FM}}} = \frac{1 + \sqrt{1 + 0.82B_{\text{CS}}(E)}}{1 + \sqrt{1 + 0.82B_{\text{FM}}(E)}} \quad (5.2)$$

The background values, in counts/keV, are given in Table V(3) and were obtained from the spectra in Figs. 5.3 and 5.4 by applying linear averaging over 100-keV intervals in the normalized data. (Note that in this table $0.123E 04 = 0.123 \times 10^4$).

TABLE V(3)

BACKGROUND DATA AND MINIMUM WEIGHT RATIOS FOR THE FREE MODE
AND COMPTON SUPPRESSION SYSTEMS

Energy KeV	$B_{FM}(E)$ counts/keV	$B_{CS}(E)$ counts/keV	$\frac{B_{FM}}{B_{CS}}$	R(CS/FM)
150.0	0.0	0.231E 06	0.0	154.46 *
250.0	0.0	0.703E 06	0.0	269.01 *
350.0	0.0	0.326E 06	0.0	183.24 *
450.0	0.156E 06	0.186E 06	0.84	1.09
550.0	0.150E 06	0.126E 06	1.20	0.92
650.0	0.116E 06	0.963E 05	1.20	0.91
750.0	0.863E 05	0.731E 05	1.18	0.92
850.0	0.722E 05	0.587E 05	1.23	0.90
950.0	0.635E 05	0.496E 05	1.28	0.88
1050.0	0.599E 05	0.457E 05	1.31	0.87
1150.0	0.561E 05	0.410E 05	1.37	0.86
1250.0	0.537E 05	0.378E 05	1.42	0.84
1350.0	0.525E 05	0.368E 05	1.43	0.84
1450.0	0.477E 05	0.348E 05	1.37	0.85
1550.0	0.447E 05	0.311E 05	1.44	0.83
1650.0	0.400E 05	0.281E 05	1.42	0.84
1750.0	0.378E 05	0.257E 05	1.47	0.83
1850.0	0.361E 05	0.243E 05	1.48	0.82
1950.0	0.332E 05	0.224E 05	1.48	0.82
2050.0	0.320E 05	0.214E 05	1.49	0.82
2150.0	0.310E 05	0.202E 05	1.54	0.81
2250.0	0.296E 05	0.193E 05	1.53	0.81
2350.0	0.279E 05	0.180E 05	1.55	0.81
2450.0	0.279E 05	0.176E 05	1.58	0.80
2550.0	0.263E 05	0.168E 05	1.57	0.80
2650.0	0.255E 05	0.162E 05	1.57	0.80
2750.0	0.247E 05	0.151E 05	1.63	0.78
2850.0	0.235E 05	0.147E 05	1.60	0.79
2950.0	0.233E 05	0.141E 05	1.65	0.78
3050.0	0.225E 05	0.140E 05	1.61	0.79
3150.0	0.219E 05	0.133E 05	1.65	0.78
3250.0	0.213E 05	0.126E 05	1.69	0.77
3350.0	0.198E 05	0.119E 05	1.67	0.78
3450.0	0.200E 05	0.118E 05	1.70	0.77
3550.0	0.195E 05	0.111E 05	1.76	0.76
3650.0	0.189E 05	0.108E 05	1.75	0.76
3750.0	0.183E 05	0.106E 05	1.73	0.76
3850.0	0.178E 05	0.105E 05	1.69	0.77
3950.0	0.181E 05	0.100E 05	1.81	0.75

* Disregard

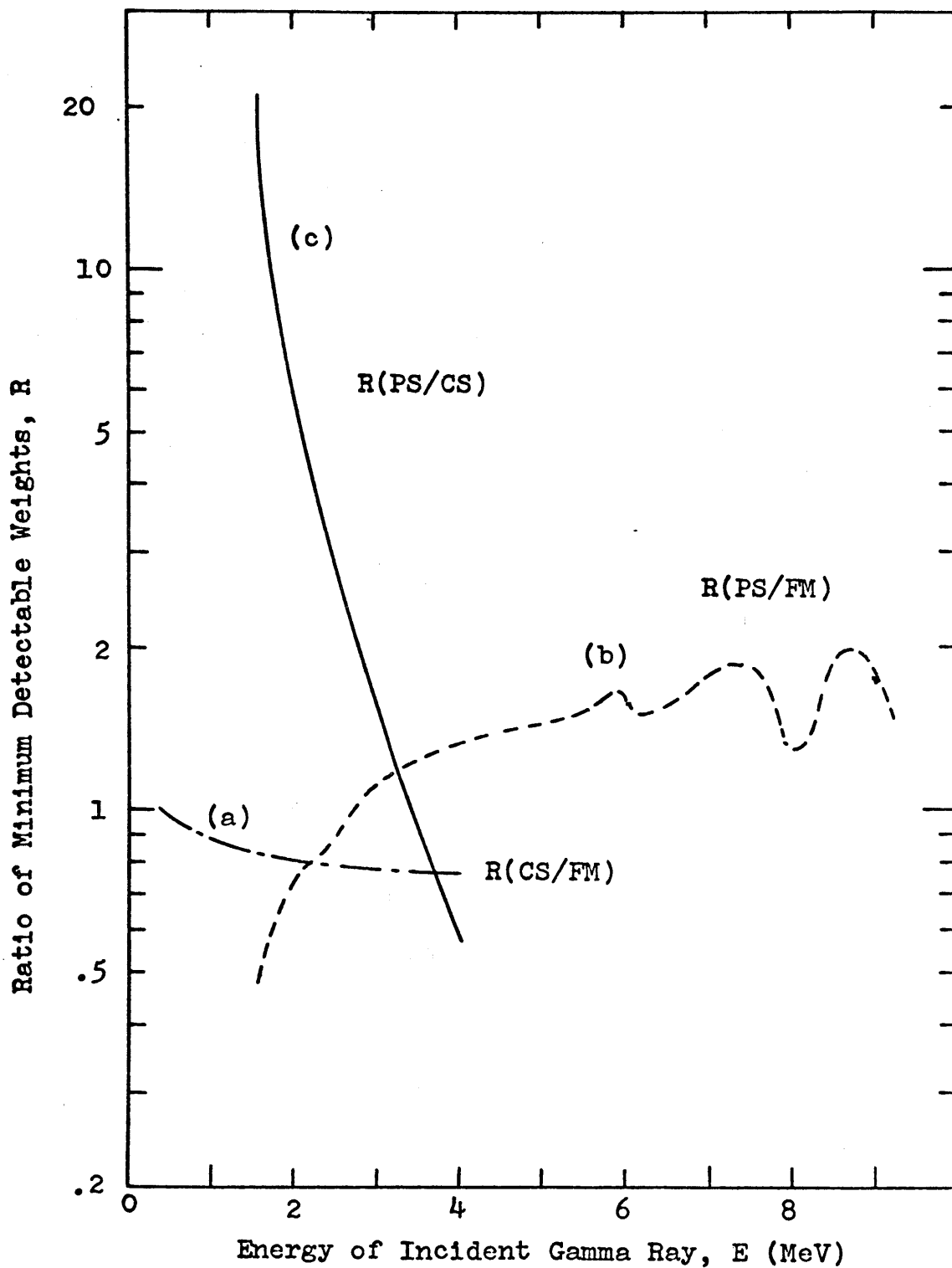


Fig. 5.6 Ratio of the minimum detectable weights by the different gamma-detection modes

On the average, use of the Compton suppression mode can increase the sensitivity of the system by a factor of approximately $(1/0.8) = 1.25$. With a system involving more sophisticated electronics and larger NaI crystals the increase in sensitivity can be improved to about 2.

For elemental analysis based on high energy gamma rays it is not immediately apparent whether a pair spectrometer would have a higher sensitivity than one operated in the free mode. The pair spectrometer reduces both the background continuum and the detection efficiency. As a result, the advantages of background suppression can become off set by the reduction in efficiency. In our system the average reduction factor in the continuum at high energies is approximately 36 and is achieved at the cost of lowering the efficiency by a factor of about 7. Therefore, in this case, the pair spectrometer is, on the average, a factor of $(7/\sqrt{36}) = 1.16$ less sensitive than the free mode system. The actual loss of sensitivity for different energies has been evaluated using the spectra in Figures 5.3 and 5.5. The results are presented in Table V(4) and Fig. 5.6(b) in terms of the ratio of the minimum detectable weights required for analysis by the pair spectrometer and the system operated in the free mode. From equation (3.24) this ratio is

$$R(\text{PS}/\text{FM}) = \frac{m_{\text{PS}}}{m_{\text{FM}}} = \frac{\epsilon_{\text{FM}} [1 + \sqrt{1 + 0.82B_{\text{PS}}(E - 1022)}]}{\epsilon_{\text{PS}} [1 + \sqrt{1 + 0.82B_{\text{FM}}(E - 1022)}]} \quad (5.3)$$

The ratio of the efficiencies for the detection of double-

TABLE V(4)

BACKGROUND DATA AND MINIMUM WEIGHT RATIOS FOR THE FREE MODE
SYSTEM AND THE PAIR SPECTROMETER

Energy keV	$B_{FM}(E-1022)$ counts/keV	$B_{PS}(E-1022)$ counts/keV	$\frac{B_{FM}}{B_{PS}}$	R(PS/FM)
1600.0	0.144E 06	0.678E 03	211.88	0.51
1800.0	0.827E 05	0.587E 03	140.97	0.63
2000.0	0.628E 05	0.608E 03	103.41	0.73
2200.0	0.554E 05	0.636E 03	87.18	0.79
2400.0	0.506E 05	0.661E 03	76.50	0.84
2600.0	0.433E 05	0.685E 03	63.20	0.93
2800.0	0.370E 05	0.715E 03	51.75	1.02
3000.0	0.334E 05	0.727E 03	46.01	1.08
3200.0	0.307E 05	0.748E 03	40.98	1.15
3400.0	0.280E 05	0.764E 03	36.70	1.21
3600.0	0.261E 05	0.736E 03	35.48	1.23
3800.0	0.242E 05	0.722E 03	33.50	1.27
4000.0	0.231E 05	0.704E 03	32.88	1.28
4200.0	0.216E 05	0.727E 03	29.70	1.35
4400.0	0.202E 05	0.732E 03	27.67	1.39
4600.0	0.193E 05	0.689E 03	27.96	1.39
4800.0	0.181E 05	0.694E 03	26.10	1.44
5000.0	0.177E 05	0.675E 03	26.26	1.43
5200.0	0.164E 05	0.654E 03	25.04	1.47
5400.0	0.160E 05	0.666E 03	24.02	1.50
5600.0	0.155E 05	0.708E 03	21.91	1.57
5800.0	0.152E 05	0.748E 03	20.36	1.62
6000.0	0.151E 05	0.792E 03	19.10	1.67
6200.0	0.146E 05	0.612E 03	23.77	1.51
6400.0	0.135E 05	0.561E 03	24.06	1.50
6600.0	0.126E 05	0.559E 03	22.60	1.55
6800.0	0.119E 05	0.596E 03	19.89	1.65
7000.0	0.114E 05	0.629E 03	18.09	1.73
7200.0	0.115E 05	0.746E 03	15.28	1.86
7400.0	0.125E 05	0.788E 03	15.91	1.83
7600.0	0.123E 05	0.771E 03	16.00	1.83
7800.0	0.117E 05	0.505E 03	23.10	1.54
8000.0	0.895E 04	0.271E 03	33.03	1.32
8200.0	0.745E 04	0.228E 03	32.66	1.33
8400.0	0.544E 04	0.271E 03	20.05	1.68
8600.0	0.408E 04	0.285E 03	14.30	1.98
8800.0	0.363E 04	0.236E 03	15.39	1.92
9000.0	0.314E 04	0.175E 03	17.95	1.81
9200.0	0.254E 04	0.881E 02	28.88	1.49

escape peaks is approximately equal to 7, as noted above, and is independent of energy. The background values given in the table are the means obtained by applying linear averaging over 200-keV intervals in the normalized data.

Note that the energy symbol in this equation represents the energy of the incident gamma ray. The background data were evaluated at $(E - 1022)$ keV since the interest here is in double-escape peaks. The humps appearing at the high energy end in Fig. 5.6(b) are a result of the humps present in the background data underneath the intense peaks. The pair spectrometer is more efficient than the free mode at gamma energies less than 3 MeV; it is less efficient above this energy.

Adjustement in the electronics to impose more strict conditions for triple coincidence will not have a significant influence on the results. This is because further suppression of the background continuum is normally accompanied by a reduction in the intrinsic efficiency of the system.

In the energy interval between approximately 1.5 MeV and 3 MeV an analysis can be based on either the full-energy peak or on the double-escape peak. The ratio of the minimum weight requirements with the system operated as a pair spectrometer or in the Compton suppression mode was evaluated for different energies by the equation

$$R(\text{PS/CS}) = \frac{m_{\text{PS}}}{m_{\text{CS}}} = \frac{\epsilon_{\text{CS}} \bar{w}(E-1022) [1 + \sqrt{1 + 0.82B_{\text{PS}}(E-1022)}]}{\epsilon_{\text{PS}} \bar{w}(E) [1 + \sqrt{1 + 0.82B_{\text{CS}}(E)}]} \quad (5.4)$$

Values for this ratio are given in the last column of Table V(5), and are shown in Fig. 5.6(c). The background values listed were obtained, where necessary, by direct interpolation applied to the data appearing in Tables V(3) and V(4). The ratios of fwhm and the efficiencies for this energy interval are also given for comparison. Note that corrections for gamma self-shielding and gamma attenuation by the masonite absorber in the beam cancel out since gamma rays of the same energy are used in both cases. At 1.6 MeV the Compton suppression system is more sensitive by a factor of 17. At higher energies this factor drops off very fast and is equal to unity at about 3.5 MeV.

As a simple application of the above results consider the measurement of a given element in the stainless steel sample. Let us assume that a characteristic gamma ray of this element has an energy of 3 MeV and that the analysis is based on the full-energy peak of this gamma ray in the free-mode spectrum. Assume further that such a measurement yields the value of m grams as the minimum measurable weight. If the analysis were based on the double-escape peak of this gamma ray, or if the background suppression techniques were employed, the minimum weight requirements would have been as follows:

<u>Mode</u>	<u>Peak Type</u>	<u>Minimum Weight</u>
Free	Full-energy	m
Compton Sup.	Full-energy	$0.79 m$
Pair Spectrom	Double-esc.	$1.54 \times 0.79m = 1.22m$
Free	Double-esc.	$1.22m/1.08 = 1.13m$

TABLE V(5)

BACKGROUND DATA, EFFICIENCY, WIDTH AND MINIMUM WEIGHT RATIOS
FOR THE COMPTON SUPPRESSION SYSTEM AND THE PAIR SPECTROMETER

Energy keV	$B_{PS}(E-1022)$ counts/keV	$B_{CS}(E)$ counts/keV	$\epsilon_{CS}(E)$ $\epsilon_{PS}(E)$	$\bar{w}(E-1022)$ $\bar{w}(E)$	$R(PS/CS)$
1600	678	29600	107.	1.01	17.0
1800	587	25000	55.6	1.00	8.85
2000	608	21900	35.2	0.99	6.04
2200	636	19750	21.7	0.98	3.97
2400	661	17800	16.8	0.97	3.27
2600	685	16500	12.04	0.97	2.45
2800	715	14900	8.97	0.96	1.94
3000	727	14050	6.92	0.95	1.54
3200	748	12950	5.35	0.94	1.25
3400	764	11850	4.30	0.93	1.05
3600	736	10950	3.52	0.93	0.87
3800	722	10550	2.72	0.92	0.67
4000	704	9850	2.37	0.91	0.59

This example indicates that at 3 MeV, only a modest change in the sensitivity of approximately ± 20 percent can be obtained by the various methods of measurement. At other energies the changes are more significant, the pair spectrometer option being in all cases the least sensitive. The extreme simplicity of the pair spectra, however, should not be overlooked, and this fact alone will have a significant influence on the choice of detection mode.

The usefulness of the results presented above can be extended further by noting that the ratios of the minimum weight requirement are approximately equivalent to the ratios of the percent errors in the peak areas obtained by the various detection modes. Thus if a full-energy peak in a free-mode spectrum at 3 MeV has an error $[\sigma(A_G)/A_G]$, the same peak in the corresponding Compton suppression spectrum will have an error of $0.79 \times [\sigma(A_G)/A_G]$. Similarly, the errors in the double escape peaks will be $1.22 \times [\sigma(A_G)/A_G]$ in the pair spectrum and $1.13 \times [\sigma(A_G)/A_G]$ in the free mode.

The results presented above are based on the particular system and detection crystal used in this work. However, due to the square root signs in the R equations, the results are expected to hold approximately for most cases of practical interest. Further insight into the criteria for evaluating background suppression techniques can be obtained from an article by R. B. Galloway [G8].

Chapter VI

A TEST ON THE EQUATION FOR THE MINIMUM WEIGHT

6.1 Introduction

In the previous chapter extensive use was made of the minimum weight equation (3.24) for evaluating the relative sensitivity of the various experimental arrangements. The analysis that follows constitutes a test on the validity of this equation and also of the equations developed for the peak area limiting levels. The data associated with the pair spectrum in Fig. 5.5 will be used. A complete analysis of the spectrum is presented and special emphasis is given to the peaks that resulted from neutron capture in manganese.

6.2 The Method

An experimental verification of the minimum measurable weight of an element in a given sample can be obtained by irradiating samples which include different known concentrations of the element in question and then extrapolating the results to obtain the required information. In such a case the determination of the element in the sample will be based on the capture gamma ray of the element that is found to be most suitable for the purpose. This procedure, if carried out properly, will yield good results. However, it is tedious and limits the choice of target materials.

In a simpler approach to the problem, irradiation of the sample is carried out only once and use is made of a large number of capture gamma rays emitted by one of the

sample constituents. The corresponding peak areas that are expected to appear in the spectrum are computed for the given concentration of the element in the sample. If this concentration is suitable a number of these peaks will be clearly visible in the spectrum while others will be lost in the statistical fluctuations of the background continuum. The presence or absence of a peak must be in accordance with the equations for the peak area limiting levels and therefore the spectral data can be examined to verify the validity of these equations and, consequently, the equation for the minimum weight.

In this work it was decided to test the equations using the second approach. The pair spectrum shown in Fig. 5.5 was used for this purpose. The manganese content in the sample seemed to be particularly suitable for this application since intense capture gamma rays of this element yielded peak areas both above and below the limiting levels.

In order to carry out the test described above it is necessary first to obtain a complete analysis of the spectrum in question. This analysis is presented in the section that follows.

6.3 Analysis of the Pair Spectrum

Part of the GAMANL output for the analysis of the stainless steel pair spectrum is shown in Table VI(1). The table includes (a) results of the least-squares fit for the resolution of the system, (b) comparison between the original fwhm and the fitted data, and (c) the analysis of the spectrum.

TABLE VI(1) - PART OF GAMANL OUTPUT - SS 303 PAIR SPECTRUM

RESULTS OF LEAST-SQUARES FIT

NUMBER OF PEAKS USED = 46

STATISTICAL FLUCTUATIONS REDUCED BY 1.34

SUM(WEIGHT*FWHM*ENERGY(10MEV)**0) = 0.29738E 04

SUM(WEIGHT*FWHM*ENERGY(10MEV)**1) = 0.15442E 04

SUM(WEIGHT*FWHM*ENERGY(10MEV)**2) = 0.88415E 03

COEFFICIENTS OF ORIGINAL MATRIX

0.28887E 03	0.14336E 03	0.79404E 02
0.14336E 03	0.79404E 02	0.46758E 02
0.79404E 02	0.46758E 02	0.28673E 02

VALUE OF DETERMINANT = 0.71581E 03

COEFFICIENTS OF INVERTED MATRIX

0.12635E 00	-0.55594E 00	0.55670E 00
-0.55594E 00	0.27633E 01	-0.29666E 01
0.55670E 00	-0.29666E 01	0.33309E 01

EQUATION OF LEAST-SQUARES FIT

FWHM = 0.94644E 01 * ENERGY(10MEV)**0

-0.91934E 01 * ENERGY(10MEV)**1

+0.19612E 02 * ENERGY(10MEV)**2

SQRT(SUM WEIGHTED RESIDUALS/DEGREES OF FREEDOM) = 0.1291E 01

TABLE VI(1) (CONTINUED)

COMPARISON BETWEEN ORIGINAL AND FITTED DATA								
NO	PEAK ENERGY	PEAK WIDTH	S.D. (WIDTH)	WEIGHT	WIDTH FIT	WIDTH DIFF	RESIDUALS	CONF INTRVL
1	1532.03	8.53247	0.23364	18.31941	8.51622	0.01625	0.00484	0.21413
2	1612.84	8.02890	0.70184	2.03012	8.49177	-0.46288	0.43497	0.20509
3	1724.84	8.75797	0.33815	8.84960	8.46212	0.29585	0.77457	0.19328
4	1809.88	7.90863	0.66745	2.24471	8.44789	-0.53426	0.64072	0.18488
5	2112.71	7.69750	0.66398	2.26822	8.39746	-0.69996	1.11130	0.15901
6	2128.32	9.37961	1.80378	0.30735	8.39609	0.99351	0.29730	0.15785
7	2239.09	7.87282	0.51879	3.71553	8.38913	-0.51632	0.99049	0.15011
8	2320.63	7.94230	1.01302	0.97446	8.38709	-0.44479	0.19278	0.14497
9	2525.88	9.62548	2.05128	0.23766	8.39349	1.23200	0.36072	0.13406
10	2602.87	8.34800	1.46125	0.46933	8.40015	-0.05215	0.00127	0.13069
11	2721.74	8.46719	0.71675	1.94654	8.41500	0.05220	0.00530	0.12622
12	2834.85	8.51316	0.48621	1.27330	8.43427	0.07889	0.00792	0.12273
13	3025.43	10.34333	3.46142	0.08346	8.47810	1.86522	0.29037	0.11834
14	3225.27	9.66450	2.13286	0.21982	8.53937	1.12513	0.27828	0.11538
15	3267.39	9.06371	0.43334	5.32519	8.55428	0.50943	1.38200	0.11493
16	3292.20	7.16459	1.27623	0.61396	8.56319	-1.39879	1.20129	0.11468
17	3357.57	6.56808	1.03908	0.92619	8.58854	-2.02047	3.78097	0.11411
18	3413.15	9.08135	0.39192	6.31040	8.61125	0.47010	1.43876	0.11370
19	3436.58	8.54991	0.41964	5.67861	8.62118	-0.07168	0.07917	0.11355
20	3616.63	10.88853	1.04490	0.91591	8.70472	2.18381	4.36803	0.11261
21	3720.26	9.91946	1.05205	0.90350	8.75856	1.16090	1.21764	0.11221
22	4010.66	8.57998	1.19021	0.70591	8.93188	-0.35191	0.08742	0.11111
23	4218.79	9.27591	0.16158	38.30257	9.07647	0.19944	1.52361	0.11001
24	4323.01	7.90275	0.93453	1.14503	9.15524	-1.25249	1.79624	0.10927
25	4406.52	8.57517	0.31784	9.89907	9.22144	-0.64627	4.13455	0.10858
26	4462.51	10.57905	1.46093	0.46853	9.26736	1.31169	0.80613	0.10806
27	4724.96	9.02897	1.79379	0.31078	9.49897	-0.47001	0.06965	0.10504
28	4809.98	9.27858	0.43977	5.17075	9.57980	-0.30121	0.46914	0.10386
29	4949.86	8.50889	0.58877	2.88472	9.71895	-1.21006	4.27393	0.10174
30	5015.30	9.23101	0.74923	1.78145	9.78668	-0.55567	0.55006	0.10069
31	5068.62	7.35438	1.01034	0.97964	9.84311	-2.48824	6.06528	0.09981
32	5180.39	7.65420	1.04592	0.91411	9.96532	-2.31082	4.88125	0.09793
33	5436.26	9.84998	1.37555	0.52850	10.26254	-0.41257	0.08996	0.09378
34	5493.52	9.84944	1.08211	0.85401	10.33265	-0.48321	0.19940	0.09296
35	5529.35	10.01781	1.01815	0.96467	10.37717	-0.35935	0.12457	0.09248
36	5619.14	9.63564	0.52603	3.61395	10.49094	-0.85530	2.64376	0.09143
37	5920.49	11.12906	0.11905	70.55710	10.89590	0.73316	3.83571	0.09023
38	6018.88	11.07828	0.13272	56.77052	11.03583	0.04245	0.10232	0.09095
39	6280.94	9.60784	1.94518	0.26429	11.42707	-1.81922	0.87469	0.09645
40	6444.48	10.50422	0.51447	3.77809	12.01440	-1.51019	8.61653	0.11429
41	6837.32	12.28093	0.37376	7.15951	12.34700	-0.06607	0.03124	0.12858
42	7099.12	10.74368	0.97622	1.04932	12.82188	-2.07821	4.53195	0.15290
43	7539.35	12.20183	0.99155	1.01711	13.68102	-1.47919	2.22544	0.20492
44	7821.15	13.70487	0.76691	1.70024	14.27087	-0.56600	0.54467	0.24470
45	7940.69	14.91661	0.27197	13.51915	14.53050	0.38611	2.01540	0.26296
46	8121.52	13.08751	1.17595	0.72315	14.93390	-1.84639	2.46532	0.29211

TABLE VI(1) (CONTINUED)

NO.	ENERGY KEV	PK CNTR CHAN NO	HEIGHT COUNTS	H TO BG RATIO	PEAK ANALYSIS		INT(B)	ERROR(B) PERCENT	W(A) KEV	W(B) KEV	BASE CHAN	TYPF
					AREA(A) COUNTS	AREA(R) COUNTS						
1	1513.0	224.9	137.9	0.079	297.2	597.4	1.33	28.64	4.89	8.52	5.	S
2	1532.0	233.4	1824.4	1.106	8211.2	7791.2	16.24	3.72	4.53	8.52	19.	*S
3	1612.8	269.4	477.3	0.337	1817.8	2032.6	3.70	8.50	8.03	8.49	9.	*S
4	1711.2	313.5	118.6	0.093	487.4	503.1	0.61	29.28	8.46	8.46	17.	D 0.00
5	1724.8	319.7	906.4	0.700	1795.9	1846.8	4.48	5.01	8.46	8.46	17.	D 0.00
6	1747.1	329.7	113.9	0.092	260.4	482.9	0.53	29.90	4.99	8.46	5.	S
7	1783.7	346.3	265.6	0.204	741.9	1125.1	1.15	13.75	5.83	8.45	8.	S
8	1809.9	358.1	601.5	0.451	2503.1	2544.6	2.46	6.71	7.91	8.44	14.	*S
9	1900.0	398.9	109.2	0.082	123.3	461.3	0.38	31.50	6.47	8.43	6.	S
10	1951.0	422.0	84.5	0.066	179.8	356.9	0.27	39.64	4.87	8.42	4.	S
11	1993.5	441.3	155.7	0.116	503.4	656.6	0.46	22.79	8.41	8.41	12.	D C.05
12	2001.6	445.0	102.6	0.077	339.4	432.9	0.70	33.39	8.41	8.41	12.	D 0.05
13	2044.7	464.5	109.3	0.083	443.6	460.4	0.70	33.27	10.61	8.40	8.	S
14	2065.5	473.9	161.9	0.120	841.3	682.1	0.43	21.60	13.07	8.40	11.	S
15	2112.7	495.4	443.2	0.310	1752.6	1866.4	1.09	9.02	7.70	8.40	11.	*S
16	2128.3	502.5	188.2	0.128	776.9	792.4	0.45	20.37	9.38	8.40	8.	*S
17	2153.2	513.8	111.9	0.077	248.5	471.2	0.26	32.27	4.84	8.39	5.	S
18	2189.1	530.2	100.5	0.073	307.4	422.8	0.22	34.89	8.39	8.39	10.	D 0.05
19	2221.7	545.1	151.4	0.106	796.8	637.0	0.32	23.72	8.39	8.39	9.	D 0.05
20	2239.1	553.0	608.6	0.423	2328.9	2560.3	1.27	6.69	7.87	8.39	9.	*S
21	2320.6	590.3	442.3	0.300	2195.5	1847.4	0.84	8.99	7.94	8.39	16.	*S
22	2375.8	615.4	146.3	0.098	484.0	615.3	0.26	26.37	6.72	8.39	7.	S
23	2429.7	640.0	99.4	0.068	345.2	415.1	0.17	35.93	6.16	8.39	7.	S
24	2469.7	658.2	223.0	0.150	1083.7	938.3	0.36	16.79	10.98	8.39	11.	S
25	2525.9	683.8	161.4	0.107	900.4	679.5	0.25	22.86	9.63	8.39	11.	*S
26	2555.2	697.2	205.7	0.137	605.1	865.9	0.31	18.34	5.90	8.40	8.	S
27	2572.9	705.3	104.3	0.069	392.0	439.2	0.15	35.95	5.11	8.40	8.	S
28	2582.9	709.9	106.7	0.072	215.4	449.3	0.16	34.01	4.45	8.40	4.	S
29	2602.9	719.0	234.9	0.159	1065.2	999.4	0.34	15.77	8.35	8.40	12.	*S
30	2620.4	726.9	132.1	0.087	273.5	556.9	0.19	27.79	4.63	8.40	4.	S
31	2653.9	742.2	96.5	0.063	361.1	406.8	0.13	38.49	9.38	8.41	7.	S
32	2670.5	749.8	132.7	0.083	445.7	559.4	0.18	28.48	8.41	8.41	12.	D 0.01
33	2682.4	755.7	265.7	0.167	899.9	1120.5	0.36	14.69	5.41	8.41	12.	D 0.01
34	2696.9	761.8	156.1	0.095	445.0	659.4	0.21	24.80	5.94	8.41	8.	S
35	2721.7	773.1	671.3	0.418	3073.5	2837.9	0.88	6.35	8.47	8.41	14.	*S
36	2781.9	800.5	111.8	0.073	323.6	472.3	0.14	34.69	5.77	8.42	7.	S
37	2834.8	824.7	439.8	0.272	1917.5	1860.0	0.53	9.34	8.51	8.43	11.	*S
38	2873.3	842.3	271.0	0.170	749.4	1147.2	0.32	14.58	5.97	8.44	7.	S
39	2955.5	879.9	263.3	0.168	1372.7	1125.7	0.30	14.50	8.46	8.46	19.	D 0.00
40	2969.7	886.3	234.8	0.149	1198.9	996.4	0.26	16.49	8.46	8.46	19.	D 0.00
41	3025.4	911.8	199.7	0.125	941.0	844.9	0.21	19.23	10.34	8.48	11.	*S
42	3060.8	928.0	122.8	0.077	286.4	522.5	0.13	30.46	5.34	8.49	5.	S
43	3103.0	947.3	458.8	0.288	1920.2	1955.7	0.47	8.90	8.50	8.50	13.	D 0.01
44	3112.3	951.6	147.3	0.093	611.8	624.2	0.15	26.01	8.50	8.50	13.	D 0.01
45	3168.6	977.3	329.0	0.202	1498.7	1406.4	0.32	12.25	8.52	8.52	19.	D 0.00
46	3186.0	985.2	491.5	0.297	2263.1	2100.7	0.48	8.45	8.52	8.52	19.	D 0.00
47	3225.3	1003.2	173.4	0.103	822.5	743.0	0.17	22.47	9.66	8.54	12.	*S
48	3240.3	1010.1	190.7	0.113	604.7	816.9	0.18	20.50	6.96	8.54	6.	S
49	3267.4	1022.5	905.6	0.539	4138.3	3837.5	0.85	5.15	9.06	8.55	12.	*S
50	3292.2	1033.8	238.4	0.141	885.7	1023.8	0.22	16.62	7.16	8.56	11.	*S
51	3357.6	1063.7	247.1	0.146	748.3	1064.4	0.22	16.23	6.57	8.59	6.	*S
52	3371.0	1069.9	97.9	0.059	211.6	422.0	0.09	38.87	4.85	8.59	5.	S
53	3413.1	1089.2	1237.0	0.714	5540.3	5345.1	1.08	3.98	8.62	8.62	26.	D 0.00
54	3436.6	1099.9	1148.9	0.681	5171.1	4964.6	1.00	4.15	8.62	8.62	26.	D C.00
55	3486.6	1122.8	256.3	0.158	1467.8	1111.6	0.22	15.19	8.65	8.65	21.	D 0.00
56	3506.5	1131.9	217.9	0.132	1250.7	945.0	0.18	17.82	8.65	8.65	21.	D 0.00
57	3545.2	1149.6	107.1	0.069	501.4	465.7	0.09	34.76	8.67	8.67	13.	D 0.20

TABLE VI(1) (CONTINUED)

58	3553.5	1153.4	196.4	0.126	899.9	854.3	0.16	19.99	8.67	8.67	13. D	0.20
59	3565.1	1159.7	116.6	0.075	435.1	508.0	0.10	31.95	8.69	8.69	16. T	0.00 C.06
60	3580.8	1165.9	186.6	0.123	702.4	812.9	0.15	19.93	8.69	8.69	16. T	0.00 C.06
61	3588.9	1169.6	103.6	0.066	365.7	451.4	0.09	37.96	8.69	8.69	16. T	0.00 C.06
62	3616.6	1182.2	228.5	0.143	1077.8	997.2	0.19	16.92	10.89	8.70	8.	*S
63	3677.0	1209.8	165.4	0.105	807.1	724.9	0.13	22.83	8.74	8.74	18. D	0.06
64	3687.1	1214.4	209.3	0.133	977.1	917.4	0.17	18.93	8.74	8.74	18. D	0.06
65	3706.3	1223.2	98.0	0.064	476.9	430.3	0.08	37.35	8.76	8.76	15. D	0.00
66	3720.3	1229.6	473.3	0.306	2257.8	2078.2	0.37	8.64	8.76	8.76	15. D	0.00

NUMBER OF PEAKS IN MULTIPLET = 5

THE 3 STRONGEST PEAKS ARE ANALYSED AS A TRIPLET. CHECK BACKGROUND SUBTRACTED DATA.												
67	3776.3	1255.2	229.3	0.149	1283.1	1011.0	0.18	16.49	8.79	8.79	28. T	0.21 C.06
68	3781.7	1257.6	222.5	0.144	1205.7	981.0	0.17	17.33	8.79	8.79	28. T	0.21 C.06
69	3792.1	1262.4	230.3	0.150	1248.3	1015.8	0.18	16.84	8.79	8.79	28. T	0.21 C.06
70	3844.1	1286.2	234.5	0.144	1135.2	1039.4	0.18	16.57	8.83	8.83	27. D	0.01
71	3855.0	1291.2	1037.2	0.639	5022.8	4594.1	0.79	4.44	8.83	8.83	27. D	0.01
72	3930.0	1325.5	168.5	0.106	575.6	750.3	0.13	23.87	7.46	8.89	7.	S
73	3956.9	1337.8	99.5	0.064	202.2	443.9	0.07	37.47	4.49	8.90	4.	S
74	4010.7	1367.4	334.5	0.216	1412.5	1498.2	0.25	11.96	8.58	8.93	11.	*S
75	4073.4	1391.1	196.7	0.126	579.7	884.9	0.14	19.16	6.23	8.97	8.	S
76	4110.7	1408.1	101.5	0.063	478.9	457.9	0.07	36.80	10.97	9.00	9.	S
77	4131.7	1417.7	115.3	0.075	469.9	521.5	0.08	32.45	9.02	9.02	11. D	0.07
78	4177.3	1438.5	100.2	0.065	482.2	455.5	0.07	39.08	9.06	9.06	33. T	0.00 C.00
79	4199.0	1448.4	208.1	0.134	1055.3	945.6	0.15	18.29	9.06	9.06	33. T	0.00 C.00
80	4218.8	1457.4	2953.9	1.877	14761.5	13424.7	2.13	2.25	9.06	9.06	33. T	0.00 C.00
81	4264.5	1478.3	170.7	0.107	607.1	780.5	0.12	22.72	9.12	9.12	16. T	0.02 C.02
82	4274.2	1487.7	410.4	0.258	1482.5	1876.6	0.30	9.77	9.12	9.12	16. T	0.02 C.02
83	4285.3	1487.8	122.3	0.077	442.7	559.1	0.09	30.78	9.12	9.12	16. T	0.02 C.02
84	4323.0	1505.1	372.7	0.235	1351.8	1711.0	0.27	10.56	7.90	9.16	7.	*S
85	4378.2	1530.3	170.8	0.102	510.5	787.6	0.12	23.18	6.58	9.20	7.	S
86	4406.5	1543.3	1202.8	0.717	4990.5	5561.9	0.86	4.01	8.58	9.22	12.	*S
87	4447.3	1561.9	156.6	0.097	729.6	727.2	0.11	24.25	9.26	9.26	16. D	0.00
88	4462.5	1569.9	504.5	0.312	2351.0	2343.4	0.36	8.09	9.26	9.26	16. D	0.00
89	4496.7	1584.6	104.9	0.066	294.9	488.9	0.07	37.30	6.29	9.30	5.	S
90	4531.2	1600.3	159.8	0.106	418.6	747.3	0.11	23.74	5.69	9.33	5.	S
91	4567.6	1617.0	136.5	0.087	926.2	640.3	0.10	27.24	11.98	9.36	12.	S
92	4675.1	1666.2	284.1	0.182	952.3	1346.7	0.21	13.61	6.62	9.45	10.	S
93	4725.0	1689.0	281.7	0.187	1549.5	1342.0	0.20	13.40	9.03	9.50	14.	*S
94	4789.7	1719.6	106.3	0.070	278.9	509.4	0.08	35.52	5.69	9.56	5.	S
95	4810.0	1727.9	1163.8	0.760	5280.6	5590.6	0.85	3.92	9.28	9.58	12.	*S
96	4847.0	1744.9	150.1	0.093	602.8	723.9	0.11	25.29	9.01	9.62	8.	S
97	4858.8	1750.2	106.2	0.067	278.6	512.9	0.08	35.68	5.52	9.63	6.	S
98	4874.0	1757.2	210.5	0.133	527.3	1017.9	0.16	18.29	5.47	9.64	6.	S
99	4949.9	1791.9	699.3	0.451	2873.4	3408.3	0.52	5.97	8.51	9.72	10.	*S
100	4982.1	1806.6	108.8	0.071	241.6	532.2	0.08	35.26	4.75	9.75	5.	S
101	5015.3	1821.8	520.6	0.347	2486.6	2554.9	0.39	7.65	9.23	9.79	15.	*S
102	5040.9	1833.5	178.4	0.085	473.1	631.9	0.10	29.45	8.16	9.81	7.	S
103	5068.6	1846.2	286.5	0.195	1145.9	1414.3	0.22	13.12	7.35	9.84	11.	*S
104	5088.4	1855.2	112.0	0.076	365.5	553.9	0.08	32.46	7.12	9.86	7.	S
105	5111.9	1866.0	111.9	0.079	491.7	554.9	0.08	31.42	11.49	9.89	9.	S
106	5138.7	1878.2	180.2	0.123	587.1	897.0	0.14	20.61	9.93	9.93	8. D	0.30
107	5180.4	1897.3	346.6	0.244	1328.6	1731.7	0.27	11.04	7.65	9.97	10.	*S
108	5220.8	1915.8	127.8	0.086	633.4	641.4	0.10	28.37	10.97	10.01	8.	S
109	5252.7	1930.4	154.0	0.107	816.2	776.8	0.12	23.96	10.06	10.06	20. D	0.00
110	5268.6	1937.7	353.4	0.245	1913.9	1782.8	0.27	10.69	10.06	10.06	20. D	0.00
111	5312.0	1957.6	182.3	0.124	738.4	925.3	0.14	20.64	10.12	10.12	10. D	0.31
112	5320.1	1961.2	93.7	0.065	398.5	475.5	0.07	37.96	10.12	10.12	10. D	0.31
113	5357.7	1978.4	129.4	0.089	506.8	660.0	0.10	28.74	6.79	10.17	9.	S
114	5391.5	1993.8	103.4	0.071	221.3	329.6	0.08	34.88	4.79	10.21	4.	S

TABLE VI(1) (CONTINUED)

115	5436.3	2014.3	258.4	0.176	1357.9	1329.6	0.21	14.52	9.85	10.26	14.	*S
116	5493.5	2040.5	288.8	0.181	1284.3	1496.2	0.23	13.71	9.85	10.33	9.	*S
117	5529.4	2056.9	444.3	0.281	1991.0	2312.2	0.36	8.97	10.02	10.38	9.	*S
118	5619.1	2098.0	895.2	0.566	4027.9	4709.5	0.74	4.84	9.64	10.49	10.	*S
119	5660.6	2116.9	105.8	0.068	505.9	559.4	0.09	34.93	10.94	10.54	8.	S
120	5673.2	2127.7	100.6	0.065	203.9	532.7	0.08	38.27	4.41	10.56	5.	S
121	5698.4	2134.2	109.8	0.070	835.4	583.7	0.09	33.70	10.60	10.62	17. D	0.62
122	5702.2	2135.9	101.9	0.065	783.4	541.9	0.09	36.16	10.60	10.60	17. D	0.62
123	5721.8	2144.9	117.1	0.072	289.0	623.9	0.10	32.15	5.60	10.62	6.	S
124	5791.4	2176.8	103.1	0.062	453.8	554.1	0.09	37.01	10.72	10.72	8. D	0.63
125	5802.9	2182.1	101.5	0.063	591.0	547.7	0.09	36.94	10.76	10.76	22. T	0.00 0.00
126	5819.0	2189.4	354.9	0.222	2069.7	1936.8	0.31	11.10	10.76	10.76	22. T	C.CC C.CC
127	5835.6	2197.0	137.4	0.083	801.0	741.3	0.12	27.75	10.76	10.76	22. T	0.00 C.CC
128	5858.5	2207.5	120.3	0.071	419.2	652.1	0.10	33.80	6.39	10.81	9.	S
129	5920.5	2235.9	5524.2	3.227	32212.4	30194.3	4.85	1.47	11.13	10.90	24.	*S
NUMBER OF PEAKS IN MULTIPLYET = 5												
THE 3 STRONGEST PEAKS ARE ANALYSED AS A TRIPLET. CHECK BACKGROUND SUBTRACTED DATA.												
130	6000.6	2272.5	686.4	0.413	3924.0	3800.7	0.62	6.29	11.04	11.04	38. T	0.00 C.CC
131	6018.9	2280.9	5395.3	3.236	30583.2	29876.9	4.85	1.48	11.04	11.04	38. T	0.00 C.CC
132	6038.1	2289.7	228.9	0.137	1270.2	1267.7	0.21	17.43	11.04	11.04	38. T	0.00 C.CC
NUMBER OF PEAKS IN MULTIPLYET = 4												
THE 3 STRONGEST PEAKS ARE ANALYSED AS A TRIPLET. CHECK BACKGROUND SUBTRACTED DATA.												
133	6104.6	2320.1	457.0	0.316	2497.3	2565.2	0.42	8.41	11.19	11.19	28. T	0.00 C.18
134	6127.2	2330.5	108.7	0.076	579.4	610.3	0.10	33.23	11.19	11.19	28. T	0.00 C.18
135	6135.4	2334.2	367.5	0.255	2005.1	2063.2	0.34	10.27	11.19	11.19	28. T	C.CC C.18
136	6152.9	2342.2	95.3	0.067	186.8	536.9	0.09	37.82	4.32	11.23	4.	S
137	6195.4	2361.6	95.2	0.072	219.6	539.2	0.09	37.50	4.90	11.30	5.	S
138	6205.0	2366.0	85.0	0.064	168.1	482.4	0.08	39.84	4.28	11.31	4.	S
139	6268.2	2394.9	88.7	0.071	282.3	507.6	0.09	37.37	5.91	11.41	7.	S
140	6280.9	2400.7	208.9	0.164	1073.7	1197.1	0.20	16.60	9.61	11.43	12.	*S
141	6324.0	2420.4	106.8	0.085	603.9	615.4	0.10	31.67	15.68	11.49	11.	S
142	6352.0	2433.1	93.9	0.075	192.5	943.6	0.09	35.41	4.54	11.54	4.	S
143	6378.1	2445.1	433.1	0.357	3461.7	2514.9	0.43	8.21	18.27	11.59	15.	S
144	6415.4	2462.1	109.4	0.089	302.4	632.9	0.11	30.36	6.20	11.64	6.	S
145	6583.5	2538.8	169.9	0.135	787.2	1015.9	0.18	20.07	11.93	11.93	14. D	0.43
146	6626.6	2558.5	152.6	0.121	734.9	918.8	0.16	23.56	12.01	12.01	17. D	0.00
147	6644.5	2566.6	1027.4	0.917	5191.5	6185.7	1.11	4.09	12.01	12.01	17. D	0.00
148	6701.3	2592.6	129.4	0.104	464.7	786.0	0.14	26.69	8.08	12.11	7.	S
149	6784.1	2630.3	159.6	0.124	714.0	982.0	0.18	21.75	12.27	12.27	13. D	0.24
150	6791.5	2633.7	102.6	0.080	460.0	631.1	0.12	33.31	12.27	12.27	13. D	0.24
151	6837.3	2654.6	1169.4	0.899	7676.6	7240.1	1.35	3.74	12.28	12.35	19.	*S
152	6887.5	2677.5	185.8	0.139	1113.4	1158.3	0.22	19.15	12.43	12.43	18. D	C.12
153	6930.5	2697.1	115.7	0.084	568.9	726.0	0.14	30.14	11.28	12.51	10.	S
154	6983.1	2721.1	99.7	0.072	375.5	630.1	0.12	35.04	4.55	12.61	7.	S
155	7000.7	2729.1	89.8	0.065	198.1	569.4	0.11	38.89	4.92	12.64	5.	S
156	7058.3	2755.4	545.2	0.372	3698.7	3484.9	0.68	7.31	13.84	12.75	18.	S
157	7099.1	2774.0	704.3	0.460	3813.1	4528.4	0.89	5.92	10.74	12.82	13.	*S
158	7158.6	2801.1	327.7	0.213	2282.7	2125.1	0.42	11.76	14.32	12.93	17.	S
NUMBER OF PEAKS IN MULTIPLYET = 4												
THE 3 STRONGEST PEAKS ARE ANALYSED AS A TRIPLET. CHECK BACKGROUND SUBTRACTED DATA.												
159	7245.7	2840.7	691.8	0.430	5034.1	4556.9	0.91	6.17	13.14	13.14	43. T	0.15 C.CC
160	7257.9	2846.3	135.0	0.084	983.7	889.3	0.18	27.98	13.14	13.14	43. T	C.15 C.CC
161	7279.8	2856.3	2292.6	1.395	16671.2	15101.4	3.10	2.60	13.14	13.14	43. T	C.15 C.CC
162	7364.5	2894.8	355.1	0.208	2876.2	2375.8	0.50	11.44	13.34	13.34	18. D	0.51
163	7371.1	2897.8	248.6	0.146	2022.3	1663.3	0.35	15.96	13.34	13.34	18. D	0.51
164	7539.4	2974.5	457.0	0.244	2486.9	3135.5	0.68	9.63	12.20	13.68	12.	*S

TABLE VI(1) (CONTINUED)

THE 3 STRONGEST PEAKS ARE ANALYSED AS A TRIPLET. CHECK BACKGROUND SUBTRACTED DATA.			NUMBER OF PEAKS IN MULTIPLET = 4											
165	7990.0	2997.6	160.1	0.093	1138.3	1112.7	C.24	25.21	13.86	13.86	52.	T	0.00	0.08
166	7633.7	3017.5	9766.5	5.794	71029.3	67869.7	15.07	1.78	13.86	13.86	52.	T	0.00	0.08
167	7646.0	3023.1	8799.9	5.280	64571.0	61152.5	13.61	1.80	13.86	13.86	52.	T	0.00	0.08
168	7699.0	3047.2	126.7	0.078	391.6	890.4	C.20	30.26	6.90	14.01	6.	S		
169	7739.8	3065.8	103.0	0.071	200.6	728.1	C.17	35.20	4.28	14.10	4.	S		
170	7821.2	3102.8	666.2	0.601	4337.7	4774.0	1.11	5.67	14.29	14.29	20.	D	0.04	
171	7871.7	3125.9	73.8	0.089	147.1	532.3	C.13	37.02	4.38	14.38	4.	S		
172	7916.2	3146.1	100.0	0.143	711.5	728.5	C.17	25.33	14.53	14.53	34.	T	0.00	0.00
173	7940.7	3157.2	1541.7	2.283	10969.0	11235.1	2.68	3.04	14.53	14.53	34.	T	0.00	0.00
174	7963.9	3167.8	95.9	0.140	645.0	662.6	0.16	26.93	14.53	14.53	34.	T	0.00	0.00
175	8071.8	3216.7	63.0	0.119	282.9	468.2	0.12	34.99	10.54	14.82	9.	S		
176	8121.5	3239.4	199.8	0.367	1220.5	1496.5	0.37	12.12	13.09	14.93	13.	S		
177	8365.8	3350.7	72.2	0.123	283.9	561.4	C.15	32.28	8.81	15.50	7.	S		
178	8432.1	3380.8	56.3	0.104	201.6	442.0	0.12	39.15	15.64	15.64	10.	D	0.26	
179	8484.4	3404.6	514.7	0.863	3860.6	4089.4	1.13	5.91	15.84	15.84	47.	T	0.00	C.C1
180	8513.6	3417.9	760.8	1.270	5734.2	6044.2	1.69	4.59	15.84	15.84	47.	T	0.00	0.01
181	8534.5	3427.4	1098.0	1.826	8215.1	8723.5	2.45	3.81	15.84	15.84	47.	T	0.00	C.C1
182	8722.9	3513.1	67.8	0.127	257.1	556.5	C.17	32.49	7.45	16.77	8.	S		
183	8884.5	3586.4	2408.1	4.652	19932.7	20288.8	6.44	3.13	16.80	16.80	33.	D	0.00	
184	8909.6	3597.7	94.5	0.185	777.4	795.9	0.26	23.46	16.80	16.80	33.	D	0.00	
185	8971.7	3625.9	52.4	0.118	420.4	448.3	0.15	38.38	17.06	17.06	31.	T	0.00	0.00
186	9000.0	3638.7	1811.7	4.206	14626.1	15501.9	5.17	3.37	17.06	17.06	31.	T	0.00	C.00
187	9025.2	3650.2	50.8	0.122	410.1	434.6	0.15	38.04	17.06	17.06	31.	T	0.00	0.00
188	9301.5	3775.3	695.2	4.708	6220.4	6241.1	2.44	4.37	17.90	17.90	35.	D	0.00	
189	9329.6	3788.1	35.2	0.247	315.4	316.3	0.13	33.05	17.90	17.90	35.	D	0.00	
190	9721.4	3965.9	374.6	8.010	5563.8	5492.2	2.84	4.70	18.44	19.06	35.	S		

The method of least-squares fit is described in Appendix II. The first page of Table VI(1) includes (a) the number of peaks used in the fit, which is 46 in this case, (b) three summation values for the parameters V_j in equation (A2.12), (c) the matrix coefficients C_{jk} evaluated by equation (A2.13), (d) the value of the determinant and the coefficients of the inverted matrix supplied by the computer program MINV, (e) the equation for the fwhm, equivalent to equation (A2.9), and (f) the square root of the weighted sum of the residuals (equation A2.14) divided by the degrees of freedom which is $46 - 3 = 43$ in this case.

The second page of table VI(1) includes data most of which were evaluated by the equations presented in Appendices II and III. This part of the table includes

- (1) the peak number
- (2) the peak energy, in keV
- (3) the peak fwhm (equation A3.7)
- (4) the standard deviation in the fwhm evaluated by equation (A3.13)
- (5) the value of the weighting function (equations A2.10, A3.8, and A3.13)
- (6) The value of the fitted fwhm, in keV, using equation (A2.9) and the constants listed in the first page of this table
- (7) the difference between the calculated and fitted fwhm
- (8) The value of the residual at each point in the

- fit, which is the product of the weight function and the square of the difference in the fwhm, and
- (9) the confidence interval (equation A2.16), which is an estimate of the uncertainty in the interpolated and extrapolated fwhm values obtained by equation (A2.9).

In the remaining pages of the table is presented the analysis of the spectrum. The various columns represent

- (1) the peak number
- (2) the energy of the incident gamma ray, in keV
- (3) the location of the peak center in the spectrum
- (4) the height of the peak evaluated by equation (A3.9)
- (5) the ratio of the peak height to the average background underneath the peak, with the background computed by equation (3.3)
- (6) the straight-sums peak area (equation 3.6)
- (7) the Gaussian area (equation 3.7)
- (8) the Gaussian peak intensity, in photons per 100 neutron captures in the sample
- (9) the percent error in the Gaussian area (eq. 3.14)
- (10) the fwhm of the peak (eq. A3.7), in keV (note that for multiplets this is set equal to the fitted fwhm)
- (11) the fitted fwhm evaluated by the least squares procedure
- (12) the width of the peak at its base line, and
- (13) the type of the peak, the symbols S, D, and T standing for singlet, doublet and triplet.

Note that in the last column, 13, an asterisk close to a singlet indicates that the gamma ray is intense and was used in the least-squares fit and in the evaluation of the area correction factor ψ for the deviation of the peak shapes from the Gaussian distribution. The numbers following the doublet and triplet symbols are a measure of the contributions to the height of a peak from the remaining peaks in the multiplet. Also note that due to the limitations of the GAMANL code to analyze high-order multiplets, the three strongest peaks of such multiplets are analyzed as triplets. This procedure does not lead into any serious trouble since, in a majority of the cases, the high-order multiplets are caused by weak peaks located at the wings of strong ones.

Other pertinent data associated with this analysis are listed below:

- (a) The gamma ray energies were corrected for system non-linearity according to the energy-dependent correction shown in Fig. 6.1 for this run
- (b) The values assigned to the smoothing parameters in equation (A1.4) were $\omega_m = 2\pi(1024/4096) = \pi/2$ and $\sigma_m = 2\pi(128/4096) = \pi/16$; the corresponding error reduction factor for this degree of smoothing is 1.34
- (c) The two energy calibration lines required by the code were the 4218.8 and the 5920.5 keV gamma rays of Fe; the energy-channel conversion factor, C, was 2.189 keV/channel

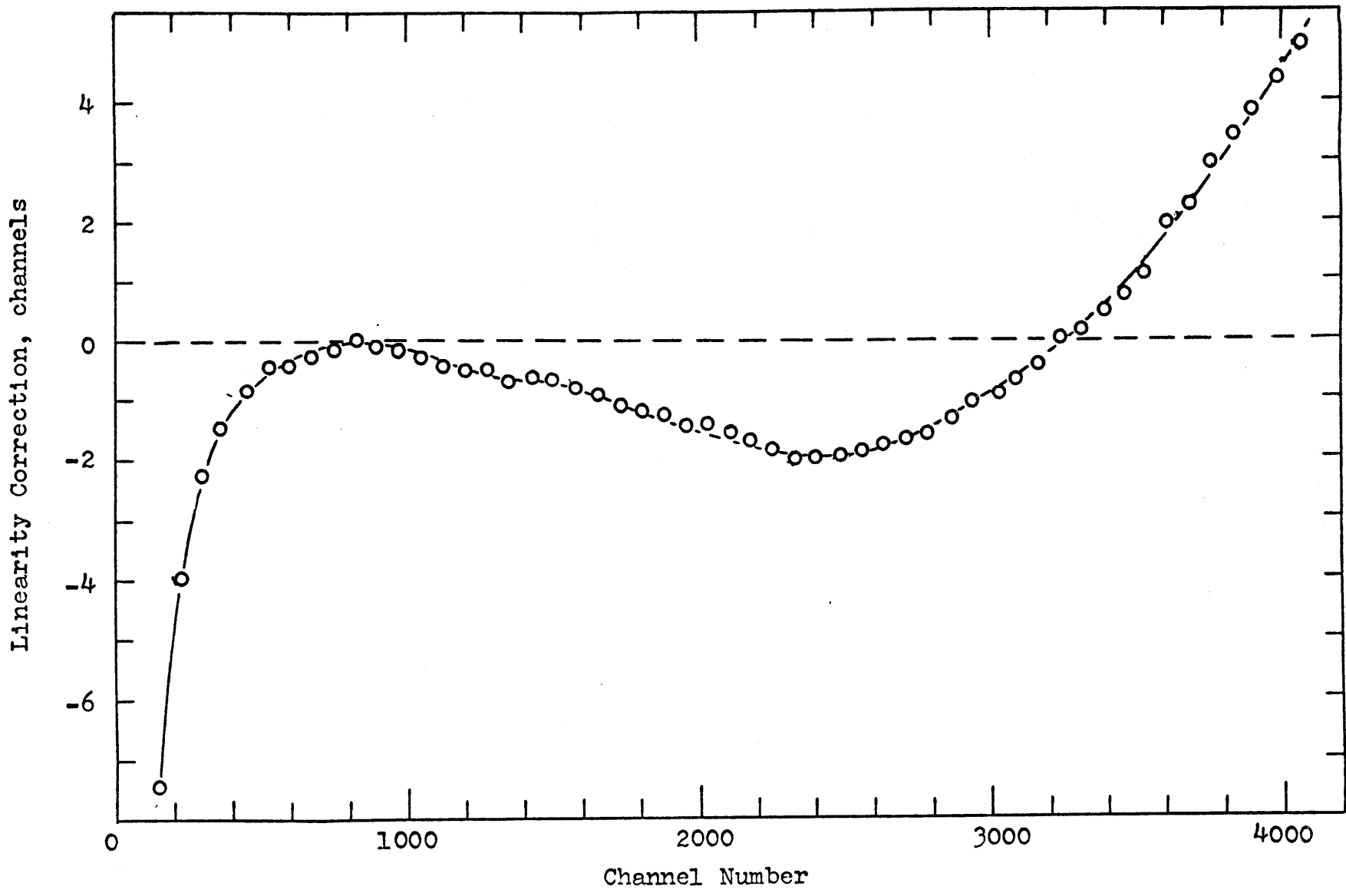


Fig. 6.1 Linearity Correction Curve

- (d) Only peaks with less than 40 percent error in the peak area are included in the Table
- (e) The correction term ψ was computed using 36 peaks; its value was 1.031
- (f) The geometry of the system included a 1/2-inch collimator which is equivalent to a fractional solid angle of 1.59×10^{-5}
- (g) The flux-time product was assigned the empirical value of 1.94×10^{13} n/cm² which was found to best fit the data analysis; it includes corrections for neutron depression and fraction of sample seen
- (h) Values for the efficiencies were taken from Table IV(2) and were corrected for the 1 1/2-inch masonite plug in the beam; gamma self-shielding was set equal to 0.89 for all energies.

The GAMANL results given above constitute the first step that must be taken in elemental analysis. The energies and peak areas of the gamma rays in the spectrum have been evaluated. These must now be used to identify the various elements in the sample and to obtain their corresponding concentrations. A computer code has been written to carry out these operation. The code, which was named WTANAL for weight analysis, is listed in Appendix V.

In this code use is made of the energies and intensities of all the gamma rays of the elements that are believed to be present in the sample. The program, working on each element separately (at first), selects from the list those gamma rays

whose energies are within specified limits and whose intensities are larger than a given value. In this manner the code can be used both for low energy and high energy applications and unnecessary computations are eliminated by rejecting low intensity gamma rays. The energies of the selected gamma rays are then compared to those in the spectrum for possible correspondence; this occurs if the energies are within a specified number of keV units. Whenever an element which could have produced the observed gamma peak in the spectrum is found, the weight M_c of the element is calculated. For this computation use is made of equation (3.25) and of the equation

$$M_c = \Lambda_G / [\phi t \Omega \epsilon I] \quad (6.1)$$

where the various symbols have already been defined. If, through such a procedure, the origin of a gamma ray is assigned to more than one element, the symbols of the interfering elements are listed. In its present form the program does not resolve interference effects.

Application of this code to the analysis of the stainless steel sample gave the results appearing in Table VI(2). On the first page of this table are listed (a) the reference sample analysed, (b) the flux time value (which in this case includes also the 0.89 correction factor for gamma self-shielding), and the solid angle, (c) the efficiency data, and (d) a list of the elements for which the spectrum is examined. Note that the maximum difference between observed and tabu-

TABLE VI(2) - PART OF WTANAL OUTPUT

ANALYSIS OF SS-303 SAMPLE - RLN 9261 - COMPUTER CLTPUT 70028

FLUX*TIME (N/CM*CM) = 0.1735E 14 SCLIC ANGLE = 0.159CE-C4

EFFICIENCY DATA INITIAL ENERGY (KEV) = 1CCC. DELTA ENERGY (KEV) = 500.

EFFICIENCY ARRAY

C.1CCCE-C5 C.575E-C4 C.158E-03 C.364E-03 0.535E-03 0.701E-03 0.823E-03 0.895E-03 0.856E-03 0.884E-03
 0.846E-03 0.742E-03 0.709E-03 0.636E-C3 C.565E-C3 0.452E-C3 0.411E-03 0.310E-03 0.208E-03 0.105E-03

ELEMENTS FOR WHICH SPECTRUM IS ANALYZED

NO PEAKS	ELEMENT	AT WEIGHT	SIGMA(BAPAS)	PIA INT	MIN ENERGY	MAX ENERGY	ENERGY DIFF
187	FE	55.85	2.62	0.1C	150C.CC	10000.00	4.00
63	CR	52.0C	3.10	0.10	1500.00	10000.00	4.00
120	NI	58.71	4.6C	0.1C	1500.00	10000.00	4.00
113	MA	54.94	13.30	0.10	1500.CC	10000.00	4.00
145	CO	5E.53	38.00	1.0C	1500.00	10000.00	4.00

TABLE VI(2) (CONTINUED)

ORDERING THE IDENTIFIED PEAKS ELEMENT WISE								
NUMBER	SAMPLE ENGY	SAPPLE AREA	ERROR P.C.	ELEMENT	TABLE ENGY	TABLE INT.	WT(GRAMS)	INTERFERENCE
3	1612.84	2032.59	8.5C	FE	1613.00	5.85	0.5125E 02	
9	1724.84	3846.83	5.C1	FE	1724.80	8.03	0.5230E 02	NI
12	2001.59	432.87	33.35	FE	2000.00	0.44	0.6358E 02	
14	2065.48	682.07	21.60	FE	2067.10	0.62	0.6431E 02	MA
15	2112.71	1866.37	5.C2	FE	2109.90	0.33	0.3088E 03	MN
16	2128.32	792.43	20.32	FE	2125.60	0.43	0.4846E 02	
17	2153.23	471.17	32.27	FE	2153.40	0.13	0.1872E 03	
23	2429.67	418.14	35.53	FE	2425.70	0.19	0.8296E 02	
24	2469.70	938.34	16.79	FE	2470.10	0.43	0.7913E 02	MN
25	2525.88	675.53	22.86	FE	2527.70	0.42	0.5564E 02	
27	2572.91	439.18	35.55	FE	2576.30	0.24	0.6031E 02	
31	2653.91	406.84	38.49	FE	2655.90	0.13	0.9625E 02	
33	2682.44	1120.45	14.69	FE	2682.30	0.41	0.8211E 02	NI
34	2696.85	656.36	24.80	FE	2698.20	0.21	0.9312E 02	MN
35	2721.74	2832.85	6.35	FE	2721.50	1.43	0.5770E 02	
37	2824.85	1860.01	9.34	FE	2835.40	0.58	0.8588E 02	
38	2873.30	1147.23	14.58	FE	2873.90	0.42	0.7121E 02	
39	2955.46	1125.72	14.50	FE	2955.60	0.36	0.7715E 02	
40	2965.66	556.42	16.45	FE	2973.40	0.20	0.1219E 03	MN NI
42	3060.79	522.48	30.46	FE	3062.10	0.11	0.1093E 03	MN
43	3103.03	1955.89	8.50	FE	3103.90	0.66	0.6638E 02	
45	3148.64	1406.41	12.25	FE	3169.30	0.31	0.9768E 02	
46	3185.56	2100.67	8.45	FE	3186.20	0.66	0.6785E 02	NI
47	3225.27	742.58	22.47	FE	3225.80	0.16	0.9683E 02	
48	3240.34	816.51	20.50	FE	3240.40	0.21	0.8046E 02	
49	3267.35	3897.48	5.15	FE	3267.80	1.15	0.6678E 02	MN NI CR
50	3292.20	1023.81	16.62	FE	3292.50	0.31	0.6644E 02	NI
51	3357.47	1064.37	16.23	FE	3356.90	0.29	0.7154E 02	
53	3413.15	5345.11	3.98	FE	3413.80	1.50	0.6770E 02	
54	3436.58	4564.61	4.15	FE	3437.40	1.35	0.6914E 02	
55	3486.63	1111.60	15.19	FE	3487.40	0.38	0.5383E 02	CR
56	3506.48	545.03	17.82	FE	3507.30	0.29	0.5948E 02	NI
67	3776.30	1011.01	16.49	FE	3777.70	0.18	0.9303E 02	NI
68	3781.65	981.03	17.33	FE	3777.70	0.18	0.9012E 02	MN NI CR
69	3792.11	1015.76	16.84	FE	3791.70	0.16	0.1046E 03	
70	3844.14	1038.45	16.57	FE	3845.10	0.27	0.6243E 02	
71	3854.95	4554.15	4.44	FE	3854.90	0.57	0.7665E 02	MN
74	4010.66	1498.18	11.56	FE	4012.50	0.39	0.5972E 02	
75	4073.44	884.94	19.16	FE	4074.20	0.12	0.1129E 03	
80	4218.80	13424.68	2.25	FE	4218.80	4.02	0.4963E 02	MN
82	4274.18	1876.61	9.77	FE	4275.50	0.37	0.7468E 02	
85	4378.18	787.63	23.18	FE	4380.10	0.17	0.9526E 02	MN
86	4406.52	5561.93	4.C1	FE	4406.80	1.31	0.6142E 02	NI
88	4462.52	2343.44	8.09	FE	4462.40	0.61	0.5525E 02	
92	4675.11	1346.73	13.61	FE	4675.80	0.27	0.7135E 02	NI
95	4809.98	5590.40	3.92	FE	4810.30	1.66	0.4816E 02	
99	4945.86	3408.29	5.97	FE	4949.00	0.80	0.6097E 02	MN
106	5139.70	897.C1	20.61	FE	5141.50	0.14	0.9182E 02	MN
113	5357.72	660.01	28.74	FE	5357.40	0.12	0.7928E 02	
116	5453.53	1496.22	13.71	FE	5493.40	0.14	0.1550E 03	CR
129	5920.50	30194.29	1.47	FE	5920.50	8.29	0.5473E 02	MN
131	6018.88	29876.85	1.48	FE	6018.50	8.08	0.5622E 02	
143	6378.14	2514.91	8.21	FE	6380.70	0.64	0.6314E 02	
161	7279.84	15101.36	2.60	FE	7278.90	4.60	0.6306E 02	

TABLE VI(2) (CONTINUED)

166	7622.73	67665.75	1.78	FE	7631.60	27.19	0.5189E 02	
167	7645.67	61152.52	1.40	FE	7645.60	22.14	0.5758E 02	
183	8884.54	20288.77	3.13	FE	8886.00	0.64	0.9426E 03	CR
188	9301.46	6241.12	4.37	FE	9298.40	3.85	0.5938E 02	
7	1783.73	1125.12	13.75	CR	1783.80	5.43	0.1560E 02	
9	1899.97	461.28	31.50	CR	1898.50	3.82	0.7263E 01	
11	1993.47	656.60	22.79	CR	1994.70	2.28	0.1483E 02	
20	2239.10	2540.32	6.65	CR	2238.90	7.45	0.1254E 02	
21	2320.63	1860.39	8.99	CR	2321.00	5.43	0.1138E 02	
22	2375.82	615.30	26.37	CR	2377.00	1.28	0.1506E 02	
26	2555.25	865.86	18.34	CR	2559.20	0.82	0.2782E 02	NI
29	2602.87	989.40	15.77	CR	2601.90	1.39	0.1798E 02	
30	2620.35	556.76	27.79	CR	2621.30	0.31	0.4470E 02	MN
32	2670.55	559.40	28.48	CR	2670.40	1.15	0.1161E 02	
41	3025.43	844.76	19.27	CR	3022.30	1.42	0.1103E 02	NI
45	3267.39	3897.48	5.15	CR	3267.50	0.46	0.1359E 03	MN NI FE
55	3486.63	1111.60	15.15	CR	3488.20	0.17	0.9469E 02	FE
62	3616.63	997.21	16.52	CR	3617.70	0.79	0.1736E 02	
66	3720.26	2078.22	8.64	CR	3720.70	2.16	0.1277E 02	
68	3781.65	561.03	17.33	CR	3785.20	0.16	0.7978E 02	MN NI FE
72	3970.00	750.35	23.87	CR	3928.10	0.36	0.2601E 02	MN NI
77	4121.74	521.46	32.45	CR	4133.90	0.32	0.1632E 02	
84	4323.01	1710.57	10.56	CR	4323.30	0.70	0.2812E 02	
90	4531.21	747.35	23.74	CR	4529.70	0.15	0.4435E 02	
96	4847.03	723.53	25.29	CR	4847.20	0.94	0.8667E 01	
98	4874.00	1017.91	18.25	CR	4872.80	0.35	0.3273E 02	MN
108	5220.77	641.41	28.37	CR	5222.90	0.61	0.1188E 02	
110	5268.65	1782.78	10.65	CR	5269.50	1.13	0.1794E 02	CO NI
116	5493.53	1496.22	13.71	CR	5493.70	0.64	0.2669E 02	FE
118	5619.14	4709.54	4.84	CR	5618.80	3.46	0.1566E 02	
124	5791.43	554.06	37.01	CR	5793.60	0.74	0.1902E 02	
128	5858.50	652.05	37.80	CR	5857.60	0.70	0.1094E 02	
130	6000.57	3800.71	6.79	CR	5999.60	2.27	0.1998E 02	
135	6135.38	2063.19	10.27	CR	6136.30	1.66	0.1513E 02	
140	6280.55	1197.13	16.60	CR	6282.40	1.18	0.1263E 02	
141	6324.01	615.38	31.67	CR	6326.40	0.49	0.1574E 02	
147	6644.48	6185.65	4.09	CR	6645.50	5.25	0.1551E 02	
152	6887.48	1158.29	19.15	CR	6890.10	1.03	0.1565E 02	NI
157	7099.13	4528.41	5.52	CR	7059.70	3.88	0.1697E 02	
162	7364.47	2375.82	11.44	CR	7366.20	6.73	0.5436E 01	
173	7940.70	11235.08	3.04	CR	7939.30	11.41	0.1733E 02	
179	8484.40	4089.36	5.51	CR	8484.30	4.06	0.2057E 02	
180	8513.57	6044.22	4.59	CR	8512.70	5.50	0.2264E 02	
183	8884.54	20288.77	3.13	CR	8884.10	24.14	0.1566E 02	FE
190	9721.42	5452.25	4.70	CR	9720.30	9.82	0.2131E 02	
5	1724.84	3846.83	5.01	NI	1726.90	0.78	0.3223E 03	FE
10	1950.96	356.83	39.64	NI	1950.30	1.49	0.1005E 02	
26	2555.25	665.86	18.34	NI	2554.10	1.44	0.1206E 02	CR
33	2682.44	1120.45	14.65	NI	2685.60	0.51	0.3952E 02	FE
40	2945.66	956.42	16.49	NI	2967.80	0.21	0.6946E 02	MN FE
41	3025.43	844.76	15.23	NI	3026.50	0.18	0.6621E 02	CR
46	3185.96	2100.67	8.45	NI	3182.40	0.28	0.9575E 02	FE
45	3267.39	3897.48	5.15	NI	3265.90	0.17	0.2759E 03	MN CR FE
90	3292.20	1023.81	16.62	NI	3296.00	0.11	0.1122E 03	FE

TABLE VI(2) (CONTINUED)

52	3371.04	422.03	38.87	NI	3367.3C	0.11	0.4449E 02	MN
58	3508.48	945.03	17.82	NI	3504.80	0.24	C.4303F C2	FE
59	3565.14	508.02	31.45	NI	3561.90	0.19	0.2854E 02	
63	3677.03	724.90	22.83	NI	3675.5C	0.41	C.1811E 02	
67	3778.30	1011.01	16.45	NI	3779.30	0.17	0.5898E 02	FE
68	3781.65	981.03	17.33	NI	3775.3C	0.17	0.5713E 02	MN CR FE
72	3530.00	750.35	23.87	NI	3530.00	0.35	0.2C36E C2	PA CR
83	4285.27	555.14	30.78	NI	4283.60	0.40	0.1230E 02	
86	4408.52	5561.93	4.01	NI	4405.10	0.14	0.3441E C3	FE
92	4675.11	1346.73	13.61	NI	4674.6C	0.18	0.6408E 02	FE
97	4858.77	512.91	35.68	NI	4858.6C	1.17	0.3754E 01	
103	5048.62	1414.35	13.12	NI	5067.50	0.11	0.1102E 03	MN
104	5088.41	553.91	32.46	NI	5087.2C	0.13	0.3654E 02	
105	5111.90	554.92	31.42	NI	5110.80	0.13	C.3661E 02	MN
107	5180.39	1731.75	11.64	NI	5178.40	0.12	0.1239E C3	CO MN
110	5268.65	1782.78	10.65	NI	5267.70	0.49	0.3130E 02	CC CR
111	5312.04	525.28	20.64	NI	5312.30	1.11	C.7182E C1	
115	5436.26	1325.56	14.42	NI	5436.00	0.95	0.2094E 02	MN
121	5648.39	583.72	33.70	NI	5645.4C	1.02	0.5041E 01	
126	5819.00	1536.75	11.10	NI	5816.80	2.34	0.7369E 01	
127	5835.55	741.31	27.75	NI	5836.7C	0.68	0.9722E 01	
132	6038.10	1267.71	17.43	NI	6034.10	0.19	0.6091F 02	
133	6104.61	2565.17	8.41	NI	6105.00	2.08	0.1137E 02	MN
136	6152.94	536.94	37.82	NI	6156.50	0.15	C.3323E 02	
145	6583.48	1015.84	20.07	NI	6583.60	1.95	0.5198E 01	
151	6837.32	7240.14	3.74	NI	6837.00	11.91	0.6373E 01	
152	6887.48	1156.25	15.15	NI	6888.40	0.11	0.1115E 03	CR
154	6983.09	630.14	35.04	NI	6983.10	0.12	0.5670F 02	CO
164	7539.36	3135.48	9.63	NI	7537.00	4.43	C.7749E 01	
168	7699.00	890.43	30.26	NI	7696.80	1.36	0.8272E C1	
170	7821.15	4773.96	5.87	NI	7818.50	9.04	0.6888E 01	
175	8071.77	468.25	34.99	NI	8069.20	0.15	C.4320E C2	
176	8121.53	1496.51	12.12	NI	8120.50	3.47	0.6045E 01	
181	8534.52	8723.46	3.81	NI	8533.4C	18.74	0.7342E 01	
186	9000.00	15501.94	3.37	NI	8958.80	41.65	0.6956E C1	
6	1747.10	482.52	29.90	PA	1747.00	2.95	C.3404E 01	
8	1809.88	2546.65	6.71	PA	1810.40	35.80	0.1249E 01	
13	2044.73	460.45	33.27	PA	2044.30	2.43	C.2215E 01	
14	2065.48	682.07	21.60	PA	2062.60	1.89	0.4088E C1	FE
15	2112.71	1866.37	9.02	MN	2113.20	18.85	0.1048E 01	FE
24	2469.70	938.34	16.79	MN	2471.50	0.98	0.1137E C2	FE
30	2620.35	556.76	27.75	PA	2621.30	0.84	0.4063E 01	CR
34	2696.85	658.36	24.80	MN	2656.50	0.36	0.1053F 02	FE
40	2569.66	596.42	16.45	PA	2969.80	0.30	0.1574E C2	NI FE
42	3060.79	522.48	30.46	PA	3060.20	0.27	0.8629E 01	FE
45	3267.35	3897.48	5.15	PA	3267.50	0.83	0.1855E C2	NI CR FE
52	3371.04	422.03	38.87	PA	3372.90	0.56	0.7829F 01	NI
58	3508.48	945.03	17.82	MN	3555.50	0.28	0.1059E 02	
60	3580.83	812.75	15.93	PA	3580.80	0.21	0.1329E 02	
68	3781.65	981.03	17.33	PA	3783.10	0.22	0.1429E 02	NI CR FE
71	3854.59	4594.15	4.44	PA	3858.40	C.57	0.2528E C2	FE
72	3930.00	750.35	23.87	PA	3929.10	0.76	0.3034E 01	NI CR
79	4158.97	945.58	18.29	PA	4155.60	0.13	0.2102E 02	
80	4218.90	13424.68	2.25	PA	4222.70	0.88	0.4394E 02	FE
81	4264.48	780.47	22.72	PA	4267.70	0.51	0.4374E 01	
85	4378.18	787.63	23.18	PA	4380.30	0.44	0.5034E 01	FE
87	4447.25	727.23	24.25	PA	4446.20	1.10	0.1845E 01	

TABLE VI(2) (CONTINUED)

91	4567.62	640.26	27.24	PA	4566.90	1.94	0.1154E C1
93	4124.56	1342.04	13.40	PN	4724.70	2.33	0.1596E 01
94	4789.69	509.40	35.52	MN	4792.80	0.23	0.6137E 01
98	4874.00	1017.51	18.29	PA	4875.60	0.84	0.3359E C1 CR
99	4949.86	3408.29	5.57	PN	4949.70	1.47	0.6430E 01 FE
101	5015.30	2594.94	7.65	PA	5014.70	5.54	0.1280E 01
103	5068.62	1414.35	13.12	PA	5067.40	3.18	0.1234E 01 NI
105	5111.90	554.92	31.42	MN	5111.40	0.31	0.4969E 01 NI
106	5138.70	897.01	20.61	PN	5135.10	0.13	0.1916E C2 FE
107	5180.39	1731.75	11.04	PN	5181.20	3.20	0.1504E 01 CO NI
109	5252.71	776.82	23.96	MN	5253.90	1.29	0.1676E 01
115	5436.26	1325.56	14.52	PA	5435.70	2.09	0.1783E C1 NI
117	5529.36	2312.20	8.57	PN	5527.20	6.94	0.9386E 00
125	5920.50	30194.29	1.47	PA	5921.30	1.01	0.8705E C2 FE
133	6104.61	2565.17	8.41	PA	6104.50	1.90	0.4028E 01 NI
145	6794.17	981.98	21.75	MN	6783.70	3.46	0.9528E 00
153	6930.48	725.98	30.14	PA	6929.00	2.57	0.9766E C0
156	7058.30	3484.54	7.31	PA	7057.90	11.35	0.1090E 01 CO
158	7158.60	2125.14	11.76	MN	7159.90	6.06	0.1272E 01
159	7245.66	4556.86	6.17	PA	7243.50	12.05	0.1397E 01
1	1512.58	585.36	28.64	CC	1515.60	2.82	0.3207E C1
107	5190.39	1731.75	11.04	CC	5181.70	2.16	0.8364E 00 MN NI
110	5268.65	1782.74	10.69	CC	5270.00	1.11	0.1679E C1 NI CR
119	5660.62	555.41	24.52	CC	5660.30	6.21	0.9613E-C1
154	6583.09	630.14	35.04	CO	6585.10	2.82	0.2931E 00 NI
156	7058.30	3484.54	7.31	CC	7055.90	1.65	0.2815E 01 MN

lated gamma ray energies for possible correspondence was 4 keV. This is approximately twice the error in the calculated energies and was set large in order to facilitate evaluation of the interference effects.

In the remaining pages of Table VI(2) are shown the results of the analysis. The first four columns of the table represent the GAMANL output data which were supplied as input to WTANAL. These are the peak number, the peak energy, the Gaussian peak area and its percent error. In columns 4, 5 and 6 are given the elements and the energies and intensities of their capture gamma rays (obtained from reference [R2]) for which there are corresponding peaks in the actual spectrum. The intensities are in photons per 100 neutron captures in the particular elements. In column 7 are given the weights of the elements evaluated by equation (6.1), and in column 8 are listed the elements, if any, that cause interference effects.

Note that the calculated weights of the elements obtained by analysing the intense gamma rays of the elements in Table VI(2) compare well with the actual concentrations given in Table V(1). The errors in the calculated weights are due to errors in the peak area measurement and in the intensity values.

A weighted average of the weight of each element considered in WTANAL was obtained using the equation

$$\bar{M}_c = \frac{\sum_i [M_{c,i} / \sigma_i^2(A_G)]}{\sum_i [1 / \sigma_i^2(A_G)]} \quad . \quad (6.2)$$

For these computations use was made of only those characteristic capture gamma rays of the elements for which the following conditions were satisfied:

- (a) gamma ray intensity greater than 1 photon per 100 neutron captures in the particular element
- (b) error in the measured peak area less than 20 percent
- (c) interference effects not significant.

The results are shown below and compared to the data supplied by the manufacturer of the sample. The agreement is good. The cobalt lines were destroyed by interference effects; the 1810 and 2113 Mn gamma rays are decay gamma rays and were not considered. It was not possible to evaluate the errors in the calculated weights since the errors in the tabulated intensities are not available.

<u>Element</u>	<u>Gamma Rays Considered</u>	<u>Calculated Weights(g)</u>	<u>Manufacturer's Data</u>
Fe	14	55.9	54.48
Cr	19	17.9	14.39
Ni	9	6.9	7.37
Mn	9	1.29	1.32
Co	-	-	0.071

6.4 Manganese Peaks in the Spectrum

From Table VI(2) it is seen that the WTANAL code has identified in the stainless steel spectrum 42 capture gamma

peaks whose energies correspond to those of Mn. Of these only 9 yielded weights that could be used reliably in equation (6.2). The remaining peaks were either too weak or subject to serious interference effects.

From reference [R2], Mn has 101 capture gamma rays of energy greater than 1.5 MeV. The purpose of this section is to examine which of these gamma rays have not appeared in the spectrum and how their expected areas compare to the peak area limiting levels.

In the first 3 columns of Table VI(3) are listed the number, the energy and the intensity of each of these 101 Mn gamma rays. The energies are in keV and the intensities are in photons per 100 neutron captures. In columns 4, 5 and 6 are given the peak area limiting levels evaluated by equations (3.21), (3.22) and (3.23). Equation (5.1a) for the fwhm was also used together with non-averaged data for the background continuum obtained from the actual smoothed spectrum. Typical values for the critical level, the detection level and the determination level are 250, 500 and 800 counts respectively. In the 7th column are listed the peak areas which the Mn in the sample is expected to produce. These were obtained from the equation

$$A(\text{expected}) = (\sum_a V)_{\text{Mn}} \phi t \Omega \epsilon_{\text{PS}} (1/100) . \quad (6.2)$$

From Table V(1) the $\sum_a V$ value for manganese is 0.193 cm^2 . Comparison of the expected areas with the limiting levels shows that

TABLE VI(3)

EXPECTED AND ACTUAL PEAK AREAS FROM MANGANESE IN SS-303 SAMPLE AND
CORRESPONDING PEAK AREA LIMITING LEVELS

MN CAPTURE GAMMA RAYS			AREA LIMITING LEVELS			EXPECTED	EXPERIMENTAL DATA	
NO.	ENERGY	INTEN.	A(CRIT)	A(DET)	A(MIN)	AREA	AREA	ERROR INTERFERENCE
1	1705.4	1.20	230.	466.	730.	72.		
2	1747.0	2.85	232.	469.	734.	188.	482.9	29.9 CU
3	1810.4	35.80	238.	481.	752.	2702.	2546.7	6.7 DECAY
4	1876.2	0.81	231.	469.	733.	69.		
5	1915.2	2.15	235.	475.	743.	197.		
6	1987.6	2.36	235.	476.	745.	244.		
7	2044.3	2.43	233.	472.	738.	275.	460.5	33.3
8	2062.6	1.89	235.	475.	742.	220.	682.1	21.6 FE
9	2090.5	0.98	240.	485.	758.	119.		
10	2113.2	18.85	243.	492.	769.	2361.	1866.4	9.0 DECAY, FE
11	2175.2	2.25	239.	483.	755.	306.		
12	2258.2	0.41	241.	489.	763.	62.		
13	2294.1	1.36	241.	488.	762.	214.		
14	2330.9	3.13	246.	498.	777.	512.	1860.4	9.0 CR
15	2369.5	0.56	247.	500.	780.	95.		
16	2437.1	1.13	245.	495.	773.	206.		
17	2453.8	0.31	250.	505.	788.	58.		
18	2471.5	0.58	246.	497.	776.	109.	938.3	16.8 FE
19	2508.8	0.32	249.	505.	787.	63.		
20	2521.8	0.94	249.	504.	786.	186.	679.5	22.9 FE
21	2593.7	0.75	245.	496.	775.	158.		
22	2610.1	0.28	249.	504.	787.	60.		
23	2621.3	0.84	252.	509.	794.	182.	556.8	27.8 CR
24	2658.0	0.66	251.	508.	793.	147.		
25	2676.9	0.97	256.	518.	808.	220.		

TABLE VI(3) (CONTINUED)

MN CAPTURE GAMMA RAYS			AREA LIMITING LEVELS			EXPECTED	EXPERIMENTAL DATA		
NO.	ENERGY	INTEN.	A(CRIT)	A(DET)	A(MIN)	AREA	AREA	ERROR	INTERFERENCE
26	2696.9	0.36	260.	526.	820.	83.	658.4	24.8	FE
27	2856.4	0.41	259.	524.	817.	106.			
28	2863.5	0.29	255.	516.	805.	75.			
29	2925.6	0.37	257.	521.	812.	100.			
30	2969.8	0.30	256.	517.	807.	84.	996.4	16.5	NI, FE
31	3003.2	0.70	256.	518.	807.	200.			
32	3060.2	0.27	259.	523.	816.	80.	552.5	30.5	FE
33	3144.4	0.24	262.	529.	826.	75.			
34	3203.6	0.28	266.	538.	839.	91.			
35	3267.5	0.83	268.	542.	844.	278.	3897.5	5.2	NI, CR, FE
36	3321.1	0.19	262.	531.	827.	65.			
37	3347.0	0.61	269.	543.	847.	213.			
38	3372.9	0.56	268.	541.	843.	198.	422.0	38.9	NI
39	3408.5	3.38	274.	553.	861.	1213.	5345.1	4.0	FE
40	3457.4	0.23	269.	543.	847.	84.			
41	3498.9	0.67	267.	540.	842.	250.			
42	3555.5	0.28	259.	523.	816.	107.	854.3	19.6	
43	3580.8	0.21	260.	525.	820.	81.	812.8	19.9	FE
44	3626.6	0.51	265.	536.	836.	200.			
45	3642.1	0.45	266.	539.	840.	178.			
46	3667.8	0.19	265.	537.	837.	76.			
47	3751.4	0.33	263.	532.	830.	135.			
48	3783.1	0.22	263.	532.	831.	91.	981.0	17.3	NI, CR, FE
49	3815.0	1.51	271.	549.	856.	630.			LOST
50	3858.4	0.57	272.	549.	856.	241.	4594.1	4.4	FE

TABLE VI(3) (CONTINUED)

MN CAPTURE GAMMA RAYS			AREA LIMITING LEVELS			EXPECTED	EXPERIMENTAL DATA		
NO.	ENERGY	INTEN.	A(CRIT)	A(DET)	A(MIN)	AREA	AREA	ERROR	INTERFERENCE
51	3929.1	0.76	269.	544.	848.	327.	750.4	23.9	NI, CR
52	3979.7	0.30	272.	550.	858.	131.			
53	4030.1	0.22	275.	556.	867.	97.			
54	4101.3	0.13	275.	556.	866.	58.			
55	4199.6	0.13	274.	554.	864.	60.	945.6	18.3	
56	4222.7	0.88	276.	558.	871.	405.	13424.7	2.3	FE
57	4267.7	0.51	277.	560.	873.	236.	780.5	22.7	
58	4348.1	0.35	283.	572.	892.	164.			
59	4380.3	0.44	287.	579.	903.	207.	787.6	23.2	FE
60	4413.1	0.24	288.	583.	908.	113.			
61	4446.2	1.10	284.	574.	895.	522.	727.2	24.3	
62	4549.8	0.33	282.	571.	890.	157.			
63	4566.9	1.54	282.	570.	890.	735.	640.3	27.2	
64	4587.8	0.33	282.	571.	891.	157.			
65	4613.8	0.14	283.	572.	892.	67.			
66	4644.6	0.77	282.	570.	889.	368.			
67	4690.0	0.85	287.	580.	905.	406.			
68	4724.7	2.33	281.	569.	889.	1113.	1342.0	13.4	
69	4780.3	0.22	281.	569.	889.	105.			
70	4792.8	0.23	283.	573.	894.	110.	509.4	35.5	
71	4829.1	0.57	299.	606.	944.	272.			
72	4875.6	0.84	290.	587.	915.	401.	1017.9	18.3	CR
73	4907.5	0.58	289.	585.	912.	277.			
74	4932.7	0.17	291.	589.	919.	81.			
75	4949.7	1.47	292.	590.	921.	702.	3408.3	6.0	FE

TABLE VI(3) (CONTINUED)

MN CAPTURE GAMMA RAYS			AREA LIMITING LEVELS			EXPECTED	EXPERIMENTAL DATA		
NO.	ENERGY	INTEN.	A(CRIT)	A(DET)	A(MIN)	AREA	AREA	ERROR	INTERFERENCE
76	4970.3	0.32	290.	587.	916.	153.			
77	5014.7	5.54	289.	585.	913.	2644.	2554.9	7.7	
78	5034.7	0.90	290.	587.	917.	429.			
79	5067.4	3.18	288.	582.	909.	1517.	1414.4	13.1	NI
80	5111.4	0.31	286.	578.	902.	148.	554.9	31.4	NI
81	5135.1	0.13	286.	579.	904.	62.	897.0	20.6	FE
82	5181.2	3.20	291.	588.	919.	1525.	1731.8	11.0	CO, NI
83	5199.0	0.38	295.	596.	931.	181.			
84	5253.9	1.29	291.	588.	919.	614.	776.8	24.0	
85	5405.2	0.28	299.	605.	944.	132.			
86	5435.7	2.09	299.	604.	944.	987.	1329.6	14.5	NI
87	5527.2	6.94	312.	632.	986.	3262.	2312.0	9.0	
88	5586.3	0.14	310.	626.	978.	66.			
89	5761.1	1.61	333.	672.	1048.	744.			LOST
90	5921.3	1.01	344.	696.	1084.	459.	30194.3	1.5	FE
91	6032.6	0.44	345.	697.	1086.	197.			
92	6104.5	1.90	324.	655.	1023.	843.	2565.2	8.4	NI
93	6430.1	0.75	311.	631.	988.	316.			
94	6556.0	0.15	318.	643.	1007.	62.			
95	6783.7	3.46	336.	680.	1063.	1365.	982.0	21.8	
96	6929.0	2.57	356.	720.	1126.	985.	726.0	30.1	
97	7038.7	0.18	370.	748.	1168.	67.			
98	7057.9	11.35	374.	757.	1181.	4234.	3484.9	7.3	CO
99	7159.9	6.06	389.	786.	1227.	2212.	2125.1	11.8	
100	7243.5	12.05	401.	810.	1263.	4320.	4556.9	6.2	
101	7270.6	3.08	408.	825.	1287.	1097.	15101.4	2.6	FE

- (a) 13 Mn gamma rays will yield peak areas greater than the determination level and can therefore be used for reliable quantitative determination
- (b) 9 gamma rays will yield areas between the detection level and the determination level, with errors ranging between 30 and 20 percent and should be restricted to qualitative analysis only
- (c) 13 gamma rays will yield areas between the critical and detection levels, with errors between 60 and 30 percent and will lead to unreliable detection if employed, and
- (d) 66 gamma rays will yield peak areas less than the critical level.

The objective of this analysis is to compare these results with the actual Mn gamma rays appearing in the spectrum. To facilitate the comparison the data obtained by the WTANAL code have been included in Table VI(3). The results are as follows:

- (a) Of the 13 Mn gamma rays expected to have peak areas above the determination level, 9 appeared in the spectrum and were used in the application of equation (6.2) for the evaluation of the average weight. Their energies were 4724.7, 5014.7, 5067.4, 5181.2, 5435.7, 5527.2, 7057.9, 7159.9 and 7243.5 keV. The two prominent decay gamma rays, of energies 1810.4 and 2113.2 keV, were also

distinctly visible but were not used in equation (6.2). Of the remaining two gamma rays, that of energy 3408.5 was masked by a strong Fe interference; the other, of energy 6783.7, had an error of 21.8 percent which is slightly larger than the 20 percent limit set for the determination level.

- (b) Of the 9 gamma rays expected to be suitable only for qualitative analysis, only the 4566.9, 5253.9 and 6929.0 keV were observed in the spectrum. Their peak area errors were 27.2, 24.0 and 30.1 percent, respectively. Two gamma peaks, the 3815.0 and the 5761.1, were probably lost in the background fit. The remaining four rays, of energies 2330.9, 4949.7, 6104.5 and 7270.6, were masked by strong interference effects from Cr, Fe, Ni and Fe, respectively.
- (c) Of the 13 gamma rays expected to have peak areas between the detection level and the critical level only two were observed in the spectrum. These were the 2044.3 keV gamma ray with a peak area error of 33.3 percent and that of energy 4446.2 with an error of 24.3 percent. The smaller error in the second case is due to either a slight error in the tabulated intensity for this peak or to some interference effect that has led to a peak area slightly larger than the one expected. Of the remaining 11 gamma rays, five were masked by interference effects; their energies are 3267.5, 3929.1, 4222.7, 4875.6, and 5921.3 keV. The other six, of energies 1987.6, 2175.2,

4644.6, 4690.0, 5034.7 and 6430.1, were not seen in the spectrum. The percent errors in the peaks corresponding to these gamma rays were probably larger than 40 percent and were therefore automatically excluded from the listing supplied by the GAMANL code.

- (d) Finally, of the 66 gamma rays expected to lead to peak areas less than the critical level were not seen, as expected. The peaks observed at the corresponding energies in the spectrum were attributed to other elements with the exceptions of those at energies 3555.5, 4199.6, 4267.7 and 4792.8 keV.

The presence or absence of peaks from the spectrum is thus seen to be in accordance with the predictions based on the peak area limiting levels, a conclusion that we set forth to prove. The minimum measurable weight of Mn in stainless steel is considered as an example in the following chapter.

Chapter VII

THE MINIMUM MEASURABLE WEIGHTS OF THE ELEMENTS

7.1 Introduction

Application of the minimum weight equation is straightforward if all the parameters on the right-hand side of equation (3.24) are known. Such information is not always available to persons who are likely to be interested in the practical applications of capture gamma rays in elemental analysis. It was therefore decided to evaluate the minimum measurable weights of the elements in cases where all the required information is known and then to develop equations that will permit extrapolation of the results to different samples and/or different experimental geometries and gamma detection systems.

The minimum weight requirements were evaluated for a stainless steel sample with the system operated in the Compton suppression mode and as a pair spectrometer. Both sets of data are presented below because, depending on the experimental arrangement, it is not immediately apparent whether it is the low energy or the high energy gamma rays that will be more advantageous or more convenient to use for elemental analysis. In practice use should be made of those characteristic capture gamma rays of the elements that yield spectral peaks whose area can be measured with the least error, irrespective of whether these are gamma rays of low or high energy. Sometimes gamma rays of lower yield are

of interest, however; for example, in large samples the high energy gamma rays with low self absorption may give a more accurate analysis.

7.2 Minimum Measurable Weights of the Elements in S. Steel

The stainless steel sample described in section 5.3.1 was used for this application together with the Compton suppression and pair spectrometer data shown in Figures 5.4 and 5.5. The spectra were in essence used to evaluate the background continuum resulting from the given experimental conditions. The presence of the photopeaks in the spectra was ignored and the minimum weight requirements were evaluated under the assumption that these peaks will not cause any interference effects.

It was noted in section 3.6 that any of the characteristic gamma rays of the elements can be used for elemental analysis. In this application, in order to evaluate the sensitivity limits, consideration was given only to twelve of the most prominent gamma rays of each element. Four of these gamma rays had energies less than 2 MeV and the other eight were above this limit. In the cases of H, C, Pb and Bi for which less than 12 capture gamma rays are reported in [R2], the analysis was applied to all the gamma rays available.

The values of the remaining parameters in equation (3.24) are now considered. The flux time product was assigned the value of 1.94×10^{13} n/cm² corresponding to the pair spectrum. As noted earlier, the Compton suppression data were multiplied by 14.6 in order to normalize them to those obtained with the

pair spectrometer. Values for the efficiencies were obtained from Tables IV(1) and IV(2) with appropriate corrections for the masonite plug in the gamma beam. Gamma ray self-shielding corrections were applied according to the information given in section 5.3.1. The solid angle was 1.59×10^{-5} . The energy-channel conversion factor was assigned the value of 2 keV/channel and the smoothing filter function chosen had $r = 1.34$. The system resolution was set equal to that obtained from the pair spectrum; the fwhm-energy equation is given by equation (5.1).

A computer program was written for the evaluation of the minimum measurable area and minimum weight of an element in a known spectrum. The code was named MINIMUM and is listed in Appendix V. Sample results of the analysis are shown in Table VII(1) for the minimum measurable weight of Mn in stainless steel. Let us consider the information presented in the first row of the Compton suppression option. Columns 2 and 3 give the energy and the intensity of a prominent Mn capture gamma ray. The intensity, which is 0.00877 in this case, is the number of gamma rays of energy 212.5 keV that will be emitted per gram of Mn of natural composition per incident thermal neutron/cm². The fourth column shows that, from equation (3.23), the minimum number of counts needed for quantitative determination at this position in the spectrum is approximately 30700 counts for the conditions described above. From equation (3.24), this number of counts corresponds to 0.33 grams of Mn (column 5). And

TABLE VII(1)

LIMITS FOR QUANTITATIVE DETERMINATION FOR MANGANESE

COMPTON SUPPRESSION

ELEM.	ENERGY KEV	INTENSITY P/G N/CM2	MIN.AREA COUNTS	MIN.WT GRAMS	WT PERCENT
MN	212.5	0.877E-02	0.307E 05	0.33E 00	0.42E 00
MN	314.3	0.517E-02	0.191E 05	0.43E 00	0.54E 00
MN	1747.0	0.415E-02	0.490E 04	0.55E 00	0.70E 00
MN	1987.6	0.344E-02	0.452E 04	0.73E 00	0.92E 00
MN	2330.9	0.456E-02	0.422E 04	0.60E 04	0.77E 00

PAIR SPECTROMETER

ELEM.	ENERGY KEV	INTENSITY P/G N/CM2	MIN.AREA COUNTS	MIN.WT GRAMS	WT PERCENT
MN	1747.0	0.415E-02	0.766E 03	0.54E 01	0.69E 01
MN	1987.6	0.344E-02	0.778E 03	0.42E 01	0.54E 01
MN	2330.9	0.456E-02	0.815E 03	0.21E 01	0.27E 01
MN	3408.5	0.492E-02	0.901E 03	0.98E 00	0.12E 01
MN	5014.7	0.807E-02	0.956E 03	0.48E 00	0.61E 00
MN	5527.2	0.101E-01	0.103E 04	0.42E 00	0.53E 00
MN	6783.7	0.504E-02	0.111E 04	0.11E 01	0.14E 01
MN	7057.9	0.165E-01	0.124E 04	0.39E 00	0.49E 00
MN	7159.9	0.883E-02	0.128E 04	0.77E 00	0.98E 00
MN	7243.5	0.175E-01	0.132E 04	0.41E 00	0.52E 00

since the stainless steel sample used had a weight of 78.83 grams, this requirement is equivalent to a Mn concentration of 0.42 percent, as shown in column 6.

In examining the results obtained for the remaining Mn gamma rays in the Compton suppression option, note that because of the rapid decrease in the background with increasing energy, the peak area determination level, column 4, decreases by as much as a factor of about 7. However, since the detection efficiency also decreases with energy, the Mn gamma ray most suitable for elemental analysis is also the most intense gamma ray of this element in this energy interval (approximately 200 to 3000 keV). (This is true for all the elements considered with the exceptions of Co, La, Mg and P). Therefore, the minimum concentration of Mn that can be measured with a 20 percent standard deviation in a stainless steel sample is 0.42 percent when the analysis is based on its 212.5 - keV gamma ray and when the data are accumulated under the experimental conditions described above.

The results obtained for the pair spectrometer are shown in the second part of the table (Table VII(1)). It is seen that for this mode of detection the minimum Mn requirement for analysis is 0.49 weight percent and corresponds to its gamma ray of energy 7057.9 keV. Observe that this is not the most intense gamma ray of Mn in this energy range (1.5 to 9 MeV). Note also that the A_{\min} values in this table are larger than those in Table VI(3) by $\sqrt{(2.189/2.0)} = 1.05$. This is because in Table VI(3) use was made of the actual energy-channel

conversion factor in the pair spectrum (2.189 keV/channel) whereas in the data presented in Table VII(1) a 2 keV/channel conversion was assumed to hold approximately for all the data obtained with the various detection modes. The dependence of the peak area limiting levels on the system resolution was discussed in the last paragraph of section 3.5.

The above results show that for an analysis based on a single capture gamma ray of Mn, both the Compton suppression system and the pair spectrometer have approximately the same analytical sensitivity. The extreme simplicity of the pair spectrum, however, favours considerably use of this detection mode.

Note that three Mn gamma rays appear in both the Compton and pair options in Table VII(1). The ratio of the minimum weight requirements for these two modes of detection are in accordance with the results shown in Fig. 5.6.

In Appendix IV are given the results for 75 elements similar to those in Table VII(1) for Mn. The data associated with the least concentration requirements by the two detection modes considered are given in Tables VII(2) and VII(3) for all the elements. The Compton suppression option is seen to be more sensitive than the pair spectrometer in all the cases with the exceptions of C, Si and Y. In a majority of the cases this is accounted for by the much higher detection efficiency at low energies. The capture gamma rays of Bi and Pb are greater than 3 MeV and therefore these elements are not present in Table VII(2). Note also that in

TABLE VII(2)

LIMITS FOR QUANTITATIVE DETERMINATION
COMPTON SUPPRESSION

ELEM.	ENERGY KEV	INTENSITY P/G N/CM2	MIN. AREA COUNTS	MIN. WT GRAMS	WT PERCENT
-----	-----	-----	-----	-----	-----
AG	199.5	0.124E 00	0.319E 05	0.24E-01	0.30E-01
AL	248.7	0.392E-03	0.251E 05	0.65E 01	0.82E 01
AS	472.2	0.147E-02	0.128E 05	0.13E 01	0.17E 01
AU	215.7	0.298E-01	0.299E 05	0.95E-01	0.12E 00
B	477.7D	0.267E-01	0.125E 05	0.74E-01	0.93E-01
B	497.5	0.126E-03	0.119E 05	0.15E 02	0.19E 02
BA	627.5	0.738E-03	0.980E 04	0.26E 01	0.33E 01
BE	853.5	0.161E-03	0.728E 04	0.11E 02	0.14E 02
BR	246.1	0.746E-02	0.259E 05	0.35E 00	0.44E 00
C	1261.2	0.497E-04	0.587E 04	0.40E 02	0.51E 02
CA	1942.5	0.339E-02	0.459E 04	0.73E 00	0.92E 00
CD	558.6	0.154E 02	0.107E 05	0.12E-03	0.16E-03
CE	662.3	0.903E-03	0.916E 04	0.21E 01	0.27E 01
CL	1951.3	0.121E 00	0.459E 04	0.20E-01	0.26E-01
CO	277.7	0.599E-01	0.224E 05	0.40E-01	0.51E-01
CR	835.1	0.863E-02	0.751E 04	0.21E 00	0.27E 00
CS	1300.9	0.790E-02	0.583E 04	0.26E 00	0.33E 00
CU	278.3	0.109E-01	0.222E 05	0.22E 00	0.28E 00
DY	185.7	0.671E 00	0.291E 05	0.39E-02	0.49E-02
ER	816.1	0.188E 00	0.770E 04	0.99E-02	0.13E-01
EU	208.0	0.931E 00	0.314E 05	0.32E-02	0.40E-02
F	596.2	0.281E-03	0.102E 05	0.69E 01	0.87E 01
FE	352.5	0.307E-02	0.172E 05	0.70E 00	0.89E 00
GA	691.7	0.276E-02	0.900E 04	0.70E 00	0.88E 00
GD	1185.4	0.888E 01	0.603E 04	0.22E-03	0.28E-03
GE	596.0	0.704E-02	0.102E 05	0.27E 00	0.35E 00
H	2223.3	0.200E 00	0.431E 04	0.13E-01	0.17E-01
HF	214.0	0.200E 00	0.304E 05	0.14E-01	0.18E-01
HG	367.8	0.922E 00	0.162E 05	0.23E-02	0.29E-02
HO	240.3	0.100E-01	0.264E 05	0.26E 00	0.33E 00
I	291.4	0.311E-02	0.213E 05	0.76E 00	0.96E 00
IN	273.3	0.734E-01	0.224E 05	0.33E-01	0.41E-01
IR	217.4	0.121E 00	0.292E 05	0.23E-01	0.29E-01
K	770.6	0.101E-01	0.790E 04	0.18E 00	0.23E 00
LA	289.1	0.385E-02	0.216E 05	0.61E 00	0.78E 00
LI	2032.5	0.841E-03	0.446E 04	0.30E 01	0.38E 01
LU	458.1	0.407E-01	0.130E 05	0.49E-01	0.62E-01

TABLE VII(2) (CONTINUED)

ELEM.	ENERGY KEV	INTENSITY P/G N/CM2	MIN.AREA COUNTS	MIN.WT GRAMS	WT PERCENT
----	-----*	-----	-----	-----	-----
MG	585.2	0.335E-03	0.102E 05	0.57E 01	0.72E 01
MN	212.5	0.877E-02	0.307E 05	0.33E 00	0.42E 00
MO	778.4	0.834E-02	0.786E 04	0.22E 00	0.28E 00
N	1887.9	0.126E-02	0.467E 04	0.19E 01	0.24E 01
NA	472.4	0.969E-02	0.128E 05	0.20E 00	0.26E 00
NB	191.0	0.294E-02	0.322E 05	0.99E 00	0.13E 01
ND	696.7	0.134E 00	0.899E 04	0.14E-01	0.18E-01
NI	465.1	0.676E-02	0.129E 05	0.29E 00	0.37E 00
OS	634.0	0.497E-02	0.973E 04	0.39E 00	0.50E 00
P	1413.1	0.571E-03	0.566E 04	0.37E 01	0.47E 01
PD	716.9	0.528E-02	0.851E 04	0.35E 00	0.45E 00
PR	178.4	0.397E-02	0.207E 05	0.46E 00	0.58E 00
PT	356.1	0.100E-01	0.170E 05	0.21E 00	0.27E 00
RB	556.8	0.658E-03	0.107E 05	0.29E 01	0.37E 01
RE	255.4	0.184E-01	0.244E 05	0.14E 00	0.17E 00
RH	217.4	0.935E-01	0.292E 05	0.30E-01	0.38E-01
RU	539.8	0.231E-02	0.109E 05	0.82E 00	0.10E 01
S	841.1	0.522E-02	0.744E 04	0.35E 00	0.45E 00
SB	332.7	0.100E-02	0.183E 05	0.22E 01	0.28E 01
SC	228.6	0.126E 00	0.280E 05	0.22E-01	0.27E-01
SE	613.9	0.122E-01	0.998E 04	0.16E 00	0.20E 00
SI	2092.9	0.919E-03	0.447E 04	0.28E 01	0.36E 01
SM	333.9	0.195E 02	0.183E 05	0.11E-03	0.14E-03
SN	1293.3	0.414E-03	0.582E 04	0.49E 01	0.62E 01
SR	1835.9	0.761E-02	0.476E 04	0.31E 00	0.39E 00
TA	271.1	0.205E-01	0.229E 05	0.12E 00	0.15E 00
TB	1442.6	0.185E-02	0.559E 04	0.12E 01	0.15E 01
TE	602.9	0.368E-02	0.101E 05	0.53E 00	0.67E 00
TI	1381.4	0.498E-01	0.580E 04	0.43E-01	0.54E-01
TL	348.6	0.310E-03	0.175E 05	0.70E 01	0.88E 01
TM	237.5	0.319E-01	0.266E 05	0.83E-01	0.10E 00
V	645.9	0.696E-02	0.956E 04	0.28E 00	0.35E 00
W	551.5	0.218E-02	0.107E 05	0.88E 00	0.11E 01
Y	776.9	0.244E-02	0.787E 04	0.76E 00	0.96E 00
YB	241.8	0.250E-01	0.257E 05	0.10E 00	0.13E 00
ZN	1077.5	0.217E-02	0.631E 04	0.87E 00	0.11E 01
ZR	934.5	0.473E-03	0.680E 04	0.38E 01	0.48E 01

TABLE VII(3)

LIMITS FOR QUANTITATIVE DETERMINATION
PAIR SPECTROMETER

ELEM.	ENERGY KEV	INTENSITY P/G N/CM2	MIN.AREA COUNTS	MIN.WT GRAMS	WT PERCENT
----	----	-----	-----	-----	-----
AG	5699.7	0.549E-02	0.106E 04	0.81E 00	0.10E 01
AL	7723.8	0.106E-02	0.135E 04	0.77E 01	0.97E 01
AS	6809.9	0.105E-02	0.111E 04	0.52E 01	0.66E 01
AU	6252.0	0.165E-01	0.102E 04	0.27E 00	0.35E 00
B	4443.0	0.153E-04	0.939E 03	0.25E 03	0.32E 03
BA	4096.3	0.873E-03	0.908E 03	0.45E 01	0.57E 01
BE	6810.0	0.397E-03	0.111E 04	0.14E 02	0.17E 02
BI	4171.1	0.362E-04	0.895E 03	0.10E 03	0.13E 03
BR	5914.2	0.363E-03	0.113E 04	0.13E 02	0.17E 02
C	4945.2	0.114E-03	0.967E 03	0.34E 02	0.43E 02
CA	6419.9	0.182E-02	0.103E 04	0.26E 01	0.33E 01
CD	2455.8	0.876E 00	0.821E 03	0.97E-02	0.12E-01
CE	4766.1	0.499E-03	0.936E 03	0.76E 01	0.96E 01
CL	6111.1	0.890E-01	0.107E 04	0.52E-01	0.66E-01
CO	5660.3	0.241E-01	0.105E 04	0.18E 00	0.23E 00
CR	8884.1	0.867E-02	0.981E 03	0.95E 00	0.12E 01
CS	5020.3	0.193E-02	0.957E 03	0.20E 01	0.25E 01
CU	7914.5	0.103E-01	0.971E 03	0.59E 00	0.75E 00
DY	5607.3	0.957E-01	0.105E 04	0.45E-01	0.58E-01
ER	6229.0	0.530E-02	0.104E 04	0.87E 00	0.11E 01
EU	2697.5	0.449E-01	0.858E 03	0.16E 00	0.20E 00
F	1889.5	0.175E-03	0.778E 03	0.98E 02	0.12E 03
FE	7631.6	0.768E-02	0.143E 04	0.11E 01	0.14E 01
GA	6360.0	0.313E-02	0.101E 04	0.15E 01	0.19E 01
GD	6749.8	0.198E 01	0.111E 04	0.27E-02	0.35E-02
GE	6116.3	0.415E-03	0.107E 04	0.11E 02	0.14E 02
H	2223.3	0.200E 00	0.803E 03	0.54E-01	0.68E-01
HF	5723.5	0.797E-02	0.107E 04	0.56E 00	0.71E 00
HG	5966.9	0.173E 00	0.112E 04	0.28E-01	0.35E-01
HO	5813.4	0.169E-02	0.109E 04	0.27E 01	0.34E 01
I	5197.8	0.566E-03	0.974E 03	0.70E 01	0.89E 01
IN	5891.9	0.633E-02	0.113E 04	0.76E 00	0.96E 00
IR	5957.7	0.200E-01	0.112E 04	0.24E 00	0.30E 00
K	5380.3	0.236E-02	0.978E 03	0.17E 01	0.21E 01
LA	5097.6	0.274E-02	0.936E 03	0.14E 01	0.18E 01
LI	2032.5	0.841E-03	0.769E 03	0.16E 02	0.20E 02
LU	5020.4	0.174E-02	0.957E 03	0.22E 01	0.28E 01

TABLE VII(3) (CONTINUED)

ELEM.	ENERGY KEV	INTENSITY P/G N/CM2	MIN.AREA COUNTS	MIN.WT GRAMS	WT PERCENT
-----	-----	-----	-----	-----	-----
MG	3916.7	0.637E-03	0.888E 03	0.63E 01	0.79E 01
MN	7057.9	0.165E-01	0.124E 04	0.39E 00	0.49E 00
MO	6919.3	0.579E-03	0.117E 04	0.10E 02	0.13E 02
N	5267.1	0.117E-02	0.965E 03	0.33E 01	0.42E 01
NA	6395.4	0.359E-02	0.104E 04	0.13E 01	0.17E 01
NB	5104.2	0.842E-04	0.938E 03	0.45E 02	0.57E 02
ND	6502.1	0.120E-01	0.106E 04	0.41E 00	0.52E 00
NI	8998.8	0.197E-01	0.912E 03	0.41E 00	0.52E 00
OS	5146.9	0.170E-03	0.954E 03	0.23E 02	0.29E 02
P	3900.3	0.649E-03	0.880E 03	0.61E 01	0.78E 01
PB	7367.7	0.476E-03	0.140E 04	0.16E 02	0.21E 02
PD	4794.6	0.493E-03	0.940E 03	0.77E 01	0.98E 01
PR	5140.2	0.133E-02	0.949E 03	0.29E 01	0.37E 01
PT	5254.6	0.144E-02	0.963E 03	0.27E 01	0.34E 01
RB	7624.1	0.987E-04	0.143E 04	0.85E 02	0.11E 03
RE	5910.2	0.184E-02	0.113E 04	0.26E 01	0.33E 01
RH	5347.2	0.122E-01	0.978E 03	0.33E 00	0.41E 00
RU	5022.8	0.166E-03	0.958E 03	0.23E 02	0.30E 02
S	5420.5	0.408E-02	0.998E 03	0.10E 01	0.13E 01
SB	6523.6	0.321E-03	0.104E 04	0.15E 02	0.19E 02
SC	8174.7	0.286E-01	0.878E 03	0.21E 00	0.26E 00
SE	6601.2	0.404E-02	0.107E 04	0.12E 01	0.16E 01
SI	4934.3	0.242E-02	0.965E 03	0.16E 01	0.20E 01
SM	5532.8	0.112E 00	0.103E 04	0.38E-01	0.48E-01
SN	3334.3	0.320E-04	0.879E 03	0.15E 03	0.19E 03
SR	1835.9	0.761E-02	0.758E 03	0.24E 01	0.31E 01
TA	5964.7	0.451E-03	0.112E 04	0.11E 02	0.13E 02
TB	5891.5	0.924E-03	0.113E 04	0.52E 01	0.66E 01
TE	2747.2	0.103E-02	0.841E 03	0.66E 01	0.84E 01
TI	6759.7	0.411E-01	0.112E 04	0.13E 00	0.17E 00
TL	5641.9	0.374E-03	0.105E 04	0.12E 02	0.15E 02
TM	5737.2	0.427E-02	0.107E 04	0.10E 01	0.13E 01
V	6517.2	0.112E-01	0.104E 04	0.43E 00	0.55E 00
W	5261.7	0.258E-02	0.964E 03	0.15E 01	0.19E 01
Y	6080.3	0.643E-02	0.109E 04	0.74E 00	0.93E 00
YB	5265.7	0.660E-02	0.965E 03	0.59E 00	0.75E 00
ZN	7862.9	0.118E-02	0.102E 04	0.53E 01	0.68E 01
ZR	6295.0	0.193E-03	0.103E 04	0.24E 02	0.30E 02

the particular case of boron, the 477.7-keV decay gamma ray resulting from the (n, α) reaction was included as additional information.

An overall impression of the sensitivity of capture gamma rays for elemental analysis can be obtained by examining Table VII(4) where the minimum weight requirements have been divided into a number of weight-percent groups. In approximately 67 percent of the cases the concentrations required for analysis range between 0.1 and 10 percent for both the Compton suppression system and the pair spectrometer. The results may be extended to the free-mode system by employing the data in Chapter V.

7.3 The development of Extrapolation Equations

The purpose of this section is to develop equations and present data that will permit extrapolation of the above results to different experimental arrangements and different samples. Consideration will be given first to the minimum weight requirements for the measurement of the elements in a stainless steel matrix, the emphasis being on changes that can be brought about by variations in the parameters on the right-hand side of equation (3.24).

In this case, of particular interest are the peak area determination level (which is specified by a standard deviation of $[100/k_2]$ percent in the peak area), the neutron flux (n/cm^2 sec), the irradiation time (secs), the fractional solid angle and the sample weight (grams). With reference to equations (3.18) and (3.24), and neglecting the 1 terms within the curly brackets, the effects of changes in these

TABLE VII(4)
LIMITS FOR QUANTITATIVE DETERMINATION
GROUPED DATA

COMPTON SUPPRESSION

Weight Percent Range	Number of Elements	Elements
10 - 100	3	B, Be, C
1 - 10	20	Al, As, Ba, Ce, F, Li, Mg, N, Nb, P, Rb, Ru, Sb, Si, Sn, Tb, Tl, W, Zn, Zr
0.1 - 1	31	Au, Br, Ca, Cr, Cs, Cu, Fe, Ga, Ge, Ho, I, K, La, Mn, Mo, Na, Ni, Os, Pd, Pr, Pt, Re, S, Se, Sr, Ta, Te, Tm, V, Y, Yb
0.01 - 0.1	13	Ag, Cl, Co, Er, H, Hf, In, Ir, Lu, Nd, Rh, Sc, Ti
0.001-0.01	3	Dy, Eu, Hg
.0001-.001	3	Cd, Gd, Sm

PAIR SPECTROMETER

> 100	5	B, Bi, F, Rb, Sn
10 - 100	14	Be, Br, C, Ge, Li, Mo, Nd, Os, Pb, Ru, Sb, Ta, Tl, Zr
1 - 10	33	Ag, Al, As, Ba, Ca, Ce, Cr, Cs, Er, Fe, Ga, Ho, I, K, La, Lu, Mg, N, Na, P, Pd, Pr, Pt, Re, S, Se, Si, Sr, Tb, Te, Tm, W, Zn
0.1 - 1	16	Au, Co, Cu, Eu, Hf, In, Ir, Mn, Nd, Ni, Rh, Sc, Ti, V, Y, Yb
0.01 - 0.1	6	Cd, Cl, Dy, H, Hg, Sm
0.001-0.01	1	Gd

parameters on the minimum weights can be approximated by the equation

$$R = \frac{(m'/M')}{(m/M)} = \frac{20.0}{(100/k_2)} \sqrt{\frac{78.83}{M'} \times \frac{1.735 \times 10^{13}}{\phi' t'} \times \frac{1.59 \times 10^{-5}}{(\Omega'/4\pi)}} \quad (7.1)$$

Here (m/M) represents the data given in the previous section and (m'/M') are the modified concentration requirements. The square root sign is a result of the linear dependence of the background continuum on M , ϕ , t and Ω . Thus, for instance, the results must be multiplied by 2 if the standard deviation in peak area is required to be 10 percent (i.e. $k_2 = 10$); and a 100-fold increase in the product $M\phi t \Omega / 4\pi$ will reduce the weight requirement by a factor of 10.

The effects of changes in the system resolution $w(\text{keV})$, the channel-energy conversion factor C ($\text{keV}/\text{channel}$), and the error reduction factor r are not as simple to evaluate. This is because, as shown in Appendix I, r depends on the number of channels occupied by typical peaks in a given spectrum and these, in turn, are a direct function of both w and C . If the smoothing filter function is chosen arbitrarily such that this correlation can be neglected, changes in these parameters will affect the weight requirements according to the equation

$$R = \frac{(m'/M')}{(m/M)} = \frac{w'(E-511y)}{w(E-511y)} \times \frac{1.34}{r} \times \sqrt{\frac{2.0}{C}} \quad (7.2)$$

where $w(E-511y)$ is given by equation (5.1). Recall that E is the energy of the incident gamma ray and that $y = 0$ for the

Compton suppression data and $\gamma = 2$ for the pair spectrometer.

An expression similar to equation (7.1) applies for changes in the detection efficiency.

Extrapolation of the results to different samples is also important. In this application it will be assumed that the parameters in equation (3.24), with the exceptions of the sample weight and the background continuum, have values identical to those given in section 7.2. The emphasis thus is on the amplitude and shape of the background continuum that will result from the irradiation of any given material. To this end let the background continuum be represented by the equation

$$B(E - 511\gamma) = N_B b(E - 511\gamma) \quad (7.3)$$

where N_B is the total number of counts between the energy limits E_1 and E_2 , and $b(E - 511\gamma)$ is a function representing the distribution of these counts over the spectrum (in counts per keV). Note that

$$\int_{E_1}^{E_2} b(E - 511\gamma) d(E - 511\gamma) = 1.0 \quad .$$

A number of spectra reported in [R2] were employed in attempts to obtain equations for N_B and $b(E - 511\gamma)$ that would be representative of all the elements. It was found that the total number of background counts could be approximated by the sum of three components according to the equation

$$N_B = N_{\text{capt}} + N_{\text{scat}} + N_{\text{backgr}} \quad (7.4)$$

where the first term represents the contribution to N_B resulting from neutron capture in the sample, N_{scat} is the contribution from neutron scattering by the sample and subsequent absorption in the surrounding structural material viewed by the detector, and N_{backgr} is the counts recorded without any sample in position. By normalizing the data obtained from [R2] to $\phi t \Omega / 4\pi = 2.745 \times 10^8 \text{ n/cm}^2$ for the stainless steel spectrum, it was possible to obtain the equation

$$N_B = [f_{\text{CS}} \sum_a V + 1.181 \sum_s V + 27.93] \times 10^6 \quad (7.5)$$

for the total Compton suppression counts between the energy limits $E_1 = 100 \text{ keV}$ and $E_2 = 2600 \text{ keV}$, and the equation

$$N_B = [f_{\text{PS}} \sum_a V + .00528 \sum_s V + .157] \times 10^6 \quad (7.6)$$

for the pair spectrometer with $E_1 = 1500 \text{ keV}$ and $E_2 = 9300 \text{ keV}$. In these equations \sum_a and \sum_s are the macroscopic neutron absorption and scattering cross sections (in cm^{-1}) and V is the sample volume (in cm^3). f_{CS} and f_{PS} are correction factors and are discussed below.

The N_{scat} numerical coefficients were evaluated by subtracting from the data the known N_{backgr} contribution and solving simultaneously the equations corresponding to two particular spectra. The carbon and nickel data given in Table VII(5) were chosen for this purpose. The f_{CS} and f_{PS} factors were then adjusted in order that the above equations agreed with the experimental data for the other

elements examined. The values obtained for these factors are given in Table VII(5) together with other pertinent data involved in the computations. In this table the weight of the materials is in grams, $(\phi t)_e$ are the effective flux time values in units of 10^{13} n/cm² which include corrections for flux depression and gamma self-shielding, and N_B' are the total counts (in units of 10^6) in the original un-normalized data between the energy limits E_1 and E_2 . To obtain the normalized counts use was made of the approximate equation

$$(N_B)_{\text{actual}} = N_B' [4\pi \cdot 2.745 \times 10^8 / (\phi t)_e \Omega] \quad (7.7)$$

The approximation involved in this equation is that the same effective flux time value was assumed to apply for all the components of N_B . Note that N_{scat} does not require a correction for gamma self-shielding and that N_{backgr} should not be adjusted for any of these two effects. These corrections amount to less than 10 to 15 percent in most cases. Moreover, since N_{scat} and N_{backgr} constitute only a small fraction of N_B , the approximations involved in obtaining equations (7.5) and (7.6) are justified.

Not included in Table VII(5) are the values for the solid angles. For the stainless steel spectra, as given in Sec. 5.3.3, the fractional solid angle was 1.59×10^{-5} . In all other cases the solid angle was 5.76×10^{-6} with the exceptions of the Sn and BaO pair spectra for which $\Omega/4\pi$ was 1.6×10^{-5} and the Mg, Al and CaO pair spectrometer data for which $\Omega/4\pi$ was 4.1×10^{-5} .

TABLE VII(5) - EXPERIMENTAL DATA EMPLOYED IN THE EVALUATION OF THE f_{CS} AND f_{PS} COEFFICIENTS
COMPTON SUPPRESSION PAIR SPECTROMETER

Sample	Weight	$\Sigma_a V$	$\Sigma_s V$	COMPTON SUPPRESSION				PAIR SPECTROMETER			
				Run	$(\phi t)_e$	N_B'	f_{CS}	Run	$(\phi t)_e$	N_B'	f_{PS}
SS303	78.83	2.64	8.38	9274	.133	14.79	67.4	9261	1.94	4.675	1.69
Backg	-	-	-	404	.104	1.055	-	414	2.57	.0848	-
C	240.7	.0411	57.98	512	.231	4.839	79.	440	2.62	.300	2.01
NaF	19.10	.1496	2.172	479	.627	11.88	399.	480	4.79	.620	2.99
Mg	10.96	.0171	.979	461	.937	6.711	296.	462	6.42	1.976	2.53
Al	28.40	.1490	.888	437	.258	3.647	258.	450	3.18	1.981	1.72
Si	46.86	.1616	1.717	471	.515	9.027	331.	470	5.97	.585	1.86
CC 4	1.748	.9097	.471	475	.245	6.429	106.	476	2.69	1.050	1.87
KF	41.93	.916	2.35	460	.251	11.06	196.	459	3.86	1.215	1.45
CaO	14.02	.0649	1.087	482	.902	8.746	261.	481	2.89	1.306	2.16
TiO ₂	9.149	.460	.936	428	.242	5.838	187.	427	3.00	.710	2.10
Fe	28.35	.8007	3.362	434	.201	6.258	146.				
	93.49	2.641	11.09					701	2.67	2.882	1.86
Ni	12.78	.6026	2.293	439	.263	4.315	79.	438	4.05	1.174	2.01
Zr	189.2	.225	9.99	402	.528	14.06	387.	401	4.44	0.418	1.06
Mo	90.7	1.54	3.98	526	.205	18.40	257.	506	4.72	2.525	1.54
Ag	5.33	1.88	.179	565	.158	19.89	306.	597	1.87	1.410	1.83
Sn	149.4	.434	3.03	594	.468	19.32	349.	602	3.71	2.363	1.94
Sb	31.65	.861	.673	559	.388	26.60	346.				
	51.3	1.39	1.09					608	3.34	1.345	1.26
BaO	51.48	.271	1.81	544	.455	15.00	468.	677	3.50	1.715	2.48
W	19.97	1.26	.327	448	.228	10.70	155.	447	3.61	.988	0.91

It is seen from Table VII(5) that the f_{CS} and f_{PS} factors can vary substantially between different materials. Nevertheless, one can still use the values of $f_{CS} = 200$ and $f_{PS} = 1.5$ for all the elements and specify that this will result in N_{capt} values that can be off by a factor of approximately 2.

The data employed in the development of equations (7.5) and (7.6) were also used to examine the shape of the background continuum. Typical $b(E - 511\gamma)$ distributions are shown in Figs. 7.1 and 7.2 for carbon, iron and silver. It was observed that the Compton suppression spectra can be characterized by the same distribution in a majority of the cases. For spectra obtained with the pair spectrometer the shape of the background continuum depends on the neutron binding energy of the irradiated sample, on the existence of intense gamma rays, and on the total fraction of capture gamma rays observed (see also reference [H8]). The distributions obtained for the elements listed in Table VII(5) are given in Tables VII(6) and VII(7). These were obtained by applying linear averaging over 100-keV intervals in the Compton suppression spectra, and over 200-keV intervals in the pair spectra.

The last three tables of this chapter present background data for a number of elements that are believed to be of practical interest. For cases where detailed information is not available, minimum weight estimates can be obtained by using the approximate N_B equations given above and by

assuming a typical shape for the background continuum. This procedure is expected to yield results accurate to within approximately a factor of 2.

Estimates for the minimum weight requirements for other materials can be obtained from the equation

$$R = [(m^*/M^*) / (m/M)]$$

$$= \frac{M}{M^*} \times \frac{\sqrt{N_B^*}}{\sqrt{N_B}} \times \frac{\sqrt{b^*(E - 511\gamma)}}{\sqrt{b(E - 511\gamma)}} \quad (7.8)$$

where the starred parameters correspond to the material of interest and the unstarred to stainless steel. Note that N_B^* is given by equation (7.7)

As a simple application of this equation let us consider the minimum weight of sulphur that can be measured in a carbon sample weighing 240.7 grams by basing the analysis on the 5420.5 - keV gamma ray of sulphur. Using the data in Table VII(5), and by applying direct interpolation to the carbon and stainless steel data in Table VII(7), equation (7.8) gives

$$R = \frac{78.83}{240.7} \times \frac{\sqrt{[1.82 \times .300 \times 10^6]}}{\sqrt{[4.675 \times 10^6]}} \times \frac{\sqrt{[0.89 \times 10^{-4}]}}{\sqrt{[1.41 \times 10^{-4}]}}$$

$$= 0.089$$

From Table VII(3), the minimum sulphur concentration for measurement in stainless steel is 1.3 percent. Therefore, for the carbon sample in question, the minimum sulphur concentration required is $1.3 \times 0.089 = 0.12$ percent approx-

ximately. It can be extended to different experimental parameters by equation (7.1). Work on coal samples [R3] is in good agreement with this result.

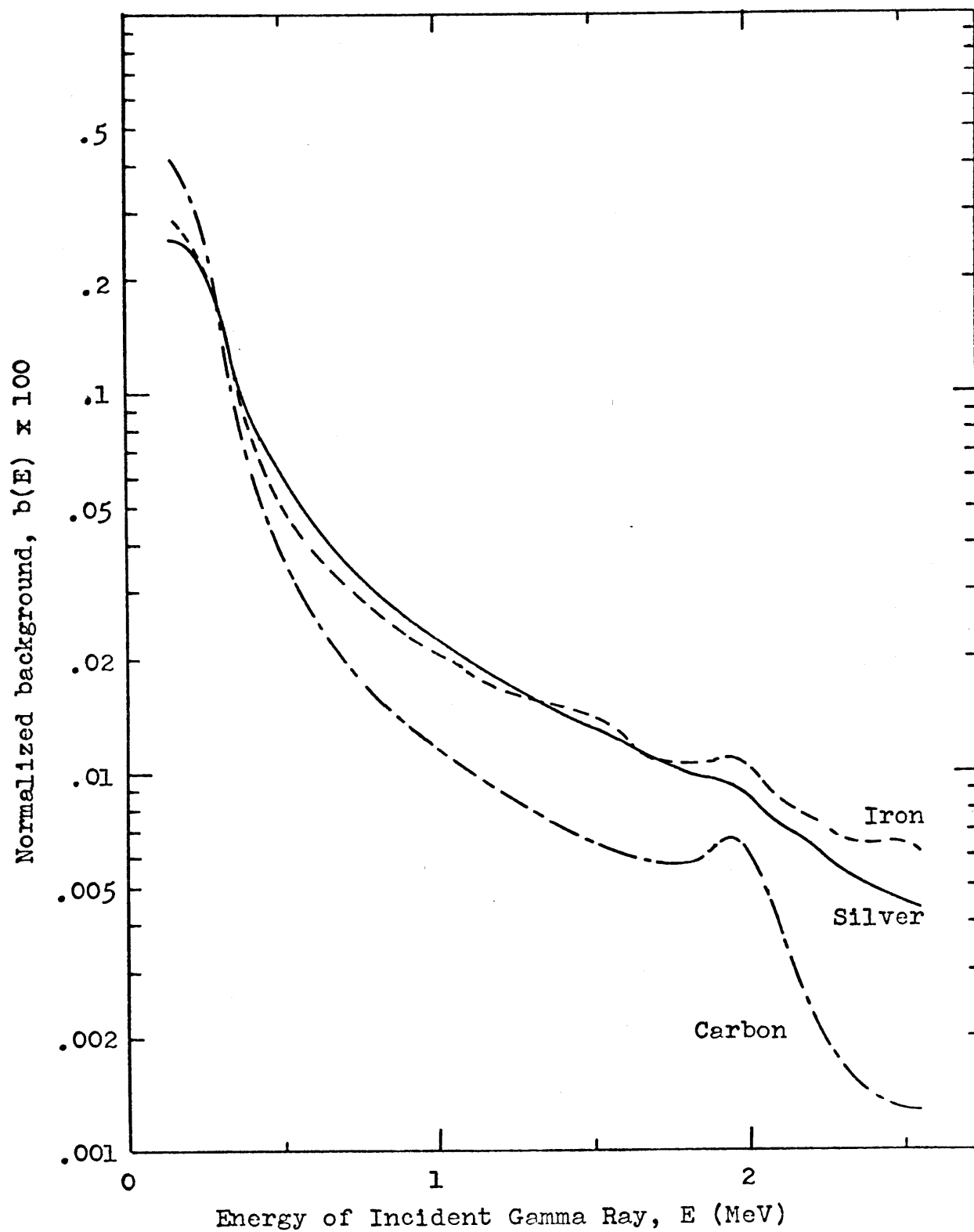


Fig. 7.1 Shape of background continuum
in Compton-suppression spectra

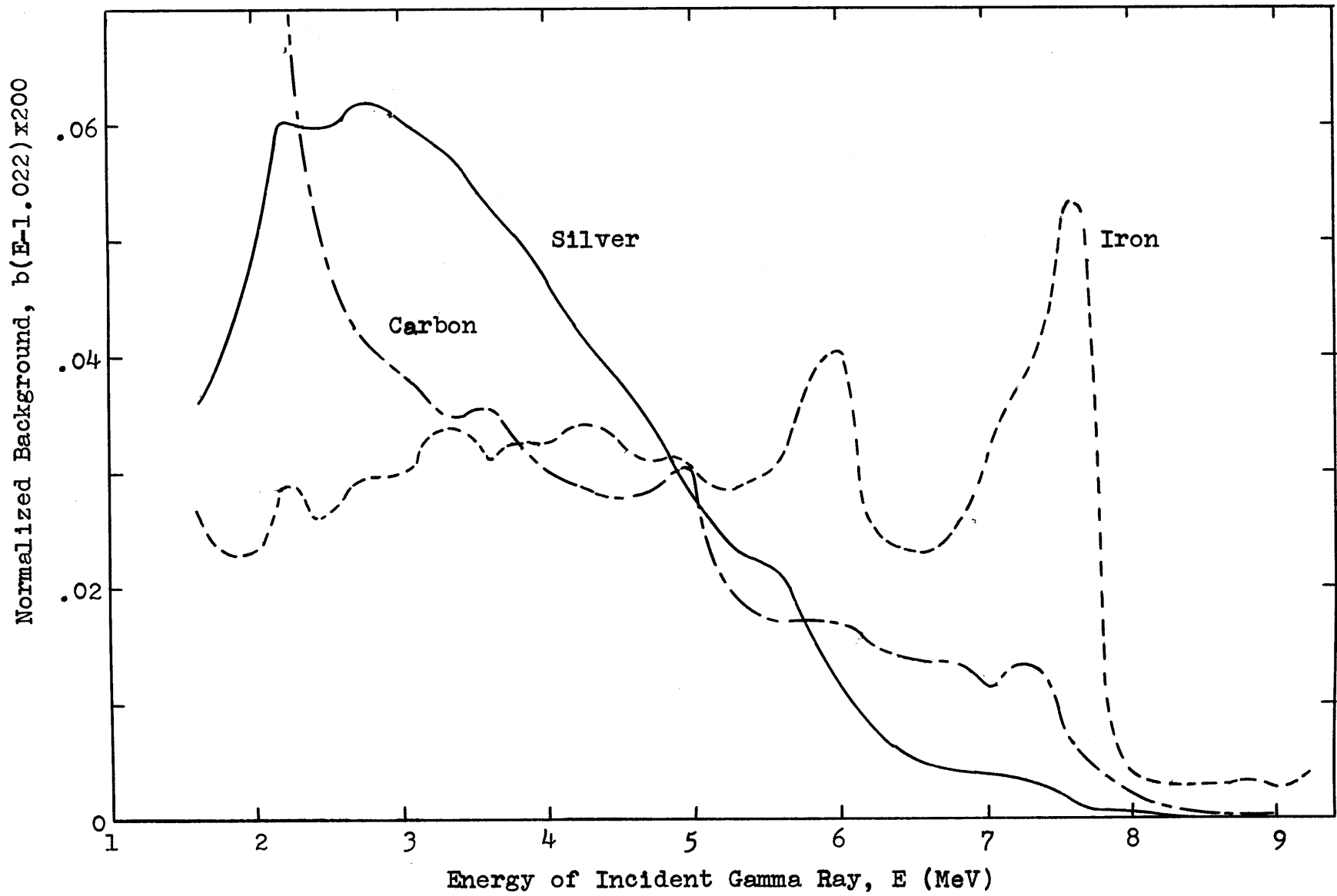


Fig. 7.2 Shape of background continuum in pair spectra

TABLE VII(6)

b(E) DISTRIBUTION IN COMPTON SUPPRESSION SPECTRA

ENERGY	S. STEEL	BACKGRND	CARBON	SODIUM	MAGNESIUM
-----	-----*	-----	-----	-----	-----
150.	0.84E-03	0.30E-02	0.41E-02	0.32E-02	0.31E-02
250.	0.29E-02	0.20E-02	0.27E-02	0.22E-02	0.23E-02
350.	0.15E-02	0.99E-03	0.89E-03	0.99E-03	0.96E-03
450.	0.86E-03	0.62E-03	0.47E-03	0.58E-03	0.58E-03
550.	0.58E-03	0.42E-03	0.29E-03	0.39E-03	0.40E-03
650.	0.45E-03	0.35E-03	0.22E-03	0.32E-03	0.32E-03
750.	0.34E-03	0.29E-03	0.17E-03	0.26E-03	0.27E-03
850.	0.27E-03	0.26E-03	0.15E-03	0.22E-03	0.23E-03
950.	0.23E-03	0.23E-03	0.13E-03	0.19E-03	0.20E-03
1050.	0.21E-03	0.20E-03	0.11E-03	0.17E-03	0.18E-03
1150.	0.19E-03	0.19E-03	0.94E-04	0.15E-03	0.16E-03
1250.	0.17E-03	0.17E-03	0.83E-04	0.14E-03	0.15E-03
1350.	0.17E-03	0.16E-03	0.73E-04	0.13E-03	0.14E-03
1450.	0.16E-03	0.15E-03	0.67E-04	0.12E-03	0.12E-03
1550.	0.14E-03	0.14E-03	0.62E-04	0.11E-03	0.12E-03
1650.	0.13E-03	0.13E-03	0.59E-04	0.11E-03	0.12E-03
1750.	0.12E-03	0.13E-03	0.58E-04	0.11E-03	0.12E-03
1850.	0.11E-03	0.13E-03	0.60E-04	0.12E-03	0.12E-03
1950.	0.10E-03	0.15E-03	0.68E-04	0.13E-03	0.15E-03
2050.	0.99E-04	0.92E-04	0.46E-04	0.94E-04	0.96E-04
2150.	0.93E-04	0.56E-04	0.32E-04	0.64E-04	0.59E-04
2250.	0.89E-04	0.35E-04	0.19E-04	0.45E-04	0.33E-04
2350.	0.83E-04	0.27E-04	0.14E-04	0.34E-04	0.22E-04
2450.	0.81E-04	0.24E-04	0.13E-04	0.33E-04	0.20E-04
2550.	0.78E-04	0.24E-04	0.13E-04	0.30E-04	0.20E-04

TABLE VII(6) (CONTINUED)

b(E) DISTRIBUTION IN COMPTON SUPPRESSION SPECTRA

ENERGY	ALUMINUM	SILICON	CHLORINE	POTASSIUM	CALCIUM
-----	-----	-----	-----	-----	-----
150.	0.32E-02	0.36E-02	0.26E-02	0.24E-02	0.29E-02
250.	0.22E-02	0.24E-02	0.20E-02	0.19E-02	0.23E-02
350.	0.94E-03	0.90E-03	0.11E-02	0.98E-03	0.10E-02
450.	0.59E-03	0.53E-03	0.71E-03	0.69E-03	0.63E-03
550.	0.41E-03	0.35E-03	0.52E-03	0.58E-03	0.42E-03
650.	0.34E-03	0.28E-03	0.40E-03	0.43E-03	0.33E-03
750.	0.29E-03	0.23E-03	0.33E-03	0.34E-03	0.27E-03
850.	0.24E-03	0.20E-03	0.28E-03	0.29E-03	0.24E-03
950.	0.21E-03	0.17E-03	0.26E-03	0.26E-03	0.21E-03
1050.	0.19E-03	0.16E-03	0.21E-03	0.24E-03	0.18E-03
1150.	0.17E-03	0.14E-03	0.18E-03	0.21E-03	0.17E-03
1250.	0.16E-03	0.12E-03	0.16E-03	0.19E-03	0.16E-03
1350.	0.15E-03	0.11E-03	0.15E-03	0.18E-03	0.15E-03
1450.	0.15E-03	0.99E-04	0.14E-03	0.16E-03	0.14E-03
1550.	0.15E-03	0.94E-04	0.13E-03	0.14E-03	0.13E-03
1650.	0.12E-03	0.91E-04	0.13E-03	0.14E-03	0.13E-03
1750.	0.99E-04	0.89E-04	0.12E-03	0.14E-03	0.13E-03
1850.	0.91E-04	0.93E-04	0.11E-03	0.13E-03	0.13E-03
1950.	0.99E-04	0.97E-04	0.11E-03	0.13E-03	0.16E-03
2050.	0.74E-04	0.70E-04	0.80E-04	0.10E-03	0.10E-03
2150.	0.53E-04	0.51E-04	0.69E-04	0.83E-04	0.58E-04
2250.	0.37E-04	0.39E-04	0.59E-04	0.71E-04	0.29E-04
2350.	0.33E-04	0.31E-04	0.54E-04	0.64E-04	0.21E-04
2450.	0.31E-04	0.31E-04	0.52E-04	0.56E-04	0.20E-04
2550.	0.30E-04	0.33E-04	0.52E-04	0.53E-04	0.19E-04

TABLE VII(6) (CONTINUED)

b(E) DISTRIBUTION IN COMPTON SUPPRESSION SPECTRA

ENERGY	TITANIUM	IRON	NICKEL	ZIRCONIUM	MOLYBDENUM
-----	-----	-----	-----	-----	-----
150.	0.25E-02	0.29E-02	0.27E-02	0.28E-02	0.24E-02
250.	0.20E-02	0.22E-02	0.22E-02	0.25E-02	0.22E-02
350.	0.98E-03	0.10E-02	0.10E-02	0.10E-02	0.11E-02
450.	0.64E-03	0.61E-03	0.64E-03	0.63E-03	0.79E-03
550.	0.48E-03	0.43E-03	0.41E-03	0.44E-03	0.67E-03
650.	0.40E-03	0.34E-03	0.36E-03	0.36E-03	0.48E-03
750.	0.35E-03	0.29E-03	0.29E-03	0.31E-03	0.36E-03
850.	0.31E-03	0.25E-03	0.25E-03	0.24E-03	0.26E-03
950.	0.28E-03	0.21E-03	0.22E-03	0.20E-03	0.22E-03
1050.	0.28E-03	0.20E-03	0.20E-03	0.17E-03	0.19E-03
1150.	0.30E-03	0.18E-03	0.18E-03	0.16E-03	0.17E-03
1250.	0.23E-03	0.17E-03	0.16E-03	0.14E-03	0.15E-03
1350.	0.18E-03	0.15E-03	0.15E-03	0.13E-03	0.13E-03
1450.	0.13E-03	0.14E-03	0.14E-03	0.11E-03	0.12E-03
1550.	0.12E-03	0.13E-03	0.13E-03	0.11E-03	0.94E-04
1650.	0.11E-03	0.11E-03	0.13E-03	0.10E-03	0.10E-03
1750.	0.10E-03	0.11E-03	0.12E-03	0.96E-04	0.96E-04
1850.	0.10E-03	0.10E-03	0.12E-03	0.93E-04	0.89E-04
1950.	0.12E-03	0.11E-03	0.13E-03	0.97E-04	0.89E-04
2050.	0.90E-04	0.91E-04	0.10E-03	0.73E-04	0.74E-04
2150.	0.67E-04	0.80E-04	0.88E-04	0.58E-04	0.63E-04
2250.	0.52E-04	0.71E-04	0.73E-04	0.48E-04	0.54E-04
2350.	0.47E-04	0.64E-04	0.67E-04	0.41E-04	0.48E-04
2450.	0.46E-04	0.65E-04	0.65E-04	0.39E-04	0.45E-04
2550.	0.45E-04	0.61E-04	0.63E-04	0.36E-04	0.41E-04

TABLE VII(6) (CONTINUED)

b (E) DISTRIBUTION IN COMPTON SUPPRESSION SPECTRA

ENERGY ENERGY	TIN SILVER	ANTIMONY TIN	BARIUM ANTIMONY	EUROPIUM BARIUM	TUNGSTEN TUNGSTEN
-----	-----+	-----	-----	-----	-----
150.	0.25E-02	0.25E-02	0.23E-02	0.25E-02	0.15E-02
250.	0.22E-02	0.22E-02	0.22E-02	0.23E-02	0.21E-02
350.	0.11E-02	0.11E-02	0.11E-02	0.11E-02	0.12E-02
450.	0.72E-03	0.67E-03	0.72E-03	0.69E-03	0.87E-03
550.	0.54E-03	0.48E-03	0.53E-03	0.47E-03	0.63E-03
650.	0.41E-03	0.38E-03	0.42E-03	0.37E-03	0.49E-03
750.	0.34E-03	0.32E-03	0.35E-03	0.30E-03	0.39E-03
850.	0.28E-03	0.28E-03	0.30E-03	0.26E-03	0.33E-03
950.	0.24E-03	0.25E-03	0.26E-03	0.22E-03	0.27E-03
1050.	0.21E-03	0.22E-03	0.22E-03	0.20E-03	0.24E-03
1150.	0.18E-03	0.19E-03	0.19E-03	0.18E-03	0.22E-03
1250.	0.17E-03	0.16E-03	0.17E-03	0.17E-03	0.20E-03
1350.	0.15E-03	0.14E-03	0.15E-03	0.14E-03	0.18E-03
1450.	0.14E-03	0.13E-03	0.14E-03	0.13E-03	0.17E-03
1550.	0.12E-03	0.12E-03	0.12E-03	0.12E-03	0.15E-03
1650.	0.11E-03	0.11E-03	0.11E-03	0.12E-03	0.14E-03
1750.	0.10E-03	0.11E-03	0.11E-03	0.11E-03	0.13E-03
1850.	0.96E-04	0.11E-03	0.11E-03	0.12E-03	0.12E-03
1950.	0.93E-04	0.11E-03	0.10E-03	0.14E-03	0.12E-03
2050.	0.79E-04	0.87E-04	0.81E-04	0.96E-04	0.10E-03
2150.	0.69E-04	0.67E-04	0.67E-04	0.64E-04	0.83E-04
2250.	0.59E-04	0.53E-04	0.54E-04	0.40E-04	0.74E-04
2350.	0.53E-04	0.46E-04	0.48E-04	0.31E-04	0.62E-04
2450.	0.48E-04	0.42E-04	0.44E-04	0.28E-04	0.58E-04
2550.	0.43E-04	0.39E-04	0.39E-04	0.26E-04	0.51E-04

TABLE VII(7)

b (E-1022) DISTRIBUTION IN PAIR SPECTROMETER SPECTRA

ENERGY	S. STEEL	BACKGRND	CARBON	SODIUM	MAGNESIUM
-----	-----+	-----	-----	-----	-----
1600.	0.14E-03	0.41E-03	0.46E-03	0.34E-03	0.32E-03
1800.	0.13E-03	0.34E-03	0.36E-03	0.30E-03	0.31E-03
2000.	0.13E-03	0.37E-03	0.33E-03	0.33E-03	0.39E-03
2200.	0.14E-03	0.52E-03	0.39E-03	0.46E-03	0.70E-03
2400.	0.14E-03	0.24E-03	0.29E-03	0.35E-03	0.43E-03
2600.	0.15E-03	0.20E-03	0.22E-03	0.27E-03	0.20E-03
2800.	0.15E-03	0.19E-03	0.20E-03	0.30E-03	0.19E-03
3000.	0.16E-03	0.18E-03	0.19E-03	0.22E-03	0.17E-03
3200.	0.16E-03	0.16E-03	0.18E-03	0.20E-03	0.15E-03
3400.	0.16E-03	0.17E-03	0.17E-03	0.18E-03	0.15E-03
3600.	0.16E-03	0.17E-03	0.18E-03	0.19E-03	0.15E-03
3800.	0.15E-03	0.15E-03	0.17E-03	0.17E-03	0.16E-03
4000.	0.15E-03	0.14E-03	0.15E-03	0.18E-03	0.15E-03
4200.	0.16E-03	0.14E-03	0.15E-03	0.14E-03	0.12E-03
4400.	0.16E-03	0.13E-03	0.14E-03	0.12E-03	0.10E-03
4600.	0.15E-03	0.14E-03	0.14E-03	0.11E-03	0.10E-03
4800.	0.15E-03	0.13E-03	0.15E-03	0.10E-03	0.98E-04
5000.	0.14E-03	0.13E-03	0.15E-03	0.10E-03	0.98E-04
5200.	0.14E-03	0.11E-03	0.10E-03	0.94E-04	0.87E-04
5400.	0.14E-03	0.11E-03	0.89E-04	0.92E-04	0.81E-04
5600.	0.15E-03	0.81E-04	0.84E-04	0.96E-04	0.75E-04
5800.	0.16E-03	0.83E-04	0.83E-04	0.83E-04	0.72E-04
6000.	0.17E-03	0.85E-04	0.84E-04	0.84E-04	0.69E-04
6200.	0.13E-03	0.76E-04	0.75E-04	0.96E-04	0.69E-04
6400.	0.12E-03	0.71E-04	0.71E-04	0.11E-03	0.69E-04
6600.	0.12E-03	0.85E-04	0.68E-04	0.61E-04	0.69E-04
6800.	0.13E-03	0.77E-04	0.68E-04	0.48E-04	0.68E-04
7000.	0.13E-03	0.78E-04	0.57E-04	0.43E-04	0.68E-04
7200.	0.16E-03	0.11E-03	0.66E-04	0.49E-04	0.86E-04
7400.	0.17E-03	0.93E-04	0.61E-04	0.52E-04	0.87E-04
7600.	0.16E-03	0.29E-04	0.33E-04	0.23E-04	0.33E-04
7800.	0.11E-03	0.10E-04	0.18E-04	0.13E-04	0.22E-04
8000.	0.58E-04	0.30E-05	0.11E-04	0.63E-05	0.15E-04
8200.	0.49E-04	0.0	0.39E-05	0.18E-05	0.93E-05
8400.	0.58E-04	0.0	0.36E-05	0.19E-05	0.48E-05
8600.	0.61E-04	0.0	0.29E-05	0.15E-05	0.38E-05
8800.	0.50E-04	0.0	0.16E-05	0.10E-05	0.33E-05
9000.	0.37E-04	0.0	0.13E-05	0.10E-05	0.24E-05
9200.	0.19E-04	0.0	0.64E-06	0.46E-06	0.18E-05

TABLE VII(7) (CONTINUED)

b (E-1022) DISTRIBUTION IN PAIR SPECTROMETER SPECTRA

ENERGY	ALUMINUM	SILICON	CHLORINE	POTASSIUM	CALCIUM
1600.	0.20E-03	0.27E-03	0.20E-03	0.22E-03	0.29E-03
1800.	0.26E-03	0.23E-03	0.18E-03	0.20E-03	0.30E-03
2000.	0.27E-03	0.26E-03	0.22E-03	0.26E-03	0.40E-03
2200.	0.47E-03	0.33E-03	0.24E-03	0.30E-03	0.69E-03
2400.	0.25E-03	0.24E-03	0.21E-03	0.25E-03	0.42E-03
2600.	0.17E-03	0.19E-03	0.19E-03	0.23E-03	0.18E-03
2800.	0.17E-03	0.20E-03	0.21E-03	0.24E-03	0.17E-03
3000.	0.19E-03	0.21E-03	0.21E-03	0.24E-03	0.15E-03
3200.	0.15E-03	0.21E-03	0.19E-03	0.23E-03	0.15E-03
3400.	0.17E-03	0.26E-03	0.19E-03	0.26E-03	0.14E-03
3600.	0.17E-03	0.33E-03	0.20E-03	0.26E-03	0.15E-03
3800.	0.17E-03	0.18E-03	0.18E-03	0.22E-03	0.13E-03
4000.	0.17E-03	0.16E-03	0.18E-03	0.23E-03	0.13E-03
4200.	0.18E-03	0.15E-03	0.17E-03	0.22E-03	0.13E-03
4400.	0.14E-03	0.16E-03	0.16E-03	0.18E-03	0.13E-03
4600.	0.16E-03	0.18E-03	0.16E-03	0.15E-03	0.11E-03
4800.	0.16E-03	0.23E-03	0.16E-03	0.14E-03	0.11E-03
5000.	0.12E-03	0.26E-03	0.16E-03	0.17E-03	0.11E-03
5200.	0.11E-03	0.98E-04	0.15E-03	0.16E-03	0.97E-04
5400.	0.10E-03	0.75E-04	0.15E-03	0.16E-03	0.94E-04
5600.	0.94E-04	0.72E-04	0.16E-03	0.15E-03	0.93E-04
5800.	0.89E-04	0.75E-04	0.17E-03	0.12E-03	0.94E-04
6000.	0.94E-04	0.76E-04	0.17E-03	0.51E-04	0.98E-04
6200.	0.94E-04	0.83E-04	0.15E-03	0.41E-04	0.10E-03
6400.	0.87E-04	0.93E-04	0.10E-03	0.36E-04	0.12E-03
6600.	0.85E-04	0.62E-04	0.11E-03	0.38E-04	0.77E-04
6800.	0.86E-04	0.61E-04	0.77E-04	0.42E-04	0.58E-04
7000.	0.84E-04	0.59E-04	0.68E-04	0.41E-04	0.55E-04
7200.	0.11E-03	0.72E-04	0.69E-04	0.35E-04	0.67E-04
7400.	0.13E-03	0.52E-04	0.82E-04	0.36E-04	0.70E-04
7600.	0.13E-03	0.19E-04	0.47E-04	0.34E-04	0.24E-04
7800.	0.87E-04	0.10E-04	0.35E-04	0.29E-04	0.16E-04
8000.	0.16E-04	0.79E-05	0.12E-04	0.69E-05	0.92E-05
8200.	0.62E-05	0.61E-05	0.74E-05	0.19E-05	0.44E-05
8400.	0.52E-05	0.54E-05	0.82E-05	0.15E-05	0.32E-05
8600.	0.40E-05	0.32E-05	0.76E-05	0.11E-05	0.23E-05
8800.	0.29E-05	0.93E-06	0.18E-05	0.67E-06	0.22E-05
9000.	0.22E-05	0.92E-06	0.50E-06	0.57E-06	0.14E-05
9200.	0.71E-06	0.26E-06	0.16E-06	0.17E-06	0.92E-06

TABLE VII(7) (CONTINUED)

b (E-1022) DISTRIBUTION IN PAIR SPECTROMETER SPECTRA

ENERGY	TITANIUM	IRON	NICKEL	ZIRCONIUM	MOLYBDENUM
-----	-----	-----	-----	-----	-----*
1600.	0.21E-03	0.13E-03	0.14E-03	0.27E-03	0.21E-03
1800.	0.17E-03	0.11E-03	0.11E-03	0.25E-03	0.21E-03
2000.	0.18E-03	0.12E-03	0.12E-03	0.28E-03	0.25E-03
2200.	0.24E-03	0.15E-03	0.15E-03	0.36E-03	0.31E-03
2400.	0.18E-03	0.13E-03	0.13E-03	0.26E-03	0.28E-03
2600.	0.15E-03	0.14E-03	0.12E-03	0.24E-03	0.28E-03
2800.	0.16E-03	0.15E-03	0.13E-03	0.23E-03	0.28E-03
3000.	0.17E-03	0.15E-03	0.14E-03	0.23E-03	0.28E-03
3200.	0.16E-03	0.17E-03	0.14E-03	0.24E-03	0.27E-03
3400.	0.17E-03	0.17E-03	0.13E-03	0.23E-03	0.26E-03
3600.	0.17E-03	0.16E-03	0.14E-03	0.23E-03	0.25E-03
3800.	0.17E-03	0.16E-03	0.14E-03	0.20E-03	0.24E-03
4000.	0.16E-03	0.16E-03	0.14E-03	0.19E-03	0.22E-03
4200.	0.16E-03	0.17E-03	0.14E-03	0.19E-03	0.21E-03
4400.	0.16E-03	0.17E-03	0.14E-03	0.17E-03	0.18E-03
4600.	0.16E-03	0.15E-03	0.14E-03	0.16E-03	0.17E-03
4800.	0.17E-03	0.16E-03	0.15E-03	0.14E-03	0.15E-03
5000.	0.17E-03	0.15E-03	0.14E-03	0.14E-03	0.13E-03
5200.	0.14E-03	0.14E-03	0.14E-03	0.13E-03	0.11E-03
5400.	0.14E-03	0.15E-03	0.14E-03	0.11E-03	0.10E-03
5600.	0.15E-03	0.16E-03	0.15E-03	0.96E-04	0.10E-03
5800.	0.16E-03	0.19E-03	0.15E-03	0.90E-04	0.80E-04
6000.	0.18E-03	0.20E-03	0.14E-03	0.95E-04	0.63E-04
6200.	0.22E-03	0.13E-03	0.13E-03	0.11E-03	0.55E-04
6400.	0.30E-03	0.12E-03	0.14E-03	0.89E-04	0.53E-04
6600.	0.25E-03	0.12E-03	0.15E-03	0.43E-04	0.52E-04
6800.	0.21E-03	0.13E-03	0.15E-03	0.43E-04	0.49E-04
7000.	0.46E-04	0.15E-03	0.12E-03	0.39E-04	0.40E-04
7200.	0.29E-04	0.18E-03	0.12E-03	0.43E-04	0.26E-04
7400.	0.27E-04	0.21E-03	0.12E-03	0.41E-04	0.26E-04
7600.	0.12E-04	0.27E-03	0.13E-03	0.21E-04	0.16E-04
7800.	0.78E-05	0.76E-04	0.12E-03	0.13E-04	0.75E-05
8000.	0.48E-05	0.18E-04	0.10E-03	0.60E-05	0.60E-05
8200.	0.30E-05	0.14E-04	0.10E-03	0.30E-05	0.51E-05
8400.	0.23E-05	0.14E-04	0.12E-03	0.28E-05	0.41E-05
8600.	0.11E-05	0.14E-04	0.12E-03	0.31E-05	0.14E-05
8800.	0.91E-06	0.15E-04	0.10E-03	0.98E-06	0.84E-06
9000.	0.96E-06	0.14E-04	0.90E-04	0.65E-06	0.63E-06
9200.	0.62E-06	0.18E-04	0.17E-04	0.42E-06	0.51E-06

TABLE VII(7) (CONTINUED)

b(E-1022) DISTRIBUTION IN PAIR SPECTROMETER SPECTRA

ENERGY	SILVER	TIN	ANTIMONY	BARIUM	TUNGSTEN
1600.	0.18E-03	0.22E-03	0.22E-03	0.32E-03	0.22E-03
1800.	0.20E-03	0.22E-03	0.24E-03	0.28E-03	0.23E-03
2000.	0.25E-03	0.27E-03	0.27E-03	0.33E-03	0.27E-03
2200.	0.30E-03	0.42E-03	0.34E-03	0.51E-03	0.35E-03
2400.	0.30E-03	0.29E-03	0.32E-03	0.32E-03	0.33E-03
2600.	0.30E-03	0.26E-03	0.30E-03	0.23E-03	0.32E-03
2800.	0.31E-03	0.27E-03	0.30E-03	0.22E-03	0.31E-03
3000.	0.30E-03	0.27E-03	0.30E-03	0.21E-03	0.29E-03
3200.	0.29E-03	0.25E-03	0.28E-03	0.20E-03	0.28E-03
3400.	0.28E-03	0.24E-03	0.27E-03	0.20E-03	0.27E-03
3600.	0.26E-03	0.23E-03	0.25E-03	0.20E-03	0.25E-03
3800.	0.25E-03	0.21E-03	0.24E-03	0.19E-03	0.22E-03
4000.	0.24E-03	0.20E-03	0.22E-03	0.22E-03	0.20E-03
4200.	0.21E-03	0.19E-03	0.20E-03	0.20E-03	0.18E-03
4400.	0.19E-03	0.17E-03	0.17E-03	0.15E-03	0.18E-03
4600.	0.18E-03	0.15E-03	0.15E-03	0.14E-03	0.17E-03
4800.	0.16E-03	0.15E-03	0.13E-03	0.13E-03	0.13E-03
5000.	0.14E-03	0.13E-03	0.11E-03	0.12E-03	0.12E-03
5200.	0.12E-03	0.11E-03	0.11E-03	0.10E-03	0.14E-03
5400.	0.11E-03	0.11E-03	0.95E-04	0.96E-04	0.11E-03
5600.	0.11E-03	0.89E-04	0.90E-04	0.93E-04	0.58E-04
5800.	0.78E-04	0.79E-04	0.81E-04	0.87E-04	0.60E-04
6000.	0.59E-04	0.73E-04	0.71E-04	0.69E-04	0.77E-04
6200.	0.40E-04	0.68E-04	0.56E-04	0.57E-04	0.86E-04
6400.	0.28E-04	0.57E-04	0.62E-04	0.52E-04	0.38E-04
6600.	0.26E-04	0.49E-04	0.39E-04	0.46E-04	0.21E-04
6800.	0.20E-04	0.45E-04	0.25E-04	0.43E-04	0.20E-04
7000.	0.20E-04	0.41E-04	0.15E-04	0.40E-04	0.20E-04
7200.	0.17E-04	0.44E-04	0.16E-04	0.44E-04	0.23E-04
7400.	0.13E-04	0.42E-04	0.15E-04	0.41E-04	0.23E-04
7600.	0.63E-05	0.18E-04	0.80E-05	0.20E-04	0.10E-04
7800.	0.36E-05	0.11E-04	0.48E-05	0.12E-04	0.46E-05
8000.	0.15E-05	0.77E-05	0.24E-05	0.79E-05	0.25E-05
8200.	0.70E-06	0.48E-05	0.12E-05	0.51E-05	0.12E-05
8400.	0.68E-06	0.37E-05	0.88E-06	0.39E-05	0.11E-05
8600.	0.38E-06	0.30E-05	0.85E-06	0.31E-05	0.89E-06
8800.	0.44E-06	0.25E-05	0.54E-06	0.25E-05	0.66E-06
9000.	0.13E-06	0.20E-05	0.52E-06	0.22E-05	0.37E-06
9200.	0.17E-06	0.21E-05	0.15E-06	0.15E-05	0.14E-06

Chapter VIII

SUMMARY AND CONCLUSIONS

This thesis evaluated the potential of neutron-capture gamma rays in elemental analysis. A large portion of the work was devoted to the development of a method for the analysis of weak peaks in gamma ray spectra. This was based on a new method of linear background fit and on equations developed for the standard deviation in the measurement of the various peak parameters. Consideration was also given to the reduction in the statistical fluctuations obtained by smoothing the data with the use of Fourier transforms. It was shown in Appendix III that the standard deviation in the number of counts H in a given channel can be represented by the equation

$$\sigma(H) = (1/r) \sqrt{H} \quad (8.1)$$

where r is the error reduction factor obtained by smoothing the data and is discussed in Appendix I.

Two methods of peak area determination were considered. These were the straight-sums approach (equation 3.6) and the Gaussian method (equation 3.7). The errors associated with these two equations were examined and it was found that the Gaussian area was to be preferred in a majority of the cases. The advantages of this method of area determination lies in the reduction of the standard deviation in the measured fwhm of a peak obtained by applying a least-squares fit to the fwhm

and energies of the intense peaks in the spectrum (Appendix II). It was therefore possible to approximate the error in the Gaussian area by the equation

$$\sigma(A_G) = 1.0645 \psi \bar{w} (1 + \alpha)(1/r) \sqrt{h + 1.5B} \quad (8.2)$$

and to use this information in chapter III to evaluate the three peak area limiting levels. These levels are denoted as the critical level, the detection level and the determination level and are given by the equations

$$A_{\text{crit}} = (2.23 \bar{w} / r) \sqrt{B} \quad (8.3)$$

$$A_{\text{det}} = (1.82 \bar{w} / r) [(1.68/r) + 2.45 \sqrt{B}] \quad (8.4)$$

$$A_{\text{min}} = (14.1 \bar{w} / r^2) [1 + \sqrt{(1 + 0.23 r^2 B)}] \quad (8.5)$$

and should be consulted in deciding whether a peak in a given spectrum is 'unreliable', 'good only for qualitative analysis' or 'good for reliable quantitative determination'. It was observed that irrespective of the amplitude of the continuum background the heights of the peaks corresponding to these three limiting levels are approximately $1.5 \sqrt{B}$, $3 \sqrt{B}$ and $5 \sqrt{B}$ when $r = 1.34$. For this value of r the limits correspond to peak area errors of approximately 60, 30 and 20 percent, respectively.

The minimum measurable concentration of an element in a given sample was considered in section 3.6. The equation derived was based on the peak area determination level and is given by

$$\frac{m}{M} = \frac{[14.1\bar{w}(E-511\gamma)/(Cr^2)]\{1 + \sqrt{[1 + 0.23Cr^2B(E-511\gamma)]}\}}{M \phi t \epsilon I (\Omega/4\pi)}. \quad (8.6)$$

Note that this equation gives the minimum weight requirement for elemental analysis based on the measurement of a single gamma ray. In practice use should be made of all the gamma rays of an element present in a given spectrum.

The equations presented above were verified (In Appendix III) by applying statistical analysis to the various parameters of 100 artificial peaks constructed with the use of a computer. The standard deviations obtained in these parameters were in agreement with the equations on which the peak area limiting levels were based. Also, in the same Appendix, an examination of three aluminum spectra for data reproducibility showed the differences in peak areas to be in accordance with the error equations.

An experimental verification of the equations was obtained in Ch. VI by examining the manganese peaks in a stainless steel pair spectrum. Since the manganese concentration in the irradiated sample was known, it was possible to compute the intensity of the 101 manganese peaks. By comparing these values with the corresponding peak area limiting levels, it was possible to specify which of the peaks would be clearly visible in the spectrum and which would be lost in the statistical fluctuations of the background. The conclusions arrived at were in good agreement with the 17 manganese peaks observed in the actual spectrum.

These equations were then used to examine the effectiveness of the two experimental arrangements and the various gamma detection modes. Results of the comparison were given in Chapter V. It was found that because of count-rate limitations both internal and external arrangements could be used with approximately the same analytical sensitivity. Comparison of the detection modes has shown that Compton suppression leads to an increase in the sensitivity of about 25 percent over that in the free mode; the pair spectrometer was found to be less sensitive than the free mode by approximately the same factor. For gamma rays of energy in the vicinity of 3 MeV, in which case the full-energy peak and the double-escape peak in our spectra have approximately the same intensity, any one of these modes can be used with the same effectiveness.

In Chapter 7 the minimum measurable weights of 75 elements were evaluated for a stainless steel matrix. In a majority of the cases the detection limits were found to range between 0.1 and 10 percent. Equations and data were then presented in Sec. 7.3 for extrapolating the results to different samples and different experimental arrangements.

In summary then, elemental analysis based on neutron-capture gamma ray spectra is characterized by complex gamma ray spectra and is insensitive in the trace-level domain for most elements. The method is likely to be found useful for on-line applications, as discussed in Chapter II, and for the detection of elements that do not satisfy the requirements of ordinary activation analysis.

APPENDIX I

EFFECTS OF SMOOTHING ON SPECTRAL DATA

A1.1 Method of Smoothing

It is general practice in the analysis of gamma ray spectra to subject the raw data to some sort of smoothing before attempting to evaluate the various peak parameters. As a result, a number of smoothing procedures may be found in the literature ([I2], [C5], [H3], [M4], [Y1]). The one used in this work is based on the use of Fourier transforms and was developed by T. Inouye. In this section will be presented a short description of this type of smoothing. Complete details may be found in references [I2] and [H1].

In this method of smoothing, the spectral data are transformed from 'energy space' to 'energy frequency space' or ω space. It is analogous to the usual transformations from time to frequency that are extensively used in communication theory. In most spectra the spectral peaks are spread over a number of channels; superimposed on these are channel to channel random fluctuations which represent the noise. As a result, this Fourier transformation separates the low frequency spectral information from the statistical noise which is of higher frequency. Thus by using an appropriate filter function in ω space and retransforming back to 'energy space' it is possible to decrease the noise content of the spectra without seriously affecting the real spectral information.

To describe the method mathematically, let the observed

data $f(E)$ be represented as the sum of two components

$$f(E) = s(E) + n(E) \quad (A1.1)$$

where $s(E)$ is the true spectral information and $n(E)$ is the noise which in this case is due principally to statistical fluctuations in the number of counts in a channel. The Fourier transform of $f(E)$, denoted by $F(\omega)$, can be written in the usual notation as

$$F(\omega) = \int_{-\infty}^{\infty} f(E) e^{-i\omega E} dE$$

or

$$F(\omega) = S(\omega) + N(\omega) \quad (A1.2)$$

where $S(\omega)$ and $N(\omega)$ stand for the Fourier transforms of the component of $f(E)$.

As was mentioned above, the success of the method depends upon $S(\omega)$ and $N(\omega)$ being different functions so that an appropriate filter function can be chosen which will eliminate at least part of $N(\omega)$ without seriously affecting $S(\omega)$. This is particularly so when the spectral peaks occupy a large number of channels in the spectrum. Denoting this filter function by $P(\omega)$, the smoothed version of the original spectrum is obtained by the inverse transform

$$s(E) = (1/2\pi) \int_{-\infty}^{\infty} F(\omega) P(\omega) e^{i\omega E} d\omega \quad (A1.3)$$

Note that all transforms have been expressed in their integral form for simplicity. In practice, where the technique is applied to discrete data, the transformations are used in their discrete form.

Al.2 Smoothing Filter Function

The method of choosing the filter function $P(\omega)$ is discussed next. As noted above, the 'w-space' subregion containing the transformed spectral information $S(\omega)$ will be large or small according to whether the peaks in the original spectrum occupy a small or a large number of channels. In practice one makes representative plots of $F(\omega)$ versus ω and attempts to identify that point where $S(\omega)$ ends. The proper filter function would then be one that passes all the frequencies below this point and eliminates those above it. Such a plot, reproduced from reference [H1], is shown in Fig. Al.1 for two typical 4096-channel spectra. The actual transformation used gives one ω point for each energy point. For clarity of presentation only every fiftieth point in ω space has been plotted. The x's represent a run where the gain was adjusted to produce a channel width of 0.971 keV. The circles represent a lower gain width of 2.063 keV. The approximate shape of the components of $F(\omega)$ are shown as the solid lines. As expected for the 0.971-keV run where the peaks contain more channels, the signal component $S(\omega)$ contains less high frequencies.

The type of filtering function employed in the analysis has the form (see figure Al.7)

$$\begin{aligned}
 P(\omega) &= 1 && \text{for } 0 \leq \omega \leq \omega_m \\
 \text{and} &&& \\
 P(\omega) &= \exp\left[-\frac{(\omega - \omega_m)^2}{2\sigma_m^2}\right] && \text{for } \omega_m \leq \omega \leq \pi
 \end{aligned}
 \tag{Al.4}$$

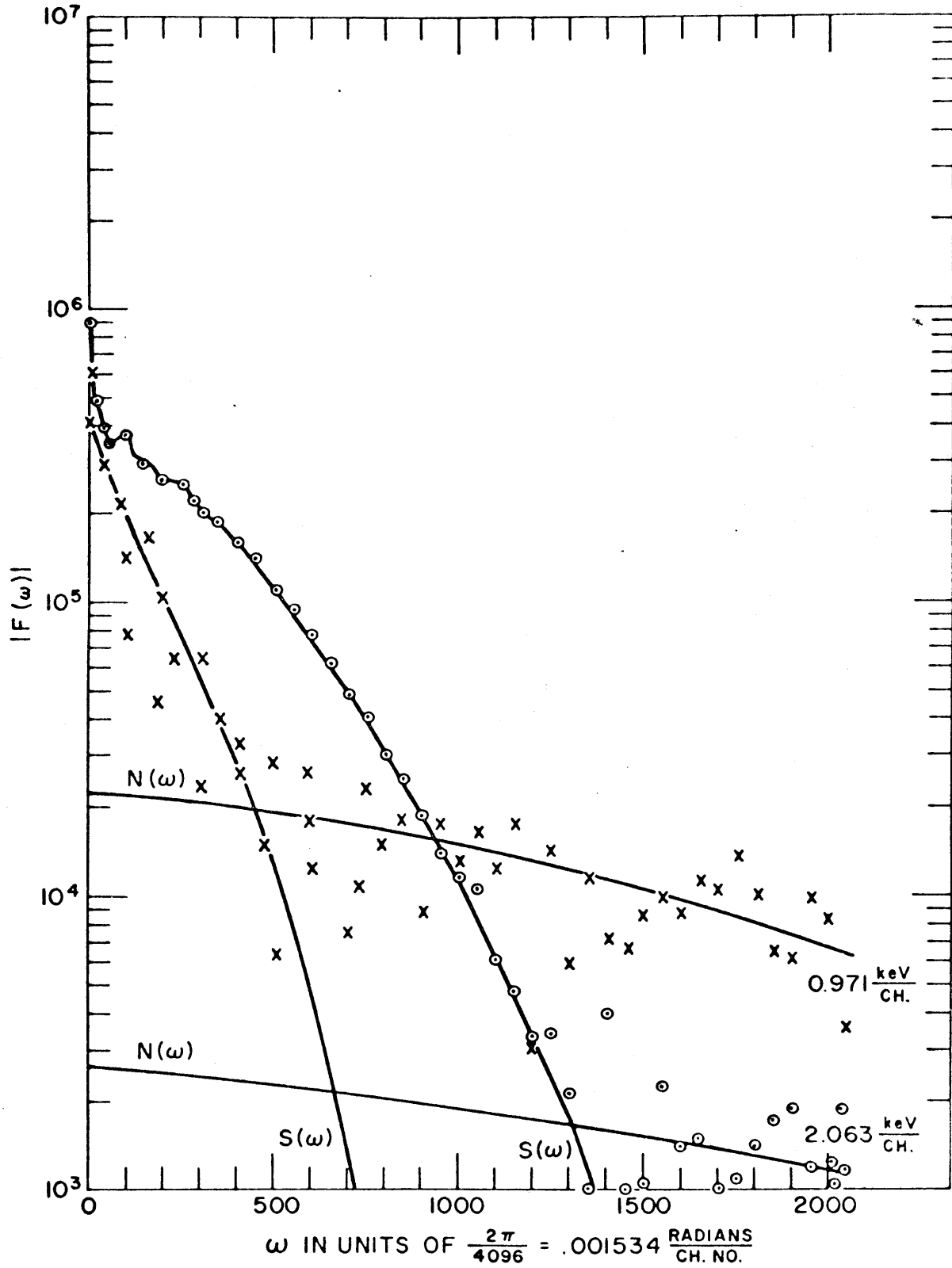


Fig. A1.1 Fourier transforms of two 4095-channel gamma ray spectra

where ω_m and σ_m must be chosen with respect to the total number of channels in the spectrum and the number of channels occupied by typical peaks. Careful analysis has revealed that the smoothing action is rather insensitive to small variations in these quantities; variations of 10 to 15 percent in either ω_m or σ_m gave appreciably the same results. Thus the same filter function can be used for all runs of approximately the same gain. If this function is properly chosen it is possible to reduce the noise content of the spectra without affecting the true spectral information. Inappropriate filter functions will lead to either insufficient smoothing (ω_m and σ_m large) or oversmoothing (ω_m and σ_m small) in which case considerable spectral information is lost.

Al.3 Degree of Smoothing

Let us represent the degree of smoothing attainable by the above technique by the equation

$$r = [\sigma(H') / \sigma(H)] \quad (\text{Al.5})$$

where $\sigma(H')$ and $\sigma(H)$ are the standard deviations in the raw (H') and smoothed (H) data of a pure noise spectrum. Thus defined, r is a measure of the average reduction in the statistical fluctuations of a large number of random data normally distributed about a fixed mean H_m . In order that these data closely approximate a Poisson distribution the standard deviation in the normal distribution was set equal to the square root of the mean H_m . r will be referred to as the

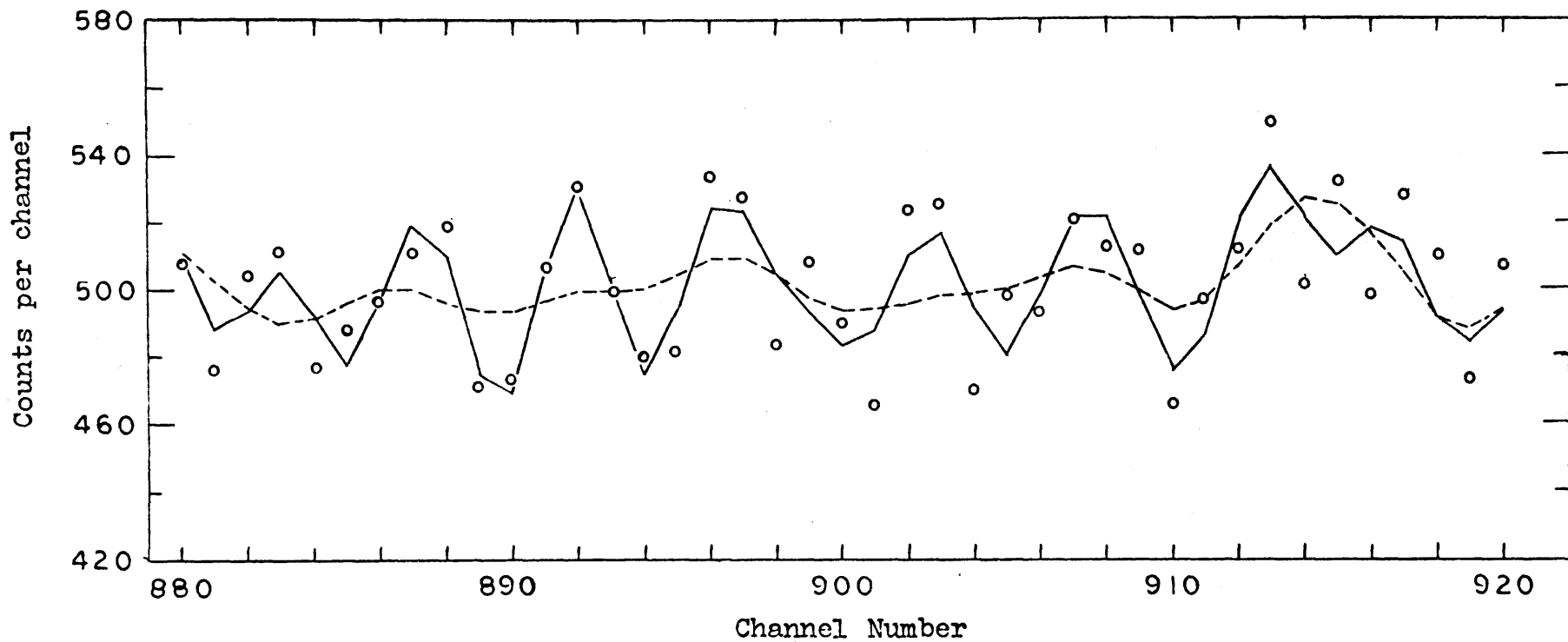
error reduction factor.

Values for r were calculated using a pseudo-experimental noise spectrum constructed by the computer code ARTSPEC and subjecting it to a number of smoothing operations. Part of this spectrum is shown in Fig. A1.2; the code is described in Appendix V. In order to examine whether both the raw and smoothed data closely approximate a normal distribution, the data were divided into a number of groups of width $\sqrt{H_m}/4$. Each group was specified by its mean value $H_k = H_m + (1/2)k\sqrt{H_m}$ where $k = \pm 1, \pm 2, \pm 3$, etc. Whenever a data point of magnitude within the interval $H_k \pm \sqrt{H_m}/4$ was encountered in the noise spectrum it was considered as being representative of the k th group. The frequency of occurrence of these groups is shown in Fig. A1.3 for three typical cases. 900 data points were considered in each case. The lines in the figure are three normal distributions given by the equation

$$y(H) = ry_0 \exp \left[- r^2 (H - H_m)^2 / 2H_m \right] \quad (\text{A1.6})$$

where $y_0 = 199.7$ and was obtained from the raw data. The mean $H_m = 500$. The error reduction factors corresponding to the three cases were $r = 1$ for the raw data, $r = 1.34$ and $r = 1.84$ and were obtained in the manner described below.

From Fig. A1.3 it is seen that both raw and smoothed data closely approximate a normal distribution. It was therefore possible to analyse the data statistically and obtain values for the standard deviations needed in equation



176

- o Original Raw Data
- Smoothing Parameters: $\omega_m = \pi/2, \sigma_m = \pi/16, r = 1.34$
- Smoothing Parameters: $\omega_m = \pi/4, \sigma_m = \pi/16, r = 1.84$

Fig. A1.2 Section of noise spectrum and typical smoothed data for light and heavy smoothing

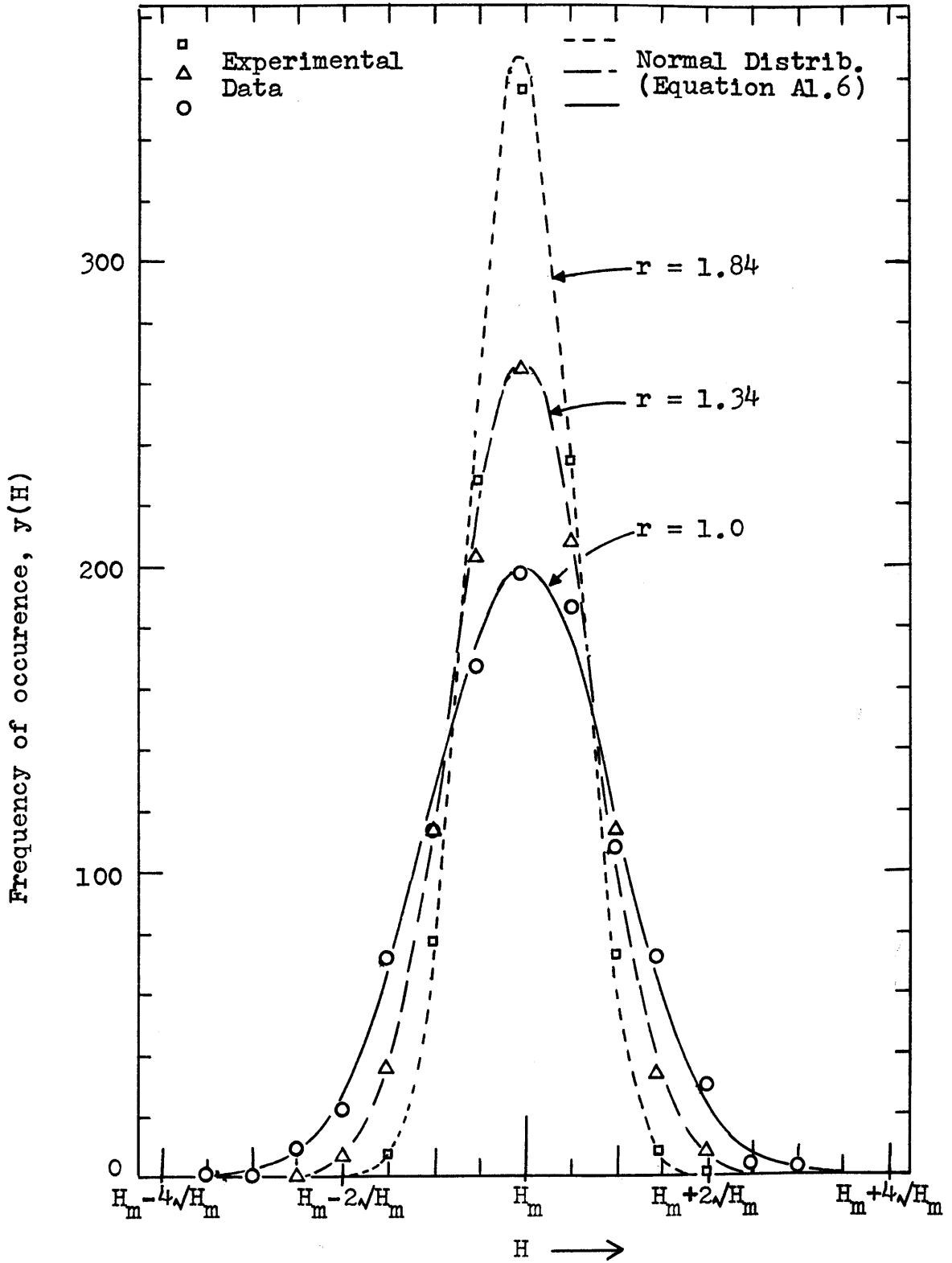


Fig. A1.3 Frequency distribution of grouped data in the raw and smoothed noise spectra

(A1.5). The results are shown in Fig. A1.4; the solid lines correspond to an empirical relation for r developed below.

It may be noted here that the smoothing operation did not affect the value of the mean; in all 18 cases considered changes in H_m were less than 0.004 percent. Also, using different noise spectra, it was observed that the reduction in the standard deviation is independent of H_m . This is an interesting result since it indicates that in a real spectrum r does not depend on the amplitude of the continuum background and so only one value for r need be specified for any given filter function.

The development of an empirical relation capable of predicting the factor r for any filter function of practical interest is now considered. Note that when a pure noise spectrum is Fourier transformed in the manner described above the resulting frequency spectrum exhibits, over its whole range, random fluctuations about a fixed mean G_m similar to those in the untransformed data. This is shown in Fig. A1.5 where, for clarity purposes, only every fifth point in the 1024-point spectrum has been plotted. To a very good approximation, therefore, the area underneath this frequency spectrum, from 0 to π degrees, is equal to πG_m . Now, since a filter function that permits the whole frequency spectrum to pass undisturbed is characterized by $r = 1$, it was anticipated that any other filter function that transmits only part of this area will have for r a value that is somehow related to the fraction of the area transmitted. In view

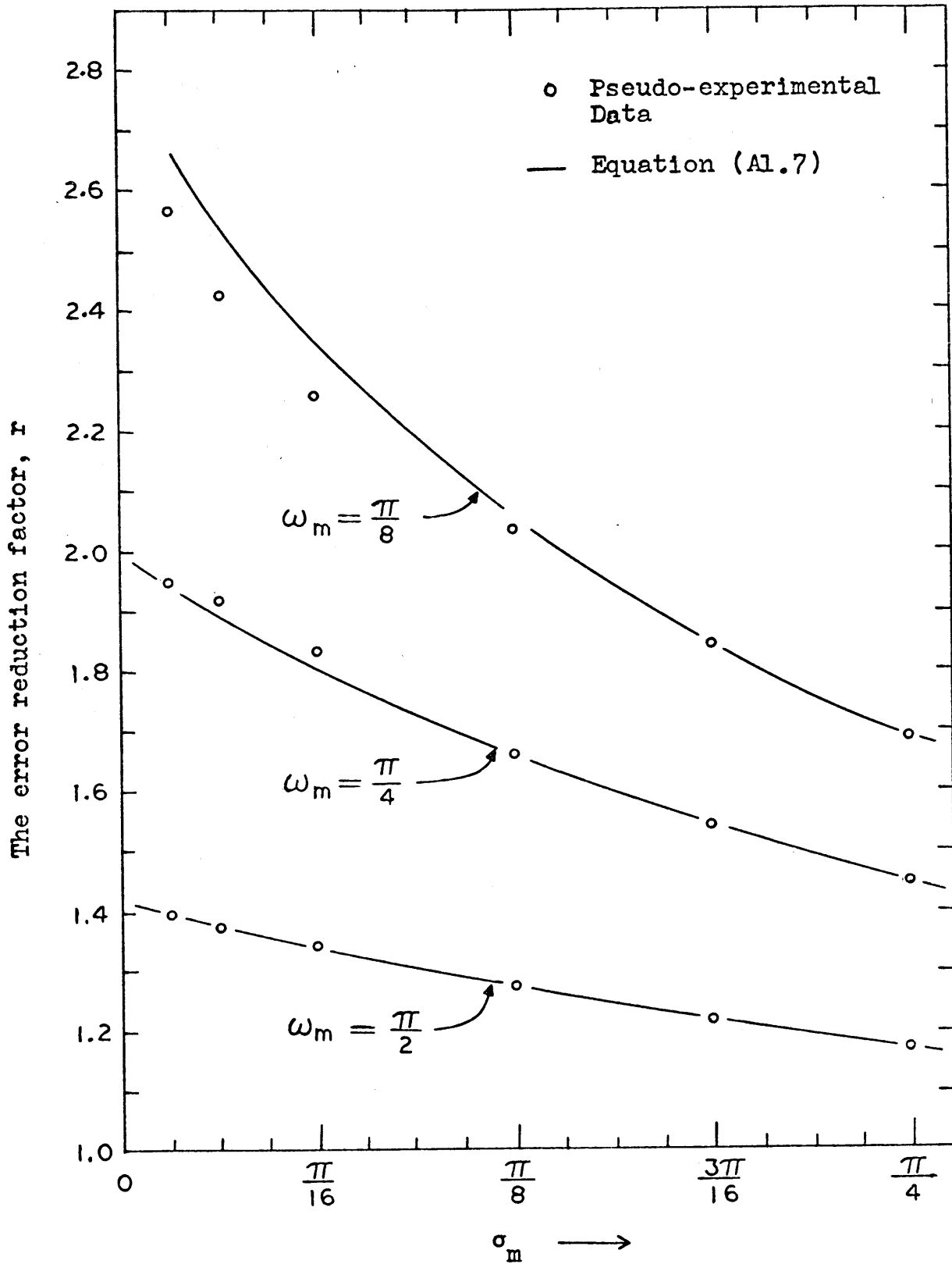


Fig. A1.4 The error reduction factor r for various combinations of the filter parameters ω_m and σ_m

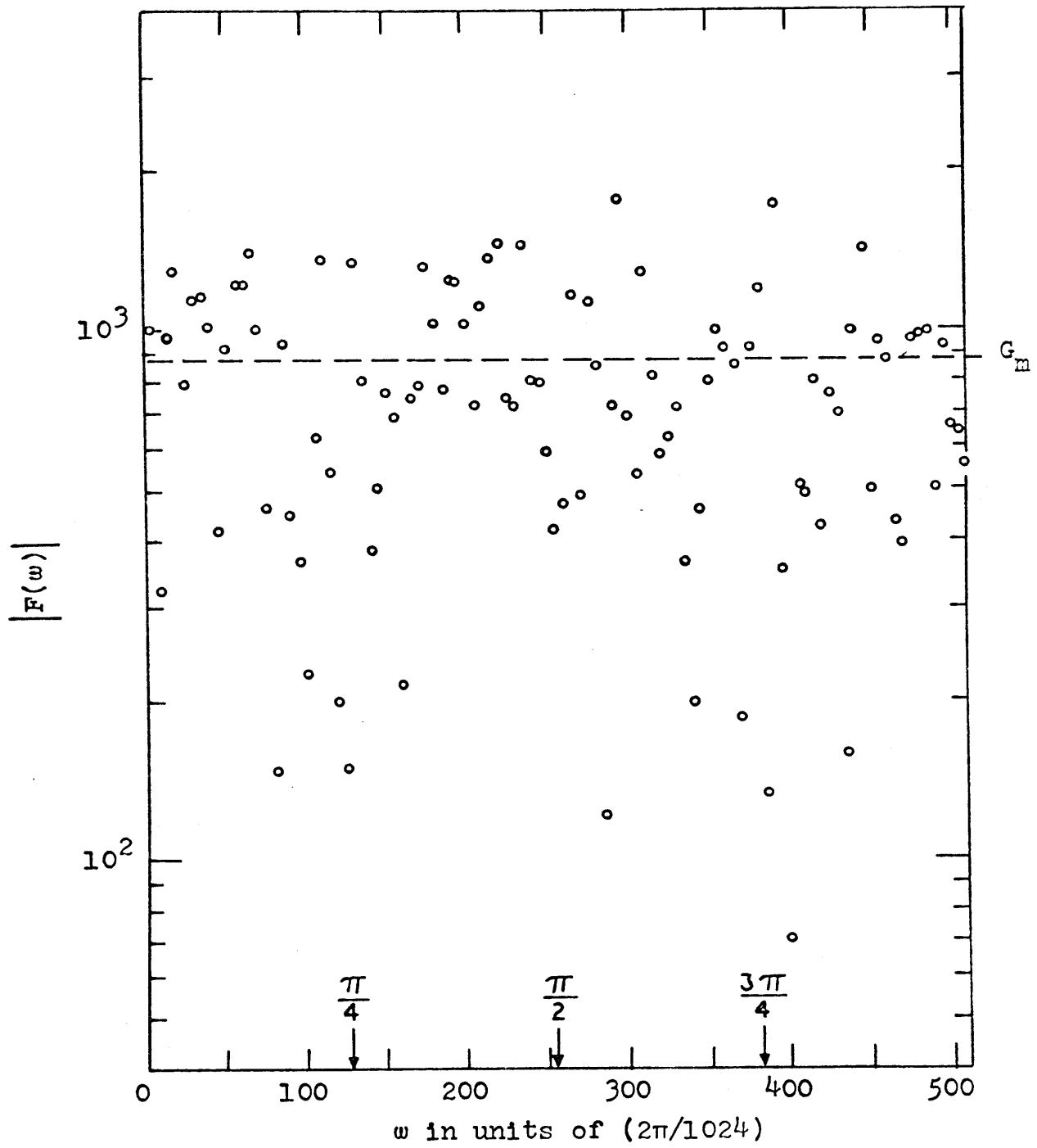


Fig. A1.5 Fourier transform of a pure noise spectrum

of the constancy of G_m over the whole frequency range, the empirical relation sought for r had the form

$$r = f \left[\pi / \left(\omega_m + \sigma_m \sqrt{\pi/2} \right) \right]$$

where the fraction may now be thought of as the inverse of the fraction of the area between 0 and π degrees that falls underneath the filter function (see Fig. A1.7). Search for such a relation to represent the pseudo-experimental data lead to the equation

$$r = \sqrt{ \left[\pi / \left(\omega_m + 0.9 \sigma_m \right) \right] } \quad (\text{A1.7})$$

(Note that the area underneath the filter function is $\omega_m + 1.25 \sigma_m$).

From the results shown in Fig. A1.4, and noting that r need only be known to within two significant figures, equation (A1.7) may be considered reliable for evaluating the effect of all filter functions that are likely to be used in practice. The equation overestimates the reduction factor for small values of σ_m .

A1.4 Effects of Smoothing on the Peak Parameters

As noted earlier, the type of filter function most suitable for the analysis of a given spectrum depends on the characteristics of the spectrum itself. Nevertheless one may still choose to apply relatively heavy smoothing for the purpose of further reducing the statistical fluctuations. In order to examine what effect this would have on the various peak parameters, a pseudo-experimental spectrum consisting

of 100 artificial peaks resting on a background continuum of 500 counts was constructed using the computer code ARTSPEC. Part of the spectrum is shown in Fig. A3.1 of Appendix III, where the same data is used to verify the equations developed for the various peak parameters. This artificial spectrum was subjected to four different smoothing operations. The error reduction factors were $r = 1$, representing the raw data, $r = 1.34$ corresponding to a filter obtained by the graphical procedure described above, and $r = 1.6$ and $r = 1.9$ arbitrarily chosen as typical values of medium and heavy smoothing. Statistical analysis was then applied in each case to the 100 values for the continuum background underneath the peaks, the peak heights above the background, the fwhm (or widths) and the peak areas. The means and standard deviations resulting from this analysis are shown in Table AI(1). These may be compared to the built-in values used in constructing the spectrum in question.

With respect to the peak areas, the main reason in the difference between the built-in and calculated values is in evaluating the background continuum. Since in our method of spectral analysis this is calculated by using count minima in the spectrum, and these minima constitute extreme points, it is not surprising that the background is underestimated in all cases. This is true despite the 1 to 5 point averaging involved in the background fit (see section 3.3). Evidently the smoothing process improves the situation by reducing the deviation of these extreme points from the actual mean. If

TABLE AI(1)

EFFECT OF VARIOUS SMOOTHING FILTER FUNCTIONS
ON THE SPECTRAL PEAK PARAMETERS
(STATISTICAL ANALYSIS BASED ON 100 PSEUDO-EXPERIMENTAL PEAKS)

	r	Background, B	Peak Height, h	Peak Width, w	Peak Area, A _{Sum}
Built-in Value		500.0	500.0	3.53	1880.0
Raw Data	1.0	480.1 ± 18.0	516.9 ± 32.7	3.67 ± 0.22	2089.2 ± 203.7
Smoothed Data	1.34	492.4 ± 14.5	504.7 ± 23.8	3.63 ± 0.17	1957.9 ± 146.9
Smoothed Data	1.60	497.3 ± 10.4	452.6 ± 20.8	3.97 ± 0.16	1915.3 ± 125.8
Smoothed Data	1.90	499.3 ± 9.5	413.6 ± 18.9	4.33 ± 0.15	1894.5 ± 130.6

the background is underestimated by an amount δB , then the peak area will be overestimated by approximately $\delta A = 3w \delta B$. Here w is the fwhm and $3w$ is approximately equal to the base width of the peak. Actual values associated with the four cases considered are:

<u>r</u>	<u>$(\delta A)_{\text{actual}}$</u>	<u>$3 w \delta B$</u>
1.0	209.2	219
1.34	77.9	82
1.6	35.3	32
1.9	14.5	9

As expected, therefore, heavy smoothing leads to more precise estimates for the background continuum. This, in turn, results in peak areas that are closer to the built-in value. But heavy smoothing also leads to shorter, broader peaks which, if sufficiently weak, will be completely smeared out and lost in the background. Consequently whether heavy smoothing should be used or not depends on whether interest lies in the strong or weak peaks in a given spectrum. Ideally one should first expose the spectral data to heavy smoothing and extract more reliable information from the strong peaks and then repeat the analysis with lighter smoothing to obtain the weak peak parameters.

Note that very heavy smoothing is not always advantageous even for the analysis of very strong peaks. This is because the standard deviation in the peak area, as shown

in Appendix III, is not decreasing monotonically with heavier smoothing as is the case with the other peak parameters. The advantages of larger reductions in the statistical fluctuations may indeed become off set by the increase in the number of channels occupied by the peak. For instance, in the pseudo-experimental spectrum considered above the standard deviation in the peak area is a minimum for r approximately equal to 1.6.

Another important point to note in the case of heavy smoothing is that the filter function parameters that will give the desired effect must be chosen with care. There is indeed an infinite number of ω_m and σ_m combinations that will yield the same error reduction factor. However, as was noted earlier, spurious peaks may appear in the spectrum for small σ_m values. This is dramatically illustrated in Fig. A1.6 where a peak, of peak height 5000 counts and a width of 4 channels resting on a background continuum of 500 counts, was subjected to heavy smoothing utilizing three different filter functions. All three filters, whose parameters are shown in Fig. A1.7, are characterized by $r = 1.9$. Note that filter (a) does not lead to any oscillations that are immediately apparent and that sharper filter cut-offs lead to fluctuations whose amplitude increases with decreasing σ_m value. Filter functions with sharp cut-offs must therefore be avoided, a fact that was pointed out by Inouye [I2]. The normal filter (d) for use with this case is also shown in Fig. A1.7 for comparison.

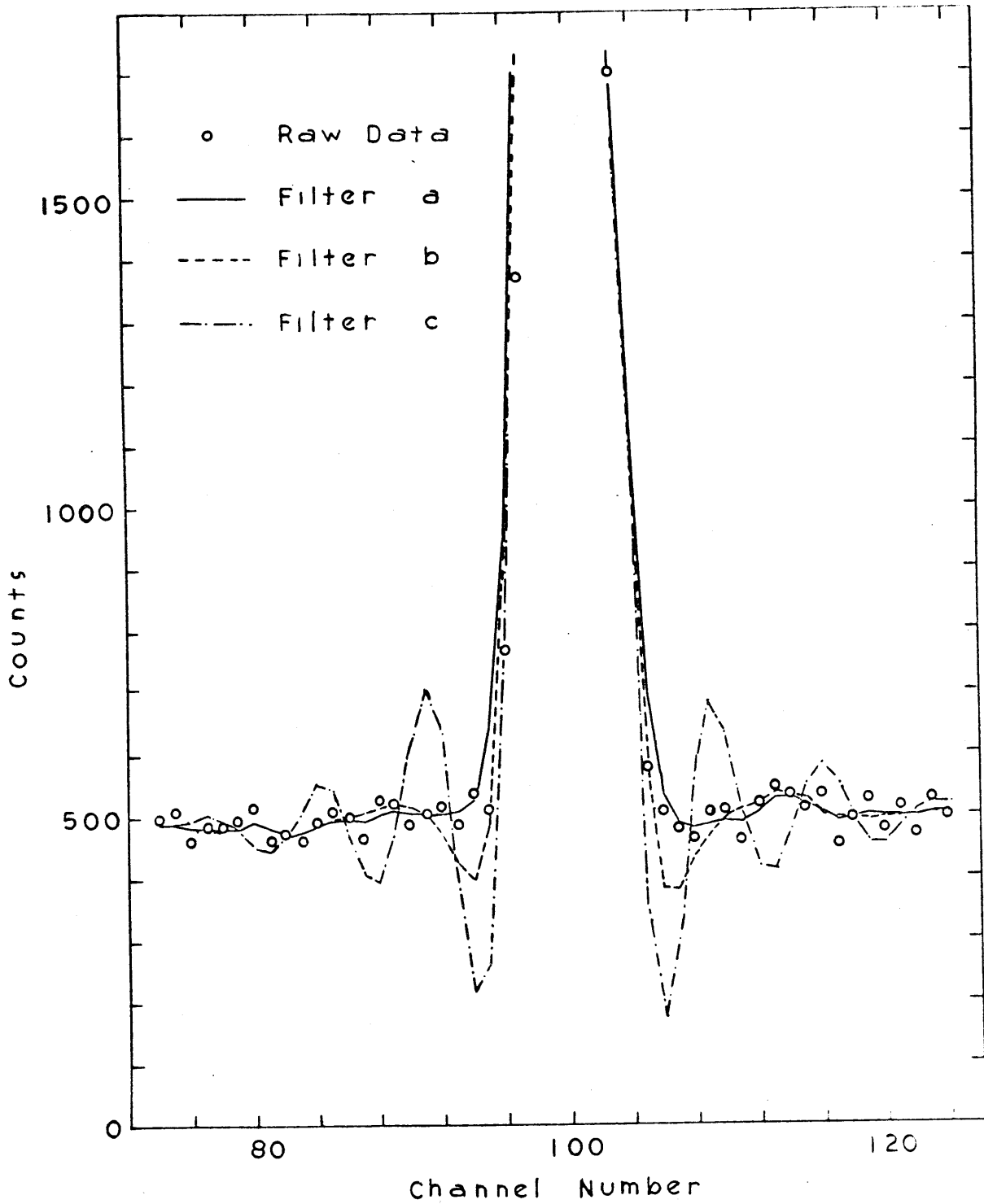


Fig. A1.6 Oscillations introduced by the filter functions shown in Fig. A1.7 for heavy smoothing

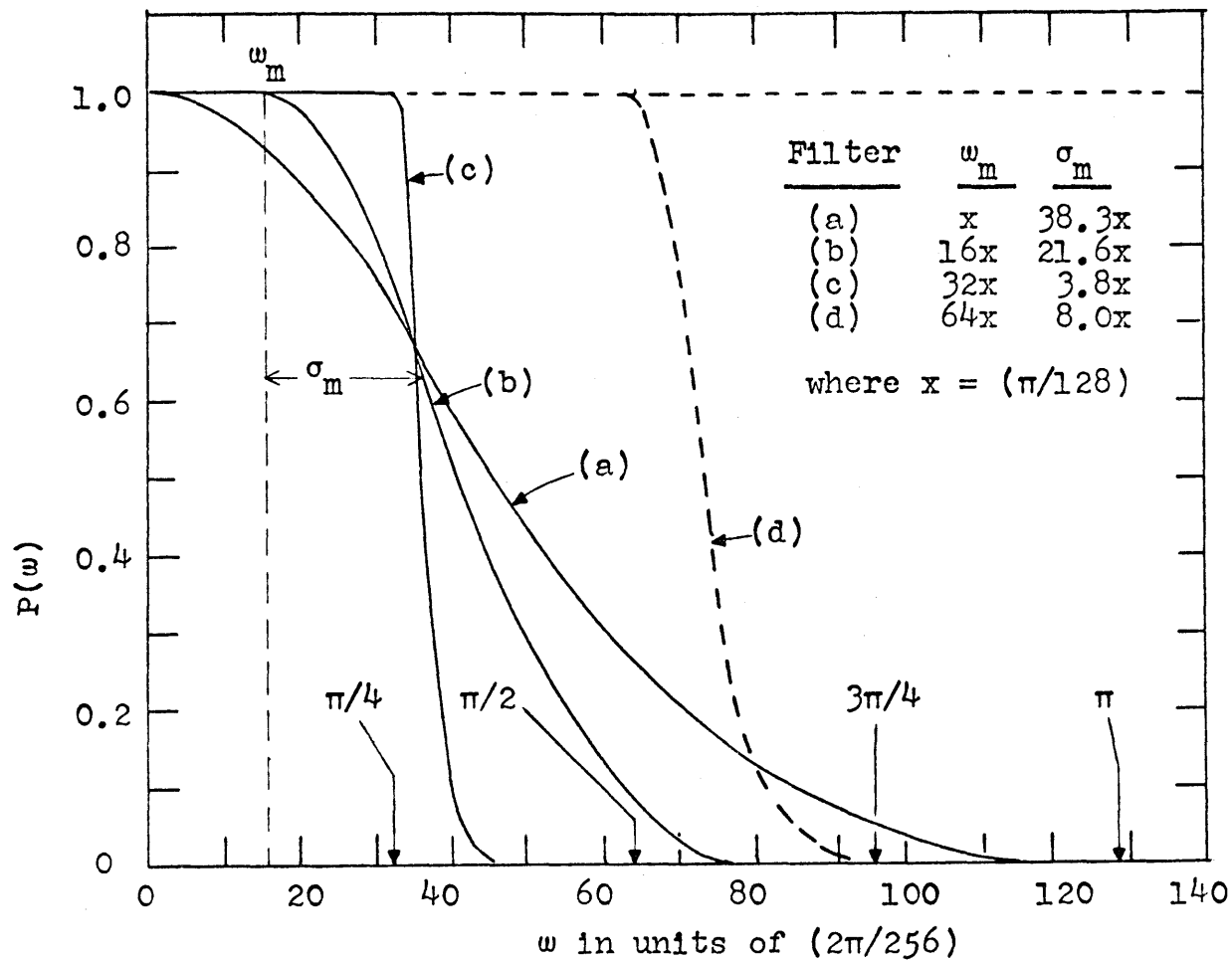


Fig. A1.7 Filter functions used in obtaining the oscillations shown in Fig. A1.6; all filters have $r = 1.9$ except filter (d) which is for normal smoothing in this case ($r = 1.34$).

Appendix II

PEAK WIDTHS AND METHOD OF LEAST-SQUARES FIT

A2.1 Reasons for the Fit

The gamma ray spectra associated with Ge(Li) spectroscopy are characterized by peaks whose parameters may be assumed to approximately coincide with the corresponding parameters of a Gaussian function. The peak areas in such spectra can therefore be obtained by the equation

$$A_G = 1.0645 \psi w h \quad (A2.1)$$

where w and h are the full-width at half-maximum (or peak width) and the peak height, and ψ is a correction term of the order of 2 percent to account for the deviation of the peaks from the Gaussian. Assuming the error in ψ is negligible, the standard deviation in peak area evaluated by this technique is

$$\sigma(A_G) = A_G \sqrt{[\sigma^2(h)/h^2] + [\sigma^2(w)/w^2]} \quad (A2.2)$$

$\sigma(h)$ and $\sigma(w)$ are the standard deviation in the height and width and are governed by counting statistics, their values being entirely dependent on the peak in question. In particular note that the widths of strong peaks may be measured with greater accuracy than those of weaker ones.

Now, for a strong and a weak peak close to each other, the widths must be comparable since they reflect the resolution of the system corresponding to that particular position in the spectrum. Yet one of them is known with greater accu-

racy. It is therefore possible to reduce the error in the area of the weaker peak by utilizing some of the information contained in the strong peak. Proceeding further, such an error may be reduced even more by incorporating more strong peaks in the analysis. In this case, however, one must allow for the possible variation of the system resolution with energy. One answer to the problem is to obtain the width as a function of energy by least-squares fitting the widths and energies of the strong peaks in the spectrum to a smoothly varying function.

A2.2 Doppler Broadening

The main assumption in the above remarks is that peak widths are expected to vary smoothly over the range of the spectrum. Physically this assumption is not quite valid since certain gamma rays will be Doppler broadened if they are emitted while the nucleus is recoiling from the emission of other gamma rays in the same cascade. Consider, for instance, a two-step cascade following thermal neutron capture. Let the energies of the first (γ_a) and second (γ_b) gamma rays emitted be E_a and E_b . The recoil velocity of the nucleus resulting from the emission of γ_a is, from conservation of momentum,

$$v = c [E_a / (m c^2)] \quad (\text{A2.3})$$

where m is the mass of the nucleus and c the velocity of light. Now, assuming that the mean life of the level at which the nucleus is left after the emission of γ_a is so

short (less than about 10^{-15} secs) that γ_b is emitted while the nucleus is still in the recoiling process, the observed energy of this transition will be Doppler shifted according to

$$E'_b = E_b [1 \pm (v/c) \cos \beta] \quad (\text{A2.4})$$

where β is the angle between the direction along which the nucleus is recoiling and the direction of emission of γ_b . The maximum spread in the observed energy is equal to twice the maximum Doppler shift which is

$$\delta E_{b,\text{max}} = (v/c) E_b = [E_a E_b / (m c^2)] \quad (\text{A2.5})$$

Moreover, since the emission of γ_a and, consequently, the nuclear recoil direction are isotropic, the observed energy E'_b will have all values between $[E_b - \delta E_{b,\text{max}}]$ and $[E_b + \delta E_{b,\text{max}}]$ specified by an intensity distribution $f_1(E_b - E'_b)$. The spectral shape of γ_b , which is broadened by two independent effects (Doppler and electronic noise (f_2)) may be represented by the convolution

$$f(E_b) = \int_{-\delta E_{b,\text{max}}}^{+\delta E_{b,\text{max}}} f_1(E_b - E'_b) f_2(E'_b) dE'_b \quad (\text{A2.6})$$

Here f_1 and f_2 are the profiles the spectral line would assume if only one of the broadening effects was present.

The system resolution function $f_2(E'_b)$ is, for the case of Ge(Li) spectroscopy, reasonably well described by a Gaussian function of width w_2 . $f_1(E_b - E'_b)$ on the other hand

depends on the angular correlation between γ_a and γ_b , a correlation which in most cases is not known. In fact the Doppler broadening effect is presently employed in the study of nuclear level structure (Wetzel[W3]).

Evaluation of equation (A2.6) is not straight-forward and in most cases requires numerical integration for each particular case considered. For the purpose of this work, where the intent is to afford some simple estimate of the Doppler broadening contribution to peak widths, it is sufficient to assume that f_1 is also a Gaussian function of width w_1 and extend the limits of integration from - infinity to + infinity. In such a case it turns out (H.C. Van de Hulst and J. J. M. Reesinck [H5]) that f is also a Gaussian having a width

$$w = \sqrt{[w_1^2 + w_2^2]} \quad (\text{A2.7})$$

Using the results reported by Wetzel on boron and nitrogen as a basis, it was found that for the case of no gamma-gamma correlation the Doppler broadening may be approximated by setting $w_1 = 1.5 \delta E_{b,\max}$. The net increase in the peak width by this effect is then

$$\delta w = w - w_2 = \sqrt{[(1.5 E_a E_b / mc^2)^2 - w_2^2]} - w_2 \quad (\text{A2.8})$$

In Table AII(1) are presented typical values of δw for a number of cases. Wetzel's results are also given for reference. The transitions used for Be, Al and Fe are not real and E_a was set equal to E_b so as to maximize the value of δw .

TABLE AII(1)

DOPPLER BROADENING CONTRIBUTION TO PEAK WIDTH

<u>Element</u>	<u>Binding En.</u>	<u>Gamma Energy</u>	<u>Gamma Energy</u>	<u>Doppler Shift</u>	<u>System Res.</u>	<u>Broadening</u>	<u>Wetzel</u>
	B_n	E_a	E_b	$\delta E_{b,max}$	w_2	δw	δw
$^{11}_B$	11453	4711	6739	3.100	7.65	1.30	1.33
		2534	8916	2.206	8.61	0.61	0.62
$^{15}_N$	10834	5534	5298	2.099	5.21	0.88	0.91
		2521	8311	1.500	6.36	0.39	0.37
$^{10}_{Be}$	6810	3405	3405	1.245	7.0	0.25	
$^{28}_{Al}$	7724	3862	3862	0.572	7.0	0.05	
$^{58}_{Fe}$	10046	5023	5023	0.467	7.0	0.035	

All entries are in keV

For gamma-gamma correlation favourable to Doppler broadening δw is approximately 50 percent larger. It may be concluded that the effect, if at all present, should be observable in those particular isotopes that have both high neutron binding energy and low atomic mass. For our case, where the samples used have their natural isotopic compositions, there is only a small number of elements for which appreciable Doppler shifts can be expected. The phenomenon can thus be neglected, but it was necessary to sidetrack for a moment to prove this point.

A2.3 The Least-Squares Fit

Reverting now to equation (A2.1), and as it was noted earlier, the error in the peak area may be reduced by utilizing the fitted width \bar{w} in place of the actual width of the peak. \bar{w} is obtained by least-squares fitting the properly weighted widths w_i and energies E_i of the strong peaks in the spectrum to the polynomial

$$\bar{w} = \sum_{j=1}^P A_j E^{(j-1)} \quad (\text{A2.9})$$

where A_j are constants evaluated in the fit and $(j-1)$ are the powers of E .

Not all the peaks in the spectrum are used in the fit since some of them are too weak to have representative widths while others are partly resolved or completely unresolved multiplets. In general the criteria employed in the selection of peaks used for the fit reject approximately 75 percent of

them. In addition, since the widths of some peaks are known with higher accuracy, it is necessary to use proper weighting functions (W_i) to accentuate the more reliable information contained in the strong peaks. The type of weighting employed in the present analysis is often called 'statistical weighting', the weights themselves being defined as the reciprocals of the squares of the standard deviations in the various measurements. The error incurred in the measurement of the independent parameter E_1 , the gamma energy, is relatively negligible; that of the dependent variable w_1 is given by equation (A3.8) in Appendix III. The weighting function used is

$$W_i = [1 / \sigma^2(w_i)] \quad (\text{A2.10})$$

where $\sigma(w_i)$ is the standard deviation in the measured width of the i th peak.

The equations used in the fit for the evaluation of the constants A_j have been put in the form

$$\begin{pmatrix} V_1 \\ V_2 \\ \cdot \\ \cdot \\ V_p \end{pmatrix} = \begin{pmatrix} C_{11} & C_{12} & \dots & C_{1p} \\ C_{21} & C_{22} & \dots & C_{2p} \\ \cdot & & & \\ \cdot & & & \\ C_{p1} & C_{p2} & & C_{pp} \end{pmatrix} \begin{pmatrix} A_1 \\ A_2 \\ \cdot \\ \cdot \\ A_p \end{pmatrix} \quad (\text{A2.11})$$

where

$$V_j = \sum_{i=1}^N W_i w_i E_i^{(j-1)} \quad j = 1, 2, \dots, p \quad (\text{A2.12})$$

$$C_{jk} = \sum_{i=1}^N W_i E_i^{(j+k-2)} \quad j, k = 1, 2, \dots, p \quad (\text{A2.13})$$

and N is the total number of peaks used in the fit. The A_j are evaluated by the usual method of matrix inversion.

The weighted sum of the squares of the residuals is

$$S = \sum_{i=1}^N W_i (w_i - \bar{w}_i)^2 \quad (\text{A2.14})$$

Also, since there are p constants in equation (A2.9) the number of degrees of freedom is $(N - p)$. J. R. Wolberg [W4] points out that if the weights W_i are not over- or under-estimated the ratio $[S / (N-p)]$ must be close to unity. That is, for an experiment repeated a large number of times, the values of S will be distributed according to a chi-squared distribution with $(N-p)$ degrees of freedom, the mean value of the distribution being equal to the number of degrees of freedom. This fact was used as a check on the error equation for the width and is discussed below.

An estimate of the uncertainty in the interpolated and extrapolated values obtainable from equation (A2.9) is given by Wolberg ([W4], page 64) as

$$s_1 = \sqrt{\frac{S}{N-p} \sum_{j=1}^p \sum_{k=1}^p \frac{\partial \bar{w}}{\partial A_j} \frac{\partial \bar{w}}{\partial A_k} C_{jk}^{-1}} \quad (\text{A2.15})$$

In the present case this reduces to

$$s_1 = \sqrt{\frac{S}{N-p} \sum_{j=1}^p \sum_{k=1}^p E^{(j+k-2)} C_{jk}^{-1}} \quad (\text{A2.16})$$

and corresponds to the parameter employed in the area error equation (3.14). The confidence interval associated with the fit is such that there is a given probability that if the experiment were repeated the value obtained for the fitted width at a given energy would fall within the interval $\bar{w}_1 - ts_1 < \bar{w}_1 < \bar{w}_1 + ts_1$. t is the student t -distribution and is used to evaluate the probability referred to; in this work it was set equal to 1.

A2.4 Application

A computer code has been written by the author to perform the above operations. It is capable of fitting the data to a p -order polynomial where p can be any integral number. However, computational accuracy restricts p to a maximum of 5 or 6. The code* is an entity in itself but was also incorporated into GAMANL. In GAMANL may also be found the various conditions used in choosing the appropriate peaks for the fit.

To choose the proper value for p the widths and energies of 46 selected peaks in Fig. 3.1 were subjected to polynomial fits of order 1, 2 and 3. In Table AII(2) is presented part of the computer output corresponding to $p = 3$. The results of the fits are shown graphically in Figs. A2.1 and A2.2. The error bars in Fig. A2.1 correspond to the standard devia-

*POLYFIT (Appendix V)

tion in the widths evaluated by equation (A3.8) Peaks whose computed errors are exceptionally large are observed to be distorted.

The values of $\sqrt{[S/(N-p)]}$ are in general greater than unity. It is believed that this reflects more the inadequacy of the criteria for choosing the appropriate peaks for the fit rather than the possible underestimation of the standard deviation in the widths. Thus, for the $p = 3$ case, if the residuals of peaks Nos. 10, 13, 27 and 28 are neglected, $\sqrt{[S/(N-p)]}$ reduces from 1.48 to the more favourable value of 1.11. The residuals in the other two cases were 2.48 for $p = 2$ and 1.44 for $p = 4$.

Consideration of the confidence interval at each data point for the various fits, the randomness of the residuals, and the chi-squared test for the value of S has lead to the choice of $p = 3$, a second order polynomial.

TABLE AII(2)

POLYFIT OUTPUT - RESULTS OF LEAST-SQUARES FIT

$$p = 3$$

Number of Peaks used = 46

$$\text{SUM}(\text{WEIGHT} * \text{WIDTH}(\text{KEV}) * \text{ENERGY}(\text{LOMEV})^{**0}) = 0.44922\text{E } 04 \quad (\text{Eq. A2.12})$$

$$\text{SUM}(\text{WEIGHT} * \text{WIDTH}(\text{KEV}) * \text{ENERGY}(\text{LOMEV})^{**1}) = 0.17189\text{E } 04 \quad (\text{Eq. A2.12})$$

$$\text{SUM}(\text{WEIGHT} * \text{WIDTH}(\text{KEV}) * \text{ENERGY}(\text{LOMEV})^{**2}) = 0.86183\text{E } 03 \quad (\text{Eq. A2.12})$$

COEFFICIENTS OF ORIGINAL MATRIX (Equation A2.13)

$$0.50838\text{E } 03 \quad 0.17204\text{E } 03 \quad 0.76364\text{E } 02$$

$$0.17204\text{E } 03 \quad 0.76364\text{E } 02 \quad 0.41894\text{E } 02$$

$$0.76364\text{E } 02 \quad 0.41894\text{E } 02 \quad 0.26394\text{E } 02$$

$$\text{VALUE OF DETERMINANT} = 0.66611\text{E } 04$$

COEFFICIENTS OF INVERTED MATRIX

$$0.39102\text{E}-01 \quad -0.20143\text{E } 00 \quad 0.20658\text{E } 00$$

$$-0.20143\text{E } 00 \quad 0.11389\text{E } 01 \quad -0.12250\text{E } 01$$

$$0.20658\text{E } 00 \quad -0.12250\text{E } 01 \quad 0.13846\text{E } 01$$

EQUATION OF LEAST-SQUARES FIT (Equation A2.9)

$$\text{FWHM (KEV)} = 0.74590\text{E } 01 * \text{ENERGY}(\text{LOMEV})^{**0}$$

$$- 0.28577\text{E } 01 * \text{ENERGY}(\text{LOMEV})^{**1}$$

$$+ 0.15605\text{E } 02 * \text{ENERGY}(\text{LOMEV})^{**2}$$

$$\text{SQRT (SUM WEIGHTED RESIDUALS/DEGREES OF FREEDOM)} = 0.14777\text{E } 01$$

(Equation A2.14)

TABLE AII(2) (CONTINUED)

COMPARISON BETWEEN ORIGINAL AND FITTED DATA									
NO	PEAK ENERGY	PEAK WIDTH	S.D. (WIDTH)	WEIGHT	WIDTH FIT	WIDTH DIFE	RESIDUALS	CONF	INTRVL
1	1531.00	7.56670	0.19920	25.20859	7.38729	0.17941	0.81145		C.11229
2	1620.02	8.41260	1.67860	0.35490	7.40562	1.00698	0.35987		C.10563
3	1778.50	7.44720	0.07200	192.72499	7.44438	0.00282	0.00153		C.09521
4	2223.64	7.55220	0.89460	1.24950	7.59518	-0.04298	0.00231		C.07699
5	2676.30	6.96380	0.84470	1.40160	7.78487	-0.82107	0.94489		C.07479
6	2680.34	8.86680	3.07910	0.10550	7.80322	1.06358	0.11934		C.07511
7	2871.65	7.78970	0.39090	6.54570	7.99512	-0.10542	0.07275		C.07737
8	2960.25	8.20410	0.19510	26.27959	7.98057	0.22353	1.31300		C.08007
9	3034.31	8.07440	0.17990	30.91489	8.02869	-0.00429	0.00057		C.08171
10	3266.17	6.22100	0.70940	1.98710	8.19040	-1.96940	7.70700		C.08731
11	3347.31	6.27490	1.27700	0.66420	8.25095	-1.97605	2.59354		C.08933
12	3411.42	9.33520	2.20580	0.20550	8.30025	1.03495	0.22012		C.09093
13	3465.56	7.64250	0.18280	29.93459	8.34298	-0.70038	14.68368		C.09276
14	3591.47	8.54670	0.32050	9.73390	8.44556	0.10114	0.09258		C.09529
15	3789.47	9.70490	0.81190	1.51730	8.61703	1.09787	1.79555		C.09973
16	3823.50	7.56630	3.25890	0.09420	8.64774	-1.08144	0.11017		C.10044
17	3849.67	9.18790	0.33710	8.80140	8.67160	0.51630	2.34619		C.10098
18	3876.12	9.04950	0.46360	4.65290	8.69593	0.35257	0.57839		C.10152
19	4017.76	11.54030	1.40380	0.50960	8.42993	2.71037	3.74357		C.10420
20	4133.32	8.81770	0.23790	17.67090	8.94390	-0.12620	0.28142		C.10616
21	4217.86	8.95770	0.85730	1.36070	9.02991	-0.07271	0.00719		C.10746
22	4259.56	9.31280	0.19670	25.84720	9.07316	0.23964	1.48431		C.10806
23	4405.68	8.41990	1.35240	0.54830	9.22899	-0.80909	0.35894		C.10993
24	4427.08	7.75520	1.18720	0.70960	9.25237	-1.49719	1.59059		C.11018
25	4566.25	7.21450	2.31390	0.18630	9.40792	-2.19342	0.89971		C.11160
26	4659.81	9.49940	0.36770	7.39720	9.51589	-0.01649	0.00201		C.11239
27	4690.37	8.67930	0.22530	19.70270	9.55174	-0.87244	14.99680		C.11263
28	4733.69	10.29900	0.24630	16.48309	9.60307	0.69593	7.98303		C.11294
29	4809.02	8.48350	4.16800	0.05760	9.69373	-1.21073	0.08436		C.11341
30	4903.16	10.38310	0.52440	3.63640	9.80950	0.57360	1.19643		C.11391
31	5014.92	8.26200	1.20310	0.69080	9.95054	-1.68854	1.96958		C.11439
32	5134.35	10.88830	0.44580	5.03290	10.10556	0.78274	3.08353		C.11478
33	5181.00	12.51830	2.18710	0.20910	10.16733	2.35097	1.15571		C.11490
34	5411.67	12.12870	0.91520	1.50500	10.48271	1.64599	4.07746		C.11542
35	5707.90	11.89870	1.24230	0.64800	10.91209	0.97661	0.61805		C.11625
36	5920.78	10.63130	0.54650	3.34850	11.23756	-0.60576	1.22871		C.11744
37	6016.90	12.43910	0.48150	4.31340	11.38916	1.04994	4.75546		C.11825
38	6102.24	12.87830	0.55370	3.26210	11.52616	1.35214	5.96400		C.11917
39	6197.64	10.56960	1.88900	0.28030	11.68201	-1.11241	0.34686		C.12043
40	6315.73	12.07520	0.86890	1.32440	11.87887	0.19633	0.05105		C.12241
41	6990.80	11.27450	1.35500	0.54460	13.08774	-1.86374	1.89267		C.14522
42	7243.96	12.07570	1.41380	0.50030	13.57776	-1.50206	1.12877		C.15977
43	7368.36	13.59150	0.42640	5.49940	13.82598	-0.23434	0.30211		C.16819
44	7723.79	14.58400	0.16850	35.20369	14.56141	0.02259	0.01797		C.19681
45	7914.70	14.80220	0.36240	7.61490	14.97275	-0.17056	0.22151		C.21488
46	8884.20	16.63759	0.72150	1.92030	17.23724	-0.59966	0.69069		C.33313

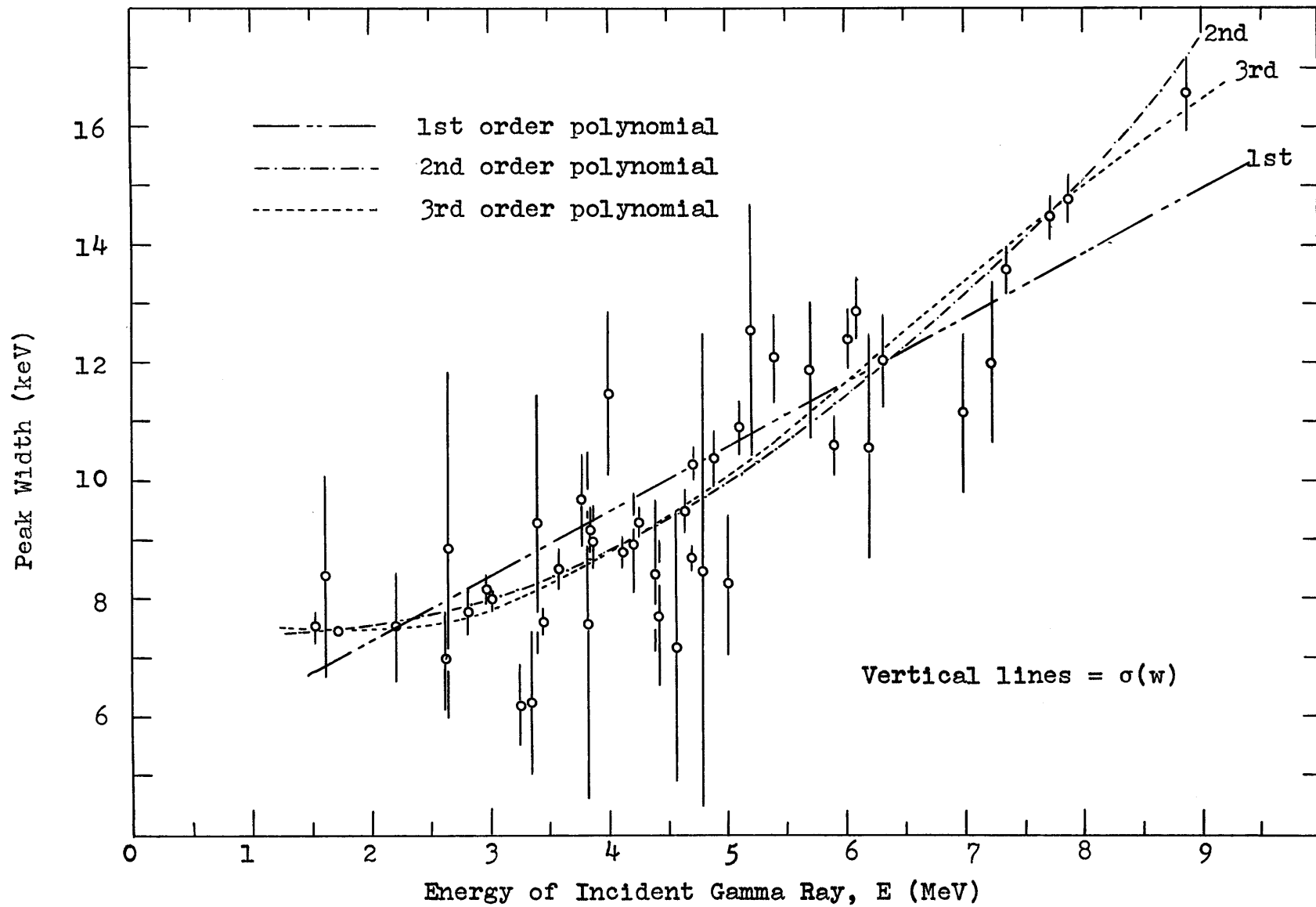


Fig. A2.1 Fitting the energy-width data to various polynomials by the method of least-squares

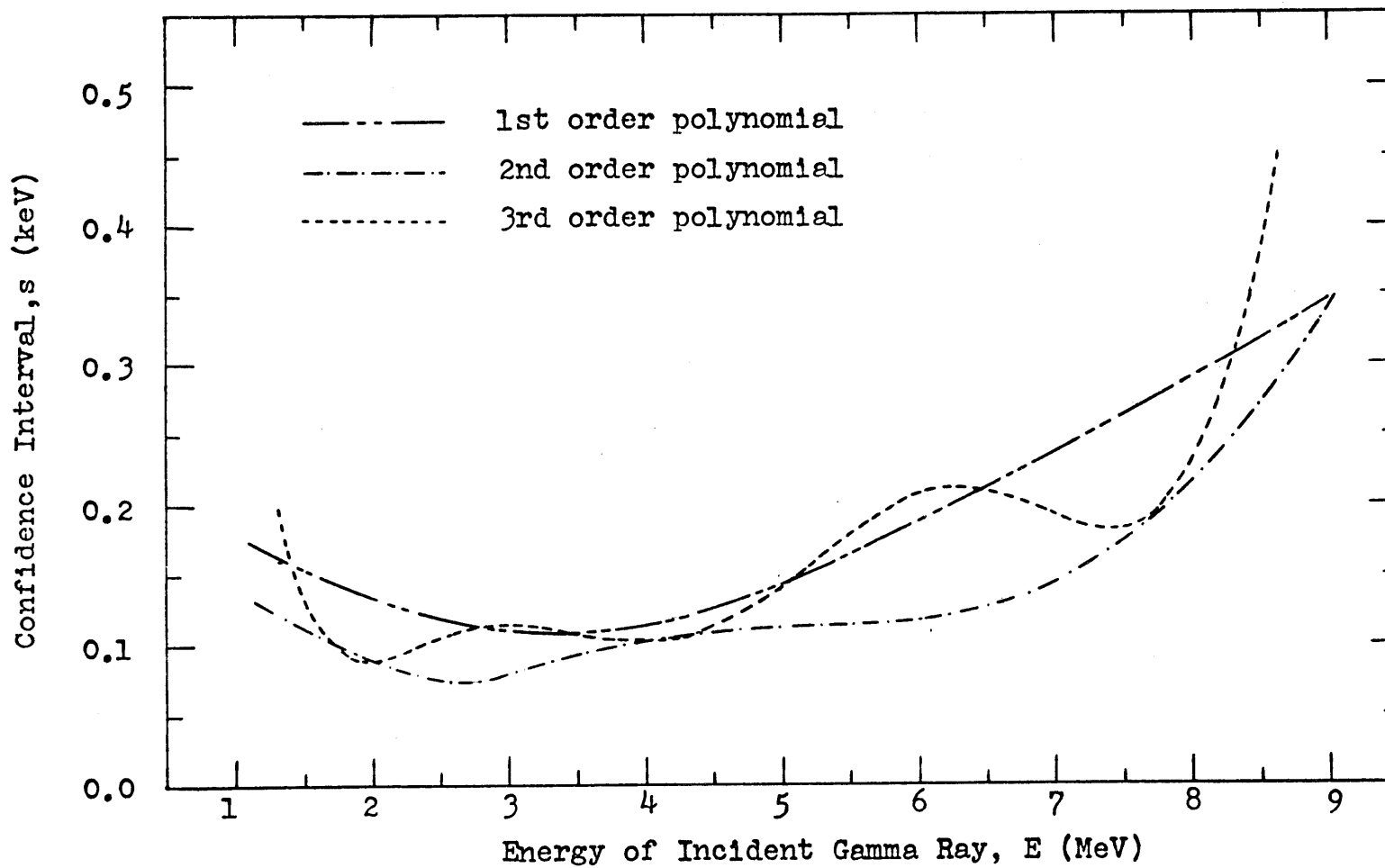


Fig. A2.2 Confidence interval in the three fits shown in Fig. A2.1

Appendix III
ERROR EQUATIONS

A3.1 The Error Equations

In order to investigate which of the two methods of peak area determination described in Chapter III is more reliable, it was necessary to develop and compare the error equations associated with the various peak parameters. To this end, note that for a large number of identical measurements the counts recorded in any one given channel in the spectrum will fluctuate independently about a mean value in a manner dictated by counting statistics [E2]. Thus if the number of counts in channel i of the original raw data is H_i the expected standard deviation, or the error as it will often be referred to, is $\sqrt{H_i}$.

Since the peak parameters are evaluated using smoothed data, it is important to extend these ideas further. The counts in neighbouring channels in the raw data fluctuate independently about their mean value. Hence the smoothing process, which reduces the intensity of the fluctuations between adjacent channels, does in fact reduce the standard deviation of the count in each channel. As shown in Appendix I, the standard deviation in the smoothed data is

$$\sigma(H_i) = (1/r) \sqrt{H_i} \quad (\text{A3.1})$$

where r represents the reduction in the statistical fluctuations by the smoothing process and depends on the particular

smoothing filter used.

Using this equation as a basis it is possible to write the error equations associated with the various peak parameters. We will consider each parameter separately.

(a) Value of Peak Minima

The equation for the value of a peak minimum in channel MO is, from equation (3.3),

$$\bar{H}_0 = \bar{H}(MO) = \frac{\sum_{j=-2}^{j=2} a_j H(MO+j)}{\sum_{j=-2}^{j=2} a_j} \quad (A3.2)$$

where $a_j = 1$ when $|H(MO+j) - H(MO)| \leq \sqrt{H(MO)}$
and $a_j = 0$ in all other cases.

Analyses of experimental data have shown that the standard deviation in H_0 can be well approximated by the equation

$$\sigma(\bar{H}_0) = (1/r) \sqrt{\bar{H}_0} \quad (A3.3)$$

The implication here is that the averaging process specified by equation (A3.2) does not reduce the standard deviation in the value of the minima. It is believed that this is due to the fact that, in our method of analysis, the averaging process always increases the value of the minima in question. Recall that the method of background evaluation described in Section (3.3) is based on count minima and that these minima constitute extreme points in the spectrum.

(b) Peak Height

The peak height h is determined by a second order

interpolation applied to the three highest points in the peak after the continuum background underneath the peak has been subtracted. Denoting these three points by h_{p-1} , h_p and h_{p+1} as shown in Fig. 3.3, the peak height equation takes the form

$$h = h_p (1 + \alpha) \quad (\text{A3.4})$$

where

$$\alpha = \frac{(h_{p+1} - h_{p-1})^2}{8h_p (2h_p - h_{p+1} - h_{p-1})}$$

For a Gaussian having a fwhm of 4 channels, α has the maximum value of 0.0366; it is even less for wider peaks. The error in α may therefore be neglected and α itself may be assumed to have the average value of 0.02 in cases where exact information is not available. Moreover, for a symmetric peak,

$$h_p = H_p - (\bar{H}_0 + \bar{H}_n)/2 = H_p - B \quad (\text{A3.5})$$

and therefore the error in the peak height is

$$\begin{aligned} \sigma(h) &= (1+\alpha) \sqrt{[H_p + (\bar{H}_0 + \bar{H}_n)/4]} / r \\ &= (1 + \alpha) (1/r) \sqrt{[h + 1.5B]} \end{aligned} \quad (\text{A3.6})$$

B is the average background underneath the peak.

(c) Peak Width

In our method of analysis the fwhm (or width) is obtained by assuming linear interpolation between the channels (h_i and h_j) whose count is just above the peak half-maximum ($h/2$), and

those (h_{i-1} and h_{j+1}) which are just below it. With reference to Fig. 3.3, this is

$$w = j - i + \lambda_i + \lambda_j \quad (\text{A3.7})$$

where

$$\lambda_i = [(h_i - h/2)/(h_i - h_{i-1})]$$

and

$$\lambda_j = [(h_j - h/2)/(h_j - h_{j+1})]$$

Such a procedure does not permit the evaluation of any error in the $(j-i)$ component and in fact it is not possible to state a priori whether a peak is exceptionally wide or exceptionally narrow. The only errors that can be assigned to w are therefore those associated with λ_i and λ_j . That is

$$\sigma(w) = \sqrt{[\sigma^2(\lambda_i) + \sigma^2(\lambda_j)]} \quad (\text{A3.8})$$

To evaluate $\sigma(\lambda_k)$ it is safer to express the λ_k parameters in terms of the data H_k . Since the h_k have been obtained by subtracting from H_k an approximately constant value, B , one may run in to the problem of accounting more than once for the error in B . Concentrating for the moment on $\sigma(\lambda_i)$, this change leads to

$$\lambda_i = [H_i - (H + B)/2] / [H_i - H_{i-1}] \quad (\text{A3.9})$$

Note that as a result of the smoothing operation, the various parameters in this equation are correlated to a degree dictated by the smoothing filter function employed and also by the number of channels existing between them. Despite its

significance, and in view of the complexity of the problem and the secondary role equation (A3.8) plays in the analysis of the data, this correlation was neglected. The final equation to be derived will essentially be valid only for unsmoothed data. For smoothed data, experimental results reported below indicate that this simplification leads to an overestimate in the standard deviation in the peak width of approximately 15 to 20 percent in the range of interest.

Use is made next of the equation for the propagation of errors which has the form

$$\sigma^2(\lambda) = \sum_k \left(\frac{\partial \lambda}{\partial x_k} \right)^2 \sigma^2(x_k) \quad (\text{A3.10})$$

where the x_k represent the various parameters in equation (A3.9). This leads to

$$\sigma(\lambda_1) = \sqrt{[(1-\lambda_1)^2 \sigma^2(H_1) + \lambda_1^2 \sigma^2(H_{1-1}) + \sigma^2(H+B)/4] / (H_1 - H_{1-1})} \quad (\text{A3.11})$$

Since we also have

$$\begin{aligned} \sigma^2(H_1) &= (1/r^2) H_1 = (1/r^2)(h_1 + B) \\ \sigma^2(H_{1-1}) &= (1/r^2) H_{1-1} = (1/r^2)(h_{1-1} + B) \end{aligned} \quad (\text{A3.12})$$

$$\text{and} \quad \sigma^2(H) = (1/r^2) H = (1/r^2)(h + B)$$

$$\sigma^2(B) = (1/r^2) B/2$$

the equation reduces, after collecting terms, to

$$\sigma(\lambda_1) = \sqrt{[(1-\lambda_1)^2 h_1 + \lambda_1^2 h_{1-1} + h/4 + (2\lambda_1^2 - 2\lambda_1 + 11/8)B] / [r(h_1 - h_{1-1})]} \quad (\text{A3.13})$$

Note that if $(h_1 - h_{1-1})$ is small, which may happen in the case of distorted peaks, the error can be very large. By definition, however, $\sigma(\lambda_1)$ cannot be larger than one channel.

It is this equation (A3.13) and the corresponding one for $\sigma(\lambda_j)$ that are presently employed in the evaluation of the weighting parameters in the least-squares fit (equations A3.8 and A2.10).

(d) Peak Areas

Two methods of area evaluation have been presented in Chapter III. According to one of them, the straight-sums technique, the area equation is

$$A_S = \sum_{k=1}^{n-1} H_k - [(n-1)/2](\bar{H}_0 + \bar{H}_n) \quad (\text{A3.15})$$

where n is the number of channel intervals occupied by the peak. The standard deviation in A_S is

$$\begin{aligned} \sigma(A_S) &= \sqrt{\left[\sum_{k=1}^{n-1} H_k + [(n-1)/2]^2 (\bar{H}_0 + \bar{H}_n) \right]} \\ &= \sqrt{\left[A_S + [(n-1)/2 + (n-1)^2/(2r)^2] (\bar{H}_0 + \bar{H}_n) \right]} \\ &= \sqrt{\left[A_S + (3\bar{w} - 1)[1 + (3\bar{w} - 1)/(2r^2)] B \right]} \end{aligned} \quad (\text{A3.16})$$

The assumptions involved here are that

(a) No counts are lost by the smoothing process, i.e.

$$\sum_{k=1}^{n-1} H_k = \sum_{k=1}^{n-1} H'_k$$

and therefore

$$\sigma\left(\sum_k H_k\right) = \sigma\left(\sum_k H'_k\right)$$

Recall that H' and H are the raw and smoothed data respectively.

- (b) No error is assumed in the number of channels occupied by the peak. However since the error equation is a strong function of n , and the position of the minima can vary appreciably depending on the statistical behaviour of the data in their immediate vicinity, it was necessary to set n equal to $3\bar{w}$, the fraction of the total area of a Gaussian distribution which falls within this interval being 99.97 percent.

In the Gaussian approach, where the peak area is given by the equation

$$A_G = 1.0645 \psi \bar{w} h \quad , \quad (A3.17)$$

ψ being the correction term for the non-truly Gaussian form of the peaks, the error equation is

$$\sigma(A_G) = A_G \sqrt{[\sigma^2(h)/h^2 + (s/\bar{w})^2]} \quad (A3.18)$$

where s stands for the error in the fitted width and is calculated by equation (A2.16). It is assumed that the error in ψ is negligible, ψ itself being approximately equal to 1.02.

A3.2 Applications

The error equations presented above are of vital importance in this work since they have been used to indicate which of the two techniques of peak area determination must be preferred and also to establish the three limiting levels in area measurements. In view of the number of assumptions involved in their derivation, it was found necessary to test their validity in a number of cases.

The first test was performed using the 100 pseudo-experimental peaks constructed by the ARTSPEC code; these were discussed earlier in Appendix I. Part of this spectrum is shown in Fig. A3.1. The analysis of this spectrum by GAMANL was carried out four times using four different filter functions for the smoothing. The error reduction factors associated with these filters were $r = 1.0, 1.34, 1.6$ and 1.9 . The two energy calibration lines required by the code were assigned values that lead to a conversion factor of 1.000 keV/channel. Part of the GAMANL output for the case $r = 1.34$ appears in Table AIII(1). This may be examined for the randomness associated with the values for the various peak parameters. The various columns in Table AIII(1) represent (1) the peak number, (2) the peak energy, in keV, (3) the location of the peak in the spectrum, (4) the peak height, (5) the height to background ratio, (6) the straight-sums area, (7) the Gaussian area, (8) the Gaussian intensity, which in this case is in arbitrary units, (9) the percent error in the Gaussian area, (10) the actual fwhm of the peaks, in keV or, in

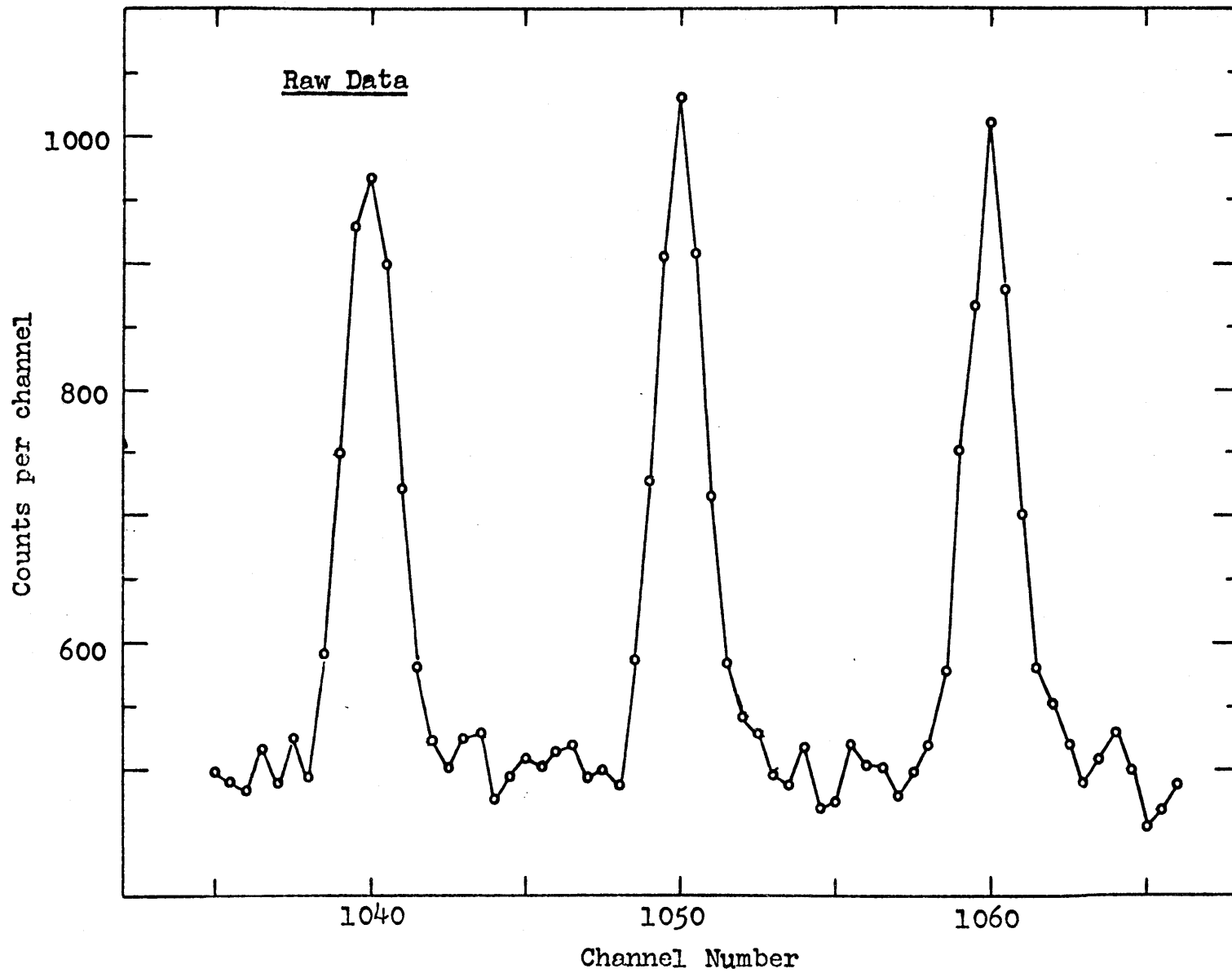


Fig. A3.1 Three of the one hundred pseudo-experimental peaks produced by the code ARTSPEC (Note that the y-scale does not start from 0)

TABLE AIII(1) - PART OF GAMANI OUTPUT FOR THE ANALYSIS OF THE 100 ARTIFICIAL PEAKS

NO.	ENERGY KEV	PK CNTR CHAN NO	HEIGHT COUNTS	H TO HG RATIO	PEAK ANALYSIS		INT(B)	ERROR(B) PERCENT	W(A) KEV	W(B) KEV	BASE CHAN	TYPE
					AREA(A) COUNTS	AREA(B) COUNTS						
1	1820.1	40.1	542.5	1.112	2321.5	2065.7	5.72	4.68	3.63	3.56	18.	*S
2	1860.0	60.0	453.8	0.872	1211.8	1729.1	4.60	5.43	3.65	3.57	9.	*S
3	1860.0	79.9	509.2	1.024	1794.1	1941.4	4.98	4.91	3.34	3.57	10.	*S
4	1880.0	100.0	510.5	1.022	1860.1	1947.3	4.81	4.89	3.51	3.57	9.	*S
5	1900.0	119.9	484.3	0.920	1694.0	1848.6	4.41	5.16	3.17	3.57	9.	*S
6	1920.0	140.0	528.4	1.071	2206.4	2018.1	4.64	4.72	3.78	3.57	14.	*S
7	1940.1	160.1	483.6	0.949	1756.3	1847.9	4.11	5.10	3.48	3.58	10.	*S
8	1960.0	180.0	531.6	1.062	2076.9	2032.4	4.37	4.70	3.59	3.58	11.	*S
9	1980.0	200.0	491.1	0.995	1952.9	1875.6	3.92	4.97	3.66	3.58	10.	*S
10	2000.0	220.0	493.6	0.988	1947.8	1889.2	3.82	4.96	3.68	3.58	12.	*S
11	2019.9	239.9	496.9	0.942	1688.3	1902.9	3.72	5.01	3.33	3.58	3.	*S
12	2040.0	260.0	478.4	0.979	1937.2	1833.7	3.47	5.04	3.64	3.59	12.	*S
13	2060.0	280.0	502.9	1.005	1892.0	1927.7	3.54	4.88	3.64	3.59	10.	*S
14	2080.0	300.0	479.8	0.960	1830.1	1840.0	3.28	5.05	3.53	3.59	12.	*S
15	2099.9	319.9	530.5	1.059	2010.7	2035.1	3.53	4.68	3.55	3.59	12.	*S
16	2120.0	340.0	442.8	0.829	1746.0	1714.7	2.90	5.36	3.61	3.59	11.	*S
17	2139.9	359.9	477.8	0.919	1853.6	1834.8	3.01	5.12	3.70	3.59	11.	*S
18	2160.0	380.0	536.9	1.089	2181.3	2062.3	3.22	4.60	3.62	3.60	13.	*S
19	2180.0	400.0	462.3	0.893	1800.0	1775.8	2.76	5.24	3.80	3.60	9.	*S
20	2200.1	420.0	528.1	1.065	2167.0	2030.2	3.08	4.66	3.71	3.60	12.	*S
21	2219.9	439.9	486.8	0.989	1990.7	1872.4	2.77	4.97	4.04	3.60	11.	*S
22	2240.1	460.1	472.4	0.847	1919.5	1830.8	2.65	5.07	3.73	3.60	11.	*S
23	2260.1	480.0	552.4	1.141	2129.4	2120.2	3.00	4.47	3.60	3.60	11.	*S
24	2280.0	500.0	560.0	1.109	2142.9	2156.0	2.97	4.47	3.62	3.60	11.	*S
25	2300.0	519.9	526.6	1.089	2215.3	2023.4	2.73	4.63	3.64	3.60	14.	*S
26	2309.7	525.7	492.7	0.846	200.3	264.5	0.36	28.21	2.91	3.61	6.	*S
27	2319.9	539.9	540.9	1.148	2143.6	2084.1	2.75	4.51	3.61	3.61	14. 0	0.00
28	2340.0	559.9	503.5	1.020	1961.0	1940.3	2.50	4.82	3.71	3.61	10.	*S
29	2360.2	580.2	505.6	1.040	2051.8	1964.5	2.43	4.78	3.74	3.61	11.	*S
30	2380.1	600.1	490.8	0.878	1951.3	1892.9	2.24	4.95	3.66	3.61	10.	*S
31	2400.1	620.1	517.7	1.063	2076.5	1997.1	2.42	4.71	3.54	3.61	15.	*S
32	2420.1	640.0	502.8	1.008	1915.7	1939.8	2.30	4.84	3.62	3.61	13.	*S
33	2435.4	655.3	81.6	0.172	287.4	314.9	0.37	24.43	3.61	3.61	13. 0	0.00
34	2439.9	659.8	492.6	1.022	1796.6	1901.2	2.21	4.89	3.61	3.61	13. 0	0.00
35	2460.2	680.2	491.4	0.955	1807.4	1897.0	2.16	5.01	3.51	3.61	10.	*S
36	2480.1	700.1	508.8	1.027	2107.8	1966.4	2.20	4.79	3.75	3.61	14.	*S
37	2500.0	720.0	497.0	0.963	1764.8	1919.3	2.11	4.94	3.38	3.61	11.	*S
38	2520.1	740.0	529.8	1.065	1987.3	2046.5	2.21	4.65	3.46	3.62	13.	*S
39	2540.0	760.0	493.9	1.022	2024.0	1903.4	2.02	4.87	4.11	3.62	9.	*S
40	2560.0	780.0	513.5	1.026	1930.8	1972.6	2.05	4.79	3.57	3.62	10.	*S
41	2580.2	800.2	519.1	1.054	2150.4	2020.4	2.05	4.74	3.87	3.62	12.	*S
42	2600.0	820.0	525.7	1.041	1841.2	2032.1	2.04	4.70	3.32	3.62	11.	*S
43	2619.9	839.9	521.5	1.016	1905.5	2010.5	1.99	4.76	3.61	3.62	8.	*S
44	2640.1	860.1	533.9	1.089	2124.7	2064.5	2.00	4.61	3.59	3.62	12.	*S
45	2659.9	879.9	517.4	1.035	1940.4	2001.0	1.91	4.76	3.57	3.62	10.	*S
46	2680.0	900.0	492.2	1.007	2087.9	1903.7	1.79	4.90	3.85	3.62	11.	*S
47	2700.1	920.1	501.8	1.014	2262.2	1941.0	1.79	4.85	3.74	3.62	17.	*S
48	2719.9	939.8	505.9	1.027	2034.6	1957.3	1.78	4.84	3.60	3.62	12.	*S
49	2740.2	960.2	484.4	0.963	1889.3	1874.2	1.68	5.03	3.67	3.62	10.	*S
50	2760.1	980.1	536.4	1.093	1906.9	2075.2	1.83	4.60	3.39	3.62	10.	*S
51	2780.0	999.9	521.1	1.054	1942.4	2016.5	1.75	4.71	3.54	3.62	12.	*S
52	2800.0	1020.0	494.3	0.980	1851.9	1912.5	1.64	4.93	3.63	3.62	9.	*S
53	2819.9	1039.9	469.3	0.906	1846.0	1816.2	1.53	5.19	3.87	3.62	9.	*S
54	2840.0	1060.0	520.3	1.040	2075.5	2011.5	1.64	4.73	3.46	3.62	13.	*S
55	2860.0	1079.9	487.5	0.975	2003.4	1888.0	1.55	4.97	3.69	3.62	12.	*S
56	2880.1	1100.0	533.6	1.059	1953.0	2065.1	1.67	4.64	3.48	3.62	10.	*S
57	2900.0	1120.0	494.4	0.983	1782.4	1913.1	1.53	4.93	3.49	3.62	9.	*S

TABLE AIII(1) - (CONTINUED)

53	2920.1	116C.1	479.4	0.971	1961.6	1855.1	1.46	5.02	3.77	3.62	13.	AS
59	2940.0	116C.C	519.4	1.048	1891.6	2009.6	1.55	4.72	3.31	3.62	12.	AS
60	2960.2	1180.1	486.8	0.987	1859.2	1875.3	1.44	4.98	3.41	3.62	10.	AS
61	2980.0	1200.0	535.0	1.098	2116.5	2070.1	1.57	4.59	3.51	3.62	13.	AS
62	3000.1	1220.1	481.2	1.009	2113.5	1861.6	1.39	4.96	4.03	3.62	12.	AS
63	3020.1	1240.C	468.5	0.971	2089.4	1812.4	1.34	5.07	4.15	3.62	13.	AS
64	3060.0	1260.C	486.6	0.966	1813.5	1832.2	1.37	5.03	3.58	3.62	11.	AS
65	3060.1	1280.0	513.3	1.013	2126.C	1995.3	1.43	4.79	3.89	3.62	12.	AS
66	3078.9	1299.8	508.3	1.039	1982.9	1965.8	1.39	4.80	3.81	3.62	7.	AS
67	3099.9	1319.9	543.4	1.122	2079.7	2101.2	1.47	4.54	3.73	3.62	9.	AS
68	3118.9	1339.8	512.1	1.032	2084.C	1973.9	1.37	4.79	3.40	3.62	12.	AS
69	3140.0	1360.0	516.6	1.061	2112.2	1999.9	1.36	4.71	3.63	3.62	12.	AS
70	3160.1	1380.C	488.5	0.955	1782.7	1841.6	1.27	4.94	3.50	3.62	9.	AS
71	3180.0	1400.C	492.7	0.999	1895.9	1903.9	1.27	4.90	3.51	3.62	13.	AS
72	3200.0	1419.9	541.3	1.089	2212.7	2091.6	1.34	4.57	3.62	3.62	14.	AS
73	3220.1	1440.C	487.8	0.935	1755.7	1894.7	1.23	5.03	3.49	3.62	9.	AS
74	3239.9	1459.9	499.1	0.978	1821.2	1923.1	1.24	4.91	3.37	3.61	11.	AS
75	3259.9	1479.9	481.3	0.964	1761.5	1859.3	1.17	5.03	3.58	3.61	8.	AS
76	3280.1	1500.C	489.C	0.966	1845.C	1842.5	1.14	4.98	3.21	3.61	8.	AS
77	3300.1	1520.C	498.9	0.983	1788.1	1925.4	1.27	4.90	3.51	3.61	8.	AS
78	3320.1	1560.C	519.6	1.019	1795.3	2006.7	1.24	4.75	3.62	3.61	8.	AS
79	3340.1	1560.C	502.5	1.011	2027.C	1934.2	1.19	4.84	3.96	3.61	9.	AS
80	3359.9	1579.9	503.9	1.039	2033.0	1966.2	1.13	4.78	3.62	3.61	12.	AS
81	3390.1	1600.C	547.2	1.100	2047.2	2109.4	1.27	4.53	3.55	3.61	10.	AS
82	3400.2	1620.1	516.9	1.052	2123.9	1992.1	1.19	4.74	3.21	3.61	15.	AS
83	3420.1	1640.1	473.1	0.945	1905.7	1822.5	1.08	5.09	3.83	3.61	11.	AS
84	3440.1	1660.1	523.1	1.065	2023.2	2016.6	1.14	4.69	3.62	3.62	12.	AS
85	3460.1	1680.1	519.2	1.044	2082.7	1993.7	1.16	4.74	3.59	3.60	12.	AS
86	3480.0	1700.C	496.5	0.955	2013.3	1803.3	1.10	4.92	3.81	3.60	11.	AS
87	3500.0	1719.9	498.5	0.955	1915.4	1917.9	1.09	4.92	3.53	3.60	12.	AS
88	3520.1	1740.1	531.8	1.020	1955.7	2065.0	1.16	4.72	3.67	3.60	8.	AS
89	3540.1	1760.C	522.4	1.083	2061.0	2013.C	1.13	4.65	3.76	3.67	10.	AS
90	3560.C	1779.9	478.6	0.960	1944.5	1832.1	1.07	5.07	3.72	3.62	14.	AS
91	3580.1	1800.1	498.1	0.960	1718.3	1913.2	1.04	4.98	3.37	3.67	9.	AS
92	3600.0	1819.9	501.6	0.955	1958.2	1925.7	1.06	4.91	3.58	3.59	11.	AS
93	3620.C	1840.C	470.4	0.924	1752.3	1805.3	0.99	5.19	3.47	3.59	11.	AS
94	3640.2	1860.1	481.2	0.941	1822.1	1844.0	1.00	5.12	3.74	3.59	8.	AS
95	3660.1	1880.0	439.4	0.853	1665.1	1694.7	0.97	5.57	3.74	3.57	8.	AS
96	3678.9	1899.9	504.1	1.019	2032.2	1932.1	1.03	4.91	3.79	3.59	12.	AS
97	3700.0	1920.0	496.C	1.011	2028.5	1903.0	1.01	4.95	3.61	3.59	14.	AS
98	3720.2	1940.1	512.1	1.056	1981.2	1871.2	1.04	4.81	3.67	3.58	13.	AS
99	3740.1	1960.0	487.9	0.948	1800.8	1867.2	0.94	5.17	3.57	3.58	11.	AS
100	3760.0	1980.C	502.2	1.002	1767.0	1911.2	1.01	4.94	3.40	3.58	8.	AS
101	3780.C	1999.9	523.4	1.032	2077.9	2033.4	1.03	4.85	3.58	3.54	13.	AS
102	3795.2	2015.2	44.3	0.135	252.8	245.4	0.11	29.87	3.58	3.53	14.	C.C.C.C
103	3800.0	2019.9	550.5	1.167	2176.6	2101.5	1.08	4.60	3.59	3.54	14.	C.C.C.C
104	3825.8	2045.8	149.5	0.300	236.5	570.7	0.29	14.26	1.67	3.52	3.	AS

this case only, in channels, (11) the least-squares width, (12) the base width in channels, and (13) the peak type, the symbols S and D standing for singlets and doublets.

Statistical analysis applied to these pseudo-experimental peaks yielded results that are summarized in Table AIII(2). The measured standard deviations in the peak parameters, defined by

$$\sigma(z) = [1/\sqrt{(n-1)}] \sqrt{\sum_{i=1}^n (z - \bar{z})^2} \quad (\text{A3.19})$$

are compared to those estimated by the error equations developed above. Three entries are given for each peak parameter; these correspond, respectively, to results obtained by applying the statistical analysis to the first 50, the last 50, and all 100 peaks.

From this table it is seen that the agreement between the actual and estimated standard deviations is satisfactory. The actual values obtained for the various peak parameters in the four different cases have already been compared in Appendix I to the built-in values used in constructing the spectrum in question; they will not, therefore, be considered any further.

The analysis presented above could have been carried out using actual gamma ray spectra. This would have involved the accumulation of 100 sets of data taken under exactly identical experimental conditions. Such a procedure is not practical and, moreover, one is faced with the problem of accounting for possible electronic shifts in the spectrometer which

TABLE AIII(2)

STATISTICAL ANALYSIS APPLIED TO THE 100

PSEUDO-EXPERIMENTAL PEAKS

Smoothing Degree	r=1.0			r=1.34			r=1.6			r=1.9		
	Mean	$\sigma_{cal.}$	$\sigma_{est.}$	Mean	$\sigma_{cal.}$	$\sigma_{est.}$	Mean	$\sigma_{cal.}$	$\sigma_{est.}$	Mean	$\sigma_{cal.}$	$\sigma_{est.}$
H (A3.1)	1001.0 999.5 1000.3	30.1 27.7 28.8	31.5	999.5 997.1 998.3	21.7 21.7 21.7	23.7	951.1 950.0 950.6	19.3 18.3 18.7	19.3	913.9 913.0 913.5	16.6 16.0 16.2	15.9
H ₀ (A3.3)	480.7 479.5 480.1	20.0 16.0 18.0	21.9	492.8 492.0 492.4	15.3 13.1 14.5	16.4	498.2 496.3 497.3	10.2 10.7 10.4	13.9	499.3 499.2 499.3	8.7 10.5 9.5	11.8
h (A3.6)	517.8 516.0 516.9	35.1 30.4 32.7	35.2	506.3 503.0 504.7	24.5 23.1 23.7	26.4	453.3 451.8 452.6	21.6 20.2 20.8	21.6	414.7 412.5 413.6	19.0 18.9 18.9	18.0
w (A3.13)x $\sqrt{2}$	3.67 3.67 3.67	0.22 0.22 0.22	0.20	3.62 3.64 3.63	0.16 0.18 0.17	0.16	3.97 3.97 3.97	0.15 0.17 0.16	0.18	4.33 4.33 4.33	0.13 0.16 0.15	0.18
A _{sum} (A3.16)	2099 2079 2089	211 198 204	176	1966 1950 1958	157 138 147	144	1922 1908 1915	118 134 126	137	1907 1882 1895	121 140 131	134

change the apparent energy resolution of the system. Furthermore, in such a case it is not possible to investigate in what way the method of analysis affects the data since no equivalent built-in values exist to which the measured peak parameters can be compared.

Despite this limitations, it was found necessary to test the error equations using also actual experimental data. Since there was also some interest in examining the reproducibility of the results obtained for a given sample, it was decided to perform an analysis that would combine both. With this in mind, the data obtained from the analysis of three aluminum runs taken under almost identical experimental conditions using the internal-sample facility were examined. The results are shown in Table AIII(4). Pertinent information on these runs is presented in Table AIII(3). Note the correction factors used to reduce all three runs to the same flux time value. Also, in Run 1, there was an extra 1/4-inch plate (Pb) between the sample and the detector and it was therefore necessary to correct for the additional attenuation of the gamma rays in passing through this extra length of lead. This was carried out using the data in Table IV(2).

Only peaks whose estimated standard deviation was less than 20 percent were considered in this comparison. The estimated errors in the peaks are those predicted by equations (A3.16) and (A3.18). The residual errors were evaluated using equation (A3.19); sample calculations are shown

in Table AIII(3).

This analysis has shown that in most cases the three different sets of peak areas, both Gaussian and straight-sums, are within the estimated standard deviation computed for each case. Also, the estimated standard deviation in the averaged peak areas are close to those obtained by equation (A3.19). Finally, in comparing the two methods of area determination, note that there is better agreement between the peak areas determined by the Gaussian approach than between the corresponding ones obtained by the straight-sums technique; the residuals in the former case are less than those in the latter.

TABLE AIII(3)

PERTINENT INFORMATION ASSOCIATED WITH THE
THREE ALUMINUM RUNS

	<u>Run 1</u>	<u>Run 2</u>	<u>Run 3</u>
Area correction factor(ψ)	1.021	1.011	1.011
Channel-energy conversion factor, C, (keV/channel)	2.172	1.989	1.988
Flux-time correction factor	0.838	1.045	1.000
1st const. in w-E equation	7.892	7.048	7.459
2nd const. in w-E equation	-3.942	0.466	-2.857
3rd const. in w-E equation	17.639	12.239	15.605

Sample Calculations

First Peak, Gaussian Method

	<u>Peak Area</u>	<u>Estim. Error</u>	<u>Error Resid.</u>
Run 1	995.3	194.4 ^(b)	
Run 2	810.1	135.4	
Run 3	759.9	143.8	
Average	855.1 ^(a)	92.4 ^(c)	71.6 ^(d)

$$(a) \quad (995.3 + 810.1 + 759.9)/3 = 855.1$$

$$(b) \quad \text{Estimated by equation (A3.18)}$$

$$(c) \quad (194.4^2 + 135.4^2 + 143.8^2)^{\frac{1}{2}}/3.0 = 92.4$$

$$(d) \quad \left(\sum_{i=1}^3 (A_i - 855.1)^2 \right)^{\frac{1}{2}}/1.414 = 71.6$$

TABLE AIII(4) COMPARISON OF THE THREE ALUMINUM RUNS -- PAIR SPECTROMETER, INTERNAL SAMPLE

NO.	ENERGY KEV	REF.	GAUSSIAN METHOD			METHOD OF SUMS		
			PEAK AREA	ERROR ESTIM	ERROR RESID	PEAK AREA	ERROR ESTIM	ERROR RESID
1	1624.7	RUN 1	995.3	194.4		1315.8	325.2	
	1620.1	RUN 2	810.1	135.4		823.1	227.4	
	1620.0	RUN 3	759.9	143.8		856.4	246.0	
		AVRGE	855.1	92.4	71.6	998.4	155.6	159.0
2	1778.5	RUN 1	25870.1	553.6		29406.6	393.2	
	1778.5	RUN 2	27293.2	453.1		30742.8	290.1	
	1778.5	RUN 3	27159.3	431.8		31924.9	280.7	
		AVRGE	26774.2	278.5	454.1	30691.4	187.8	727.7
3	1810.5	RUN 1	1593.8	210.7		1512.9	345.6	
	1810.2	RUN 2	1867.2	152.0		2143.1	245.2	
	1810.2	RUN 3	2070.1	156.7		2396.3	254.2	
		AVRGE	1843.7	101.1	138.0	2017.4	164.7	262.7
4	2112.9	RUN 1	2052.4	197.9		2642.8	317.3	
	2110.3	RUN 2	1978.6	150.4		2481.2	241.5	
	2111.5	RUN 3	1888.3	153.3		2706.6	251.7	
		AVRGE	1973.1	97.3	47.5	2610.2	157.2	67.1
5	2225.7	RUN 1	1654.1	194.9		1827.9	316.8	
	2221.6	RUN 2	1087.4	146.8		1034.9	244.4	
	2223.6	RUN 3	1115.0	150.3		1062.0	253.3	
		AVRGE	1285.5	95.5	184.5	1308.3	157.9	259.9
6	2272.8	RUN 1	1468.2	214.7		1260.4	354.7	
	2273.5	RUN 2	1086.2	150.3		1060.6	250.8	
	2272.8	RUN 3	1156.1	149.8		1387.4	252.5	
		AVRGE	1236.8	100.6	117.4	1236.2	167.5	95.1

TABLE AIII(4) (CONTINUED)

NO.	ENERGY KEV	REF.	GAUSSIAN METHOD			METHOD OF SUMS		
			PEAK AREA	ERROR ESTIM	ERROR RESID	PEAK AREA	ERROR ESTIM	ERROR RESID
7	2283.8	RUN 1	2393.0	217.3		2091.0	346.6	
	2283.2	RUN 2	2825.2	165.0		2726.3	257.4	
	2282.9	RUN 3	2691.9	162.9		3197.0	259.3	
		AVRGE	2636.7	105.9	127.8	2671.4	167.9	320.5
8	2577.7	RUN 1	1255.9	212.0		1082.6	352.1	
	2578.0	RUN 2	1576.5	162.9		1451.0	267.5	
	2578.5	RUN 3	1333.3	160.0		1217.4	268.1	
		AVRGE	1388.6	103.8	96.6	1250.3	172.4	107.6
9	2590.4	RUN 1	2864.9	225.8		2501.3	355.2	
	2591.5	RUN 2	2936.3	172.9		2675.0	270.1	
	2590.7	RUN 3	3192.6	174.6		2892.4	274.0	
		AVRGE	2997.9	111.2	99.5	2689.6	174.5	113.1
10	2626.2	RUN 1	1379.6	205.4		1370.3	338.9	
	2625.0	RUN 2	1123.3	161.3		1100.8	269.6	
	2626.3	RUN 3	1332.8	160.2		1125.7	268.2	
		AVRGE	1278.5	102.1	78.8	1198.9	169.8	86.0
11	2822.9	RUN 1	3457.4	224.4		3436.5	342.9	
	2822.5	RUN 2	3487.2	180.6		3669.5	277.3	
	2821.6	RUN 3	3260.1	177.4		3386.7	278.2	
		AVRGE	3401.6	112.8	71.3	3497.6	173.8	87.2
12	2961.8	RUN 1	8940.3	290.6		9493.6	373.5	
	2960.7	RUN 2	9265.4	239.0		9500.4	306.8	
	2960.2	RUN 3	8658.4	225.1		8472.8	296.6	
		AVRGE	8954.7	146.2	175.5	9155.6	189.0	341.4

TABLE AIII(4) (CONTINUED)

NO.	ENERGY KEY	REF.	GAUSSIAN METHOD			METHOD OF SUMS		
			PEAK AREA	ERROR ESTIM	ERROR RESID	PEAK AREA	ERROR ESTIM	ERROR RESID
13	3034.6	RUN 1	8417.4	290.4		8229.9	381.3	
	3034.5	RUN 2	8499.6	235.4		8761.0	310.6	
	3034.3	RUN 3	7830.6	224.0		7799.7	306.8	
		AVRGE	8249.2	145.3	210.7	8263.5	193.2	278.0
14	3267.4	RUN 1	1216.7	202.8		1482.6	335.0	
	3267.8	RUN 2	1302.4	164.0		1333.3	270.5	
	3266.2	RUN 3	1375.3	163.3		1086.4	271.4	
		AVRGE	1298.2	102.6	45.9	1300.8	169.7	115.5
15	3304.1	RUN 1	799.1	210.2		647.3	352.6	
	3302.9	RUN 2	986.8	171.1		824.5	286.5	
	3302.7	RUN 3	1385.9	169.4		1167.0	282.5	
		AVRGE	1057.3	106.5	173.0	879.6	178.3	152.5
16	3409.4	RUN 1	1156.5	218.8		716.0	362.4	
	3412.5	RUN 2	940.3	168.7		1022.7	282.7	
	3411.4	RUN 3	1102.3	166.7		1262.3	281.1	
		AVRGE	1066.4	107.6	64.9	1000.3	179.6	158.1
17	3437.2	RUN 1	857.4	214.7		732.7	359.6	
	3437.3	RUN 2	782.7	166.4		646.8	279.9	
	3440.3	RUN 3	1112.6	169.5		996.8	285.5	
		AVRGE	917.6	106.7	99.9	792.1	179.2	105.3
18	3466.3	RUN 1	7907.3	291.8		7684.7	383.0	
	3465.9	RUN 2	8737.6	242.9		8592.5	309.4	
	3465.6	RUN 3	8467.6	234.6		8447.7	309.6	
		AVRGE	8370.8	148.8	244.6	8241.6	193.9	281.6

TABLE AIII(4) (CONTINUED)

NC.	ENERGY KEV	REF.	GAUSSIAN METHOD			METHOD OF SUMS		
			PEAK AREA	ERROR ESTIM	ERROR RESID	PEAK AREA	ERROR ESTIM	ERROR RESID
19	3561.9	RUN 1	1089.7	218.4		1290.5	363.4	
	3562.0	RUN 2	1353.8	170.2		1588.6	280.4	
	3560.6	RUN 3	1306.3	170.7		1938.9	286.6	
		AVRGE	1250.0	108.4	81.3	1606.0	180.4	187.4
20	3592.8	RUN 1	5838.3	266.8		5541.7	372.9	
	3591.6	RUN 2	5750.2	209.9		6104.8	292.4	
	3591.5	RUN 3	6019.4	207.1		6340.9	290.5	
		AVRGE	5869.3	132.5	79.3	5995.8	185.3	237.0
21	3791.5	RUN 1	1504.1	210.9		1820.5	343.2	
	3789.4	RUN 2	1082.2	174.9		1044.9	290.8	
	3789.5	RUN 3	1566.7	167.2		1598.7	275.0	
		AVRGE	1384.4	107.0	152.1	1488.0	175.7	230.6
22	3825.5	RUN 1	967.6	221.2		796.1	368.1	
	3823.6	RUN 2	946.5	173.1		1059.0	289.3	
	3823.5	RUN 3	890.6	166.9		892.1	282.4	
		AVRGE	934.9	108.9	23.0	915.7	182.3	76.8
23	3851.8	RUN 1	4578.7	251.8		5145.5	366.5	
	3849.5	RUN 2	4625.4	206.3		5057.7	301.4	
	3849.7	RUN 3	4711.8	198.8		5017.2	291.9	
		AVRGE	4638.6	127.2	39.0	5073.5	185.7	37.9
24	3876.6	RUN 1	3635.6	245.8		3490.5	371.1	
	3875.7	RUN 2	3286.7	193.6		2824.0	295.7	
	3876.1	RUN 3	3061.5	187.4		3181.8	293.3	
		AVRGE	3327.9	121.6	167.0	3165.4	185.9	192.6

TABLE AIII(4) (CONTINUED)

NO.	ENERGY KEV	REF.	GAUSSIAN METHOD			METHOD OF SUMS		
			PEAK AREA	ERROR ESTIM	ERROR RESID	PEAK AREA	ERROR ESTIM	ERROR RESID
25	4017.0	RUN 1	1215.6	216.1		862.9	354.4	
	4013.5	RUN 2	1045.7	167.5		1126.1	277.5	
	4017.8	RUN 3	946.0	163.8		1071.8	275.8	
		AVRGE	1069.1	106.3	78.7	1020.3	176.0	80.2
26	4136.0	RUN 1	9996.3	323.9		9844.6	382.5	
	4133.9	RUN 2	10416.1	263.5		11519.9	303.1	
	4133.3	RUN 3	9766.7	249.1		9830.4	301.5	
		AVRGE	10059.7	162.1	190.1	10398.3	191.2	560.8
27	4219.1	RUN 1	2741.1	236.6		2959.6	367.5	
	4218.4	RUN 2	2495.2	188.1		2318.9	295.1	
	4217.9	RUN 3	1972.4	185.6		2005.9	302.4	
		AVRGE	2402.9	118.2	226.7	2428.1	186.6	280.7
28	4261.5	RUN 1	9818.8	323.0		9779.9	383.5	
	4259.8	RUN 2	9996.2	258.9		11030.8	300.1	
	4259.6	RUN 3	10175.7	257.4		10959.0	311.8	
		AVRGE	9996.9	162.5	103.1	10589.9	192.7	405.5
29	4381.0	RUN 1	1079.5	206.0		1270.9	337.9	
	4378.3	RUN 2	1013.4	168.5		827.9	278.1	
	4377.9	RUN 3	962.3	162.4		831.1	271.5	
		AVRGE	1018.4	103.9	33.9	976.6	171.7	147.1
30	4407.1	RUN 1	1038.6	209.6		974.8	344.3	
	4407.8	RUN 2	1135.6	169.9		1199.2	279.3	
	4405.7	RUN 3	1027.7	165.4		869.8	275.8	
		AVRGE	1067.3	105.5	34.3	1014.6	174.0	97.1

TABLE AIII(4) (CONTINUED)

NO.	ENERGY KEV	REF.	GAUSSIAN METHOD			METHOD OF SUMS		
			PEAK AREA	ERROR ESTIM	ERROR RESID	PEAK AREA	ERROR ESTIM	ERROR RESID
31	4426.5	RUN 1	1295.2	212.3		1298.5	345.1	
	4427.8	RUN 2	1600.9	171.6		1721.4	276.3	
	4427.1	RUN 3	1766.6	167.7		1530.5	270.1	
		AVRGE	1554.2	106.8	138.1	1516.8	172.7	122.3
32	4659.9	RUN 1	3587.6	251.1		3707.5	376.3	
	4660.4	RUN 2	4222.0	212.4		3879.3	312.8	
	4659.8	RUN 3	4345.2	201.6		4201.0	296.1	
		AVRGE	4051.6	128.6	234.7	3929.3	190.6	144.6
33	4690.8	RUN 1	6885.7	295.4		6878.5	395.1	
	4690.7	RUN 2	6684.5	235.3		7158.2	316.6	
	4690.4	RUN 3	7580.9	237.3		7261.5	313.4	
		AVRGE	7050.4	148.7	271.6	7099.4	198.5	114.4
34	4734.6	RUN 1	9150.0	321.2		9739.9	394.9	
	4733.6	RUN 2	8909.7	262.8		9035.9	330.4	
	4733.7	RUN 3	8904.7	247.6		9789.7	311.2	
		AVRGE	8988.1	161.1	81.1	9521.8	200.5	243.4
35	4765.6	RUN 1	1720.0	231.5		1822.7	371.7	
	4765.1	RUN 2	1487.2	189.9		981.6	308.8	
	4763.2	RUN 3	1268.6	176.2		1395.8	291.8	
		AVRGE	1492.0	115.8	130.3	1400.0	188.2	242.8
36	4811.4	RUN 1	1423.4	224.9		1102.4	363.3	
	4810.5	RUN 2	793.6	174.0		590.3	289.1	
	4809.0	RUN 3	1226.7	171.1		1045.7	282.3	
		AVRGE	1147.9	110.6	186.0	912.8	181.1	162.1

TABLE AIII(4) (CONTINUED)

NO.	ENERGY KEV	REF.	GAUSSIAN METHOD			METHOD OF SUMS		
			PEAK AREA	ERROR ESTIM	ERROR RESID	PEAK AREA	ERROR ESTIM	ERROR RESID
37	4904.3	RUN 1	4459.9	248.4		4918.1	351.6	
	4903.2	RUN 2	4911.8	203.8		5336.7	282.6	
	4903.2	RUN 3	4932.1	199.8		4928.4	280.4	
		AVRGE	4767.9	126.1	154.2	5061.1	177.0	137.9
38	4950.6	RUN 1	1110.6	216.7		803.5	352.8	
	4949.9	RUN 2	857.7	167.3		772.7	276.4	
	4947.0	RUN 3	844.1	160.1		660.6	266.9	
		AVRGE	937.5	105.7	86.7	745.6	173.9	43.4
39	5014.4	RUN 1	1588.0	215.2		1485.7	342.3	
	5014.9	RUN 2	1639.2	170.0		1248.6	269.5	
	5014.9	RUN 3	1814.1	173.1		1573.3	276.9	
		AVRGE	1680.4	108.1	68.4	1435.9	172.1	97.0
40	5103.8	RUN 1	1133.7	199.7		1419.5	322.6	
	5101.4	RUN 2	769.1	164.4		566.1	271.7	
	5104.9	RUN 3	629.1	157.3		493.9	264.3	
		AVRGE	844.0	100.9	150.4	826.5	165.9	297.2
41	5135.2	RUN 1	5031.4	249.6		5207.0	338.3	
	5134.2	RUN 2	4341.6	192.8		5260.2	269.9	
	5134.3	RUN 3	4524.0	191.8		4517.2	269.4	
		AVRGE	4632.4	123.0	206.4	4994.8	169.9	239.3
42	5184.0	RUN 1	1400.0	204.0		1781.2	325.5	
	5180.0	RUN 2	1072.3	162.5		1099.4	264.1	
	5181.0	RUN 3	1586.2	161.5		1918.7	258.9	
		AVRGE	1352.8	102.2	150.2	1599.8	164.2	253.3

TABLE AIII(4) (CONTINUED)

NO.	ENERGY KEV	REF.	GAUSSIAN METHOD			METHOD OF SUMS		
			PEAK AREA	ERROR ESTIM	ERROR RESID	PEAK AREA	ERROR ESTIM	ERROR RESID
43	5412.7	RUN 1	2948.1	225.2		3220.4	333.5	
	5410.1	RUN 2	3057.0	178.8		3382.5	262.8	
	5411.7	RUN 3	3119.5	177.2		3351.9	262.9	
		AVRGE	3041.6	112.6	50.1	3318.3	166.5	149.7
44	5525.2	RUN 1	2256.5	209.4		2232.8	315.7	
	5526.0	RUN 2	2188.6	168.1		2344.9	256.0	
	5526.6	RUN 3	1743.9	163.2		1784.3	257.5	
		AVRGE	2063.0	104.7	160.7	2120.6	160.4	171.3
45	5587.2	RUN 1	1097.9	202.1		1327.0	325.2	
	5585.0	RUN 2	1583.1	167.8		1322.6	264.3	
	5586.0	RUN 3	1819.6	161.0		1412.3	251.0	
		AVRGE	1500.2	102.7	212.4	1354.0	162.8	29.2
46	5708.2	RUN 1	702.7	194.2		668.3	317.2	
	5710.7	RUN 2	1117.8	161.2		1104.5	259.3	
	5707.9	RUN 3	940.5	151.5		923.5	247.6	
		AVRGE	920.4	98.1	120.3	898.7	159.6	126.5
47	5920.8	RUN 1	4459.3	247.0		4572.5	339.7	
	5920.2	RUN 2	4017.8	191.2		3923.8	266.3	
	5920.8	RUN 3	4624.4	186.8		4586.9	250.0	
		AVRGE	4367.2	121.3	181.1	4361.1	166.3	218.7
48	6018.3	RUN 1	4291.7	247.6		5034.2	345.2	
	6018.0	RUN 2	4320.3	197.4		4390.7	273.0	
	6016.9	RUN 3	4584.4	195.8		4490.5	269.3	
		AVRGE	4398.8	124.1	93.2	4638.5	172.0	200.0

TABLE AIII(4) (CONTINUED)

NO.	ENERGY KEV	REF.	GAUSSIAN METHOD			METHOD OF SUMS		
			PEAK AREA	ERROR ESTIM	ERROR RESID	PEAK AREA	ERROR ESTIM	ERROR RESID
49	6101.1	RUN 1	3824.9	238.3		3669.2	333.4	
	6101.2	RUN 2	3776.7	189.6		3650.2	266.0	
	6102.2	RUN 3	3823.0	184.7		4225.9	260.4	
		AVRGE	3808.2	118.7	15.9	3848.4	166.6	188.8
50	6201.1	RUN 1	947.5	196.5		794.0	313.9	
	6198.0	RUN 2	996.6	153.8		880.6	245.9	
	6197.6	RUN 3	828.4	151.3		747.8	247.0	
		AVRGE	924.1	97.3	49.9	807.5	156.3	138.9
51	6317.7	RUN 1	2447.2	216.1		2651.9	318.7	
	6316.6	RUN 2	2507.2	173.0		2406.7	254.9	
	6315.7	RUN 3	2956.2	174.4		3075.6	253.2	
		AVRGE	2636.8	109.1	160.6	2711.4	160.1	195.4
52	6438.8	RUN 1	878.2	199.9		593.5	319.7	
	6439.0	RUN 2	584.6	151.9		387.6	248.5	
	6440.5	RUN 3	799.7	149.6		660.0	243.5	
		AVRGE	754.2	97.4	87.8	547.0	157.5	82.0
53	6708.8	RUN 1	1175.1	205.9		687.2	322.2	
	6708.7	RUN 2	848.7	156.3		748.2	251.1	
	6709.6	RUN 3	1053.7	152.2		1015.4	242.7	
		AVRGE	1025.8	100.0	95.3	816.9	158.4	100.8
54	6988.6	RUN 1	749.6	203.4		444.8	325.7	
	6990.0	RUN 2	659.5	159.1		484.1	258.3	
	6990.8	RUN 3	854.7	157.9		657.7	255.3	
		AVRGE	754.6	100.9	56.4	528.9	162.6	65.4

TABLE AIII(4) (CONTINUED)

NO.	ENERGY KEV	REF.	GAUSSIAN METHOD			METHOD OF SUMS		
			PEAK AREA	ERROR ESTIM	ERROR RESID	PEAK AREA	ERROR ESTIM	ERROR RESID
55	7058.5	RUN 1	2495.2	232.5		2199.2	340.0	
	7057.2	RUN 2	2248.9	178.8		2177.4	265.3	
	7054.7	RUN 3	2259.8	179.0		2283.1	268.6	
		AVRGE	2334.6	114.5	80.4	2219.9	169.4	32.3
56	7156.6	RUN 1	960.9	224.5		653.9	357.6	
	7160.6	RUN 2	1192.2	173.0		1099.8	273.3	
	7158.1	RUN 3	1087.5	168.8		1013.0	270.3	
		AVRGE	1080.2	109.9	66.9	922.2	175.0	136.5
57	7177.2	RUN 1	882.2	226.3		596.4	362.4	
	7178.0	RUN 2	1046.3	172.8		955.7	275.5	
	7174.5	RUN 3	1000.1	171.4		922.1	276.6	
		AVRGE	976.2	110.8	48.9	824.8	177.5	114.6
58	7245.5	RUN 1	2460.0	253.6		1908.6	378.1	
	7244.0	RUN 2	2818.2	194.7		3213.9	284.0	
	7244.0	RUN 3	2453.4	194.8		2232.6	293.4	
		AVRGE	2577.2	124.8	120.5	2451.7	185.5	392.4
59	7277.7	RUN 1	1661.3	248.5		1369.6	385.7	
	7274.9	RUN 2	1479.1	183.0		1711.1	286.3	
	7275.7	RUN 3	1697.5	191.0		1446.5	299.5	
		AVRGE	1612.6	121.0	67.6	1509.0	188.7	103.4
60	7305.0	RUN 1	1856.4	246.9		1752.4	378.7	
	7306.6	RUN 2	1978.5	191.9		1607.2	292.7	
	7307.5	RUN 3	2467.1	193.9		2011.8	290.4	
		AVRGE	2100.7	122.7	186.6	1790.4	186.6	118.3

TABLE AIII(4) (CONTINUED)

NO.	ENERGY KEV	REF.	GAUSSIAN METHOD			METHOD OF SUMS		
			PEAK AREA	ERROR ESTIM	ERROR RESID	PEAK AREA	ERROR ESTIM	ERROR RESID
61	7367.1	RUN 1	7654.1	326.1		6956.6	397.6	
	7368.1	RUN 2	6375.4	241.0		6834.7	299.4	
	7368.4	RUN 3	6484.0	243.1		6366.7	308.0	
		AVRGE	6837.8	157.6	409.4	6719.3	195.1	179.8
62	7694.5	RUN 1	3515.9	279.2		3463.7	396.9	
	7693.8	RUN 2	2728.8	212.0		2296.7	312.7	
	7694.4	RUN 3	3382.4	215.8		3354.4	311.1	
		AVRGE	3209.0	137.2	243.2	3038.3	197.8	372.1
63	7723.8	RUN 1	24761.4	581.9		24562.7	420.4	
	7723.8	RUN 2	24851.0	511.9		24302.1	354.0	
	7723.8	RUN 3	24481.9	479.8		24086.8	338.7	
		AVRGE	24698.1	303.8	111.8	24317.1	215.2	139.0
64	7916.1	RUN 1	6176.4	250.8		5433.2	224.3	
	7914.3	RUN 2	6275.8	203.3		6177.3	172.3	
	7914.7	RUN 3	6283.0	202.9		5781.5	181.7	
		AVRGE	6245.1	127.1	34.4	5797.3	112.1	215.0
65	7939.0	RUN 1	1139.3	143.6		1017.6	196.5	
	7934.1	RUN 2	933.4	106.8		923.4	151.2	
	7932.4	RUN 3	662.3	105.6		612.2	159.4	
		AVRGE	911.7	69.3	138.1	851.1	98.2	122.5
66	8508.4	RUN 1	451.8	98.9		278.4	137.2	
	8511.0	RUN 2	460.8	72.8		359.3	99.6	
	8513.3	RUN 3	573.1	78.9		431.2	106.2	
		AVRGE	495.2	48.6	39.0	356.3	66.7	44.2

TABLE AIII(4) (CONTINUED)

NO.	ENERGY KEV	REF.	GAUSSIAN METHOD			METHOD OF SUMS		
			PEAK AREA	ERROR ESTIM	ERROR RESID	PEAK AREA	ERROR ESTIM	ERROR RESID
67	8534.7	RUN 1	553.9	104.0		341.8	140.6	
	8533.1	RUN 2	543.1	74.9		558.9	99.8	
	8532.8	RUN 3	698.3	80.4		531.7	102.0	
		AVRGE	598.4	50.4	50.0	477.4	66.8	68.3
68	8886.0	RUN 1	1787.4	140.1		1820.0	131.6	
	8881.5	RUN 2	1318.9	97.9		1267.2	101.8	
	8884.2	RUN 3	1497.6	100.9		1423.0	98.1	
		AVRGE	1534.6	66.2	136.5	1503.4	64.4	164.6
69	8997.1	RUN 1	1243.1	116.5		1165.9	109.4	
	8995.4	RUN 2	898.5	83.6		820.2	92.8	
	8995.0	RUN 3	988.2	83.8		845.6	85.9	
		AVRGE	1043.2	55.4	103.2	943.9	55.7	111.3

Appendix IV

PROMINENT CAPTURE GAMMA RAYS OF THE ELEMENTS AND THEIR
MINIMUM MEASURABLE WEIGHTS IN STAINLESS STEEL

It was pointed out in Section 3.6, and again later in Sec. 7.2, that any of the characteristic capture gamma rays of an element can be used in the application of equation (3.24) for the evaluation of its minimum measurable weight in a given sample. In order to evaluate the limits of analytical sensitivity, however, consideration was given only to 12 of the most prominent capture gamma rays of each element.

The limits of analytical sensitivity for the detection of 75 elements in stainless steelware given in Chapter VII for the Compton suppression system and the pair spectrometer. In that chapter, however, it is only the data associated with the most effective gamma ray of each element that was reported. This Appendix is devoted, in part, to the presentation of the minimum weight requirements associated with all the 12 gamma rays chosen for each element. The data is presented in a form similar to Table VII(1) where the limits for quantitative determination of Mn were considered. The experimental information required for the application of equation (3.24) is given in Sec. 7.2 and will not be repeated here. The results for the Compton suppression system appear in Table AIV(1); those for the pair spectrometer are listed in Table AIV(2).

It was noted in Sec. 7.2 that the minimum weight require-

ments were evaluated under the assumption that interference effects are not present. As an aid to resolving such effects in cases where their presence cannot be neglected, there is presented in Table AIV(3) an ordered list of the prominent capture gamma rays of the elements. The data in this table were extracted from reference [R2]. The intensities were converted to number of gamma rays emitted per gram of element of natural composition per incident thermal neutron/cm² by using equation (3.25). In this set of units interference effects may be resolved with less effort since the relative significance of gamma rays originating from different elements may now be evaluated directly.

Recall that in all three tables listed below only twelve gamma rays have been considered for each element. Four of these have energies below 2 MeV and the rest are above this energy limit. Note that H, C, Pb and Bi have less than 12 prominent gamma rays. The symbol D next to the 477.7-keV gamma ray of boron and the 2754.4-keV gamma ray of sodium indicates that these are decay gamma rays and were included accidentally. The symbol E which appears throughout these tables stands for the exponential power on the base 10; thus $0.123E\ 02 = 12.3$ and $0.123E-02 = 0.00123$.

A complete ordered list which includes all the identified capture gamma rays of 75 elements was published recently in a separate report [H7].

TABLE AIV(1) COMPTON SUPPRESSION

LIMITS FOR QUANTITATIVE DETERMINATION

ELEM.	ENERGY	INTENSITY	MIN.AREA	MIN.WT	WT PERCENT
AG	199.5	0.124E 00	0.319E 05	0.24E-01	0.30E-01
AG	237.0	0.477E-01	0.266E 05	0.55E-01	0.70E-01
AG	295.6	0.198E-01	0.209E 05	0.12E 00	0.15E 00
AG	380.4	0.129E-01	0.153E 05	0.16E 00	0.20E 00
AG	2048.6	0.169E-02	0.445E 04	0.15E 01	0.19E 01
AL	248.7	0.392E-03	0.251E 05	0.65E 01	0.82E 01
AL	329.4	0.333E-03	0.185E 05	0.66E 01	0.84E 01
AL	583.4	0.205E-03	0.666E 04	0.90E 01	0.11E 02
AL	1623.1	0.168E-03	0.527E 04	0.14E 02	0.17E 02
AL	2960.4	0.323E-03	0.385E 04	0.11E 02	0.14E 02
AS	236.7	0.109E-02	0.266E 05	0.24E 01	0.31E 01
AS	299.2	0.503E-03	0.205E 05	0.46E 01	0.58E 01
AS	472.2	0.147E-02	0.128E 05	0.13E 01	0.17E 01
AS	1465.9	0.781E-03	0.557E 04	0.28E 01	0.35E 01
AU	193.5	0.123E-01	0.319E 05	0.24E 00	0.30E 00
AU	215.7	0.298E-01	0.299E 05	0.95E-01	0.12E 00
AU	248.2	0.169E-01	0.257E 05	0.15E 00	0.20E 00
AU	261.5	0.175E-01	0.237E 05	0.14E 00	0.18E 00
B	258.1	0.938E-04	0.238E 05	0.26E 02	0.33E 02
B	477.7 D	0.267E-01	0.125E 05	0.74E-01	0.93E-01
B	497.5	0.126E-03	0.119E 05	0.15E 02	0.19E 02
B	501.7	0.109E-03	0.118E 05	0.18E 02	0.22E 02
B	2072.7	0.301E-04	0.451E 04	0.86E 02	0.11E 03
B	2532.3	0.199E-04	0.411E 04	0.15E 03	0.19E 03
BA	627.5	0.738E-03	0.980E 04	0.26E 01	0.33E 01
BA	818.7	0.507E-03	0.768E 04	0.37E 01	0.47E 01
BA	1245.9	0.270E-03	0.587E 04	0.73E 01	0.93E 01
BA	1435.5	0.515E-03	0.566E 04	0.42E 01	0.53E 01
BA	2186.0	0.123E-03	0.431E 04	0.21E 02	0.27E 02
BA	2639.4	0.114E-03	0.402E 04	0.28E 02	0.35E 02
BE	853.5	0.161E-03	0.728E 04	0.11E 02	0.14E 02
BE	2589.9	0.152E-03	0.403E 04	0.20E 02	0.26E 02
BR	196.9	0.339E-02	0.320E 05	0.86E 00	0.11E 01
BR	246.1	0.746E-02	0.259E 05	0.35E 00	0.44E 00
BR	315.9	0.266E-02	0.191E 05	0.83E 00	0.11E 01
BR	1199.1	0.233E-02	0.596E 04	0.84E 00	0.11E 01
C	1261.2	0.497E-04	0.587E 04	0.40E 02	0.51E 02
CA	520.0	0.384E-03	0.114E 05	0.50E 01	0.64E 01
CA	726.9	0.138E-03	0.842E 04	0.14E 02	0.17E 02
CA	1388.3	0.142E-03	0.579E 04	0.15E 02	0.19E 02

TABLE AIV(1) (CONTINUED)

LIMITS FOR QUANTITATIVE DETERMINATION

ELEM.	ENERGY	INTENSITY	MIN. AREA	MIN. WT	WT PERCENT
CA	1724.0	0.136E-03	0.495E 04	0.17E 02	0.21E 02
CA	1942.5	0.339E-02	0.459E 04	0.73E 00	0.92E 00
CA	2129.8	0.163E-03	0.444E 04	0.16E 02	0.20E 02
CA	2811.0	0.154E-03	0.385E 04	0.22E 02	0.28E 02
CD	558.6	0.154E 02	0.107E 05	0.12E-03	0.16E-03
CD	651.3	0.295E 01	0.946E 04	0.65E-03	0.83E-03
CD	806.0	0.989E 00	0.771E 04	0.19E-02	0.24E-02
CD	1364.2	0.105E 01	0.580E 04	0.20E-02	0.25E-02
CD	2455.8	0.876E 00	0.416E 04	0.34E-02	0.43E-02
CD	2550.1	0.310E 00	0.405E 04	0.98E-02	0.12E-01
CD	2659.8	0.603E 00	0.391E 04	0.52E-02	0.66E-02
CD	2767.3	0.279E 00	0.386E 04	0.12E-01	0.15E-01
CD	3000.0	0.310E 00	0.381E 04	0.12E-01	0.15E-01
CE	662.3	0.903E-03	0.916E 04	0.21E 01	0.27E 01
CE	1436.8	0.130E-03	0.567E 04	0.17E 02	0.21E 02
CE	1454.3	0.104E-03	0.561E 04	0.21E 02	0.27E 02
CE	1810.1	0.142E-03	0.476E 04	0.16E 02	0.21E 02
CE	2041.5	0.294E-04	0.445E 04	0.86E 02	0.11E 03
CE	2272.3	0.367E-04	0.427E 04	0.73E 02	0.93E 02
CL	518.3	0.620E-01	0.115E 05	0.31E-01	0.40E-01
CL	1165.4	0.615E-01	0.604E 04	0.31E-01	0.40E-01
CL	1951.3	0.121E 00	0.459E 04	0.20E-01	0.26E-01
CL	1957.5	0.853E-01	0.459E 04	0.29E-01	0.37E-01
CL	2864.4	0.382E-01	0.385E 04	0.91E-01	0.11E 00
CO	230.5	0.684E-01	0.282E 05	0.40E-01	0.51E-01
CO	277.7	0.599E-01	0.224E 05	0.40E-01	0.51E-01
CO	556.2	0.455E-01	0.107E 05	0.42E-01	0.53E-01
CO	1830.3	0.191E-01	0.473E 04	0.12E 00	0.16E 00
CR	749.2	0.355E-02	0.809E 04	0.52E 00	0.66E 00
CR	835.1	0.863E-02	0.751E 04	0.21E 00	0.27E 00
CR	1783.8	0.195E-02	0.480E 04	0.12E 01	0.15E 01
CR	1898.5	0.137E-02	0.467E 04	0.18E 01	0.22E 01
CR	2238.9	0.268E-02	0.421E 04	0.97E 00	0.12E 01
CR	2321.0	0.195E-02	0.419E 04	0.14E 01	0.18E 01
CS	234.8	0.439E-02	0.274E 05	0.61E 00	0.78E 00
CS	308.0	0.620E-02	0.197E 05	0.56E 00	0.46E 00
CS	1300.9	0.790E-02	0.583E 04	0.26E 00	0.33E 00
CS	1376.7	0.414E-02	0.583E 04	0.52E 00	0.65E 00
CS	2074.2	0.138E-02	0.451E 04	0.19E 01	0.24E 01
CU	278.3	0.109E-01	0.222E 05	0.22E 00	0.28E 00
CU	385.2	0.254E-02	0.151E 05	0.79E 00	0.10E 01
CU	608.9	0.289E-02	0.100E 05	0.67E 00	0.85E 00
CU	1672.4	0.423E-03	0.495E 04	0.52E 01	0.66E 01

TABLE AIV(1) (CONTINUED)

LIMITS FOR QUANTITATIVE DETERMINATION

ELEM.	ENFRGY	INTENSITY	MIN.AREA	MIN.WT	WT PERCENT
DY	185.7	0.671E 00	0.291E 05	0.39E-02	0.49E-02
DY	413.2	0.237E 00	0.142E 05	0.84E-02	0.11E-01
DY	497.6	0.150E 00	0.119E 05	0.13E-01	0.16E-01
DY	538.4	0.244E 00	0.109E 05	0.78E-02	0.99E-02
DY	2067.4	0.300E-01	0.450E 04	0.86E-01	0.11E 00
DY	2703.4	0.809E-01	0.398E 04	0.40E-01	0.51E-01
DY	2733.6	0.410E-01	0.393E 04	0.80E-01	0.10E 00
DY	2948.5	0.444E-01	0.381E 04	0.81E-01	0.10E 00
ER	285.2	0.683E-01	0.220E 05	0.35E-01	0.44E-01
ER	730.6	0.433E-01	0.835E 04	0.43E-01	0.55E-01
ER	816.1	0.188E 00	0.770E 04	0.99E-02	0.13E-01
ER	914.5	0.259E-01	0.687E 04	0.69E-01	0.88E-01
ER	2159.7	0.287E-02	0.430E 04	0.89E 00	0.11E 01
ER	2341.6	0.380E-02	0.425E 04	0.73E 00	0.93E 00
ER	2668.7	0.380E-02	0.395E 04	0.84E 00	0.11E 01
EU	208.0	0.931E 00	0.314E 05	0.32E-02	0.40E-02
EU	374.6	0.124E 00	0.157E 05	0.16E-01	0.21E-01
EU	1658.6	0.501E-01	0.502E 04	0.44E-01	0.56E-01
EU	1890.2	0.605E-01	0.469E 04	0.40E-01	0.51E-01
EU	2048.0	0.363E-01	0.445E 04	0.70E-01	0.88E-01
EU	2093.5	0.363E-01	0.446E 04	0.71E-01	0.90E-01
EU	2412.0	0.225E-01	0.422E 04	0.13E 00	0.16E 00
EU	2697.5	0.449E-01	0.401E 04	0.73E-01	0.93E-01
EU	2859.7	0.311E-01	0.385E 04	0.11E 00	0.14E 00
F	326.7	0.115E-03	0.186E 05	0.19E 02	0.24E 02
F	596.2	0.281E-03	0.102E 05	0.69E 01	0.87E 01
F	1749.0	0.158E-03	0.490E 04	0.14E 02	0.18E 02
F	1889.5	0.175E-03	0.468E 04	0.14E 02	0.18E 02
F	2452.8	0.354E-04	0.412E 04	0.82E 02	0.10E 03
F	2528.1	0.292E-04	0.412E 04	0.10E 03	0.13E 03
F	2601.9	0.310E-04	0.408E 04	0.10E 03	0.13E 03
F	2682.8	0.268E-04	0.401E 04	0.12E 03	0.15E 03
FE	352.5	0.307E-02	0.172E 05	0.70E 00	0.89E 00
FE	692.1	0.139E-02	0.900E 04	0.14E 01	0.18E 01
FE	1613.0	0.165E-02	0.525E 04	0.14E 01	0.17E 01
FE	1724.8	0.227E-02	0.496E 04	0.10E 01	0.13E 01
GA	250.9	0.232E-02	0.250E 05	0.11E 01	0.14E 01
GA	393.7	0.158E-02	0.148E 05	0.13E 01	0.16E 01
GA	651.0	0.103E-02	0.946E 04	0.19E 01	0.24E 01
GA	691.7	0.276E-02	0.900E 04	0.70E 00	0.88E 00
GD	780.3	0.253E 01	0.785E 04	0.73E-03	0.93E-03
GD	943.7	0.635E 01	0.673E 04	0.28E-03	0.36E-03
GD	961.8	0.461E 01	0.674E 04	0.40E-03	0.50E-03

TABLE AIV(1) (CONTINUED)

LIMITS FOR QUANTITATIVE DETERMINATION

ELEM.	ENERGY	INTENSITY	MIN.AREA	MIN.WT	WT PERCENT
GD	1185.4	0.888E 01	0.603E 04	0.22E-03	0.28E-03
GD	2107.0	0.374E 00	0.446E 04	0.69E-02	0.88E-02
GD	2314.4	0.389E 00	0.418E 04	0.69E-02	0.88E-02
GD	2600.1	0.389E 00	0.408E 04	0.81E-02	0.10E-01
GD	2678.7	0.464E 00	0.400E 04	0.70E-02	0.89E-02
GE	326.1	0.119E-02	0.186E 05	0.18E 01	0.23E 01
GE	596.0	0.704E-02	0.102E 05	0.27E 00	0.35E 00
GE	868.1	0.384E-02	0.721E 04	0.47E 00	0.60E 00
GE	1100.6	0.189E-02	0.630E 04	0.10E 01	0.13E 01
GE	2013.0	0.285E-03	0.454E 04	0.89E 01	0.11E 02
H	2223.3	0.200E 00	0.431E 04	0.13E-01	0.17E-01
HF	214.0	0.200E 00	0.304E 05	0.14E-01	0.18E-01
HF	325.8	0.223E-01	0.187E 05	0.99E-01	0.13E 00
HF	1206.4	0.168E-01	0.591E 04	0.12E 00	0.15E 00
HF	1228.9	0.141E-01	0.589E 04	0.14E 00	0.18E 00
HF	2064.9	0.230E-02	0.450E 04	0.11E 01	0.14E 01
HF	2468.5	0.290E-02	0.410E 04	0.10E 01	0.13E 01
HG	367.8	0.922E 00	0.162E 05	0.23E-02	0.29E-02
HG	661.1	0.538E-01	0.922E 04	0.35E-01	0.45E-01
HG	1570.3	0.441E-01	0.528E 04	0.50E-01	0.64E-01
HG	1693.3	0.961E-01	0.496E 04	0.23E-01	0.30E-01
HG	2002.1	0.853E-01	0.458E 04	0.30E-01	0.38E-01
HG	2639.9	0.484E-01	0.402E 04	0.66E-01	0.84E-01
HO	240.3	0.100E-01	0.264E 05	0.26E 00	0.33E 00
HO	290.4	0.662E-02	0.213E 05	0.35E 00	0.45E 00
HO	426.3	0.717E-02	0.137E 05	0.27E 00	0.35E 00
HO	543.2	0.650E-02	0.109E 05	0.29E 00	0.37E 00
HO	2118.3	0.831E-03	0.448E 04	0.32E 01	0.40E 01
HO	2589.9	0.926E-03	0.403E 04	0.34E 01	0.43E 01
I	291.4	0.311E-02	0.213E 05	0.76E 00	0.96E 00
I	336.7	0.265E-02	0.181E 05	0.82E 00	0.10E 01
I	421.0	0.105E-02	0.139E 05	0.19E 01	0.24E 01
I	614.2	0.592E-03	0.998E 04	0.33E 01	0.42E 01
I	1887.9	0.253E-03	0.467E 04	0.95E 01	0.12E 02
IN	273.3	0.734E-01	0.224E 05	0.33E-01	0.41E-01
IN	335.6	0.238E-01	0.182E 05	0.92E-01	0.12E 00
IN	819.3	0.287E-01	0.768E 04	0.65E-01	0.83E-01
IN	1752.8	0.146E-01	0.490E 04	0.16E 00	0.20E 00
IN	2337.4	0.259E-02	0.423E 04	0.11E 01	0.14E 01
IR	217.4	0.121E 00	0.292E 05	0.23E-01	0.29E-01
IR	351.8	0.571E-01	0.173E 05	0.38E-01	0.48E-01
IR	418.3	0.202E-01	0.140E 05	0.98E-01	0.12E 00

TABLE AIV(1) (CONTINUED)

LIMITS FOR QUANTITATIVE DETERMINATION

ELEM.	ENERGY	INTENSITY	MIN.AREA	MIN.WT	WT PERCENT
IR	1551.6	0.161E-01	0.522E 04	0.14E 00	0.18E 00
IR	2454.2	0.649E-02	0.414E 04	0.45E 00	0.57E 00
K	770.6	0.101E-01	0.790E 04	0.18E 00	0.23E 00
K	1159.0	0.190E-02	0.609E 04	0.10E 01	0.13E 01
K	1617.5	0.255E-02	0.526E 04	0.89E 00	0.11E 01
K	1929.3	0.818E-03	0.454E 04	0.29E 01	0.37E 01
K	2073.2	0.331E-02	0.451E 04	0.78E 00	0.99E 00
K	2291.2	0.111E-02	0.422E 04	0.24E 01	0.31E 01
K	2545.9	0.117E-02	0.402E 04	0.26E 01	0.33E 01
LA	219.6	0.454E-02	0.293E 05	0.62E 00	0.78E 00
LA	289.1	0.385E-02	0.216E 05	0.61E 00	0.78E 00
LA	423.2	0.267E-02	0.138E 05	0.74E 00	0.93E 00
LA	722.2	0.121E-02	0.848E 04	0.15E 01	0.20E 01
LA	2765.3	0.436E-03	0.385E 04	0.75E 01	0.95E 01
LI	558.8	0.156E-03	0.107E 05	0.12E 02	0.16E 02
LI	869.1	0.839E-04	0.721E 04	0.22E 02	0.28E 02
LI	980.7	0.914E-04	0.666E 04	0.20E 02	0.25E 02
LI	1891.4	0.851E-04	0.469E 04	0.28E 02	0.36E 02
LI	2032.5	0.841E-03	0.446E 04	0.30E 01	0.38E 01
LI	2117.4	0.584E-04	0.448E 04	0.45E 02	0.57E 02
LI	2184.0	0.211E-03	0.432E 04	0.12E 02	0.16E 02
LU	269.4	0.109E-01	0.229E 05	0.22E 00	0.28E 00
LU	367.5	0.144E-01	0.164E 05	0.15E 00	0.19E 00
LU	458.1	0.407E-01	0.130E 05	0.49E-01	0.62E-01
LU	762.0	0.109E-01	0.793E 04	0.17E 00	0.21E 00
LU	2056.2	0.156E-02	0.449E 04	0.16E 01	0.21E 01
LU	2091.2	0.192E-02	0.447E 04	0.13E 01	0.17E 01
MG	390.0	0.876E-04	0.150E 05	0.23E 02	0.29E 02
MG	585.2	0.335E-03	0.102E 05	0.57E 01	0.72E 01
MG	1129.4	0.111E-03	0.622E 04	0.17E 02	0.22E 02
MG	1808.9	0.393E-03	0.476E 04	0.59E 01	0.75E 01
MG	2828.1	0.557E-03	0.392E 04	0.62E 01	0.79E 01
MN	212.5	0.877E-02	0.307E 05	0.33E 00	0.42E 00
MN	314.3	0.517E-02	0.191E 05	0.43E 00	0.54E 00
MN	1747.0	0.415E-02	0.490E 04	0.55E 00	0.70E 00
MN	1987.6	0.344E-02	0.452E 04	0.73E 00	0.92E 00
MN	2330.9	0.456E-02	0.422E 04	0.60E 00	0.77E 00
MO	719.9	0.150E-02	0.851E 04	0.13E 01	0.16E 01
MO	778.4	0.834E-02	0.786E 04	0.22E 00	0.28E 00
MO	849.0	0.296E-02	0.735E 04	0.62E 00	0.78E 00
MO	1091.0	0.745E-03	0.627E 04	0.25E 01	0.32E 01
MO	2400.9	0.167E-03	0.416E 04	0.17E 02	0.21E 02
MO	2664.5	0.215E-03	0.392E 04	0.15E 02	0.19E 02

TABLE AIV(1) (CONTINUED)

LIMITS FOR QUANTITATIVE DETERMINATION

ELEM.	ENERGY	INTENSITY	MIN.AREA	MIN.WT	WT PERCENT
N	253.1	0.150E-03	0.244E 05	0.17E 02	0.21E 02
N	596.8	0.141E-03	0.101E 05	0.14E 02	0.17E 02
N	1678.6	0.195E-03	0.494E 04	0.11E 02	0.14E 02
N	1887.9	0.126E-02	0.467E 04	0.19E 01	0.24E 01
NA	472.4	0.969E-02	0.128E 05	0.20E 00	0.26E 00
NA	870.6	0.355E-02	0.720E 04	0.51E 00	0.65E 00
NA	781.1	0.428E-03	0.785E 04	0.43E 01	0.55E 01
NA	1634.4	0.120E-02	0.517E 04	0.19E 01	0.24E 01
NA	2027.2	0.277E-02	0.452E 04	0.92E 00	0.12E 01
NA	2517.6	0.239E-02	0.407E 04	0.13E 01	0.16E 01
NA	2754.4 D	0.143E-01	0.384E 04	0.23E 00	0.29E 00
NA	2862.7	0.164E-02	0.383E 04	0.21E 01	0.27E 01
NB	191.0	0.294E-02	0.322E 05	0.99E 00	0.13E 01
NB	255.1	0.143E-02	0.244E 05	0.17E 01	0.22E 01
NB	945.9	0.143E-03	0.674E 04	0.13E 02	0.16E 02
NB	1724.5	0.112E-03	0.495E 04	0.20E 02	0.26E 02
NB	1979.7	0.413E-04	0.458E 04	0.61E 02	0.77E 02
ND	454.5	0.118E-01	0.131E 05	0.17E 00	0.21E 00
ND	618.5	0.513E-01	0.990E 04	0.38E-01	0.48E-01
ND	696.7	0.134E 00	0.899E 04	0.14E-01	0.18E-01
ND	814.5	0.192E-01	0.770E 04	0.97E-01	0.12E 00
ND	2371.5	0.253E-02	0.413E 04	0.11E 01	0.14E 01
NI	283.1	0.174E-02	0.221E 05	0.14E 01	0.18E 01
NI	339.5	0.145E-02	0.180E 05	0.15E 01	0.19E 01
NI	465.1	0.676E-02	0.129E 05	0.29E 00	0.37E 00
NI	877.9	0.201E-02	0.717E 04	0.91E 00	0.12E 01
OS	187.3	0.448E-02	0.307E 05	0.62E 00	0.78E 00
OS	478.3	0.328E-02	0.125E 05	0.60E 00	0.76E 00
OS	569.3	0.250E-02	0.106E 05	0.77E 00	0.98E 00
OS	634.0	0.497E-02	0.973E 04	0.39E 00	0.50E 00
OS	2261.3	0.116E-03	0.421E 04	0.23E 02	0.29E 02
OS	2458.8	0.484E-04	0.415E 04	0.61E 02	0.77E 02
P	636.2	0.495E-03	0.971E 04	0.39E 01	0.50E 01
P	1070.6	0.348E-03	0.634E 04	0.54E 01	0.68E 01
P	1413.1	0.571E-03	0.566E 04	0.37E 01	0.47E 01
P	1890.0	0.246E-03	0.469E 04	0.98E 01	0.12E 02
P	2114.3	0.282E-03	0.447E 04	0.93E 01	0.12E 02
P	2154.2	0.620E-03	0.433E 04	0.42E 01	0.53E 01
PD	245.7	0.267E-02	0.259E 05	0.98E 00	0.12E 01
PD	616.1	0.485E-02	0.995E 04	0.40E 00	0.51E 00
PD	716.9	0.528E-02	0.851E 04	0.35E 00	0.45E 00

TABLE AIV(1) (CONTINUED)

LIMITS FOR QUANTITATIVE DETERMINATION

ELEM.	ENERGY	INTENSITY	MIN.AREA	MIN.WT	WT PERCENT
PD	1047.9	0.419E-02	0.638E 04	0.44E 00	0.56E 00
PD	2196.9	0.498E-03	0.430E 04	0.52E 01	0.67E 01
PD	2457.5	0.461E-03	0.415E 04	0.64E 01	0.81E 01
PD	2484.3	0.466E-03	0.411E 04	0.64E 01	0.81E 01
PR	178.4	0.397E-02	0.207E 05	0.46E 00	0.58E 00
PR	645.8	0.753E-03	0.956E 04	0.26E 01	0.33E 01
PR	699.8	0.705E-03	0.893E 04	0.27E 01	0.35E 01
PR	1006.6	0.478E-03	0.655E 04	0.38E 01	0.49E 01
PR	2839.8	0.304E-03	0.392E 04	0.11E 02	0.14E 02
PT	333.3	0.577E-02	0.183E 05	0.38E 00	0.48E 00
PT	356.1	0.100E-01	0.170E 05	0.21E 00	0.27E 00
PT	1491.3	0.492E-03	0.551E 04	0.45E 01	0.56E 01
PT	1978.7	0.492E-03	0.460E 04	0.51E 01	0.65E 01
PT	2067.8	0.368E-03	0.450E 04	0.70E 01	0.89E 01
PT	2311.4	0.513E-03	0.417E 04	0.52E 01	0.66E 01
PT	2469.6	0.415E-03	0.410E 04	0.70E 01	0.89E 01
RB	476.0	0.224E-03	0.126E 05	0.88E 01	0.11E 02
RB	556.8	0.658E-03	0.107E 05	0.29E 01	0.37E 01
RB	872.7	0.159E-03	0.719E 04	0.11E 02	0.15E 02
RB	1030.8	0.202E-03	0.650E 04	0.92E 01	0.12E 02
RB	2130.0	0.226E-04	0.444E 04	0.12E 03	0.15E 03
RB	2149.7	0.236E-04	0.435E 04	0.11E 03	0.14E 03
RB	2176.8	0.586E-04	0.431E 04	0.44E 02	0.56E 02
RE	209.8	0.154E-01	0.307E 05	0.19E 00	0.24E 00
RE	255.4	0.184E-01	0.244E 05	0.14E 00	0.17E 00
RE	291.1	0.110E-01	0.213E 05	0.21E 00	0.27E 00
RE	317.6	0.843E-02	0.190E 05	0.26E 00	0.33E 00
RE	2004.4	0.103E-02	0.457E 04	0.25E 01	0.31E 01
RH	217.4	0.935E-01	0.292E 05	0.30E-01	0.38E-01
RH	267.9	0.338E-01	0.231E 05	0.72E-01	0.91E-01
RH	645.0	0.193E-01	0.956E 04	0.10E 00	0.13E 00
RH	789.7	0.120E-01	0.775E 04	0.15E 00	0.19E 00
RU	475.3	0.151E-02	0.126E 05	0.13E 01	0.17E 01
RU	539.8	0.231E-02	0.109E 05	0.82E 00	0.10E 01
RU	630.6	0.779E-03	0.976E 04	0.25E 01	0.32E 01
RU	687.1	0.531E-03	0.900E 04	0.21E 01	0.26E 01
RU	2298.3	0.823E-04	0.421E 04	0.33E 02	0.42E 02
RU	2530.4	0.128E-03	0.411E 04	0.24E 02	0.30E 02
S	841.1	0.522E-02	0.744E 04	0.35E 00	0.45E 00
S	1358.5	0.416E-03	0.580E 04	0.50E 01	0.64E 01
S	1597.8	0.113E-02	0.524E 04	0.20E 01	0.25E 01
S	1890.5	0.681E-03	0.469E 04	0.36E 01	0.45E 01
S	2379.7	0.307E-02	0.416E 04	0.91E 00	0.12E 01

TABLE AIV(1) (CONTINUED)

LIMITS FOR QUANTITATIVE DETERMINATION

ELEM.	ENERGY	INTENSITY	MIN.AREA	MIN.WT	WT PERCENT
S	2753.2	0.403E-03	0.384E 04	0.81E 01	0.10E 02
S	2931.1	0.154E-02	0.379E 04	0.23E 01	0.29E 01
SB	283.1	0.900E-03	0.221E 05	0.27E 01	0.34E 01
SB	332.7	0.100E-02	0.183E 05	0.22E 01	0.28E 01
SB	921.1	0.383E-03	0.688E 04	0.47E 01	0.60E 01
SB	1402.0	0.318E-03	0.575E 04	0.67E 01	0.85E 01
SB	2074.2	0.125E-03	0.451E 04	0.21E 02	0.26E 02
SC	228.6	0.126E 00	0.280E 05	0.22E-01	0.27E-01
SC	295.6	0.506E-01	0.209E 05	0.46E-01	0.58E-01
SC	627.9	0.226E-01	0.980E 04	0.86E-01	0.11E 00
SC	1692.0	0.112E-01	0.495E 04	0.20E 00	0.25E 00
SC	2111.4	0.655E-02	0.447E 04	0.40E 00	0.50E 00
SC	2635.6	0.977E-02	0.400E 04	0.32E 00	0.41E 00
SE	239.6	0.120E-01	0.264E 05	0.22E 00	0.28E 00
SE	520.6	0.332E-02	0.114E 05	0.58E 00	0.74E 00
SE	613.9	0.122E-01	0.998E 04	0.16E 00	0.20E 00
SE	886.9	0.273E-02	0.714E 04	0.67E 00	0.85E 00
SI	246.9	0.147E-03	0.257E 05	0.18E 02	0.22E 02
SI	250.5	0.142E-03	0.250E 05	0.18E 02	0.23E 02
SI	1273.2	0.420E-03	0.587E 04	0.48E 01	0.61E 01
SI	1332.2	0.388E-04	0.577E 04	0.53E 02	0.67E 02
SI	2092.9	0.919E-03	0.447E 04	0.28E 01	0.36E 01
SI	2425.9	0.135E-03	0.420E 04	0.22E 02	0.27E 02
SM	333.9	0.195E 02	0.183E 05	0.11E-03	0.14E-03
SM	439.4	0.107E 02	0.134E 05	0.18E-03	0.23E-03
SM	737.5	0.217E 01	0.825E 04	0.85E-03	0.11E-02
SM	1169.7	0.103E 01	0.605E 04	0.19E-02	0.24E-02
SM	2119.8	0.936E-01	0.448E 04	0.28E-01	0.36E-01
SM	2161.0	0.655E-01	0.429E 04	0.39E-01	0.50E-01
SM	2332.0	0.398E-01	0.422E 04	0.69E-01	0.88E-01
SN	251.9	0.596E-04	0.250E 05	0.43E 02	0.54E 02
SN	1171.3	0.254E-03	0.605E 04	0.76E 01	0.97E 01
SN	1229.5	0.221E-03	0.589E 04	0.89E 01	0.11E 02
SN	1293.3	0.414E-03	0.582E 04	0.49E 01	0.62E 01
SN	2112.7	0.488E-04	0.447E 04	0.53E 02	0.68E 02
SN	2179.0	0.371E-04	0.432E 04	0.70E 02	0.89E 02
SN	2651.7	0.183E-04	0.394E 04	0.17E 03	0.22E 03
SR	558.5	0.120E-02	0.107E 05	0.16E 01	0.20E 01
SR	850.4	0.106E-02	0.733E 04	0.17E 01	0.22E 01
SR	897.9	0.246E-02	0.703E 04	0.74E 00	0.94E 00
SR	1835.9	0.761E-02	0.476E 04	0.31E 00	0.39E 00
SR	2276.8	0.266E-03	0.428E 04	0.10E 02	0.13E 02
SR	2391.5	0.383E-03	0.418E 04	0.74E 01	0.93E 01

TABLE AIV(1) (CONTINUED)

LIMITS FOR QUANTITATIVE DETERMINATION

ELEM.	ENERGY	INTENSITY	MIN. AREA	MIN. WT	WT PERCENT
TA	271.1	0.205E-01	0.229E 05	0.12E 00	0.15E 00
TA	297.6	0.406E-02	0.207E 05	0.57E 00	0.72E 00
TA	361.4	0.132E-02	0.168E 05	0.16E 01	0.20E 01
TA	402.9	0.107E-01	0.146E 05	0.19E 00	0.24E 00
TB	596.6	0.593E-03	0.101E 05	0.33E 01	0.41E 01
TB	1442.6	0.185E-02	0.559E 04	0.12E 01	0.15E 01
TB	1689.0	0.662E-03	0.494E 04	0.34E 01	0.43E 01
TB	1745.8	0.819E-03	0.492E 04	0.28E 01	0.36E 01
TB	2120.2	0.349E-03	0.448E 04	0.75E 01	0.95E 01
TE	602.9	0.368E-02	0.101E 05	0.53E 00	0.67E 00
TE	1437.0	0.125E-02	0.567E 04	0.17E 01	0.22E 01
TE	1487.1	0.120E-02	0.551E 04	0.18E 01	0.23E 01
TE	1918.9	0.920E-03	0.455E 04	0.26E 01	0.33E 01
TE	2039.1	0.425E-03	0.444E 04	0.59E 01	0.75E 01
TE	2386.0	0.270E-03	0.420E 04	0.10E 02	0.13E 02
TE	2610.5	0.602E-03	0.404E 04	0.52E 01	0.67E 01
TE	2747.2	0.103E-02	0.393E 04	0.32E 01	0.41E 01
TI	341.7	0.233E-01	0.179E 05	0.94E-01	0.12E 00
TI	1381.4	0.498E-01	0.580E 04	0.43E-01	0.54E-01
TI	1586.0	0.650E-02	0.522E 04	0.34E 00	0.43E 00
TI	1761.6	0.601E-02	0.477E 04	0.37E 00	0.47E 00
TL	348.6	0.310E-03	0.175E 05	0.70E 01	0.88E 01
TL	737.0	0.242E-03	0.825E 04	0.77E 01	0.97E 01
TL	873.1	0.259E-03	0.719E 04	0.70E 01	0.89E 01
TL	911.1	0.253E-03	0.687E 04	0.71E 01	0.90E 01
TM	205.2	0.240E-01	0.313E 05	0.12E 00	0.15E 00
TM	220.4	0.109E-01	0.293E 05	0.26E 00	0.33E 00
TM	237.5	0.319E-01	0.266E 05	0.83E-01	0.10E 00
TM	565.5	0.979E-02	0.106E 05	0.20E 00	0.25E 00
TM	2115.2	0.898E-03	0.448E 04	0.29E 01	0.37E 01
V	436.6	0.409E-02	0.134E 05	0.48E 00	0.61E 00
V	645.9	0.696E-02	0.956E 04	0.28E 00	0.35E 00
V	823.5	0.267E-02	0.762E 04	0.70E 00	0.88E 00
V	1777.8	0.317E-02	0.481E 04	0.72E 00	0.92E 00
W	201.2	0.122E-02	0.314E 05	0.24E 01	0.30E 01
W	551.5	0.218E-02	0.107E 05	0.88E 00	0.11E 01
W	772.7	0.857E-03	0.789E 04	0.21E 01	0.27E 01
W	891.5	0.769E-03	0.709E 04	0.24E 01	0.30E 01
Y	203.2	0.141E-02	0.316E 05	0.21E 01	0.26E 01
Y	455.2	0.744E-03	0.131E 05	0.27E 01	0.34E 01
Y	574.6	0.978E-03	0.104E 05	0.20E 01	0.25E 01

TABLE AIV(1) (CONTINUED)

LIMITS FOR QUANTITATIVE DETERMINATION

ELEM.	ENERGY	INTENSITY	MIN.AREA	MIN.WT	WT PERCENT
Y	776.9	0.244E-02	0.787E 04	0.76E 00	0.96E 00
Y	2546.6	0.205E-03	0.402E 04	0.15E 02	0.19E 02
Y	2749.5	0.253E-03	0.390E 04	0.13E 02	0.17E 02
YB	241.8	0.250E-01	0.257E 05	0.10E 00	0.13E 00
YB	341.9	0.820E-02	0.178E 05	0.26E 00	0.34E 00
YB	475.4	0.310E-02	0.126E 05	0.64E 00	0.81E 00
YB	636.2	0.448E-02	0.971E 04	0.43E 00	0.55E 00
YB	2585.0	0.144E-02	0.405E 04	0.22E 01	0.27E 01
ZN	445.7	0.533E-03	0.133E 05	0.37E 01	0.47E 01
ZN	1007.6	0.297E-03	0.655E 04	0.62E 01	0.79E 01
ZN	1077.5	0.217E-02	0.631E 04	0.87E 00	0.11E 01
ZN	1883.5	0.777E-03	0.466E 04	0.31E 01	0.39E 01
ZN	2858.2	0.142E-03	0.386E 04	0.24E 02	0.31E 02
ZR	251.2	0.125E-03	0.250E 05	0.20E 02	0.26E 02
ZR	561.0	0.110E-03	0.106E 05	0.17E 02	0.22E 02
ZR	934.5	0.473E-03	0.680E 04	0.38E 01	0.48E 01
ZR	1404.7	0.108E-03	0.573E 04	0.20E 02	0.25E 02
ZR	2190.9	0.247E-04	0.430E 04	0.11E 03	0.13E 03
ZR	2694.0	0.299E-04	0.402E 04	0.11E 03	0.14E 03
ZR	2933.2	0.152E-04	0.379E 04	0.23E 03	0.30E 03

TABLE AIV(2) PAIR SPECTROMETER

LIMITS FOR QUANTITATIVE DETERMINATION

ELEM.	ENERGY	INTENSITY	MIN.AREA	MIN.WT	WT PERCENT
AG	2048.6	0.169E-02	C.774E C3	0.78E 01	0.98E 01
AG	4720.2	0.172E-02	C.93CE C3	0.22E C1	0.28E 01
AG	5240.2	0.236E-02	0.960E 03	0.17E 01	0.21E 01
AG	5577.9	0.204E-02	C.102E 04	0.21E C1	0.26E 01
AG	5699.7	0.549E-02	0.106E 04	0.81E CC	C.10E 01
AG	5793.1	0.366E-02	0.109E 04	0.12E 01	0.16E 01
AG	6056.1	0.408E-02	C.112E 04	C.12E C1	0.15E 01
AG	7268.9	0.201E-02	0.134E 04	0.36E 01	0.46E C1
AL	1623.1	0.168E-03	C.805E C3	0.19E C3	0.25E 03
AL	2960.4	0.323E-03	0.846E 03	0.18E 02	0.23E 02
AL	3034.4	C.305E-C3	C.858E 03	0.19E 02	0.24E 02
AL	3465.5	0.225E-03	0.889E C3	0.21E C2	0.26E C2
AL	3591.7	0.148E-03	0.869E 03	0.29E 02	0.37E C2
AL	4133.7	C.223E-03	C.897E C3	0.17E 02	0.22E 02
AL	4259.9	0.213E-03	0.911E 03	0.18E C2	C.23E C2
AL	4734.1	0.183E-03	0.931E 03	0.21E 02	0.26E 02
AL	7723.8	0.106E-02	C.135E 04	C.77E C1	0.97E 01
AS	4783.0	C.304E-03	0.927E 03	0.12E 02	0.16E 02
AS	5416.5	0.210E-03	C.100E C4	0.19E 02	0.25E 02
AS	5784.7	0.199E-03	0.110E 04	0.23E 02	0.29E C2
AS	6058.3	0.224E-C3	0.112E 04	0.22E 02	0.27E 02
AS	6294.5	0.655E-03	0.103E 04	C.7CE C1	0.89E C1
AS	6809.9	0.105E-02	0.111E 04	0.52E 01	0.66E 01
AS	6926.1	0.376E-C3	C.118E C4	C.16E C2	0.20E 02
AS	7019.5	0.872E-03	0.121E 04	0.71E C1	0.90E 01
AU	4189.0	0.134E-02	0.901E C3	C.28E C1	0.36E 01
AU	5148.2	0.399E-02	0.955E C3	C.97E CC	0.12E 01
AU	5710.4	C.399E-C2	0.107E 04	0.11E 01	0.14E 01
AU	5982.8	0.417E-02	0.113E 04	C.12E C1	C.15E 01
AU	6252.0	0.165E-01	0.102E 04	0.27E 00	0.35E 00
AU	6319.1	0.106E-01	C.103E C4	C.44E CC	0.55E 00
AU	6456.8	0.682E-02	0.104E 04	C.7CE CC	0.89E 00
AU	6512.1	0.505E-C2	C.106E 04	0.97E 00	0.12E 01
B	2072.7	0.301E-04	0.784E 03	0.43E C3	0.54E 03
B	2532.3	0.199E-C4	C.822E 03	0.40E 03	0.51E 03
B	3308.0	0.909E-05	0.882E C3	0.55E C3	0.69E C3
B	3505.0	0.108E-04	0.885E 03	0.42E 03	0.54E 03
B	4443.0	C.153E-C4	C.939E 03	0.25E 03	0.32E 03
B	4710.2	0.682E-05	0.930E 03	0.55E C3	0.70E 03
B	6759.3	0.796E-05	0.112E 04	0.69E 03	0.87E 03
B	7005.1	0.966E-05	C.118E 04	C.63E C3	0.80E 03
BA	2186.0	0.123E-03	0.782E 03	C.89E 02	0.11E 03
BA	2639.4	0.114E-03	C.819E C3	C.63E 02	0.80E C2
BA	3641.7	0.304E-03	0.879E 03	0.14E 02	0.18E C2
BA	4096.3	0.873E-C3	0.908E 03	0.45E 01	0.57E 01

TABLE AIV(2) (CONTINUED)

LIMITS FOR QUANTITATIVE DETERMINATION

ELEM.	ENERGY	INTENSITY	MIN.AREA	MIN.WT	WT PERCENT
EA	4723.8	0.114E-03	0.930E 03	0.33E 02	0.42E 02
BA	5730.7	0.309E-03	0.106E 04	0.14E 02	0.18E 02
EA	6027.9	0.457E-04	0.114E 04	0.11E 03	0.14E 03
BA	9108.8	0.210E-04	0.738E 03	0.33E 03	0.42E 03
BE	2589.9	0.152E-03	0.809E 03	0.49E 02	0.62E 02
BE	3368.2	0.217E-03	0.883E 03	0.22E 02	0.28E 02
BE	3444.4	0.749E-04	0.890E 03	0.63E 02	0.80E 02
BE	5958.1	0.127E-03	0.112E 04	0.38E 02	0.48E 02
BE	6810.0	0.397E-03	0.111E 04	0.14E 02	0.17E 02
BI	4054.7	0.260E-04	0.894E 03	0.15E 03	0.19E 03
BI	4101.8	0.174E-04	0.907E 03	0.22E 03	0.28E 03
BI	4171.1	0.362E-04	0.895E 03	0.10E 03	0.13E 03
BR	5507.7	0.186E-03	0.104E 04	0.23E 02	0.29E 02
BR	5914.2	0.363E-03	0.113E 04	0.13E 02	0.17E 02
BR	6354.7	0.262E-03	0.101E 04	0.17E 02	0.22E 02
BR	6745.5	0.227E-03	0.111E 04	0.24E 02	0.30E 02
BR	7030.1	0.247E-03	0.121E 04	0.25E 02	0.32E 02
BR	7076.3	0.267E-03	0.125E 04	0.24E 02	0.31E 02
BR	7420.7	0.328E-03	0.141E 04	0.24E 02	0.31E 02
BR	7575.8	0.585E-03	0.143E 04	0.14E 02	0.18E 02
C	3683.9	0.542E-04	0.875E 03	0.78E 02	0.99E 02
C	4945.2	0.114E-03	0.967E 03	0.34E 02	0.43E 02
CA	1724.0	0.136E-03	0.767E 03	0.17E 03	0.22E 03
CA	1942.5	0.339E-02	0.771E 03	0.46E 01	0.58E 01
CA	2129.8	0.163E-03	0.813E 03	0.75E 02	0.95E 02
CA	2811.0	0.154E-03	0.849E 03	0.42E 02	0.54E 02
CA	3610.2	0.296E-03	0.877E 03	0.15E 02	0.19E 02
CA	4418.9	0.697E-03	0.951E 03	0.56E 01	0.71E 01
CA	4749.7	0.128E-03	0.935E 03	0.30E 02	0.37E 02
CA	5900.6	0.198E-03	0.113E 04	0.24E 02	0.31E 02
CA	6419.9	0.182E-02	0.103E 04	0.26E 01	0.33E 01
CD	2455.8	0.876E 00	0.821E 03	0.97E-02	0.12E-01
CD	2550.1	0.310E 00	0.822E 03	0.25E-01	0.32E-01
CD	2659.8	0.603E 00	0.834E 03	0.12E-01	0.15E-01
CD	2767.3	0.279E 00	0.843E 03	0.24E-01	0.30E-01
CD	3000.0	0.310E 00	0.845E 03	0.18E-01	0.23E-01
CD	4810.0	0.122E 00	0.964E 03	0.32E-01	0.40E-01
CD	5431.4	0.209E 00	0.991E 03	0.19E-01	0.25E-01
CD	5823.9	0.451E 00	0.110E 04	0.10E-01	0.13E-01
CE	1810.1	0.142E-03	0.788E 03	0.14E 03	0.18E 03
CE	2041.5	0.294E-04	0.773E 03	0.45E 03	0.57E 03
CE	2272.3	0.367E-04	0.805E 03	0.28E 03	0.35E 03
CE	3018.4	0.439E-04	0.849E 03	0.13E 03	0.16E 03

TABLE AIV(2) (CONTINUED)

LIMITS FOR QUANTITATIVE DETERMINATION

ELEM.	ENERGY	INTENSITY	MIN.AREA	MIN.WT	WT PERCENT
CE	3090.6	0.342E-04	0.854E 03	0.16E 03	0.20E 03
CE	3619.8	0.420E-04	0.876E 03	0.10E 03	0.13E 03
CE	4291.2	0.286E-03	0.923E 03	0.13E 02	0.17E 02
CE	4336.8	0.133E-03	0.928E 03	0.29E 02	0.37E 02
CE	4766.1	0.499E-03	0.936E 03	0.76E 01	0.96E 01
CL	1951.3	0.121E 00	0.765E 03	0.13E 00	0.16E 00
CL	1957.5	0.853E-01	0.766E 03	0.18E 00	0.22E 00
CL	2864.4	0.382E-01	0.845E 03	0.16E 00	0.21E 00
CL	3062.2	0.210E-01	0.858E 03	0.27E 00	0.34E 00
CL	4980.0	0.215E-01	0.953E 03	0.18E 00	0.23E 00
CL	5715.2	0.261E-01	0.108E 04	0.17E 00	0.22E 00
CL	6111.1	0.890E-01	0.107E 04	0.52E-01	0.66E-01
CL	6620.1	0.564E-01	0.106E 04	0.89E-01	0.11E 00
CL	7413.8	0.481E-01	0.139E 04	0.16E 00	0.21E 00
CL	7790.0	0.374E-01	0.126E 04	0.21E 00	0.26E 00
CO	1830.3	0.191E-01	0.752E 03	0.97E 00	0.12E 01
CO	4029.2	0.621E-02	0.909E 03	0.64E 00	0.81E 00
CO	5181.7	0.839E-02	0.962E 03	0.46E 00	0.59E 00
CO	5660.3	0.241E-01	0.105E 04	0.18E 00	0.23E 00
CO	6706.0	0.280E-01	0.110E 04	0.19E 00	0.24E 00
CO	6876.9	0.302E-01	0.115E 04	0.19E 00	0.24E 00
CO	6985.1	0.110E-01	0.119E 04	0.55E 00	0.70E 00
CO	7214.1	0.177E-01	0.130E 04	0.39E 00	0.50E 00
CO	7491.1	0.113E-01	0.148E 04	0.74E 00	0.94E 00
CR	1783.8	0.195E-02	0.775E 03	0.11E 02	0.14E 02
CR	1898.5	0.137E-02	0.776E 03	0.12E 02	0.16E 02
CR	2238.9	0.268E-02	0.804E 03	0.39E 01	0.50E 01
CR	2321.0	0.195E-02	0.810E 03	0.50E 01	0.63E 01
CR	5618.8	0.124E-02	0.106E 04	0.35E 01	0.45E 01
CR	6645.5	0.190E-02	0.110E 04	0.27E 01	0.35E 01
CR	7939.3	0.410E-02	0.955E 03	0.15E 01	0.19E 01
CR	8512.3	0.198E-02	0.100E 04	0.37E 01	0.47E 01
CR	8884.1	0.867E-02	0.981E 03	0.95E 00	0.12E 01
CR	9720.3	0.353E-02	0.448E 03	0.17E 01	0.22E 01
CS	2074.2	0.138E-02	0.785E 03	0.93E 01	0.12E 02
CS	5020.3	0.193E-02	0.957E 03	0.20E 01	0.25E 01
CS	5252.6	0.122E-02	0.962E 03	0.32E 01	0.41E 01
CS	5377.2	0.117E-02	0.980E 03	0.34E 01	0.43E 01
CS	5505.4	0.946E-03	0.104E 04	0.45E 01	0.57E 01
CS	5570.6	0.151E-02	0.102E 04	0.28E 01	0.35E 01
CS	5637.4	0.841E-03	0.106E 04	0.52E 01	0.66E 01
CS	6051.9	0.108E-02	0.113E 04	0.45E 01	0.57E 01
CU	1672.4	0.423E-03	0.775E 03	0.64E 02	0.82E 02
CU	4320.8	0.518E-03	0.918E 03	0.73E 01	0.93E 01
CU	5417.7	0.737E-03	0.100E 04	0.55E 01	0.70E 01

TABLE AIV(2) (CONTINUED)

LIMITS FOR QUANTITATIVE DETERMINATION

ELEM.	ENERGY	INTENSITY	MIN.AREA	MIN.WT	WT PERCENT
CU	6599.5	0.806E-03	0.106E 04	0.62E 01	0.79E 01
CU	6678.0	0.142E-02	0.110E 04	0.37E 01	0.47E 01
CU	7251.9	0.124E-02	0.133E 04	0.58E 01	0.73E 01
CU	7306.2	0.271E-02	0.138E 04	0.28E 01	0.35E 01
CU	7636.6	0.528E-02	0.143E 04	0.16E 01	0.20E 01
CU	7914.5	0.103E-01	0.971E 03	0.59E 00	0.75E 00
DY	2067.4	0.300E-01	0.782E 03	0.43E 00	0.54E 00
DY	2703.4	0.809E-01	0.855E 03	0.88E-01	0.11E 00
DY	2733.6	0.410E-01	0.842E 03	0.17E 00	0.21E 00
DY	2948.5	0.444E-01	0.848E 03	0.13E 00	0.17E 00
DY	3444.7	0.434E-01	0.890E 03	0.11E 00	0.14E 00
DY	5143.8	0.468E-01	0.952E 03	0.82E-01	0.10E 00
DY	5556.9	0.768E-01	0.103E 04	0.55E-01	0.70E-01
DY	5607.3	0.957E-01	0.105E 04	0.45E-01	0.58E-01
ER	2159.7	0.287E-02	0.790E 03	0.40E 01	0.51E 01
ER	2341.6	0.380E-02	0.821E 03	0.25E 01	0.32E 01
ER	2668.7	0.380E-02	0.841E 03	0.19E 01	0.24E 01
ER	4109.4	0.236E-02	0.900E 03	0.16E 01	0.21E 01
ER	4921.4	0.294E-02	0.955E 03	0.13E 01	0.17E 01
ER	5211.6	0.344E-02	0.973E 03	0.11E 01	0.15E 01
ER	6229.0	0.530E-02	0.104E 04	0.87E 00	0.11E 01
ER	6676.8	0.308E-02	0.110E 04	0.17E 01	0.22E 01
EU	1658.6	0.501E-01	0.775E 03	0.56E 00	0.72E 00
EU	1890.2	0.605E-01	0.778E 03	0.28E 00	0.36E 00
EU	2048.0	0.363E-01	0.774E 03	0.36E 00	0.46E 00
EU	2093.5	0.363E-01	0.796E 03	0.35E 00	0.44E 00
EU	2412.0	0.225E-01	0.810E 03	0.39E 00	0.49E 00
EU	2657.5	0.449E-01	0.858E 03	0.16E 00	0.20E 00
EU	2859.7	0.311E-01	0.847E 03	0.20E 00	0.26E 00
EU	5379.7	0.225E-01	0.978E 03	0.18E 00	0.22E 00
EU	5918.3	0.242E-01	0.113E 04	0.20E 00	0.25E 00
EU	6228.5	0.190E-01	0.104E 04	0.24E 00	0.31E 00
F	1749.0	0.158E-03	0.762E 03	0.14E 03	0.18E 03
F	1889.5	0.175E-03	0.778E 03	0.98E 02	0.12E 03
F	2452.8	0.354E-04	0.825E 03	0.24E 03	0.31E 03
F	2528.1	0.292E-04	0.822E 03	0.27E 03	0.35E 03
F	2601.9	0.310E-04	0.819E 03	0.24E 03	0.30E 03
F	2682.8	0.268E-04	0.851E 03	0.27E 03	0.34E 03
F	3074.4	0.318E-04	0.860E 03	0.17E 03	0.22E 03
F	3589.3	0.384E-04	0.867E 03	0.11E 03	0.14E 03
F	6017.1	0.334E-04	0.113E 04	0.15E 03	0.18E 03
F	6600.7	0.279E-04	0.107E 04	0.18E 03	0.23E 03
FE	1613.0	0.165E-02	0.803E 03	0.20E 02	0.26E 02
FE	1724.8	0.227E-02	0.768E 03	0.10E 02	0.13E 02
FE	4218.8	0.114E-02	0.911E 03	0.34E 01	0.43E 01

TABLE AIV(2) (CONTINUED)

LIMITS FOR QUANTITATIVE DETERMINATION

ELEM.	ENERGY	INTENSITY	MIN.AREA	MIN.WT	WT PERCENT
FE	4810.3	0.469E-03	0.964E 03	0.83E 01	0.11E 02
FE	5920.5	0.234E-02	0.113E 04	0.21E 01	0.26E 01
FE	6018.5	0.228E-02	0.113E 04	0.21E 01	0.27E 01
FE	7278.9	0.130E-02	0.135E 04	0.56E 01	0.72E 01
FE	7631.6	0.768E-02	0.143E 04	0.11E 01	0.14E 01
FE	7645.6	0.626E-02	0.142E 04	0.13E 01	0.17E 01
FE	9298.4	0.109E-02	0.585E 03	0.55E 01	0.70E 01
GA	3130.9	0.552E-03	0.858E 03	0.97E 01	0.12E 02
GA	4840.5	0.835E-03	0.973E 03	0.47E 01	0.60E 01
GA	5195.0	0.853E-03	0.974E 03	0.46E 01	0.59E 01
GA	5339.1	0.173E-02	0.976E 03	0.23E 01	0.29E 01
GA	5601.5	0.121E-02	0.104E 04	0.35E 01	0.45E 01
GA	6008.0	0.149E-02	0.113E 04	0.33E 01	0.41E 01
GA	6111.4	0.118E-02	0.107E 04	0.40E 01	0.50E 01
GA	6360.0	0.313E-02	0.101E 04	0.15E 01	0.19E 01
GD	2107.0	0.374E 00	0.802E 03	0.33E-01	0.42E-01
GD	2314.4	0.389E 00	0.806E 03	0.25E-01	0.32E-01
GD	2600.1	0.389E 00	0.817E 03	0.19E-01	0.24E-01
GD	2678.7	0.464E 00	0.847E 03	0.16E-01	0.20E-01
GD	5582.6	0.359E 00	0.102E 04	0.12E-01	0.15E-01
GD	5902.9	0.704E 00	0.113E 04	0.68E-02	0.86E-02
GD	6419.3	0.329E 00	0.103E 04	0.14E-01	0.18E-01
GD	6749.8	0.198E 01	0.111E 04	0.27E-02	0.35E-02
GE	2013.0	0.285E-03	0.776E 03	0.49E 02	0.62E 02
GE	5450.2	0.291E-03	0.985E 03	0.14E 02	0.18E 02
GE	5518.3	0.311E-03	0.104E 04	0.14E 02	0.17E 02
GE	6036.7	0.380E-03	0.114E 04	0.13E 02	0.16E 02
GE	6116.3	0.415E-03	0.107E 04	0.11E 02	0.14E 02
GE	6707.9	0.398E-03	0.111E 04	0.13E 02	0.17E 02
GE	6915.5	0.321E-03	0.117E 04	0.18E 02	0.23E 02
GE	7259.8	0.264E-03	0.134E 04	0.27E 02	0.35E 02
H	2223.3	0.200E 00	0.803E 03	0.54E-01	0.68E-01
HF	2064.9	0.230E-02	0.780E 03	0.56E 01	0.71E 01
HF	2468.5	0.290E-02	0.812E 03	0.29E 01	0.36E 01
HF	4343.5	0.315E-02	0.936E 03	0.12E 01	0.16E 01
HF	5418.4	0.209E-02	0.100E 04	0.20E 01	0.25E 01
HF	5505.6	0.311E-02	0.104E 04	0.14E 01	0.17E 01
HF	5694.4	0.230E-02	0.106E 04	0.19E 01	0.24E 01
HF	5723.5	0.797E-02	0.107E 04	0.56E 00	0.71E 00
HF	6112.3	0.262E-02	0.107E 04	0.18E 01	0.23E 01
HG	1570.3	0.441E-01	0.832E 03	0.90E 00	0.11E 01
HG	1693.3	0.961E-01	0.770E 03	0.27E 00	0.34E 00
HG	2002.1	0.853E-01	0.777E 03	0.17E 00	0.21E 00
HG	2639.9	0.484E-01	0.820E 03	0.15E 00	0.19E 00

TABLE AIV(2) (CONTINUED)

LIMITS FOR QUANTITATIVE DETERMINATION

ELEM.	ENERGY	INTENSITY	MIN. AREA	MIN. WT	WT PERCENT
HG	4739.5	0.761E-01	0.931E 03	0.49E-01	0.63E-01
HG	4842.5	0.585E-01	0.972E 03	0.67E-01	0.85E-01
HG	5050.2	0.598E-01	0.953E 03	0.65E-01	0.82E-01
HG	5658.1	0.741E-01	0.105E 04	0.59E-01	0.75E-01
FG	5966.9	0.173E 00	0.112E 04	0.28E-01	0.35E-01
HG	6457.8	0.668E-01	0.104E 04	0.71E-01	0.91E-01
HO	2118.3	0.831E-03	0.810E 03	0.15E 02	0.19E 02
HC	2589.9	0.926E-03	0.809E 03	0.80E 01	0.10E 02
HO	5082.8	0.688E-03	0.954E 03	0.56E 01	0.71E 01
HO	5181.9	0.831E-03	0.962E 03	0.47E 01	0.59E 01
HO	5212.7	0.712E-03	0.973E 03	0.55E 01	0.70E 01
HO	5763.1	0.854E-03	0.110E 04	0.54E 01	0.68E 01
HC	5813.4	0.169E-02	0.109E 04	0.27E 01	0.34E 01
HO	6052.1	0.593E-03	0.113E 04	0.82E 01	0.10E 02
I	1887.9	0.253E-03	0.775E 03	0.68E 02	0.86E 02
I	4103.3	0.115E-03	0.905E 03	0.34E 02	0.43E 02
I	4950.2	0.441E-03	0.964E 03	0.88E 01	0.11E 02
I	5093.7	0.335E-03	0.941E 03	0.11E 02	0.14E 02
I	5197.8	0.566E-03	0.974E 03	0.70E 01	0.89E 01
I	5559.6	0.306E-03	0.103E 04	0.14E 02	0.18E 02
I	6307.4	0.297E-03	0.101E 04	0.15E 02	0.19E 02
I	6693.0	0.278E-03	0.107E 04	0.19E 02	0.24E 02
IN	1752.8	0.146E-01	0.759E 03	0.15E 01	0.19E 01
IN	2337.4	0.259E-02	0.819E 03	0.37E 01	0.47E 01
IN	3876.6	0.207E-02	0.890E 03	0.20E 01	0.25E 01
IN	4227.5	0.259E-02	0.913E 03	0.15E 01	0.19E 01
IN	4774.9	0.467E-02	0.936E 03	0.81E 00	0.10E 01
IN	4969.4	0.467E-02	0.960E 03	0.83E 00	0.11E 01
IN	5103.4	0.446E-02	0.936E 03	0.85E 00	0.11E 01
IN	5141.1	0.425E-02	0.951E 03	0.91E 00	0.11E 01
IN	5891.9	0.633E-02	0.113E 04	0.76E 00	0.96E 00
IR	1591.6	0.161E-01	0.812E 03	0.22E 01	0.29E 01
IR	2454.2	0.649E-02	0.821E 03	0.13E 01	0.17E 01
IR	4860.2	0.850E-02	0.965E 03	0.46E 00	0.58E 00
IR	4943.5	0.908E-02	0.968E 03	0.43E 00	0.55E 00
IR	5564.6	0.118E-01	0.103E 04	0.36E 00	0.46E 00
IR	5667.2	0.177E-01	0.105E 04	0.25E 00	0.31E 00
IR	5782.6	0.120E-01	0.110E 04	0.38E 00	0.49E 00
IR	5957.7	0.200E-01	0.112E 04	0.24E 00	0.30E 00
IR	6081.8	0.176E-01	0.109E 04	0.27E 00	0.34E 00
K	1617.5	0.255E-02	0.804E 03	0.13E 02	0.16E 02
K	1929.3	0.818E-03	0.770E 03	0.19E 02	0.25E 02
K	2073.2	0.331E-02	0.784E 03	0.39E 01	0.49E 01
K	2291.2	0.111E-02	0.798E 03	0.89E 01	0.11E 02
K	2545.9	0.117E-02	0.821E 03	0.67E 01	0.85E 01

TABLE AIV(2) (CONTINUED)

LIMITS FOR QUANTITATIVE DETERMINATION					
ELEM.	ENERGY	INTENSITY	MIN. AREA	MIN. WT	WT PERCENT
K	3546.6	0.137E-02	0.865E 03	0.32E 01	0.41E 01
K	5380.3	0.236E-02	0.978E 03	0.17E 01	0.21E 01
K	5695.6	0.150E-02	0.106E 04	0.29E 01	0.37E 01
K	5752.0	0.142E-02	0.109E 04	0.32E 01	0.41E 01
K	7769.0	0.146E-02	0.126E 04	0.52E 01	0.66E 01
LA	2765.3	0.436E-03	0.846E 03	0.15E 02	0.20E 02
LA	3082.6	0.501E-03	0.856E 03	0.11E 02	0.14E 02
LA	3608.6	0.551E-03	0.876E 03	0.79E 01	0.10E 02
LA	4389.4	0.972E-03	0.950E 03	0.40E 01	0.51E 01
LA	4416.3	0.945E-03	0.951E 03	0.41E 01	0.52E 01
LA	4502.8	0.659E-03	0.917E 03	0.56E 01	0.71E 01
LA	4842.7	0.276E-02	0.972E 03	0.14E 01	0.18E 01
LA	5097.6	0.274E-02	0.936E 03	0.14E 01	0.18E 01
LI	1891.4	0.851E-04	0.778E 03	0.20E 03	0.25E 03
LI	2032.5	0.841E-03	0.769E 03	0.16E 02	0.20E 02
LI	2117.4	0.584E-04	0.810E 03	0.21E 03	0.27E 03
LI	2184.0	0.211E-03	0.786E 03	0.52E 02	0.66E 02
LI	3492.7	0.172E-04	0.880E 03	0.27E 03	0.34E 03
LI	3585.2	0.140E-04	0.864E 03	0.31E 03	0.39E 03
LI	4508.3	0.135E-04	0.917E 03	0.28E 03	0.35E 03
LI	6017.3	0.129E-04	0.113E 04	0.38E 03	0.48E 03
LI	7246.7	0.375E-04	0.133E 04	0.19E 03	0.24E 03
LU	2056.2	0.156E-02	0.776E 03	0.83E 01	0.11E 02
LU	2091.2	0.192E-02	0.795E 03	0.66E 01	0.84E 01
LU	3852.1	0.151E-02	0.896E 03	0.27E 01	0.34E 01
LU	5020.4	0.174E-02	0.957E 03	0.22E 01	0.28E 01
LU	5320.4	0.119E-02	0.967E 03	0.33E 01	0.42E 01
LU	5569.6	0.169E-02	0.102E 04	0.25E 01	0.32E 01
LU	5601.7	0.183E-02	0.104E 04	0.24E 01	0.30E 01
LU	6803.8	0.160E-02	0.110E 04	0.34E 01	0.43E 01
MG	1808.9	0.393E-03	0.788E 03	0.51E 02	0.65E 02
MG	2828.1	0.557E-03	0.853E 03	0.12E 02	0.15E 02
MG	3054.1	0.169E-03	0.853E 03	0.33E 02	0.42E 02
MG	3301.1	0.116E-03	0.886E 03	0.43E 02	0.55E 02
MG	3413.6	0.848E-04	0.900E 03	0.57E 02	0.72E 02
MG	3830.7	0.880E-04	0.896E 03	0.47E 02	0.59E 02
MG	3916.7	0.637E-03	0.888E 03	0.63E 01	0.79E 01
MG	5451.8	0.432E-04	0.988E 03	0.94E 02	0.12E 03
MG	8154.4	0.621E-04	0.864E 03	0.93E 02	0.12E 03
MN	1747.0	0.415E-02	0.766E 03	0.54E 01	0.69E 01
MN	1987.6	0.344E-02	0.778E 03	0.42E 01	0.54E 01
MN	2330.9	0.456E-02	0.815E 03	0.21E 01	0.27E 01
MN	3408.5	0.492E-02	0.901E 03	0.98E 00	0.12E 01
MN	5014.7	0.807E-02	0.956E 03	0.48E 00	0.61E 00
MN	5527.2	0.101E-01	0.103E 04	0.42E 00	0.53E 00

TABLE AIV(2) (CONTINUED)

LIMITS FOR QUANTITATIVE DETERMINATION					
ELEM.	ENERGY	INTENSITY	MIN.AREA	MIN.WT	WT PERCENT
MN	6783.7	0.504E-02	0.111E 04	0.11E 01	0.14E 01
MN	7057.9	0.165E-01	0.124E 04	0.39E 00	0.49E 00
MN	7159.9	0.883E-02	0.128E 04	0.77E 00	0.98E 00
MN	7243.5	0.175E-01	0.132E 04	0.41E 00	0.52E 00
MC	2400.9	0.167E-03	0.810E 03	0.53E 02	0.67E 02
MC	2664.5	0.215E-03	0.837E 03	0.34E 02	0.43E 02
MO	5602.4	0.128E-03	0.104E 04	0.34E 02	0.43E 02
MC	5713.1	0.225E-03	0.108E 04	0.20E 02	0.25E 02
MO	6364.6	0.127E-03	0.102E 04	0.36E 02	0.46E 02
MO	6625.1	0.123E-03	0.107E 04	0.41E 02	0.52E 02
MO	6919.3	0.579E-03	0.117E 04	0.10E 02	0.13E 02
MO	7527.1	0.132E-03	0.148E 04	0.64E 02	0.82E 02
N	1678.6	0.195E-03	0.773E 03	0.14E 03	0.17E 03
N	1887.9	0.126E-02	0.775E 03	0.14E 02	0.17E 02
N	3530.5	0.441E-03	0.889E 03	0.10E 02	0.13E 02
N	4507.6	0.728E-03	0.917E 03	0.51E 01	0.65E 01
N	5267.1	0.117E-02	0.965E 03	0.33E 01	0.42E 01
N	5296.7	0.856E-03	0.975E 03	0.46E 01	0.59E 01
N	5532.0	0.819E-03	0.103E 04	0.51E 01	0.65E 01
N	6321.4	0.767E-03	0.103E 04	0.60E 01	0.77E 01
N	7299.5	0.385E-03	0.137E 04	0.19E 02	0.25E 02
NA	1634.4	0.120E-02	0.805E 03	0.26E 02	0.33E 02
NA	2027.2	0.277E-02	0.774E 03	0.49E 01	0.62E 01
NA	2517.6	0.239E-02	0.823E 03	0.34E 01	0.43E 01
NA	2754.4D	0.143E-01	0.846E 03	0.47E 00	0.60E 00
NA	2862.7	0.164E-02	0.845E 03	0.38E 01	0.48E 01
NA	3098.1	0.135E-02	0.855E 03	0.40E 01	0.51E 01
NA	3588.0	0.242E-02	0.867E 03	0.18E 01	0.23E 01
NA	3982.0	0.301E-02	0.896E 03	0.13E 01	0.17E 01
NA	6395.4	0.359E-02	0.104E 04	0.13E 01	0.17E 01
NB	1724.5	0.112E-03	0.768E 03	0.21E 03	0.27E 03
NB	1979.7	0.413E-04	0.785E 03	0.36E 03	0.46E 03
NB	4739.7	0.443E-04	0.932E 03	0.85E 02	0.11E 03
NB	5104.2	0.842E-04	0.938E 03	0.45E 02	0.57E 02
NB	5253.6	0.428E-04	0.962E 03	0.91E 02	0.12E 03
NB	5496.9	0.601E-04	0.104E 04	0.71E 02	0.90E 02
NB	5895.3	0.631E-04	0.113E 04	0.76E 02	0.96E 02
NB	6830.7	0.752E-04	0.113E 04	0.74E 02	0.94E 02
NB	7186.1	0.345E-04	0.129E 04	0.20E 03	0.25E 03
ND	2371.5	0.253E-02	0.821E 03	0.37E 01	0.47E 01
ND	4790.9	0.169E-02	0.932E 03	0.22E 01	0.28E 01
ND	4949.0	0.184E-02	0.964E 03	0.21E 01	0.27E 01
ND	5380.9	0.178E-02	0.978E 03	0.22E 01	0.28E 01
ND	5448.2	0.260E-02	0.981E 03	0.15E 01	0.20E 01
ND	5521.2	0.225E-02	0.104E 04	0.19E 01	0.24E 01

TABLE AIV(2) (CONTINUED)

LIMITS FOR QUANTITATIVE DETERMINATION

ELEM.	ENERGY	INTENSITY	MIN.AREA	MIN.WT	WT PERCENT
ND	6255.9	0.544E-02	0.101E 04	0.83E 00	0.11E 01
ND	6502.1	0.120E-01	0.106E 04	0.41E 00	0.52E 00
NI	5816.8	0.110E-02	0.110E 04	0.42E 01	0.53E 01
NI	6105.0	0.982E-03	0.107E 04	0.47E 01	0.60E 01
NI	6837.0	0.562E-02	0.113E 04	0.10E 01	0.13E 01
NI	7536.1	0.233E-02	0.148E 04	0.36E 01	0.46E 01
NI	7818.9	0.427E-02	0.118E 04	0.17E 01	0.21E 01
NI	8120.5	0.164E-02	0.899E 03	0.36E 01	0.46E 01
NI	8533.4	0.884E-02	0.101E 04	0.85E 00	0.11E 01
NI	8958.8	0.197E-01	0.912E 03	0.41E 00	0.52E 00
OS	2261.3	0.116E-03	0.802E 03	0.88E 02	0.11E 03
OS	2458.8	0.484E-04	0.813E 03	0.17E 03	0.22E 03
OS	4530.7	0.484E-04	0.911E 03	0.76E 02	0.97E 02
OS	4812.8	0.678E-04	0.967E 03	0.58E 02	0.73E 02
OS	5146.9	0.170E-03	0.954E 03	0.23E 02	0.29E 02
OS	5274.0	0.111E-03	0.966E 03	0.35E 02	0.45E 02
OS	5684.0	0.775E-04	0.105E 04	0.56E 02	0.71E 02
OS	6587.2	0.436E-04	0.106E 04	0.12E 03	0.15E 03
P	1890.0	0.246E-03	0.778E 03	0.70E 02	0.88E 02
P	2114.3	0.282E-03	0.807E 03	0.44E 02	0.56E 02
P	2154.2	0.620E-03	0.802E 03	0.19E 02	0.24E 02
P	3058.3	0.239E-03	0.855E 03	0.23E 02	0.30E 02
P	3522.8	0.535E-03	0.891E 03	0.85E 01	0.11E 02
P	3900.3	0.649E-03	0.880E 03	0.61E 01	0.78E 01
P	4671.3	0.561E-03	0.943E 03	0.68E 01	0.86E 01
P	6785.3	0.528E-03	0.111E 04	0.10E 02	0.13E 02
P	7421.2	0.216E-03	0.141E 04	0.37E 02	0.46E 02
PB	6736.4	0.255E-04	0.111E 04	0.21E 03	0.27E 03
PB	7367.7	0.476E-03	0.140E 04	0.16E 02	0.21E 02
PD	2156.9	0.498E-03	0.789E 03	0.22E 02	0.28E 02
PD	2457.5	0.461E-03	0.817E 03	0.18E 02	0.23E 02
PD	2484.3	0.466E-03	0.817E 03	0.18E 02	0.22E 02
PD	4794.6	0.493E-03	0.940E 03	0.77E 01	0.98E 01
PD	5212.9	0.221E-03	0.974E 03	0.18E 02	0.23E 02
PD	5828.4	0.371E-03	0.110E 04	0.13E 02	0.16E 02
PD	6652.5	0.163E-03	0.111E 04	0.32E 02	0.41E 02
PD	8331.0	0.724E-04	0.942E 03	0.91E 02	0.12E 03
PR	2839.8	0.304E-03	0.856E 03	0.21E 02	0.27E 02
PR	3652.0	0.555E-03	0.877E 03	0.77E 01	0.98E 01
PR	4692.2	0.111E-02	0.945E 03	0.34E 01	0.44E 01
PR	4801.4	0.574E-03	0.951E 03	0.67E 01	0.85E 01
PR	5095.9	0.734E-03	0.939E 03	0.52E 01	0.66E 01
PR	5140.2	0.133E-02	0.949E 03	0.29E 01	0.37E 01
PR	5665.7	0.134E-02	0.105E 04	0.32E 01	0.41E 01

TABLE AIV(2) (CONTINUED)

LIMITS FOR QUANTITATIVE DETERMINATION

ELEM.	ENERGY	INTENSITY	MIN. AREA	MIN. WT	WT PERCENT
PR	5842.9	0.468E-03	0.111E 04	0.10E 02	0.13E 02
PT	1978.7	0.492E-03	0.785E 03	0.30E 02	0.38E 02
PT	2067.8	0.368E-03	0.782E 03	0.35E 02	0.44E 02
PT	2311.4	0.513E-03	0.803E 03	0.19E 02	0.24E 02
PT	2469.6	0.415E-03	0.812E 03	0.20E 02	0.25E 02
PT	5173.4	0.525E-03	0.953E 03	0.74E 01	0.93E 01
PT	5254.6	0.144E-02	0.963E 03	0.27E 01	0.34E 01
PT	5307.0	0.344E-03	0.977E 03	0.12E 02	0.15E 02
PT	5611.4	0.308E-03	0.106E 04	0.14E 02	0.18E 02
PT	6033.5	0.326E-03	0.114E 04	0.15E 02	0.19E 02
RB	2130.0	0.226E-04	0.813E 03	0.54E 03	0.69E 03
RB	2149.7	0.236E-04	0.806E 03	0.50E 03	0.64E 03
RB	2176.8	0.586E-04	0.794E 03	0.19E 03	0.24E 03
RB	5760.6	0.313E-04	0.110E 04	0.15E 03	0.19E 03
RB	6470.7	0.262E-04	0.103E 04	0.18E 03	0.23E 03
RB	6520.2	0.293E-04	0.103E 04	0.16E 03	0.21E 03
RB	6831.4	0.308E-04	0.113E 04	0.18E 03	0.23E 03
RB	7624.1	0.987E-04	0.143E 04	0.85E 02	0.11E 03
RE	2004.4	0.103E-02	0.777E 03	0.14E 02	0.17E 02
RE	3153.2	0.668E-03	0.865E 03	0.79E 01	0.10E 02
RE	4861.0	0.974E-03	0.966E 03	0.40E 01	0.51E 01
RE	5007.9	0.890E-03	0.954E 03	0.43E 01	0.55E 01
RE	5074.3	0.134E-02	0.953E 03	0.29E 01	0.36E 01
RE	5137.2	0.106E-02	0.948E 03	0.36E 01	0.46E 01
RE	5277.7	0.640E-03	0.967E 03	0.61E 01	0.78E 01
RE	5910.2	0.184E-02	0.113E 04	0.26E 01	0.33E 01
RH	4510.3	0.401E-02	0.919E 03	0.93E 00	0.12E 01
RH	5266.2	0.931E-02	0.965E 03	0.42E 00	0.53E 00
RH	5347.2	0.122E-01	0.978E 03	0.33E 00	0.41E 00
RH	5517.2	0.129E-01	0.113E 04	0.37E 00	0.47E 00
RH	6046.4	0.703E-02	0.114E 04	0.70E 00	0.89E 00
RH	6082.8	0.593E-02	0.108E 04	0.79E 00	0.10E 01
RH	6171.8	0.611E-02	0.106E 04	0.76E 00	0.96E 00
RH	6211.4	0.630E-02	0.104E 04	0.73E 00	0.92E 00
RU	2298.3	0.823E-04	0.806E 03	0.12E 03	0.15E 03
RU	2530.4	0.128E-03	0.822E 03	0.62E 02	0.79E 02
RU	4351.3	0.960E-04	0.934E 03	0.40E 02	0.51E 02
RU	4627.4	0.106E-03	0.933E 03	0.36E 02	0.45E 02
RU	5022.8	0.166E-03	0.958E 03	0.23E 02	0.30E 02
RU	6273.7	0.122E-03	0.104E 04	0.38E 02	0.48E 02
RU	6342.1	0.128E-03	0.103E 04	0.36E 02	0.46E 02
RU	7102.9	0.823E-04	0.126E 04	0.80E 02	0.10E 03
S	1597.8	0.113E-02	0.810E 03	0.31E 02	0.40E 02
S	1890.5	0.681E-03	0.778E 03	0.25E 02	0.32E 02

TABLE AIV(2) (CONTINUED)

LIMITS FOR QUANTITATIVE DETERMINATION					
ELEM.	ENERGY	INTENSITY	MIN. AREA	MIN. WT	WT PERCENT
S	2379.7	0.307E-02	0.818E 03	0.30E C1	0.38E 01
S	2753.2	0.403E-03	0.846E 03	0.17E 02	0.21E 02
S	2931.1	0.154E-02	0.852E 03	0.39E C1	0.50E 01
S	3220.8	0.187E-02	0.881E 03	0.28E 01	0.35E 01
S	3370.4	0.363E-03	0.883E 03	0.13E 02	0.17E 02
S	4869.8	0.792E-03	0.963E 03	0.49E C1	0.62E 01
S	5420.5	0.408E-02	0.998E 03	0.10E 01	0.13E 01
S	7800.0	0.270E-03	0.123E 04	0.28E C2	0.35E 02
SB	2074.2	0.125E-03	0.785E 03	0.10E 03	0.13E 03
SB	5562.9	0.176E-03	0.103E 04	0.24E 02	0.31E 02
SB	5684.3	0.897E-04	0.105E 04	0.49E C2	0.62E 02
SB	5886.2	0.163E-03	0.113E 04	0.29E 02	0.37E 02
SB	6380.1	0.141E-03	0.103E 04	0.33E 02	0.42E 02
SB	6468.1	0.119E-03	0.103E 04	0.40E 02	0.51E C2
SB	6523.6	0.321E-03	0.104E 04	0.15E 02	0.19E 02
SB	6728.0	0.217E-03	0.110E 04	0.25E C2	0.31E 02
SC	1692.0	0.112E-01	0.770E C3	0.23E C1	0.29E C1
SC	2111.4	0.655E-02	0.805E 03	0.19E 01	0.24E 01
SC	2635.6	0.977E-02	0.817E 03	0.74E 00	0.94E 00
SC	4975.1	0.672E-02	0.957E C3	0.58E 00	0.73E 00
SC	6054.9	0.733E-02	0.112E 04	0.66E 00	0.84E C0
SC	6839.5	0.155E-01	0.114E 04	0.36E 00	0.46E 00
SC	7635.9	0.829E-02	0.143E 04	0.10E 01	0.13E 01
SC	8531.6	0.147E-01	0.101E 04	0.51E 00	0.65E 00
SC	8174.7	0.286E-01	0.878E C3	0.21E 00	0.26E 00
SE	4565.7	0.122E-02	0.932E 03	0.31E 01	0.39E 01
SE	5601.7	0.202E-02	0.104E 04	0.21E 01	0.27E 01
SE	6008.0	0.271E-02	0.113E 04	0.18E 01	0.23E 01
SE	6232.7	0.142E-02	0.104E 04	0.32E 01	0.41E 01
SE	6601.2	0.404E-02	0.107E 04	0.12E C1	0.16E 01
SE	7179.7	0.154E-02	0.129E 04	0.44E 01	0.56E C1
SE	7418.7	0.240E-02	0.140E 04	0.33E 01	0.42E 01
SI	2092.9	0.919E-03	0.795E 03	0.14E 02	0.17E 02
SI	2425.9	0.135E-03	0.806E C3	0.64E 02	0.81E 02
SI	3539.3	0.273E-02	0.879E 03	0.16E C1	0.21E 01
SI	3661.3	0.158E-03	0.876E 03	0.27E 02	0.34E 02
SI	4934.3	0.242E-02	0.965E C3	0.16E 01	0.20E 01
SI	5107.3	0.126E-03	0.941E 03	0.30E 02	0.38E 02
SI	6380.1	0.433E-03	0.103E 04	0.11E 02	0.14E 02
SI	7199.3	0.246E-03	0.130E 04	0.28E C2	0.36E 02
SM	2119.8	0.936E-01	0.811E 03	0.13E 00	0.17E 00
SM	2161.0	0.655E-01	0.790E 03	0.17E 00	0.22E 00
SM	2332.0	0.398E-01	0.816E 03	0.24E 00	0.31E 00
SM	4484.3	0.398E-01	0.926E C3	0.94E-01	0.12E 00
SM	4809.1	0.912E-01	0.964E 03	0.43E-C1	0.54E-01

TABLE AIV(2) (CONTINUED)

LIMITS FOR QUANTITATIVE DETERMINATION					
ELEM.	ENERGY	INTENSITY	MIN.AREA	MIN.WT	WT PERCENT
SM	5532.8	0.112E 00	0.103E 04	0.38E-01	0.48E-01
SM	6537.9	0.468E-01	0.104E 04	0.10E 00	0.13E 00
SM	7213.0	0.175E 00	0.130E 04	0.40E-01	0.51E-01
SN	2112.7	0.488E-04	0.805E 03	0.25E 03	0.32E 03
SN	2179.0	0.371E-04	0.796E 03	0.30E 03	0.38E 03
SN	2651.7	0.183E-04	0.826E 03	0.39E 03	0.50E 03
SN	3334.3	0.320E-04	0.879E 03	0.15E 03	0.19E 03
SN	3459.2	0.177E-04	0.885E 03	0.26E 03	0.33E 03
SN	5392.5	0.136E-04	0.975E 03	0.29E 03	0.37E 03
SN	6268.0	0.139E-04	0.103E 04	0.33E 03	0.42E 03
SN	9326.1	0.110E-04	0.581E 03	0.55E 03	0.70E 03
SR	1835.9	0.761E-02	0.758E 03	0.24E 01	0.31E 01
SR	2276.8	0.266E-03	0.805E 03	0.38E 02	0.48E 02
SR	2391.5	0.383E-03	0.810E 03	0.23E 02	0.30E 02
SR	3009.5	0.448E-03	0.846E 03	0.13E 02	0.16E 02
SR	6101.9	0.295E-03	0.107E 04	0.16E 02	0.20E 02
SR	6267.3	0.463E-03	0.103E 04	0.99E 01	0.13E 02
SR	6660.6	0.460E-03	0.111E 04	0.12E 02	0.15E 02
SR	6941.9	0.282E-03	0.119E 04	0.21E 02	0.27E 02
SR	7527.7	0.386E-03	0.148E 04	0.22E 02	0.28E 02
TA	4220.6	0.337E-03	0.911E 03	0.11E 02	0.14E 02
TA	4315.5	0.299E-03	0.917E 03	0.13E 02	0.16E 02
TA	4483.0	0.197E-03	0.924E 03	0.19E 02	0.24E 02
TA	4617.7	0.191E-03	0.932E 03	0.20E 02	0.25E 02
TA	4781.8	0.210E-03	0.931E 03	0.18E 02	0.23E 02
TA	5342.9	0.172E-03	0.977E 03	0.23E 02	0.29E 02
TA	5964.7	0.451E-03	0.112E 04	0.11E 02	0.13E 02
TA	6062.5	0.273E-03	0.111E 04	0.18E 02	0.22E 02
TB	1689.0	0.662E-03	0.771E 03	0.39E 02	0.50E 02
TB	1745.8	0.819E-03	0.769E 03	0.28E 02	0.35E 02
TB	2120.2	0.349E-03	0.811E 03	0.35E 02	0.45E 02
TB	5099.6	0.471E-03	0.934E 03	0.80E 01	0.10E 02
TB	5777.2	0.680E-03	0.110E 04	0.68E 01	0.86E 01
TB	5891.5	0.924E-03	0.113E 04	0.52E 01	0.66E 01
TB	5953.7	0.384E-03	0.113E 04	0.12E 02	0.16E 02
TB	5994.7	0.453E-03	0.113E 04	0.11E 02	0.14E 02
TB	6138.8	0.471E-03	0.107E 04	0.10E 02	0.13E 02
TB	6218.2	0.697E-03	0.103E 04	0.66E 01	0.83E 01
TE	1918.9	0.920E-03	0.777E 03	0.18E 02	0.22E 02
TE	2039.1	0.425E-03	0.773E 03	0.31E 02	0.40E 02
TE	2386.0	0.270E-03	0.815E 03	0.34E 02	0.43E 02
TE	2610.5	0.602E-03	0.826E 03	0.12E 02	0.16E 02
TE	2747.2	0.103E-02	0.841E 03	0.66E 01	0.84E 01
TE	3544.0	0.270E-03	0.868E 03	0.16E 02	0.21E 02
TE	5668.1	0.222E-03	0.105E 04	0.20E 02	0.25E 02

TABLE AIV(2) (CONTINUED)

LIMITS FOR QUANTITATIVE DETERMINATION

ELEM.	ENERGY	INTENSITY	MIN.AREA	MIN.WT	WT PERCENT
TE	6211.1	0.210E-03	0.104E 04	0.22E 02	0.28E 02
TE	6323.0	0.700E-03	0.103E 04	0.66E 01	0.84E 01
TI	1586.0	0.650E-02	0.820E 03	0.57E 01	0.73E 01
TI	1761.6	0.601E-02	0.756E 03	0.36E 01	0.45E 01
TI	3026.8	0.264E-02	0.854E 03	0.22E 01	0.27E 01
TI	3475.5	0.178E-02	0.874E 03	0.26E 01	0.33E 01
TI	3920.4	0.132E-02	0.891E 03	0.30E 01	0.38E 01
TI	4881.3	0.431E-02	0.950E 03	0.89E 00	0.11E 01
TI	4966.6	0.284E-02	0.959E 03	0.14E 01	0.17E 01
TI	6418.0	0.277E-01	0.103E 04	0.17E 00	0.22E 00
TI	6555.6	0.493E-02	0.105E 04	0.10E 01	0.13E 01
TI	6759.7	0.411E-01	0.112E 04	0.13E 00	0.17E 00
TL	4752.8	0.194E-03	0.936E 03	0.19E 02	0.25E 02
TL	4914.2	0.204E-03	0.955E 03	0.19E 02	0.24E 02
TL	5180.8	0.182E-03	0.962E 03	0.21E 02	0.27E 02
TL	5280.5	0.236E-03	0.967E 03	0.17E 02	0.21E 02
TL	5603.6	0.323E-03	0.104E 04	0.13E 02	0.17E 02
TL	5641.9	0.374E-03	0.105E 04	0.12E 02	0.15E 02
TL	6166.9	0.204E-03	0.106E 04	0.23E 02	0.29E 02
TL	6515.2	0.157E-03	0.104E 04	0.31E 02	0.39E 02
TM	2115.2	0.898E-03	0.808E 03	0.14E 02	0.18E 02
TM	4733.2	0.166E-02	0.931E 03	0.23E 01	0.29E 01
TM	5152.2	0.166E-02	0.958E 03	0.23E 01	0.30E 01
TM	5737.2	0.427E-02	0.107E 04	0.10E 01	0.13E 01
TM	5942.7	0.418E-02	0.114E 04	0.12E 01	0.15E 01
TM	6001.6	0.243E-02	0.113E 04	0.20E 01	0.25E 01
TM	6387.4	0.364E-02	0.104E 04	0.13E 01	0.16E 01
TM	6552.9	0.247E-02	0.105E 04	0.20E 01	0.25E 01
V	1777.8	0.317E-02	0.770E 03	0.67E 01	0.84E 01
V	5142.2	0.293E-02	0.951E 03	0.13E 01	0.17E 01
V	5209.9	0.332E-02	0.974E 03	0.12E 01	0.15E 01
V	5515.5	0.574E-02	0.104E 04	0.74E 00	0.94E 00
V	5751.9	0.524E-02	0.109E 04	0.87E 00	0.11E 01
V	6464.8	0.565E-02	0.104E 04	0.85E 00	0.11E 01
V	6517.2	0.112E-01	0.104E 04	0.43E 00	0.55E 00
V	6873.9	0.672E-02	0.115E 04	0.85E 00	0.11E 01
V	7162.7	0.822E-02	0.129E 04	0.83E 00	0.11E 01
W	3470.7	0.594E-03	0.882E 03	0.78E 01	0.99E 01
W	4249.2	0.844E-03	0.918E 03	0.45E 01	0.58E 01
W	4684.7	0.788E-03	0.949E 03	0.49E 01	0.62E 01
W	5164.3	0.123E-02	0.962E 03	0.32E 01	0.40E 01
W	5261.7	0.258E-02	0.964E 03	0.15E 01	0.19E 01
W	5320.5	0.179E-02	0.967E 03	0.22E 01	0.28E 01
W	6144.3	0.957E-03	0.107E 04	0.49E 01	0.62E 01
W	6190.5	0.274E-02	0.105E 04	0.17E 01	0.21E 01

TABLE AIV(2) (CONTINUED)

LIMITS FOR QUANTITATIVE DETERMINATION

ELEM.	ENERGY	INTENSITY	MIN. AREA	MIN. WT	WT PERCENT
Y	2546.6	0.205E-03	0.821E 03	0.38E 02	0.48E 02
Y	2749.5	0.253E-03	0.843E 03	0.27E 02	0.34E 02
Y	3163.4	0.114E-03	0.868E 03	0.46E 02	0.55E 02
Y	3301.4	0.116E-03	0.886E 03	0.43E 02	0.55E 02
Y	4107.5	0.441E-03	0.900E 03	0.88E 01	0.11E 02
Y	4352.4	0.137E-03	0.933E 03	0.28E 02	0.36E 02
Y	5645.4	0.138E-03	0.105E 04	0.31E 02	0.40E 02
Y	6080.3	0.643E-02	0.109E 04	0.74E 00	0.93E 00
YB	2585.0	0.144E-02	0.818E 03	0.52E 01	0.66E 01
YB	3087.5	0.149E-02	0.854E 03	0.37E 01	0.46E 01
YB	3632.8	0.191E-02	0.876E 03	0.23E 01	0.29E 01
YB	3884.9	0.310E-02	0.880E 03	0.13E 01	0.16E 01
YB	3929.6	0.148E-02	0.887E 03	0.27E 01	0.34E 01
YB	4829.6	0.114E-02	0.988E 03	0.35E 01	0.44E 01
YB	5265.7	0.660E-02	0.965E 03	0.59E 00	0.75E 00
YB	6780.1	0.489E-03	0.112E 04	0.11E 02	0.14E 02
ZN	1883.5	0.777E-03	0.769E 03	0.22E 02	0.28E 02
ZN	2858.2	0.142E-03	0.847E 03	0.44E 02	0.56E 02
ZN	4137.9	0.178E-03	0.898E 03	0.22E 02	0.27E 02
ZN	5474.2	0.384E-03	0.102E 04	0.11E 02	0.14E 02
ZN	6867.6	0.204E-03	0.114E 04	0.28E 02	0.35E 02
ZN	6958.5	0.325E-03	0.118E 04	0.18E 02	0.23E 02
ZN	7069.2	0.163E-03	0.124E 04	0.40E 02	0.50E 02
ZN	7112.0	0.163E-03	0.126E 04	0.41E 02	0.51E 02
ZN	7862.9	0.118E-02	0.102E 04	0.53E 01	0.68E 01
ZR	2190.9	0.247E-04	0.785E 03	0.44E 03	0.56E 03
ZR	2694.0	0.299E-04	0.859E 03	0.24E 03	0.31E 03
ZR	2933.2	0.152E-04	0.852E 03	0.40E 03	0.50E 03
ZR	3474.7	0.153E-04	0.874E 03	0.30E 03	0.38E 03
ZR	4530.3	0.201E-04	0.911E 03	0.18E 03	0.23E 03
ZR	5263.7	0.323E-04	0.964E 03	0.12E 03	0.15E 03
ZR	6295.0	0.193E-03	0.103E 04	0.24E 02	0.30E 02
ZR	8634.2	0.916E-05	0.980E 03	0.82E 03	0.10E 04

TABLE AIV(3)

TWELVE OF THE MOST PROMINENT CAPTURE GAMMA RAYS OF 75 ELEMENTS LISTED IN TERMS OF INCREASING GAMMA RAY ENERGY

ENERGY (KEV)	INTENSITY (P/G-N/CM2)	ELEMENT	ENERGY (KEV)	INTENSITY (P/G-N/CM2)	ELEMENT
178.4	0.40E-02	PR	283.1	0.17E-02	NI
185.7	0.67E 00	DY	283.1	0.90E-03	SB
187.3	0.45E-02	OS	285.2	0.68E-01	ER
191.0	0.29E-02	NB	289.1	0.38E-02	LA
193.5	0.12E-01	AU	290.4	0.66E-02	HO
196.9	0.34E-02	BR	291.1	0.11E-01	RE
199.5	0.12E 00	AG	291.4	0.31E-02	I
201.2	0.12E-02	W	295.6	0.51E-01	SC
203.2	0.14E-02	Y	295.6	0.20E-01	AG
205.2	0.24E-01	TM	297.6	0.41E-02	TA
208.0	0.93E 00	EU	299.2	0.50E-03	AS
209.8	0.15E-01	RE	308.0	0.62E-02	CS
212.5	0.88E-02	MN	314.3	0.52E-02	MN
214.0	0.20E 00	HF	315.9	0.27E-02	BR
215.7	0.30E-01	AU	317.6	0.84E-02	RE
217.4	0.93E-01	RH	325.8	0.22E-01	HF
217.4	0.12E 00	IR	326.1	0.12E-02	GE
219.6	0.45E-02	LA	326.7	0.11E-03	F
220.4	0.11E-01	TM	329.4	0.33E-03	AL
228.6	0.13E 00	SC	332.7	0.10E-02	SB
230.5	0.68E-01	CO	333.3	0.58E-02	PT
234.8	0.44E-02	CS	333.9	0.19E 02	SM
236.7	0.11E-02	AS	335.6	0.24E-01	IN
237.0	0.48E-01	AG	336.7	0.26E-02	I
237.5	0.32E-01	TM	339.5	0.14E-02	NI
239.6	0.12E-01	SE	341.7	0.23E-01	TI
240.3	0.10E-01	HO	341.9	0.82E-02	YB
241.8	0.25E-01	YB	348.6	0.31E-03	TL
245.7	0.27E-02	PD	351.8	0.57E-01	IR
246.1	0.75E-02	BR	352.5	0.31E-02	FE
246.9	0.15E-03	SI	356.1	0.10E-01	PT
248.2	0.17E-01	AU	361.4	0.13E-02	TA
248.7	0.39E-03	AL	367.5	0.14E-01	LU
250.5	0.14E-03	SI	367.8	0.92E 00	HG
250.9	0.23E-02	GA	374.6	0.12E 00	EU
251.2	0.12E-03	ZR	380.4	0.13E-01	AG
251.9	0.60E-04	SN	385.2	0.25E-02	CU
253.1	0.15E-03	N	390.0	0.88E-04	MG
255.1	0.14E-02	NB	393.7	0.16E-02	GA
255.4	0.18E-01	RE	402.9	0.11E-01	TA
258.1	0.94E-04	B	413.2	0.24E 00	DY
261.5	0.17E-01	AU	418.3	0.20E-01	IR
267.9	0.34E-01	RH	421.0	0.10E-02	I
269.4	0.11E-01	LU	423.2	0.27E-02	LA
271.1	0.20E-01	TA	426.3	0.72E-02	HO
273.3	0.73E-01	IN	436.6	0.41E-02	V
277.7	0.60E-01	CO	439.4	0.11E 02	SM
278.3	0.11E-01	CU	445.7	0.53E-03	ZN

TABLE AIV(3) (CONTINUED)

ENERGY (KEV)	INTENSITY (P/G-N/CM2)	ELEMENT	ENERGY (KEV)	INTENSITY (P/G-N/CM2)	ELEMENT
-----	-----	-----	-----	-----	-----
454.5	0.12E-01	ND	645.8	0.75E-03	PR
455.2	0.74E-03	Y	645.9	0.70E-02	V
458.1	0.41E-01	LU	651.0	0.10E-02	GA
465.1	0.68E-02	NI	651.3	0.29E 01	CD
472.2	0.15E-02	AS	661.1	0.54E-01	HG
472.4	0.97E-02	NA	662.3	0.90E-03	CE
475.3	0.15E-02	RU	687.1	0.93E-03	RU
475.4	0.31E-02	YB	691.7	0.28E-02	GA
476.0	0.22E-03	RB	692.1	0.14E-02	FE
477.7 D	0.27E-01	B	696.7	0.13E 00	ND
478.3	0.33E-02	OS	699.8	0.70E-03	PR
497.5	0.13E-03	B	716.9	0.53E-02	PD
497.6	0.15E 00	DY	719.9	0.15E-02	MO
501.7	0.11E-03	B	722.2	0.12E-02	LA
518.3	0.62E-01	CL	726.9	0.14E-03	CA
520.0	0.38E-03	CA	730.6	0.43E-01	ER
520.6	0.33E-02	SE	737.0	0.24E-03	TL
538.4	0.24E 00	DY	737.5	0.22E 01	SM
539.8	0.23E-02	RU	749.2	0.35E-02	CR
543.2	0.65E-02	HO	762.0	0.11E-01	LU
551.5	0.22E-02	W	770.6	0.10E-01	K
556.2	0.45E-01	CO	772.7	0.86E-03	W
556.8	0.66E-03	RB	776.9	0.24E-02	Y
558.5	0.12E-02	SR	778.4	0.83E-02	MO
558.6	0.15E 02	CD	780.3	0.25E 01	GD
558.8	0.16E-03	LI	781.1	0.43E-03	NA
561.0	0.11E-03	ZR	789.7	0.12E-01	RH
565.5	0.98E-02	TM	806.0	0.99E 00	CD
569.3	0.25E-02	OS	814.5	0.19E-01	ND
574.6	0.98E-03	Y	816.1	0.19E 00	ER
585.2	0.33E-03	MG	818.7	0.51E-03	BA
596.0	0.70E-02	GE	819.3	0.29E-01	IN
596.2	0.28E-03	F	823.5	0.27E-02	V
596.6	0.59E-03	TB	835.1	0.86E-02	CR
596.8	0.14E-03	N	841.1	0.52E-02	S
602.9	0.37E-02	TE	849.0	0.30E-02	MO
608.9	0.29E-02	CU	850.4	0.11E-02	SR
613.9	0.12E-01	SE	853.5	0.16E-03	BE
614.2	0.59E-03	I	868.1	0.38E-02	GE
616.1	0.48E-02	PD	869.1	0.84E-04	LI
618.5	0.51E-01	ND	870.6	0.35E-02	NA
627.5	0.74E-03	BA	872.7	0.16E-03	RB
627.9	0.23E-01	SC	873.1	0.26E-03	TL
630.6	0.78E-03	RU	877.9	0.20E-02	NI
634.0	0.50E-02	OS	886.9	0.27E-02	SE
636.2	0.49E-03	P	891.5	0.77E-03	W
636.2	0.45E-02	YB	897.9	0.25E-02	SR
645.0	0.19E-01	RH	911.1	0.25E-03	TL

TABLE AIV(3) (CONTINUED)

ENERGY (KEV)	INTENSITY (P/G-N/CM2)	ELEMENT	ENERGY (KEV)	INTENSITY (P/G-N/CM2)	ELEMENT
914.5	0.26E-01	ER	1570.3	0.44E-01	HG
921.1	0.38E-03	SB	1586.0	0.65E-02	TI
934.5	0.47E-03	ZR	1591.6	0.16E-01	IR
943.7	0.63E 01	GD	1597.8	0.11E-02	S
945.9	0.14E-03	NB	1613.0	0.16E-02	FE
961.8	0.46E 01	GD	1617.5	0.25E-02	K
980.7	0.91E-04	LI	1623.1	0.17E-03	AL
983.4	0.20E-03	AL	1634.4	0.12E-02	NA
1006.6	0.48E-03	PR	1658.6	0.50E-01	EU
1007.6	0.30E-03	ZN	1672.4	0.42E-03	CU
1030.8	0.20E-03	RB	1678.6	0.19E-03	N
1047.9	0.42E-02	PD	1689.0	0.66E-03	TB
1070.6	0.35E-03	P	1692.0	0.11E-01	SC
1077.5	0.22E-02	ZN	1693.3	0.96E-01	HG
1091.0	0.74E-03	MO	1724.0	0.14E-03	CA
1100.6	0.19E-02	GE	1724.5	0.11E-03	NB
1129.4	0.11E-03	MG	1724.8	0.23E-02	FE
1159.0	0.19E-02	K	1745.8	0.82E-03	TB
1165.4	0.61E-01	CL	1747.0	0.41E-02	MN
1169.7	0.10E 01	SM	1749.0	0.16E-03	F
1171.3	0.25E-03	SN	1752.8	0.15E-01	IN
1185.4	0.89E 01	GD	1761.6	0.60E-02	TI
1199.1	0.23E-02	BR	1777.8	0.32E-02	V
1206.4	0.17E-01	HF	1783.8	0.19E-02	CR
1228.9	0.14E-01	HF	1808.9	0.39E-03	MG
1229.5	0.22E-03	SN	1810.1	0.14E-03	CE
1245.9	0.27E-03	BA	1830.3	0.19E-01	CO
1261.2	0.50E-04	C	1835.9	0.76E-02	SR
1273.2	0.42E-03	SI	1883.5	0.78E-03	ZN
1293.3	0.41E-03	SN	1887.9	0.13E-02	N
1300.9	0.79E-02	CS	1887.9	0.25E-03	I
1332.2	0.39E-04	SI	1889.5	0.17E-03	F
1358.5	0.42E-03	S	1890.0	0.25E-03	P
1364.2	0.10E 01	CD	1890.2	0.60E-01	EU
1376.7	0.41E-02	CS	1890.5	0.68E-03	S
1381.4	0.50E-01	TI	1891.4	0.85E-04	LI
1388.3	0.14E-03	CA	1898.5	0.14E-02	CR
1402.0	0.32E-03	SB	1918.9	0.92E-03	TE
1404.7	0.11E-03	ZR	1942.5	0.34E-02	CA
1413.1	0.57E-03	P	1929.3	0.82E-03	K
1435.5	0.51E-03	BA	1951.3	0.12E 00	CL
1436.8	0.13E-03	CE	1957.5	0.85E-01	CL
1437.0	0.12E-02	TE	1978.7	0.49E-03	PT
1442.6	0.18E-02	TB	1979.7	0.41E-04	NB
1454.3	0.10E-03	CE	1987.6	0.34E-02	MN
1465.9	0.78E-03	AS	2002.1	0.85E-01	HG
1487.1	0.12E-02	TE	2004.4	0.10E-02	RE
1491.3	0.49E-03	PT	2013.0	0.28E-03	GE

TABLE AIV(3) (CONTINUED)

ENERGY (KEV)	INTENSITY (P/G-N/CM2)	ELEMENT	ENERGY (KEV)	INTENSITY (P/G-N/CM2)	ELEMENT
2027.2	0.28E-02	NA	2330.9	0.46E-02	MN
2032.5	0.84E-03	LI	2332.0	0.40E-01	SM
2039.1	0.42E-03	TE	2337.4	0.26E-02	IN
2041.5	0.29E-04	CE	2341.6	0.38E-02	ER
2048.0	0.36E-01	EU	2371.5	0.25E-02	ND
2048.6	0.17E-02	AG	2379.7	0.31E-02	S
2056.2	0.16E-02	LU	2386.0	0.27E-03	TE
2064.9	0.23E-02	HF	2391.5	0.38E-03	SR
2067.4	0.30E-01	DY	2400.9	0.17E-03	MO
2067.8	0.37E-03	PT	2412.0	0.22E-01	EU
2072.7	0.30E-04	B	2425.9	0.13E-03	SI
2073.2	0.33E-02	K	2452.8	0.35E-04	F
2074.2	0.12E-03	SB	2454.2	0.65E-02	IR
2074.2	0.14E-02	CS	2455.8	0.88E 00	CD
2091.2	0.19E-02	LU	2457.5	0.46E-03	PD
2092.9	0.92E-03	SI	2458.8	0.48E-04	OS
2093.5	0.36E-01	EU	2468.5	0.29E-02	HF
2107.0	0.37E 00	GD	2469.6	0.41E-03	PT
2111.4	0.65E-02	SC	2484.3	0.47E-03	PD
2112.7	0.49E-04	SN	2517.6	0.24E-02	NA
2114.3	0.28E-03	P	2528.1	0.29E-04	F
2115.2	0.90E-03	TM	2530.4	0.13E-03	RU
2117.4	0.58E-04	LI	2532.3	0.20E-04	B
2118.3	0.83E-03	HO	2545.9	0.12E-02	K
2119.8	0.94E-01	SM	2546.6	0.20E-03	Y
2120.2	0.35E-03	TB	2550.1	0.31E 00	CD
2129.8	0.16E-03	CA	2585.0	0.14E-02	YB
2130.0	0.23E-04	RB	2589.9	0.93E-03	HO
2149.7	0.24E-04	RB	2589.9	0.15E-03	BE
2154.2	0.62E-03	P	2600.1	0.39E 00	GD
2159.7	0.29E-02	ER	2601.9	0.31E-04	F
2161.0	0.65E-01	SM	2610.5	0.60E-03	TE
2176.8	0.59E-04	RB	2635.6	0.98E-02	SC
2179.0	0.37E-04	SN	2639.4	0.11E-03	BA
2184.0	0.21E-03	LI	2639.9	0.48E-01	HG
2186.0	0.12E-03	BA	2651.7	0.18E-04	SN
2190.9	0.25E-04	ZR	2659.8	0.60E 00	CD
2196.9	0.50E-03	PD	2664.5	0.21E-03	MO
2223.3	0.20E 00	H	2668.7	0.38E-02	ER
2238.9	0.27E-02	CR	2678.7	0.46E 00	GD
2261.3	0.12E-03	OS	2682.8	0.27E-04	F
2272.3	0.37E-04	CE	2694.0	0.30E-04	ZR
2276.8	0.27E-03	SR	2697.5	0.45E-01	EU
2291.2	0.11E-02	K	2703.4	0.81E-01	DY
2298.3	0.82E-04	RU	2733.6	0.41E-01	DY
2311.4	0.51E-03	PT	2747.2	0.10E-02	TE
2314.4	0.39E 00	GD	2749.5	0.25E-03	Y
2321.0	0.19E-02	CR	2753.2	0.40E-03	S

TABLE AIV(3) (CONTINUED)

ENERGY (KEV)	INTENSITY (P/G-N/CM2)	ELEMENT	ENERGY (KEV)	INTENSITY (P/G-N/CM2)	ELEMENT
-----	-----	-----	-----	-----	-----
2754.4 D	0.14E-01	NA	3522.8	0.53E-03	P
2765.3	0.44E-03	LA	3530.5	0.44E-03	N
2767.3	0.28E 00	CD	3539.3	0.27E-02	SI
2811.0	0.15E-03	CA	3544.0	0.27E-03	TE
2828.1	0.56E-03	MG	3546.6	0.14E-02	K
2839.8	0.30E-03	PR	3585.2	0.14E-04	LI
2858.2	0.14E-03	ZN	3588.0	0.24E-02	NA
2859.7	0.31E-01	EU	3589.3	0.38E-04	F
2862.7	0.16E-02	NA	3591.7	0.15E-03	AL
2864.4	0.38E-01	CL	3608.6	0.55E-03	LA
2931.1	0.15E-02	S	3610.2	0.30E-03	CA
2933.2	0.15E-04	ZR	3619.8	0.42E-04	CE
2948.5	0.44E-01	DY	3632.8	0.19E-02	YB
2960.4	0.32E-03	AL	3641.7	0.30E-03	BA
3000.0	0.31E 00	CD	3652.0	0.55E-03	PR
3009.5	0.45E-03	SR	3661.3	0.16E-03	SI
3018.4	0.44E-04	CE	3683.9	0.54E-04	C
3026.8	0.26E-02	TI	3830.7	0.88E-04	MG
3034.4	0.30E-03	AL	3852.1	0.15E-02	LU
3054.1	0.17E-03	MG	3876.6	0.21E-02	IN
3058.3	0.24E-03	P	3884.9	0.31E-02	YB
3062.2	0.21E-01	CL	3900.3	0.65E-03	P
3074.4	0.32E-04	F	3916.7	0.64E-03	MG
3082.6	0.50E-03	LA	3920.4	0.13E-02	TI
3087.5	0.15E-02	YB	3929.6	0.15E-02	YB
3090.6	0.34E-04	CE	3982.0	0.30E-02	NA
3098.1	0.13E-02	NA	4029.2	0.62E-02	CO
3130.9	0.55E-03	GA	4054.7	0.26E-04	BI
3153.2	0.67E-03	RE	4096.3	0.87E-03	BA
3163.4	0.11E-03	Y	4101.8	0.17E-04	BI
3220.8	0.19E-02	S	4103.3	0.11E-03	I
3301.1	0.12E-03	MG	4107.5	0.44E-03	Y
3301.4	0.12E-03	Y	4109.4	0.24E-02	ER
3308.0	0.91E-05	B	4133.7	0.22E-03	AL
3334.3	0.32E-04	SN	4137.9	0.18E-03	ZN
3368.2	0.22E-03	BE	4171.1	0.36E-04	BI
3370.4	0.36E-03	S	4189.0	0.13E-02	AU
3408.5	0.49E-02	MN	4218.8	0.11E-02	FE
3413.6	0.85E-04	MG	4220.6	0.34E-03	TA
3444.4	0.75E-04	BE	4227.5	0.26E-02	IN
3444.7	0.43E-01	DY	4249.2	0.84E-03	W
3459.2	0.18E-04	SN	4259.9	0.21E-03	AL
3465.5	0.22E-03	AL	4291.2	0.29E-03	CE
3470.7	0.59E-03	W	4315.5	0.30E-03	TA
3474.7	0.15E-04	ZR	4320.8	0.52E-03	CU
3475.5	0.18E-02	TI	4336.8	0.13E-03	CE
3492.7	0.17E-04	LI	4343.5	0.31E-02	HF
3505.0	0.11E-04	B	4351.3	0.96E-04	RU

TABLE AIV(3) (CONTINUED)

ENERGY (KEV)	INTENSITY (P/G-N/CM2)	ELEMENT -----*	ENERGY (KEV)	INTENSITY (P/G-N/CM2)	ELEMENT -----
4352.4	0.14E-03	Y	4921.4	0.29E-02	ER
4389.4	0.97E-03	LA	4934.3	0.24E-02	SI
4416.3	0.94E-03	LA	4943.5	0.91E-02	IR
4418.9	0.70E-03	CA	4945.2	0.11E-03	C
4443.0	0.15E-04	B	4949.0	0.18E-02	ND
4483.0	0.20E-03	TA	4950.2	0.44E-03	I
4484.3	0.40E-01	SM	4966.6	0.28E-02	TI
4502.8	0.66E-03	LA	4969.4	0.47E-02	IN
4507.6	0.73E-03	N	4975.1	0.67E-02	SC
4508.3	0.13E-04	LI	4980.0	0.21E-01	CL
4510.3	0.40E-02	RH	5007.9	0.89E-03	RE
4530.3	0.20E-04	ZR	5014.7	0.81E-02	MN
4530.7	0.48E-04	OS	5020.3	0.19E-02	CS
4565.7	0.12E-02	SE	5020.4	0.17E-02	LU
4617.7	0.19E-03	TA	5022.8	0.17E-03	RU
4627.4	0.11E-03	RU	5050.2	0.60E-01	HG
4671.3	0.56E-03	P	5074.3	0.13E-02	RE
4684.7	0.79E-03	W	5082.8	0.69E-03	HO
4692.2	0.11E-02	PR	5093.7	0.33E-03	I
4710.2	0.68E-05	B	5095.9	0.73E-03	PR
4720.2	0.17E-02	AG	5097.6	0.27E-02	LA
4723.8	0.11E-03	BA	5099.6	0.47E-03	IB
4733.2	0.17E-02	TM	5103.4	0.45E-02	IN
4734.1	0.18E-03	AL	5104.2	0.84E-04	NB
4739.5	0.76E-01	HG	5107.3	0.13E-03	SI
4739.7	0.44E-04	NB	5137.2	0.11E-02	RE
4749.7	0.13E-03	CA	5140.2	0.13E-02	PR
4752.8	0.19E-03	TL	5141.1	0.42E-02	IN
4766.1	0.50E-03	CE	5142.2	0.29E-02	V
4774.9	0.47E-02	IN	5143.8	0.47E-01	DY
4781.8	0.21E-03	TA	5146.9	0.17E-03	OS
4783.0	0.30E-03	AS	5148.2	0.40E-02	AU
4790.9	0.17E-02	ND	5152.2	0.17E-02	TM
4794.6	0.49E-03	PD	5164.3	0.12E-02	W
4801.4	0.57E-03	PR	5173.4	0.52E-03	PT
4809.1	0.91E-01	SM	5180.8	0.18E-03	TL
4810.0	0.12E 00	CD	5181.7	0.84E-02	CO
4810.3	0.47E-03	FE	5181.9	0.83E-03	HO
4812.8	0.68E-04	OS	5195.0	0.85E-03	GA
4829.6	0.11E-02	YB	5197.8	0.57E-03	I
4840.5	0.83E-03	GA	5209.9	0.33E-02	V
4842.5	0.58E-01	HG	5211.6	0.34E-02	ER
4842.7	0.28E-02	LA	5212.7	0.71E-03	HO
4860.2	0.85E-02	IR	5212.9	0.22E-03	PD
4861.0	0.97E-03	RE	5240.2	0.24E-02	AG
4869.8	0.79E-03	S	5252.6	0.12E-02	CS
4881.3	0.43E-02	TI	5253.6	0.43E-04	NB
4914.2	0.20E-03	TL	5254.6	0.14E-02	PT

TABLE AIV(3) (CONTINUED)

ENERGY (KEV)	INTENSITY (P/G-N/CM2)	ELEMENT	ENERGY (KEV)	INTENSITY (P/G-N/CM2)	ELEMENT
5261.7	0.26E-02	W	5601.7	0.18E-02	LU
5263.7	0.32E-04	ZR	5601.7	0.20E-02	SE
5265.7	0.66E-02	YB	5602.4	0.13E-03	MO
5266.2	0.93E-02	RH	5603.6	0.32E-03	TL
5267.1	0.12E-02	N	5607.3	0.96E-01	DY
5274.0	0.11E-03	OS	5611.4	0.31E-03	PT
5277.7	0.64E-03	RE	5618.8	0.12E-02	CR
5280.5	0.24E-03	TL	5637.4	0.84E-03	CS
5296.7	0.86E-03	N	5641.9	0.37E-03	TL
5307.0	0.34E-03	PT	5645.4	0.14E-03	Y
5320.4	0.12E-02	LU	5658.1	0.74E-01	HG
5320.5	0.18E-02	W	5660.3	0.24E-01	CO
5339.1	0.17E-02	GA	5665.7	0.13E-02	PR
5342.9	0.17E-03	TA	5667.2	0.18E-01	IR
5347.2	0.12E-01	RH	5668.1	0.22E-03	TE
5377.2	0.12E-02	CS	5684.0	0.77E-04	OS
5379.7	0.22E-01	EU	5684.3	0.90E-04	SB
5380.3	0.24E-02	K	5694.4	0.23E-02	HF
5380.9	0.18E-02	ND	5695.6	0.15E-02	K
5392.5	0.14E-04	SN	5699.7	0.55E-02	AG
5416.5	0.21E-03	AS	5710.4	0.40E-02	AU
5417.7	0.74E-03	CU	5713.1	0.22E-03	MO
5418.4	0.21E-02	HF	5715.2	0.26E-01	CL
5420.5	0.41E-02	S	5723.5	0.80E-02	HF
5431.4	0.21E 00	CD	5730.7	0.31E-03	BA
5448.2	0.26E-02	ND	5737.2	0.43E-02	TM
5450.2	0.29E-03	GE	5751.9	0.52E-02	V
5451.8	0.43E-04	MG	5752.0	0.14E-02	K
5474.2	0.38E-03	ZN	5760.6	0.31E-04	RB
5496.9	0.60E-04	NB	5763.1	0.85E-03	HO
5505.4	0.95E-03	CS	5777.2	0.68E-03	TB
5505.6	0.31E-02	HF	5782.6	0.12E-01	IR
5507.7	0.19E-03	BR	5784.7	0.20E-03	AS
5515.5	0.57E-02	V	5793.1	0.37E-02	AG
5518.3	0.31E-03	GE	5813.4	0.17E-02	HO
5521.2	0.22E-02	ND	5816.8	0.11E-02	NI
5527.2	0.10E-01	MN	5823.9	0.45E 00	CD
5532.0	0.82E-03	N	5828.4	0.37E-03	PD
5532.8	0.11E 00	SM	5842.9	0.47E-03	PR
5556.9	0.77E-01	DY	5886.2	0.16E-03	SB
5559.6	0.31E-03	I	5891.5	0.92E-03	TB
5562.9	0.18E-03	SB	5891.9	0.63E-02	IN
5564.6	0.12E-01	IR	5895.3	0.63E-04	NB
5569.6	0.17E-02	LU	5900.6	0.20E-03	CA
5570.6	0.15E-02	CS	5902.9	0.70E 00	GD
5577.9	0.20E-02	AG	5910.2	0.18E-02	RE
5582.6	0.36E 00	GD	5914.2	0.36E-03	BR
5601.5	0.12E-02	GA	5917.2	0.13E-01	RH

TABLE AIV(3) (CONTINUED)

ENERGY (KEV)	INTENSITY (P/G-N/CM2)	ELEMENT	ENERGY (KEV)	INTENSITY (P/G-N/CM2)	ELEMENT
-----	-----	-----	-----	-----	-----
5918.3	0.24E-01	EU	6267.3	0.46E-03	SR
5920.5	0.23E-02	FE	6268.0	0.14E-04	SN
5942.7	0.42E-02	TM	6273.7	0.12E-03	RU
5953.7	0.38E-03	TB	6294.5	0.65E-03	AS
5957.7	0.20E-01	IR	6295.0	0.19E-03	ZR
5958.1	0.13E-03	BE	6307.4	0.30E-03	I
5964.7	0.45E-03	TA	6319.1	0.11E-01	AU
5966.9	0.17E 00	HG	6321.4	0.77E-03	N
5982.8	0.42E-02	AU	6323.0	0.70E-03	TE
5994.7	0.45E-03	TB	6342.1	0.13E-03	RU
6001.6	0.24E-02	TM	6354.7	0.26E-03	BR
6008.0	0.27E-02	SE	6360.0	0.31E-02	GA
6008.0	0.15E-02	GA	6364.6	0.13E-03	MO
6017.1	0.33E-04	F	6380.1	0.14E-03	SB
6017.3	0.13E-04	LI	6380.1	0.43E-03	SI
6018.5	0.23E-02	FE	6387.4	0.36E-02	TM
6027.9	0.46E-04	BA	6395.4	0.36E-02	NA
6033.5	0.33E-03	PT	6418.0	0.28E-01	TI
6036.7	0.38E-03	GE	6419.3	0.33E 00	GD
6046.4	0.70E-02	RH	6419.9	0.18E-02	CA
6051.9	0.11E-02	CS	6456.8	0.68E-02	AU
6052.1	0.59E-03	HO	6457.8	0.67E-01	HG
6054.9	0.73E-02	SC	6464.8	0.56E-02	V
6056.1	0.41E-02	AG	6468.1	0.12E-03	SB
6058.3	0.22E-03	AS	6470.7	0.26E-04	RB
6062.5	0.27E-03	TA	6502.1	0.12E-01	ND
6080.3	0.64E-02	Y	6512.1	0.50E-02	AU
6081.8	0.18E-01	IR	6515.2	0.16E-03	TL
6082.8	0.59E-02	RH	6517.2	0.11E-01	V
6101.9	0.29E-03	SR	6520.2	0.29E-04	RB
6105.0	0.98E-03	NI	6523.6	0.32E-03	SB
6111.1	0.89E-01	CL	6537.9	0.47E-01	SM
6111.4	0.12E-02	GA	6552.9	0.25E-02	TM
6112.3	0.26E-02	HF	6555.6	0.49E-02	TI
6116.3	0.41E-03	GE	6587.2	0.44E-04	OS
6138.8	0.47E-03	TB	6599.5	0.81E-03	CU
6144.3	0.96E-03	W	6600.7	0.28E-04	F
6166.9	0.20E-03	TL	6601.2	0.40E-02	SE
6171.8	0.61E-02	RH	6620.1	0.56E-01	CL
6190.5	0.27E-02	W	6625.1	0.12E-03	MO
6211.1	0.21E-03	TE	6645.5	0.19E-02	CR
6211.4	0.63E-02	RH	6652.5	0.16E-03	PD
6218.2	0.70E-03	TB	6660.6	0.46E-03	SR
6228.5	0.19E-01	EU	6676.8	0.31E-02	ER
6229.0	0.53E-02	ER	6678.0	0.14E-02	CU
6232.7	0.14E-02	SE	6693.0	0.28E-03	I
6252.0	0.16E-01	AU	6706.0	0.28E-01	CO
6255.9	0.54E-02	ND	6707.9	0.40E-03	JE

TABLE AIV(3) (CONTINUED)

ENERGY (KEV)	INTENSITY (P/G-N/CM2)	ELEMENT	ENERGY (KEV)	INTENSITY (P/G-N/CM2)	ELEMENT
-----	-----	-----	-----	-----	-----
6728.0	0.22E-03	SB	7268.9	0.20E-02	AG
6736.4	0.25E-04	PB	7278.9	0.13E-02	FE
6745.5	0.23E-03	BR	7299.5	0.38E-03	N
6749.8	0.20E 01	GD	7306.2	0.27E-02	CU
6759.3	0.80E-05	B	7367.7	0.48E-03	PB
6759.7	0.41E-01	TI	7413.8	0.48E-01	CL
6780.1	0.49E-03	YB	7418.7	0.24E-02	SE
6783.7	0.50E-02	MN	7420.7	0.33E-03	BR
6785.3	0.53E-03	P	7421.2	0.22E-03	P
6803.8	0.16E-02	LU	7491.1	0.11E-01	CO
6809.9	0.10E-02	AS	7527.1	0.13E-03	MO
6810.0	0.40E-03	BE	7527.7	0.39E-03	SR
6830.7	0.75E-04	NB	7536.1	0.23E-02	NI
6831.4	0.31E-04	RB	7575.8	0.58E-03	BR
6837.0	0.56E-02	NI	7624.1	0.99E-04	RB
6839.5	0.15E-01	SC	7631.6	0.77E-02	FE
6867.6	0.20E-03	ZN	7635.9	0.83E-02	SC
6873.9	0.67E-02	V	7636.6	0.53E-02	CU
6876.9	0.30E-01	CO	7645.6	0.63E-02	FE
6915.5	0.32E-03	GE	7723.8	0.11E-02	AL
6919.3	0.58E-03	MO	7769.0	0.15E-02	K
6926.1	0.38E-03	AS	7790.0	0.37E-01	CL
6941.9	0.28E-03	SR	7800.0	0.27E-03	S
6958.5	0.32E-03	ZN	7818.9	0.43E-02	NI
6985.1	0.11E-01	CO	7862.9	0.12E-02	ZN
7005.1	0.97E-05	B	7914.5	0.10E-01	CU
7019.5	0.87E-03	AS	7939.3	0.41E-02	CR
7030.1	0.25E-03	BR	8120.5	0.16E-02	NI
7057.9	0.16E-01	MN	8154.4	0.62E-04	MG
7069.2	0.16E-03	ZN	8174.7	0.29E-01	SC
7076.3	0.27E-03	BR	8331.0	0.72E-04	PD
7102.9	0.82E-04	RU	8512.3	0.20E-02	CR
7112.0	0.16E-03	ZN	8531.6	0.15E-01	SC
7159.9	0.88E-02	MN	8533.4	0.88E-02	NI
7162.7	0.82E-02	V	8634.2	0.92E-05	ZR
7179.7	0.15E-02	SE	8884.1	0.87E-02	CR
7186.1	0.34E-04	NB	8998.8	0.20E-01	NI
7199.3	0.25E-03	SI	9108.8	0.21E-04	BA
7213.0	0.17E 00	SM	9298.4	0.11E-02	FE
7214.1	0.18E-01	CO	9326.1	0.11E-04	SN
7243.5	0.17E-01	MN	9720.3	0.35E-02	CR
7246.7	0.37E-04	LI	9882.9	0.13E-02	SE
7251.9	0.12E-02	CU	10827.7	0.48E-03	N
7259.8	0.26E-03	GE			

Appendix V
COMPUTER CODES

In this Appendix are presented the listings of the various computer codes that have been used extensively in the present thesis. It is believed that the information included in the codes is sufficient to enable interested readers to follow the various computational operations without difficulty. The programs are written in FORTRAN IV language for the MIT 360/65 computer.

The codes and their functions are as follows:

(1) ARTSPEC

This code computes normally distributed random numbers with a given mean and given standard deviation on which may be superimposed Gaussian peaks of specified height, width and channel number. It smooths the data by the method of Fourier transforms and any number of filter functions. It calculates means and standard deviation over a specified range of channels. Both smoothing and statistical analysis may be applied to data supplied externally. The program calls Subroutines GAUSS and FOURT.

(2) Subroutine GAUSS

This subroutine computes a normally distributed random number with a given mean and standard deviation. It was supplied by the MIT computational center. It calls Subroutine RANDU (also supplied by MIT) and uses 12 random numbers to compute normal random numbers by the central limit theorem.

The result is then adjusted to match the given mean and standard deviation.

(3) Subroutine RANDU

Subroutine RANDU computes normally distributed random real numbers between 0 and 1.0 and random integers between zero and 2^{31} . Each entry uses as input an integer random number and produces a new integer and real random number. This subroutine uses the power residue method discussed in the IBM manual C20-8011, Random Number Generation and Testing, and will produce 2^{29} terms before repeating. It was supplied by the MIT computational center and is specific to the MIT 360/65 computer.

(4) POLYFIT

This code has been written to perform the least-squares fit described in Appendix AII. It is capable of fitting the width-energy data to a p-order polynomial. p can be any number but computational accuracy limits its value to a maximum of 5 or 6. It calls subroutine MINV for the evaluation of the inverse matrix coefficients and the value of the determinant.

(5) Subroutine MINV

This subroutine was supplied(also)by the MIT computational center. It inverts a matrix by the standard Gauss-Jordan method. The determinant is also calculated.

(6) WTANAL

The code WTANAL, for weight analysis, analyses the constituents of a given spectrum for a number of elements supplied as input by operating on data obtained with the GAMANL code. Use is made of the energies and intensities of all the gamma rays of the elements that are believed to be present in the sample. The program, working on each element separately, selects from the list those gamma rays whose energies are within specified limits and whose intensities are larger than a given value. The energies of the selected gamma rays are then compared to those in the spectrum for possible correspondence. Whenever an element which could have produced an observed gamma peak in the spectrum is found, the weight of the element is calculated. If through such a procedure the origin of a gamma ray is assigned to more than one element the symbols of the interfering elements are listed. In its present form the program does not resolve interfering effects.

(7) MINIMUM

The code has been written for the evaluation of the peak area limiting levels in a given spectrum and the minimum weight requirements for a number of elements supplied as input. Use is made of the energies and intensities of the elements examined. The experimental conditions under which the spectrum in question was obtained must also be supplied. The program calls subroutine BAKSUB for evaluation of the background continuum.

(8) Subroutine BAKSUB

This subroutine, which is also used by GAMANL with a slight modification in the COMMON card, performs the subtraction of the background continuum from the spectral information. Its method of operation was described in Sec. 3.3.

The GAMANL code, which was used in this thesis more extensively than any other of the codes listed above, may be found in Reference [H1]. The same report also includes the subroutine FOURT for the fast-Fourier transforms employed in smoothing the data. FOURT is also called by ARTSPEC.

In the pages that follow are presented the listings of these codes in the order they were discussed.


```

C      COMPUTER PROGRAM 'ARTSPEC'
C      COMPUTES NORMALLY DISTRIBUTED RANDOM NUMBERS WITH A GIVEN MEAN
C      AND GIVEN STANDARD DEVIATION ON WHICH MAY BE SUPERIMPOSED GAUSSIAN
C      PEAKS OF SPECIFIED HEIGHT, WIDTH, AND CHANNEL NUMBER. SMOOTHS
C      THE DATA BY THE METHOD OF FAST FOURIER TRANSFORMS AND ANY NUMBER
C      OF FILTER FUNCTIONS. CALCULATES MEANS AND STANDARD DEVIATIONS
C      OVER A SPECIFIED RANGE OF CHANNELS. BOTH SMOOTHING AND
C      STATISTICAL ANALYSIS MAY BE APPLIED TO DATA SUPPLIED EXTERNALLY.
C      PROGRAM CALLS SUBROUTINE 'FOURT' FOR THE FAST-FOURIER TRANSFORM
C
C      DIMENSION TBK(5000),TBL(5000),WT(5000),CHAN(500),HT(500),
1 SGMA(500), GRUP(500), IGRUP(500)
C      COMPLEX DATA(5000), DATA2(5000)
C
C      4 CONTINUE
C      READ(5,5) IX,NUMRUN,N,IPEAK,ISAME,AMB,S
C      5 FORMAT(3X,I7,4I5,2F10.0)
C      IX MUST CONTAIN AN ODD INTEGER NUMBER WITH NINE OR LESS DIGITS
C      ON THE FIRST ENTRY TO GAUSS.
C      NUMRUN IS THE REFERENCE NUMBER
C      N IS THE NUMBER OF RANDOM DATA POINTS TO BE GENERATED, AMB IS
C      THEIR MEAN AND S THEIR STANDARD DEVIATION
C      N+1 MUST BE EVEN AND A POWER OF 2 FOR FASTEST RESULTS.
C      IPEAK LESS THAN ZERO = DATA MUST BE SUPPLIED
C      IPEAK =0 IMPLIES PROGRAM PRODUCES RANDOM DATA WITHOUT PEAKS.
C      IPEAK GREATER THAN ZERO, PROGRAM PRODUCES RANDOM DATA ON WHICH ARE
C      SUPERIMPOSED IPEAK NUMBER OF PEAKS.
C      IX1 = IX
C      IF(IPEAK) 30,26,6
C
C
C      6 CONTINUE
C      PROGRAM SUPERIMPOSES IPEAK PEAKS ON BACKGROUND DATA OF SPECIFIED
C      MEAN, EACH PEAK HAVING ITS PARAMETERS READ IN AS INPUT DATA.

```

```

C   USE ISAME=1 TO SUPERIMPOSE ON THE BACKGROUND IPEAK PEAKS ALL OF
C   SAME HEIGHT AND SAME WIDTH AND A FIXED NUMBER OF CHANNELS APART.
    IF(ISAME) 7,7,9
  7  CONTINUE
    READ(5,8) (CHAN(I), HT(I), SGMA(I), I = 1,IPEAK)
  8  FORMAT(3F10.2)
    GO TO 12
  9  READ(5,10) CHAN1, HT1,SGMA1, DCHAN
 10  FORMAT(4F10.2)
    DO 11 J =1,IPEAK
      HT(J) = HT1
      SGMA(J) = SGMA1
      CHAN(J) = CHAN1 + FLOAT(J)*DCHAN
 11  CONTINUE
C
 12  DO 17 J =1,N
      GH = 0.0
      DO 16 K = 1,IPEAK
        CB = CHAN(K)
        CA = FLOAT(J)
        EX = (CA-CB)*(CA-CB)/(2.0*SGMA(K)*SGMA(K))
        IF(EX - 15.0) 13,13,16
 13  GH = GH + HT(K)*EXP(-EX)
 16  CONTINUE
      AM = AMB + GH
      S = SQRT(AM)
      CALL GAUSS(IX,S,AM,V)
 17  TBK(J) = V
C
    WRITE(6,18) NUMRUN,IX1
 18  FORMAT(1H1,35X, 'RANDOM DATA PRODUCED',I7, ',IX = ',I8)
    WRITE(6,19) IPEAK
 19  FORMAT(1HC,15X, 'NUMBER OF PEAKS SUPERIMPOSED', I5)
    WRITE(6,21) (I,CHAN(I),HT(I),SGMA(I),I=1,IPEAK)

```

```

21 FORMAT(1H0,15X,'NO.',I5,10X,'CHANNEL NO.',F10.1,10X,'HEIGHT',
1 F10.1,10X,'S.D.',F10.2)
WRITE(6,22)
22 FORMAT(1H0)
GO TO 33

C
C
26 CONTINUE
C PROGRAM PRODUCES N RANDOM DATA POINTS OF SPECIFIED MEAN AND S.D.
C IF S IS LESS OR EQUAL TO 0 IT IS SET EQUAL TO SQRT(AM)
IF(S) 27,27,28
27 S = SQRT(AMB)
28 CONTINUE
C GENERATION OF THE RANDOM NUMBERS
AM = AMB
DO 29 J = 1,N
CALL GAUSS(IX,S,AM,V)
29 TBK(J) = V
WRITE(6,18) NUMRUN,IX1
GO TO 33

C
C
C STATISTICAL ANALYSIS AND SMOOTHING MAY BE APPLIED TO DATA SUPPLIED
30 READ(5,31) (TBK(J), J=1,N)
31 FORMAT (7X,7(F6.0,1X))/(8(F6.0,1X)))
WRITE(6,32)NUMRUN
32 FORMAT(1H1,35X, 'RANDOM DATA FED IN', I7)

C
C
33 CONTINUE
C STORE ORIGINAL DATA FOR MULTIPLE SMOOTHING PROCESSES.
DO 34 J = 1,N
34 TBL(J) = TBK(J)
C USE MRPT TO CHECK IF ORIGINAL DATA HAS ALREADY BEEN TRANSFORMED.

```

```

MRPT = 0
35 CONTINUE
C PRINTOUT OF ORIGINAL AND SMOOTHED DATA.
  LK = N/10
  DO 37 J = 1,LK
  JU = J*10
  JL = JU - 9
C JU IS THE CHANNEL NUMBER FOR EVERY TENTH POINT
  WRITE(6,36) (TBK(I),I=JL,JU),JU
36 FORMAT(2X,10(F9.2,2X),I6)
37 CONTINUE
  JA = JU+1
  WRITE(6,38) (TBK(I), I=JA,N)
38 FORMAT(2X,10(F9.2,2X))
C
C READ(5,39) IPUNCH,IAVRG,MINAV,MAXAV,ISMUTH
39 FORMAT(5I5)
C IPUNCH GREATER THAN ZERO PUNCHES OUT RANDOM AND SMOOTHED DATA.
  IF(IPUNCH) 41,41,40
40 WRITE(7,31) (TBK(I),I=1,N)
C IAVRG GREATER THAN ZERO CALCULATES MEAN AND STANDARD DEVIATION
C BETWEEN CHANNELS MINAV AND MAXAV. GROUPS DATA INTO IAVRG SUBGROUPS
C USE IAVRG = I*9 + 1, I = 1,2,3,... .
41 IF(IAVRG) 60,60,42
C
C
C STATISTICAL ANALYSIS APPLIED TO ORIGINAL AND SMOOTHED DATA.
C COMPUTATION OF THE MEAN AND STANDARD DEVIATION
42 SUMX1 = 0.0
  SUMX2 = 0.0
  NT = MAXAV - MINAV + 1
  DO 44 J = MINAV, MAXAV
44 SUMX1 = SUMX1 + TBK(J)
  AVR = SUMX1/FLOAT(NT)

```

```

DO 45 J = MINAV, MAXAV
45 SUMX2 = SUMX2 + (TBK(J) - AVR)**2
SDPTS = SQRT(SUMX2/FLCAT(NT-1))
C GROUPING OF DATA INTO IAVRG SUBGROUPS.
C PCINTS LYING 4.5 S.D. FROM THE MEAN ARE EXCLUDED.
DO 47 I = 1,IAVRG
S = SQRT(AVR)
DX = 9.0*S/FLOAT(IAVRG-1)
X = AVR + DX*FLOAT(I - (IAVRG+1)/2)
GRUP(I) = X
IGRUP(I) = 0
DO 47 J = MINAV, MAXAV
Y = TBK(J)
IF(ABS(X-Y-0.01) - DX/2.0) 46,47,47
46 IGRUP(I) = IGRUP(I) + 1
47 CONTINUE

C WRITE(6,52)
WRITE(6,53) NT, MINAV, MAXAV
WRITE(6,54) AM
WRITE(6,55) AVR
WRITE(6,56) S
WRITE(6,57) SDPTS
WRITE(6,58)
WRITE(6,59) (GRUP(I), IGRUP(I), I = 1,IAVRG)
52 FORMAT(1H1,35X, 'STATISTICAL ANALYSIS')
53 FORMAT(1H0,10X, 'NUMBER OF DATA POINTS = ', I7, 'BETWEEN CHANNELS ',
1 I7, ' AND ', I7)
54 FORMAT(1H0,10X, 'MEAN (READ IN) = ' F10.2)
55 FORMAT(1H0,10X, 'CALCULATED MEAN = ' F10.2)
56 FORMAT(1H0,10X, 'S.D. READ IN = ' F10.2)
57 FORMAT(1H0,10X, 'CALCULATED S.D. = ' F10.2)
58 FORMAT(1H0,10X, 'DATA GROUPING')
59 FORMAT(25X,F10.2, 5X, I6)

```

```

C
C
60 CONTINUE
C   ISMUTH LESS THAN 0 PROGRAM RETURNS TO THE FIRST READ STATEMENT.
C   IF ISMUTH IS LESS THAN 0 RETURN TO THE FIRST READ STATEMENT
C   IF ISMUTH = 0, CALL EXIT
C   IF ISMUTH = 1 SMOOTH THE DATA
C   IF(ISMUTH) 4,100,61
61 CONTINUE
C   WT ARRAY DATA READ IN.
C   READ(5,62) SIGB, MWTB, WTC1
62 FORMAT(F5.0,I5, F5.0)
C   WTC1 IS THE AMPLITUDE OF THE FILTER FUNCTION BEFORE THE CUTOFF
C   MWTB IS THE CHANNEL NUMBER CORRESPONDING TO THE FILTER CUTOFF.
C   SIGB IS THE STANDARD DEVIATION OF THE GAUSSIAN IN THE CUTOFF.
C
C   FOURIER TRANSFORM OF ORIGINAL DATA AND PRINTOUT.
C   NUM = N + 1
C   TBK(NUM) = 0.0
C   IF(MRPT) 65,65,77
65 CONTINUE
C   DO 68 I = 1,NUM
C   DATA(I) = CMPLX(TBK(I),0.0)
68 CONTINUE
C   FAST FOURIER TRANSFORM ON DATA.
C
C       CALL FOURT (DATA,NUM,1,+1,+1,0)
C
C   DO 70 I = 1,NUM
C   AR = REAL(DATA(I))
C   AI = AIMAG(DATA(I))
C   TBK(I) = SQRT(AR*AR + AI*AI)
C   TBK IS USED TO STORE THE MAGNITUDE OF EACH TRANSFORMED POINT.
70 CONTINUE

```

```

W8= 6.2831873/FLOAT(NUM)
NUM2 = NUM/2 + 2
C PRINT OUT OF TRANSFORMED DATA.
WRITE(6,71) W8
71 FORMAT (1H1,26H DELTA OMEGA IN RADIANS = ,F10.6)
WRITE(6,72)
72 FORMAT (1H ,19H TRANSFORM INTEGRAL)
WRITE(6,73) (TBK(I),I=1,NUM2)
73 FORMAT (1H ,10E11.4)
C
IF(MRPT) 74,74,79
74 CONTINUE
C STORE ORIGINAL TRANSFORMED DATA FOR REFILTERING.
DO 75 I = 1,NUM
75 DATA2(I) = DATA(I)
GO TO 79
77 CONTINUE
C RECALL ORIGINAL TRANSFORMED DATA.
DO 78 I = 1,NUM
78 DATA(I) = DATA2(I)
C
79 CONTINUE
MRPT = 1
C EVALUATION OF THE FILTERING DATA.
NUP = NUM/2
SIGB2 = 2.0*SIGB*SIGB
WT(NUM) = WTC1
DO 80 I = 1, MWTB
J = NUM - I
WT(I) = WTC1
80 WT(J) = WT(I)
DO 82 I = MWTB, NUP
J = NUM - I
EX2 = (I-MWTB)*(I-MWTB)

```

```

      WT(I) = WTC1*EXP(-EX2/SIGB2)
82  WT(J) = WT(I)
C   FILTERING THE TRANSFORMED DATA WITH WT(I).
      DO 84 I = 1,NUM
84  DATA(I) = DATA(I)*WT(I)
C
C   INVERSE FOURIER TRANSFORM
      CALL FOURT(DATA,NUM,1,-1,+1,0)
C
      DO 85 I = 1,NUM
      AR = REAL(DATA(I))
      AI = AIMAG(DATA(I))
      TBK(I) = SQRT(AR*AR + AI*AI)/FLOAT(NUM)
C   DIVIDING BY NUM IS TO CORRECTLY NORMALIZE THE OUTPUT DATA.
85  CONTINUE
C
      IF(ISMUTH - 1) 94,94,86
94  WRITE(6,95) NUMRUN
95  FORMAT(1H1,10X,'SMOOTHED DATA OF RUN NO ', I5)
      WRITE(6,96) SIGB,MWTB,WTC1
96  FORMAT(1H0,'SIGB =',F6.1,' MWTB =',I5,' WTC1 =',F5.2)
C
      GO TO 35
100 CALL EXIT
      END

```


C	<u>SUBROUTINE GAUSS(IX,S,AM,V)</u>	GAUS 390
C	PURPOSE	GAUS 50
C	COMPUTES A NORMALLY DISTRIBUTED RANDOM NUMBER WITH A GIVEN	GAUS 60
C	MEAN AND STANDARD DEVIATION	GAUS 70
C		GAUS 80
C	USAGE	GAUS 90
C	CALL GAUSS(IX,S,AM,V)	GAUS 100
C		GAUS 110
C	DESCRIPTION OF PARAMETERS	GAUS 120
C	IX -IX MUST CONTAIN AN ODD INTEGER NUMBER WITH NINE OR	GAUS 130
C	LESS DIGITS ON THE FIRST ENTRY TO GAUSS. THEREAFTER	GAUS 140
C	IT WILL CONTAIN A UNIFCRMLY DISTRIBUTED INTEGER RANDOM	GAUS 150
C	NUMBER GENERATED BY THE SUBROUTINE FOR USE ON THE NEXT	GAUS 160
C	ENTRY TO THE SUBROUTINE.	GAUS 170
C	S -THE DESIRED STANDARD DEVIATION OF THE NORMAL	GAUS 180
C	DISTRIBUTION.	GAUS 190
C	AM -THE DESIRED MEAN OF THE NCRMAL DISTRIBUTION	GAUS 200
C	V -THE VALUE OF THE COMPUTED NORMAL RANDOM VARIABLE	GAUS 210
C		GAUS 220
C	REMARKS	GAUS 230
C	THIS SUBROUTINE USES RANDU WHICH IS MACHINE SPECIFIC	GAUS 240
C		GAUS 250
C	SUBROUTINES AND FUNCTION SUBPROGRAMS REQUIRED	GAUS 260
C	RANDU	GAUS 270
C		GAUS 280
C	METHCD	GAUS 290
C	USES 12 UNIFCRM RANDCM NUMBERS TO COMPUTE NORMAL RANDOM	GAUS 300
C	NUMBERS BY CENTRAL LIMIT THEOREM. THE RESULT IS THEN	GAUS 310
C	ADJUSTED TO MATCH THE GIVEN MEAN AND STANDARD DEVIATION.	GAUS 320
C	THE UNIFORM RANDOM NUMBERS COMPUTED WITHIN THE SUBROUTINE	GAUS 330
C	ARE FCUND BY THE POWER RESIDUE METHOD.	GAUS 340
C		GAUS 350
C		GAUS 360
C	GAUS 370

C

```
A=0.0  
DO 50 I=1,12  
CALL RANDU(IX,IY,Y)  
IX=IY  
50 A=A+Y  
V=(A-6.0)*S+AM  
RETURN  
END
```

```
GAUS 380  
GAUS 400  
GAUS 410  
GAUS 420  
GAUS 430  
GAUS 440  
GAUS 450  
GAUS 460
```


C	GIVEN IN THE REFERENCE BELOW. ALSO, IT SHOULD BE NOTED THAT	RAND 380
C	IF FLOATING POINT RANDOM NUMBERS ARE DESIRED, AS ARE	RAND 390
C	AVAILABLE FROM RANDU, THE RANDOM CHARACTERISTICS OF THE	RAND 400
C	FLOATING POINT DEVIATES ARE MODIFIED AND IN FACT THESE	RAND 410
C	DEVIATES HAVE HIGH PROBABILITY OF HAVING A TRAILING LOW	RAND 420
C	ORDER ZERO BIT IN THEIR FRACTIONAL PART.	RAND 430
C		RAND 440
C	SUBROUTINES AND FUNCTION SUBPROGRAMS REQUIRED	RAND 450
C	NONE	RAND 460
C		RAND 470
C	METHOD	RAND 480
C	POWER RESIDUE METHOD DISCUSSED IN IBM MANUAL C20-8011,	RAND 490
C	RANDOM NUMBER GENERATION AND TESTING	RAND 500
C		RAND 510
C	RAND 520
C		RAND 530
	IY=IX*65539	RAND 550
	IF(IY)5,6,6	RAND 560
5	IY=IY+2147483647+1	RAND 570
6	YFL=IY	RAND 580
	YFL=YFL*.4656613E-9	RAND 590
	RETURN	RAND 600
	END	RAND 610

```

C   COMPUTER CODE 'POLYFIT'
C   LEAST-SQUARES FITTING THE WIDTH-ENERGY EQUATION
C
      DIMENSION E(100),W(100),WT(100),HT(100),SDWID(100)
      DIMENSION WEO(50),EO(50),CF(50),MACA(50),LACA(50),
1    AO(50), FA(50), WIDCL(100), WIDER(100), WIDDF(100),WIDRS(100)
95  CCNTINUE
      READ(5,100) N, NACA
100  FORMAT(2I5)
      READ(5,105) (E(I),W(I),SDWID(I),WT(I),HT(I),I=1,N)
105  FORMAT((10X,F10.2,3(2X,F8.4),2X,F8.2))
C   N IS THE NUMBER OF POINTS TO BE LEAST-SQUARES FITTED
C   E IS THE ENERGY, W IS THE WIDTH, WT IS THE WEIGHT AND HT THE
C   HEIGHT
C   SDWID IS THE STANDARD DEVIATION IN THE WIDTH, IN KEV
C   NACA IS THE DEGREE OF THE POLYNOMIAL TO WHICH THE DATA IS FITTED
      WRITE(6,202)
202  FORMAT(1H1,34X, 'PEAKS USED IN COMPUTING LSF OF FWHM')
      WRITE(6,203)
203  FORMAT(1HC, '
1    SD-KEV          PEAK NO.      ENERGY KEV      WIDTH KEV
          WEIGHT          HEIGHT')
      WRITE(6,205) (I,E(I),W(I),SDWID(I),WT(I),HT(I),I = 1,N)
205  FORMAT(15X,I5,5X,F10.2,5X,F10.3,5X,F10.3,5X,F10.3,5X,F10.2)
C
206  CONTINUE
      WRITE(6,207)
207  FORMAT(1H1,20X, 'RESULTS OF LEAST-SQUARES FIT')
C   EVALUATION OF THE SUM(WIDTH*WEIT*ENERGY**J) COEFFICIENTS.
      DO 215 I = 1,NACA
      SUMWE = 0.0
      DO 210 J = 1, N
      K = I - 1
      EGM = E(J)/10000.0
210  SUMWE = SUMWE + WT(J)*W(J)*EGM**K

```

```

      WEC(I) = SUMWE
215 CONTINUE
C
      DO 216 I = 1, NACA
        J = I - 1
        WRITE(6,218) J, WEO(I)
218 FORMAT(1H0,5X,'SUM(WEIGHT*WIDTH(KEV)*ENERGY(10MEV)**',I2,') = ',
1 E12.5)
216 CONTINUE
C
C      EVALUATION OF THE SUM(WEIGHT*ENERGY**K) COEFFICIENTS
      NACB = 2*NACA - 1
      DO 225 I = 1, NACB
        SUME = 0.0
        DO 220 J = 1, N
          K = I - 1
          EGM = E(J)/10000.0
220 SUME = SUME + WT(J)*EGM**K
          EO(I) = SUME
225 CONTINUE
C      FORMATION OF THE COEFFICIENT MATRIX.
      DO 230 I = 1, NACA
        DO 230 J = 1, NACA
          K = (I-1)*NACA + J
          L = I + J - 1
230 CF(K) = EO(L)
232 CONTINUE
C      PRINTOUT OF ORIGINAL MATRIX COEFFICIENTS.
      WRITE(6,235)
235 FORMAT(1H0, 5X, ' COEFFICIENTS OF ORIGINAL MATRIX')
240 FORMAT(8(5X,E12.5))
      DO 245 I = 1, NACA
        J = (I-1)*NACA + 1
        K = J + NACA - 1

```

```

WRITE(6,240) (CF(L), L = J,K)
245 CONTINUE
C
      CALL MINV(CF,NACA,DTN,LACA,MACA)
C
C   SUBROUTINE MINV CALCULATES THE INVERSE OF THE COEFFICIENT MATRIX.
WRITE(6,250) DTN
250 FORMAT(1H0,5X,' VALUE OF DETERMINANT = ',E12.5)
WRITE(6,255)
255 FORMAT(1HC, 5X, ' COEFFICIENTS OF INVERTED MATRIX')
DO 260 I = 1, NACA
  J = (I-1)*NACA + 1
  K = J + NACA - 1
  WRITE(6,240) (CF(L), L = J,K)
260 CONTINUE
C
C   EVALUATION OF THE LSF COEFFICIENTS
DO 280 I = 1, NACA
  SUMAO = 0.0
  DO 270 L = 1, NACA
    J = (I - 1)*NACA + L
270 SUMAO = SUMAO + CF(J)*WEO(L)
  AO(I) = SUMAO
280 CONTINUE
  WRITE(6,282)
282 FORMAT(1H0,5X, 'EQUATION OF LEAST-SQUARES FIT')
  WRITE(6,283)
283 FORMAT(1H0, 5X, 'FWHM(KEV) =')
  DO 286 I = 1, NACA
    J = I - 1
    WRITE(6,284) AO(I), J
284 FORMAT(16X,E12.5,'*ENERGY(10MEV)**',I2)
286 CONTINUE
C   EVALUATION OF THE RMS ERROR IN FITTING THE DATA

```

```

QWAP = 0.0
DO 290 I = 1,N
EGM = E(I)/10000.0
SUMFW = 0.0
DO 285 J = 1,NACA
K = J - 1
285 SUMFW = SUMFW + A0(J)*EGM**K
WIDCL(I) = SUMFW
QWIP = W(I) - WIDCL(I)
WIDDF(I) = QWIP
WIDRS(I) = WT(I)*QWIP*QWIP
QWAP = QWAP + WIDRS(I)
290 CONTINUE
DGF = N - NACA
S = SQRT(QWAP/DGF)
WRITE(6,291) S
291 FORMAT(1H0,5X,'SQRT(SUM WEIGHTED RESIDUALS/DEGREES OF FREEDOM) =
1 ',E12.5)

```

```

C
C EVALUATION OF THE ERRORS IN THE FIT.

```

```

DO 300 I = 1,N
EGM = E(I)/10000.0
DO 294 K = 1, NACA
L = K - 1
294 FA(K) = EGM**L
SUMA = 0.0
DO 296 J = 1, NACA
DO 296 K = 1, NACA
L = (J-1)*NACA + K
296 SUMA = SUMA + FA(J)*FA(K)*CF(L)
WIDER(I) = S*SQRT(SUMA)
300 CONTINUE

```

```

C
WRITE(6,305)

```



```

305 FORMAT(1H1, 45X, 'COMPARISON BETWEEN ORIGINAL AND FITTED DATA')
      WRITE(6,306)
306 FORMAT(1HC,'          NO    PEAK ENERGY    PEAK WIDTH  S.D.(WIDTH)
1    WEIGHT    WIDTH FIT    WIDTH DIFF    RESIDUALS  CONF INTRVL')
      WRITE(6,310) (I,E(I), W(I), SDWID(I), WT(I), WIDCL(I),WIDDF(I),
1    WIDRS(I), WIDER(I), I = 1,N)
310 FORMAT((6X,I5,5X,F10.2,7(3X,F10.5)))
C
      READ(5,315) NACA
315 FORMAT(I5)
C    USE THIS STATEMENT TO PERFORM DIFFERENT DEGREE FITS TO THE DATA.
      IF(NACA) 325,95,206
325 CONTINUE
      CALL EXIT
      END

```


C	C IN COLUMN 1 SHOULD BE REMOVED FROM THE DOUBLE PRECISION	MINV 390
C	STATEMENT WHICH FOLLOWS.	MINV 400
C		MINV 410
C	DOUBLE PRECISION A,C,BIGA,HOLD	MINV 420
C		MINV 430
C	THE C MUST ALSO BE REMOVED FROM DOUBLE PRECISION STATEMENTS	MINV 440
C	APPEARING IN OTHER ROUTINES USED IN CONJUNCTION WITH THIS	MINV 450
C	ROUTINE.	MINV 460
C		MINV 470
C	THE DOUBLE PRECISION VERSION OF THIS SUBROUTINE MUST ALSO	MINV 480
C	CONTAIN DOUBLE PRECISION FORTRAN FUNCTIONS. ABS IN STATEMENT	MINV 490
C	10 MUST BE CHANGED TO DABS.	MINV 500
C		MINV 510
C	MINV 520
C		MINV 530
C	SEARCH FOR LARGEST ELEMENT	MINV 540
C		MINV 550
	D=1.0	MINV 560
	NK=-N	MINV 570
	DO 80 K=1,N	MINV 580
	NK=NK+N	MINV 590
	L(K)=K	MINV 600
	M(K)=K	MINV 610
	KK=NK+K	MINV 620
	BIGA=A(KK)	MINV 630
	DO 20 J=K,N	MINV 640
	IZ=N*(J-1)	MINV 650
	DO 20 I=K,N	MINV 660
	IJ=IZ+I	MINV 670
	10 IF(ABS(BIGA)- ABS(A(IJ))) 15,20,20	MINV 680
	15 BIGA=A(IJ)	MINV 690
	L(K)=I	MINV 700
	M(K)=J	MINV 710
	20 CONTINUE	MINV 720

C
C
C

INTERCHANGE ROWS

J=L(K)
IF(J-K) 35,35,25
25 KI=K-N
DO 30 I=1,N
KI=KI+N
HOLD=-A(KI)
JI=KI-K+J
A(KI)=A(JI)
30 A(JI) =HOLD

C
C
C

INTERCHANGE COLUMNS

35 I=M(K)
IF(I-K) 45,45,38
38 JP=N*(I-1)
DO 40 J=1,N
JK=NK+J
JI=JP+J
HOLD=-A(JK)
A(JK)=A(JI)
40 A(JI) =HOLD

C
C
C
C

DIVIDE COLUMN BY MINUS PIVOT (VALUE OF PIVOT ELEMENT IS
CONTAINED IN BIGA)

45 IF(BIGA) 48,46,48
46 D=0.0
RETURN
48 DO 55 I=1,N
IF(I-K) 50,55,50
50 IK=NK+I

MINV 730
MINV 740
MINV 750
MINV 760
MINV 770
MINV 780
MINV 790
MINV 800
MINV 810
MINV 820
MINV 830
MINV 840
MINV 850
MINV 860
MINV 870
MINV 880
MINV 890
MINV 900
MINV 910
MINV 920
MINV 930
MINV 940
MINV 950
MINV 960
MINV 970
MINV 980
MINV 990
MINV1000
MINV1010
MINV1020
MINV1030
MINV1040
MINV1050
MINV1060

	A(IK)=A(IK)/(-BIGA)	MINV1070
55	CONTINUE	MINV1080
C		MINV1090
C	REDUCE MATRIX	MINV1100
C		MINV1110
	DO 65 I=1,N	MINV1120
	IK=NK+I	MINV1130
	HOLD=A(IK)	MINV1140
	IJ=I-N	MINV1150
	DO 65 J=1,N	MINV1160
	IJ=IJ+N	MINV1170
	IF(I-K) 60,65,60	MINV1180
60	IF(J-K) 62,65,62	MINV1190
62	KJ=IJ-I+K	MINV1200
	A(IJ)=HCLD*A(KJ)+A(IJ)	MINV1210
65	CONTINUE	MINV1220
C		MINV1230
C	DIVIDE RCW BY PIVOT	MINV1240
C		MINV1250
	KJ=K-N	MINV1260
	DO 75 J=1,N	MINV1270
	KJ=KJ+N	MINV1280
	IF(J-K) 70,75,70	MINV1290
70	A(KJ)=A(KJ)/BIGA	MINV1300
75	CONTINUE	MINV1310
C		MINV1320
C	PRODUCT OF PIVOTS	MINV1330
C		MINV1340
	D=D*BIGA	MINV1350
C		MINV1360
C	REPLACE PIVOT BY RECIPROCAL	MINV1370
C		MINV1380
	A(KK)=1.0/BIGA	MINV1390
80	CONTINUE	MINV1400

C
C FINAL ROW AND COLUMN INTERCHANGE
C

 K=N
100 K=(K-1)
 IF(K) 150,150,105
105 I=L(K)
 IF(I-K) 120,120,108
108 JQ=N*(K-1)
 JR=N*(I-1)
 DO 110 J=1,N
 JK=JQ+J
 HOLD=A(JK)
 JI=JR+J
 A(JK)=-A(JI)
110 A(JI) =HOLD
120 J=M(K)
 IF(J-K) 100,100,125
125 KI=K-N
 DO 130 I=1,N
 KI=KI+N
 HOLD=A(KI)
 JI=KI-K+J
 A(KI)=-A(JI)
130 A(JI) =HOLD
 GO TO 100
150 RETURN
 END

MINV1410
MINV1420
MINV1430
MINV1440
MINV1450
MINV1460
MINV1470
MINV1480
MINV1490
MINV1500
MINV1510
MINV1520
MINV1530
MINV1540
MINV1550
MINV1560
MINV1570
MINV1580
MINV1590
MINV1600
MINV1610
MINV1620
MINV1630
MINV1640
MINV1650
MINV1660
MINV1670
MINV1680

```

C      COMPUTER CODE 'WTANAL'
C      ELEMENTAL ANALYSIS THROUGH PROMPT GAMMA SPECTROSCOPY
C      PROGRAM ANALYZES THE CONSTITUENTS OF A GIVEN SPECTRUM FOR A NUMBER
C      OF ELEMENTS SUPPLIED AS INPUT, BY OPERATING ON THE GAMANL OUTPUT.
C
      DIMENSION REF(18), ES(500), ER(500), AREAG(500), SES(2000),
1     SER(2000), SAREA(2000), EFFCY(50), NPEAK(25), ELM(25), AW(25),
2     SIGMA(25), ATMIN(25), ETMIN(25), ETMAX(25), DENG(25), ET(25,300),
3     AT(25,300), SM(2000), LS(2000), SELM(2000), SET(2000), SAT(2000),
4     INTRF(2000), SELMX(2000,10)
      READ(5,90) (REF(I), I = 1, 18)
90    FORMAT(18A4)
C      USE THIS STATEMENT FOR REFERENCE NUMBER AND OTHER INFORMATION
      READ(5,95) NS, FLUXT, SLDAN
95    FORMAT(I5,2E10.4)
C      NS IS THE NUMBER OF PEAKS IN THE SPECTRUM TO BE ANALYZED
C      FLUXT IS THE INTEGRATED FLUX (NEUTRONS/SQUARE CM)
C      SLDAN IS THE SOLID ANGLE
      READ(5,100) (ES(I), ER(I), AREAG(I), I = 1, NS)
100   FORMAT(8X,F10.2, 16X,F10.2,3X,F10.2)
C      ES = PEAK ENERGY, ER = ERROR PERCENT, AREAG = GAUSSIAN AREA
      READ(5,105) J2, FIRENG, DELENG
105   FORMAT(I5,2F5.0)
C      J2 = NUMBER OF POINTS IN EFFICIENCY ARRAY
C      FIRENG = FIRST ENERGY (KEV) USED IN EFFICIENCY CALCULATION
C      DELENG = ENERGY DIFFERENCE BETWEEN EFFICIENCY POINTS
      READ(5,110) (EFFCY(I), I = 1, J2)
110   FORMAT(7E10.3)
C      EFFCY = EFFICIENCY DATA ARRAY
      READ(5,115) NEL
115   FORMAT(I5)
C      NEL = NUMBER OF ELEMENTS USED IN THE ANALYSIS
      DO 140 I = 1, NEL
      READ(5,120) NPEAK(I),ELM(I),AW(I),SIGMA(I),ATMIN(I),ETMIN(I),

```

```

      1 ETMAX(I), DENG(I)
120 FORMAT(I5,3X,A2,6F10.2)
C     ELM = ELEMENT EXAMINED
C     NPEAK = NUMBER OF TABULATED PEAKS FOR THIS ELEMENT
C     AW = ATOMIC WEIGHT, SIGMA = THERMAL NEUTRON ABSORPTION X-SECTION
C     ATMIN = MIN VALUE OF PEAK INTENSITY USEABLE FOR ANALYSIS
C     ETMIN AND ETMAX SPECIFY THE ENERGY RANGE OF THE SPECTRUM
C     DENG = MAX DIFF BETWEEN SAMPLE AND TABULATED ENERGIES FOR POSSIBLE
C           AGREEMENT
      NPK = NPEAK(I)
      READ(5,125) (ET(I,K), AT(I,K), K = 1, NPK)
125 FORMAT(2(10X,F10.2))
C     ET = TABULATED ENERGIES OF SPECIFIED ELEMENT
C     AT = TABULATED INTENSITIES (GAMMAS/100 NEUTRON CAPTURES)
140 CONTINUE
C
C     PRINTOUT OF PERTINENT INFORMATION
      WRITE(6,145) (REF(I), I = 1,18)
145 FORMAT(1H1, 25X, 18A4)
      WRITE(6,150) FLUXT, SLDAN
150 FORMAT(1H0, 10X, 'FLUX*TIME (N/CM*CM) = ', E11.4, 10X, 'SOLID ANGLE
      l= ', E11.4)
      WRITE(6,155) FIRENG, DELENG
155 FORMAT(1H0, 10X, 'EFFICIENCY DATA INITIAL ENERGY (KEV) = ', F6.0,
      1 5X, 'DELTA ENERGY (KEV) = ', F6.0)
      WRITE(6,160) (EFFCY(I), I = 1,J2)
160 FORMAT(1H0, 10X, 'EFFICIENCY ARRAY'/( 10X,10E10.3))
      WRITE(6,165)
165 FORMAT(1H0, 25X, ' ELEMENTS FOR WHICH SPECTRUM IS ANALYZED')
      WRITE(6,170)
170 FORMAT(1H0, 7X, ' NO PEAKS      ELEMENT      AT WEIGHT      SIGMA(BARNS
      1)      MIN INT      MIN ENERGY      MAX ENERGY      ENERGY DIFF')
      WRITE(6,175) (NPEAK(I), ELM(I), AW(I), SIGMA(I), ATMIN(I), ETMIN(I),
      1 ETMAX(I), DENG(I), I = 1, NEL)

```



```

175 FORMAT((10X,I5,8X,A2,6(5X,F10.2)))
C
C ONLY THE PEAKS OF EACH ELEMENT WHICH LIE WITHIN THE SPECIFIED
C RANGE OF THE SPECTRUM AND WHOSE INTENSITIES ARE LARGER THAN THE
C SPECIFIED VALUE ARE EXAMINED.
DO 200 I = 1, NEL
KN = 0
NPK = NPEAK(I)
DO 195 K = 1, NPK
IF(ET(I,K) - ETMIN(I)) 195,180,180
180 IF(ET(I,K) - ETMAX(I))185,185,195
185 IF(AT(I,K) - ATMIN(I)) 195,195,190.
190 KN = KN + 1
ET(I,KN) = ET(I,K)
AT(I,KN) = AT(I,K)
195 CONTINUE
NPEAK(I) = KN
200 CONTINUE
C
C PART ONE - CORRESPONDENCE BETWEEN SAMPLE AND TABULATED PEAKS
C EACH GAMMA RAY IN THE SPECTRUM IS CHECKED WITH THE TABULATED
C ENERGIES OF ALL THE DESIRED ELEMENTS FOR POSSIBLE CORRESPONDENCE.
WRITE(6,205)
205 FORMAT(1H1, 40X, 'DETECTED ENERGIES AND POSSIBLE CONSTITUENTS')
WRITE(6,210)
210 FORMAT(1HC,4X,'NUMBER SAMPLE ENGY SAMPLE AREA ERROR P.C.
1 ELEMENT TABLE ENGY TABLE INT. WT(GRAMS)')
L = 0
Y = FLUXT*SLDAN*C.006023
DO 265 IS = 1, NS
INTF = 0
EGAM = ES(IS)
C EVALUATION OF THE SYSTEM EFFICIENCY AT THIS ENERGY
IEGAM=2

```

```

215 XEGAM = DELENG*FLOAT(IEGAM-1) + FIRENG
    IF (XEGAM-EGAM) 220,220,225
220 IEGAM=IEGAM+1
    GO TO 215
225 E1 = XEGAM - DELENG
    E2=XEGAM
    E3 = XEGAM + DELENG
    G1=EFFCY(IEGAM-1)
    G2=EFFCY(IEGAM)
    G3=EFFCY(IEGAM+1)
    D12=(G2-G1)/(E2-E1)
    D23=(G3-G2)/(E3-E2)
    D123=(D23-D12)/(E3-E1)
    GX=G1+(EGAM-E1)*D12+(EGAM-E2)*(EGAM-E1)*D123
C   GX      SECOND ORDER INTERPOLATED EFFICIENCY AT GAMMA ENERGY EGAM.
    WRITE(6,230) IS, ES(IS), AREAG(IS), ER(IS)
230 FORMAT(1H ,5X,I5,3(5X,F10.2))
    DO 250 I = 1, NEL
    NPK = NPEAK(I)
    DO 250 K = 1, NPK
    IF(ABS(ES(IS)-ET(I,K)) - DENG(I)) 235,235,250
235 L = L + 1
    INTF = INTF + 1
    SM(L) = AREAG(IS)*AW(I)/(GX*SIGMA(I)*AT(I,K)*Y)
C   THE FOLLOWING PARAMETERS ARE STORED IN NEW ARRAYS FOR THE SECOND
C   PART OF THE ANALYSIS.
    LS(L) = IS
    SES(L) = ES(IS)
    SAREA(L) = AREAG(IS)
    SER(L) = ER(IS)
    SELM(L) = ELM(I)
    SET(L) = ET(I,K)
    SAT(L) = AT(I,K)
    WRITE(6,240) SELM(L), SET(L), SAT(L), SM(L)

```

```

240 FORMAT(1H ,60X,8X,A2,5X,F10.2,5X,F10.2,5X,E10.4)
250 CONTINUE
C   STORING THE SYMBOL OF THE ELEMENTS WHICH INTERFERE WITH EACH OTHER
   IF(INTF) 265,265,252
252 DC 260 INT = 1, INTF
   LK = L + 1 - INT
   INTRF(LK) = INTF - 1
   JK = 0
   DO 260 JA = 1, INTF
   IF(JA - INT) 255, 260, 255
255 JK = JK + 1
   LJ = L + 1 - JA
   SELMX(LK,JK) = SELM(LJ)
260 CONTINUE
265 CONTINUE
C
C   PART TWO - ORDERING THE SAMPLE CONSTITUENTS ELEMENT WISE
   WRITE(6,270)
270 FORMAT(1H1, 35X,'ORDERING THE IDENTIFIED PEAKS ELEMENT WISE')
   WRITE(6,272)
272 FORMAT(1H0,4X,'NUMBER      SAMPLE ENGY      SAMPLE AREA      ERROR P.C.
1      ELEMENT      TABLE ENGY      TABLE INT.      WT(GRAMS)  INTE
2RFRERENCE')
   DO 305 K = 1, NEL
   WRITE(6,275)
275 FORMAT(1H0,/)
   DO 305 I = 1, L
   IF(ELM(K) - SELM(I)) 305,280,305
280 IA = INTRF(I)
   IF(IA) 285,285,295
285 WRITE(6,290) LS(I), SES(I), SAREA(I), SER(I), SELM(I), SET(I), SAT(I),
1 SM(I)
290 FORMAT(1H ,5X,I5,3(5X,F10.2),11X,A2,5X,F10.2,3X,F10.2,9X,E10.4)
   GO TO 305

```

```
295 WRITE(6,300) LS(I),SES(I),SAREA(I),SER(I),SELM(I),SET(I),SAT(I),  
1 SM(I), (SELMX(I,IC), IC = 1, IA)  
300 FORMAT(1H ,5X,I5,3(5X,F10.2),11X,A2,5X,F10.2,3X,F10.2,9X,E10.4,  
1 2X,6(A2,1X))  
305 CONTINUE  
CALL EXIT  
END
```

```

C      COMPUTER PROGRAM MINIMUM
C      EVALUATION OF MINIMUM DETECTABLE AREAS AND MINIMUM DETECTABLE
C      WEIGHTS IN A KNOWN BACKGROUND.
COMMON TBL(4096), TBK(4096),DTS(4096)
COMMON IPUNCH,JREAD,JPRINT,JPUNCH
DIMENSION EGAM(50), AINT(50), EFFCY (50), REF(50)
JREAD = 5
JPRINT = 6
JPUNCH = 7

C      READ(5,90) (REF(I), I = 1, 18)
90  FORMAT(18A4)
C      USE THIS STATEMENT FOR REFERENCE NUMBER AND OTHER INFORMATION
READ(JREAD,95) NUMRUN,NOCHAN,IMAX,DCR
95  FORMAT(3I5,F5.0)
C      NUMRUN IS THE SPECTRUM RUN NUMBER, NOCHAN IS THE NUMBER OF CHANNELS
C      IN THE SPECTRUM, IMAX IS THE CHANNEL NUMBER AT WHICH THE BACKGROUND
C      SUBTRACTION BEGINS, AND DCR IS THE SLOPE CRITERION USED IN BAKSUB.
READ (JREAD,100) (TBK(I),I=1,NOCHAN)
100 FORMAT (7X,7(F6.0,1X))/(8(F6.0,1X)))
C      TBK IS THE DATA ARRAY. EGAM1 AND EGAM2 ARE THE ENERGIES OF THE TWO
C      CALIBRATION GAMMA RAYS AND IP1,IP2 ARE THEIR POSITIONS IN THE
C      SPECTRUM, IN CHANNEL NUMBERS.
READ (JREAD,102) EGAM1,IP1,EGAM2,IP2
102 FORMAT (4X,F6.1,4X,I6,4X,F6.1,4X,I6)
READ(5,105) J2, FIRENG, DELENG
105 FORMAT(I5,2F5.0)
C      J2 = NUMBER OF POINTS IN EFFICIENCY ARRAY
C      FIRENG = FIRST ENERGY (KEV) USED IN EFFICIENCY CALCULATION
C      DELENG = ENERGY DIFFERENCE BETWEEN EFFICIENCY POINTS
READ(5,110) (EFFCY(I), I = 1, J2)
110 FORMAT(7E10.3)
C      EFFCY = EFFICIENCY DATA ARRAY
READ(JREAD,112) A0, A1, A2

```

```

112 FORMAT(3F10.3)
C   A0, A1, AND A2 ARE THE CONSTANTS DETERMINING THE SYSTEM RESOLUTION
READ(JREAD,112) C1, C2
C   USE THESE CONSTANTS IN THE EQUATION FOR A(MIN)
READ(5,114) FLUXT, SANGLE,FACTR
C   FLUX IS THE INTEGRATED FLUX, AND SANGLE IS THE SOLID ANGLE.
C   FACTR IS USED TO MULTIPLY THE INPUT TBK DATA, IF SO DESIRED, AFTER
C   SUBROUTINE BAKSUB IS CALLED.
114 FORMAT(2E10.4,F10.3)
READ(5,112) ELIM1, ELIM2, SMPLW
C   ELIM1 AND ELIM2 ARE ENERGY LIMITS WITHIN WHICH THE ANALYSIS IS DONE.
C   SMPLW IS THE SAMPLE WEIGHT, IN GRAMS
C
C   EVALUATION OF THE ENERGY-CHANNEL CONVERSION FACTOR
SLP = (EGAM2 -EGAM1)/FLOAT(IP2-IP1)
C
C   PRINTOUT OF PERTINENT INFORMATION
WRITE(6,120) (REF(I), I = 1,18)
120 FORMAT(1H1, 25X, 18A4)
WRITE (JPRINT,122) NUMRUN, NOCHAN
122 FORMAT (1H0,4X,9H RUN NO = ,I5,5X,22H NUMBER OF CHANNELS = ,I5)
WRITE (JPRINT,123) IMAX
123 FORMAT (5X,41H CHANNEL NUMBER SLOPE CRITERION (IMAX) = ,I5)
WRITE (JPRINT,125) DCR
125 FORMAT(5X,51H SLOPE CRITERION FOR BACKGROUND IN UNITS OF SQRT OF,
114H BACKGROUND = , F6.2)
WRITE (JPRINT,130) SLP
130 FORMAT (' ',4X,' ENERGY PER CH.NO (KEV) = ',F6.3)
WRITE (JPRINT,149) SANGLE,FLUXT
149 FORMAT (' ',4X,' SOLID ANGLE RADIANS = ',E10.4,2X,' FLUXT = ',
1 E10.4)
WRITE(JPRINT,150)
150 FORMAT(1H0,20X, ' EQUATION OF LEAST-SQUARES FITTED FWHM')
WRITE(JPRINT, 152) A0, A1, A2

```

```

152 FORMAT ('0',10X,' FWHM(KEV)=' ,F9.3,' + ' ,F9.3,
1 ' *E(10MEV) + ' ,F9.3,' *E(10MEV)**2 ')
WRITE(JPRINT, 153) C1, C2
153 FORMAT( 1H0, 10X, ' AREA(MIN) = ' ,F8.4,'*WIDTH*(1.0 + SQRT(1. + ' ,
1 F7.3,'*BACKGROUND))'//)
WRITE(6,155) FIRENG, DELENG
155 FORMAT(1H0,5X,'EFFICIENCY DATA INITIAL ENERGY(KEV) = ' ,F6.0,
1 5X,'DELTA ENERGY (KEV) = ' , F6.0)
WRITE(6,160) (EFFCY(I), I = 1,J2)
160 FORMAT(1H0, 10X,'EFFICIENCY ARRAY'/( 10X,10E10.3))
WRITE(6,165) FACTR
165 FORMAT(1H0,5X,'INPUT SPECTRAL DATA AND FLUXT WERE MULTIPLIED BY',
1 F10.3)
C
C SUBROUTINE BAKSUB IS CALLED FOR THE EVALUATION OF THE BACKGROUND
C CONTINUUM UNDERNEATH THE PEAKS.
C
C CALL BAKSUB(NOCHAN,IMAX,DCR)
C
C DO 170 I = 1, NOCHAN
170 TBL(I) = TBL(I)*FACTR
FLUXT = FLUXT*FACTR
ISUM = 50
C
175 READ(5,95) ILINE
C ILINE IS THE NUMBER OF GAMMA RAYS OF THE ELEMENT CONSIDERED.
IF(ILINE) 260,260,180
180 WRITE(6,185)
185 FORMAT(1H )
ISUM = ISUM + 1
WTLIM = 1000000.
READ(5, 190) (EGAM(I), AINT(I), ZET, I = 1, ILINE)
190 FORMAT(10X,F10.1,10X,E9.2, 13X, A2)
C EGAM(I) AND AINT(I) ARE THE ENERGIES AND INTENSITIES OF THE

```

```

C   GAMMA RAYS OF THE ELEMENTS. ZET IS THE ELEMENTAL SYMBOL.
C
C   EVALUATION OF THE LIMITS FOR QUANTITATIVE DETERMINATION
DO 250 J = 1, ILINE
  IF(ISUM - 49) 210,210,195
195 WRITE(6,200)
200 FORMAT(1H1,///30X,' LIMITS FOR QUANTITATIVE DETERMINATION')
  WRITE(6,205)
205 FORMAT(1H0, 15X, ' ELEM. ENERGY INTENSITY MIN.AREA MI
IN.WT WT PERCENT',/)
  ISUM = 0
210 CONTINUE
  EGA = EGAM(J)
  IF(EGA - ELIM1) 250,250,215
215 IF(EGA - ELIM2) 220,220,250
220 CONTINUE
  IPX = (EGA - EGAM1)/SLP
  IPY = IPX + IPI
C   IPY IS THE POSITION IN THE SPECTRUM CORRESPONDING TO AN ENERGY EGAM(I).
C   BG IS THE VALUE OF THE BACKGROUND AT IPY. IT IS MODIFIED TO
C   A CHANNEL ENERGY CONVERSION OF 2 KEV PER CHANNEL.
  BG = TBL(IPY)*2.0/SLP
  EGM = EGA/10000.0
  W = (A0 + A1*EGM + A2*EGM*EGM)/2.0
C   W IS THE SYTEM RESOLUTION IN CHANNELS.
C   AMIN IS THE PEAK AREA DETERMINATION LEVEL
  AMIN = C1*W *(1. + SQRT(1.0 + C2*BG))
C
C   EVALUATION OF EFFICIENCY
  IEGAM=2
225 XEGAM = DELENG*FLOAT(IEGAM-1) + FIRENG
  IF (XEGAM-EGA) 230,235,235
230 IEGAM=IEGAM+1
  GO TO 225

```



```

235 E1 = XEGAM - DELENG
    E2=XEGAM
    E3 = XEGAM + DELENG
    G1=EFFCY(IEGAM-1)
    G2=EFFCY(IEGAM)
    G3=EFFCY(IEGAM+1)
    D12=(G2-G1)/(E2-E1)
    D23=(G3-G2)/(E3-E2)
    D123=(D23-D12)/(E3-E1)
    GX=G1+(EGA -E1)*D12+(EGA -E2)*(EGA -E1)*D123
C   GX IS THE EFFICIENCY OF THE DETECTOR AT EGAM(I). IT IS
C   OBTAINED BY A SECOND ORDER INTERPOLATION.
C
C   EVALUATION OF MINIMUM DETECTABLE WEIGHT
    WTMIN = AMIN/(AINT(J)*GX*FLUXT*SANGLE)
C   EVALUATION OF WEIGHT PERCENT
    WTPC = WTMIN*100.0/SMPLW
    WRITE(6,240) ZET,EGA,AINT(J),AMIN,WTMIN,WTPC
240 FORMAT(1H ,18X,A2,2X,F8.1,3X,E10.3,3X,E10.3,2X,E10.2,2X,E10.2)
    ISUM = ISUM + 1
C   IDENTIFICATION OF THE OPTIMUM GAMMA RAY FOR ELEMENTAL ANALYSIS.
    IF(WTPC -WTLIM) 245,245,250
245 WTLIM = WTPC
    ENER = EGA
    AINTN = AINT(J)
    AMINN = AMIN
    WTMNN = WTMIN
250 CONTINUE
C
    WRITE(7, 255) ZET,ENER,AINTN,AMINN,WTMNN,WTLIM
255 FORMAT(5X,A2,2X,F8.1,3X,E10.3,3X,E10.3,2X,E10.2,2X,E10.2)
    GO TO 175
260 CALL EXIT
    END

```

```

SUBROUTINE BAKSUB (NOCHAN,IMAX,DCR)
C SUBROUTINE BACKSUB PERFORMS THE BACKGROUND SUBTRACTION ON ARRAY
C TBK. THE ORIGINAL TBK ARRAY IS REPLACED BY THE BACKGROUND
C SUBTRACTED ARRAY.
COMMON TBL(4096), TBK(4096),DTS(4096)
COMMON IPUNCH,JREAD,JPRINT,JPUNCH
C
WRITE (JPRINT,498)
498 FORMAT(1H1,40X,37H CHOSEN MINIMA AND SLOPE BETWEEN THEM)
WRITE (JPRINT,499)
499 FORMAT(20X,29H NO. L CH. LEFT MIN ,
142H RIGHT MIN SLOPE BASE PNTS-AV.)
C
JJ = NOCHAN - 1
DO 302 I = 1,JJ
302 DTS(I)=TBK(I+1)-TBK(I)
C IMAX LOWER LIMIT ON SLOPE CRITERION.
LA = IMAX + 1
M2 = IMAX + 2
M3 = IMAX + 3
I = IMAX + 4
ILOOP = 0
IMIN = 0
IAVL = 1
C XM NEGATIVE, DB POSITIVE DETERMINES A PEAK.
333 XM=DTS(I)*DTS(I-1)
DB=QTS(I)-DTS(I-1)
IF (XM) 305,305,303
305 IF (DB) 303,303,304
304 CONTINUE
C
C EXAMINING THE MINIMA OF ADJACENT PEAKS FOR POSSIBLE MULTIPLETS.
C LA IS THE ACCEPTED MINIMUM ON THE LEFT-HAND-SIDE OF THE PEAK.
C M1,M2 AND M3 ARE THE NEXT THREE MINIMA CONSIDERED.

```

```

C      B2MT IS THE MEASURED VALUE OF THE BACKGROUND AT POINT M2, AN
C      B2ME IS THE VALUE IT WOULD HAVE HAD IT BEEN ON THE LA TO M1 LINE.
C      SIMILAR REMARKS FOR B3ME.
C      IF THE GRADIENT OF THE LA TO M1 LINE IS NEGATIVE THE TEST
C      FOR MULTIPLETS IS APPLIED TO ONLY THE FIRST TWO MINIMA M1 & M2.
C      WHEN THE GRADIENT IS POSITIVE THE MINIMA CONSIDERED FOR THE FIT
C      ARE M1, M2 AND M3.
C      THE VALUES (B2ME - B2MT) AND (B3ME - B3MT) MUST SATISFY
C      CERTAIN CRITERIA IF POINT M1 IS TO BE ACCEPTED AS A POSSIBLE
C      MINIMUM IN THE LINEAR BACKGROUND FIT.
C      IF THE CRITERIA ARE NOT MET THE ANALYSIS CONTINUES WITH M2 NOW
C      BECOMING M1, M3 BECOMING M2 AND THE NEWLY CALCULATED NEXT MINIMUM
C      BECOMING M3. THE PROCEDURE IS REPEATED TILL THERE IS A MAXIMUM
C      OF FIVE PEAKS BETWEEN LA AND M1, THE TEST BEING IGNORED THEREAFTER
C
310  M1 = M2
      M2 = M3
      M3 = I
      GRAD1 = (TBK(M1) - TBK(LA))/FLOAT(M1-LA)
      B2ME = TBK(LA) + GRAD1*FLOAT(M2-LA)
      B2MT = TBK(M2)
      IF(GRAD1) 370,370,371
370  IF(B2ME-B2MT) 308,308,365
C      DCR IS READ IN AND HAS A VALUE OF APPROXIMATELY 1.0
365  CRIT = DCR*SQRT(B2MT*FLOAT(M2-M1))
      IF(B2ME - B2MT - CRIT) 308,308,366
371  B3ME = TBK(LA) + GRAD1*FLOAT(M3-LA)
      B3MT = TBK(M3)
      CRIT2 = DCR*SQRT(B2MT*FLOAT(M2-M1))
      IF(ABS(B2MT - B2ME) - CRIT2) 309,309,366
309  CRIT3 = DCR*SQRT(B3MT*FLOAT(M3-M1))
      IF(ABS(B3MT - B3ME) - CRIT3) 308,308,366
366  ILOOP = ILOOP + 1
      IF(ILOOP - 5) 303,308,308

```

```

C
C ONCE M1 IS CHOSEN, ITS VALUE TBK(M1) IS AVERAGED BY WEIGHING
C IT EQUALLY WITH THE VALUES IN THE NEARBY FIVE CHANNELS, TWO
C ON EACH SIDE. THESE HOWEVER MUST BE WITHIN ONE STANDARD DEVIATION
C FROM TBK(M1) TO BE CONSIDERED IN THE AVERAGING.
308 LL = M1
      ILOOP = 0
      X = 0.0
      TBSQ = SQRT(TBK(LL))
      IAVM = 5
      IAV = 0
      DO 603 IV = 1, IAVM
      LIV = LL - (IAVM+1)/2 + IV
      TC = ABS(TBK(LIV) - TBK(LL))
      IF(TC - TBSQ) 602,602,603
602 IAV = IAV + 1
      X = X + TBK(LIV)
      TB = X/FLOAT(IAV)
603 CONTINUE
C
      TBK(LL) = TB
      IAVR = IAV
C
C LA IS LOWER CHAN NO LIMIT FOR LINEAR BACKGROUND FIT.
C LL IS UPPER CHAN NO LIMIT FOR LINEAR BACKGROUND FIT.
533 LB=LA+1
      LX=LL-1
C LBASE IS THE NUMBER OF CHANNELS OCCUPIED BY THE PEAK (FIRST CH=0)
      LBASE = LL - LA
C QSLOP IS THE SLOPE BETWEEN THE TWO MINIMA OF A PEAK
      QSLOP = (TBK(LL)-TBK(LA))/FLOAT (LBASE)
C TBL IS A DUMMY ARRAY USED FOR CALCULATING THE BACKGROUND.
      TBL(LA)=TBK(LA)
      IMIN = IMIN + 1

```

```

      IF (LBASE - 8) 550,551,551
551 CONTINUE
      WRITE (JPRINT,500) IMIN,LA,TBK(LA),TBK(LL),QSLOP,LBASE,IAVL,IAVR
500 FORMAT(20X, I7,3X,I6,3X,F9.2,3X,F9.2,3X,F9.3,3X,3I5)
550 CONTINUE
C      BACKGROUND - LINEAR FIT.
      DO 306 IK=LB,LX
306 TBL(IK)=(TBK(LA)*FLOAT (LL-IK)+TBK(LL)*FLOAT (IK-LA))/
      IFLOAT (LL-LA)
      MZ = LA
      LA=LL
      IAVL = IAVR
C
C303 IF (I-JJ) 334,335,335
334 I=I+1
      GO TO 333
C
C      THE LAST FOUR PEAKS ARE CONSIDERED TO BE SINGLET. NO AVERAGING
C      IS APPLIED
C335 TBL(MZ) = TBK(MZ)
      TBL(M1) = TBK(M1)
      TBL(M2) = TBK(M2)
      TBL(M3) = TBK(M3)
      TBL(NOCHAN) = TBK(NOCHAN)
      TBL(1) = FLOAT(MZ)
      TBL(2) = FLOAT(M1)
      TBL(3) = FLOAT(M2)
      TBL(4) = FLOAT(M3)
      TBL(5) = FLOAT(NOCHAN)
      DO 311 IM = 1,4
      LA = TBL(IM)
      LB = LA + 1
      LL = TBL(IM+1)
      LX = LL - 1

```

```

      DO 307 IK=LB,LX
307  TBL(IK)=(TBK(LA)*FLOAT (LL-IK)+TBK(LL)*FLOAT (IK-LA))/
      1 FLOAT (LL - LA)
311 CONTINUE
C
      DO 404 I = 1,IMAX
      TBK(I) = TBK(I)
      TBK(I) = 0.0
      DTS(I) = 0.0
      IF (TBL(I)) 405,404,404
405  TBL(I) = 0.0
404  CONTINUE
      DO 401 I = IMAX,NOCHAN
      TBK(I) = TBK(I) - TBL(I)
      DTS(I-1) = TBK(I) - TBK(I-1)
C  CORRECTION FOR NEGATIVE VALUES.
      IF (TBL(I)) 406,407,407
406  TBL(I) = 0.0
407  CONTINUE
      IF(TBK(I)) 403,403,401
403  TBK(I) = 0.0
401  CONTINUE
      RETURN
      END

```

REFERENCES

- [A1(a)] S.E. Arnell, R. Hardell, A. Hasselgren, L. Jonsson and O. Skeppstedt, "Thermal Neutron Capture Gammas Measured with Ge(Li)-Spectrometers and Internal Reactor Targets", Nucl. Instr. and Methods 54 (1967), p 165
- [A1(b)] S.E. Arnell and E.G. Nadjakov, "Thermal Neutron Capture Gamma Measurement with a Three-crystal Pair Spectrometer with Internal Target", Nucl. Instr. and Methods 24 (1963), p 185
- [B1] G. A. Bartholomew and M. R. Gunye, "Gamma-Gamma Angular Correlation Measurements of Thermal Neutron Capture Gamma Rays in Cr-53 and Cr-54", Can. J. Physics 43, p 1128 (1965)
- [C1] R. L. Caldwell, W. R. Mills, Jr., L.S. Allen, P. R. Bell, and R. L. Heath, "Combination Neutron Experiment for Remote Analysis", Science, 152, p457 (1966)
- [C2] D. F. Covell, "Determination of Gamma Ray Abundance Directly from the Total Absorption Peak", Anal. Chem. 31, No 11, p1787 (Nov 1959)
- [C3] C. L. Carnahan, "A Method for the Analysis of Complex Peaks Occuring in Gamma Ray Pulse Height Distributions", Nucl. Instr. and Methods 30, p165(1964)
- [C4] Lloyd A. Currie, "Limits of Qualitative Detection and Quantitative Determination", Anal. Chem 40, No. 3, pp 586-592 (1968)
- [C5] M. Ciampi, L. Daddi and V. D'Angelo, "Fitting of Gaussians to Peaks by a Maximum Probability Method", Nucl. Instr. and Meth. 66, pp 102-104 (1968)
- [C6] D. Comar, C. Crouzel, M. Chasteland, R. Riviere and C. Kellershohn, "The Use of Neutron-Capture Gamma Radiation for the Analysis of Biological Samples", Nucl. Appl. 6, pp 344-351 (April 1969)
- [D1(a)] L. Daddi and V. D'Angelo, "Evaluation of Peaks in Nuclear Spectroscopy", Nucl. Instr. and Meth. 42, pp 134-136 (1966)
- [D1(b)] L. Daddi and V. D'Angelo, "Statistical Fluctuations in Nuclear Spectrometry Peaks", Int. J. Applied Rad. and Isotopes 19, pp 407-410 (1968)
- [E1] G. T. Ewan and A. J. Tavendale, Can. J. Phys. 42, p 2286 (1964)

- [E2] N. D. Eckhoff, "A Study of Variance-Covariance Matrix for Gamma Ray Spectra", Nucl. Instr. and Meth. 68, pp 93 - 102 (1969)
- [E3] Ahmed Elkady, "Identification of Gold in Mixtures by Neutron Capture Gamma Rays", Trans. Am. Nucl. Soc. Vol 12, No. 1, p 42 (1969)
- [G1] Margaret B. Glos, "Activation Analysis Ready for Routine Use", Nucleonics 23, No. 6, p 62 (1965)
- [G2(a)] R. C. Greenwood and J. Reed, "Scintillation Spectrometer Measurements of Capture Gamma Rays from Natural Elements", Proc. Modern Trends in Activ. Anal., 1961 Int. Conf., College station, Texas, Dec. 1961
- [G2(b)] R. C. Greenwood et al., "Use of Neutron Capture Gamma Rays from A Lunar-Surface Compositional Analysis", Trans. Am. Nucl. Soc. 6, p 179 (1963)
- [G3] B. W. Garbrah and J. E. Whitley, "Determination of Boron by Thermal Neutron Capture Gamma-ray Analysis", Anal. Chem. 39, No. 3, p 345 (March 1967)
- [G4] Groshev et al., "De-Excitation of Ni Nuclei after Thermal Neutron Capture", Fiz. 3, pp 444-8 (March 1966)
- [G5] R. C. Greenwood, "Elemental Analysis using the Neutron Capture Gamma-Ray Technique with a Ge(Li) Detector", Trans. Am. Nucl. Soc. 10, 1, p28 (1967)
- [G6] H. D. Graber and D. D. Watson, "A Method for the Analysis of Pulse Height Spectra", Nucl. Instr. and Meth. 43, pp 355-360 (1966)
- [G7] B. W. Garbrah and J. E. Whitley, "Assessment of Neutron Capture Gamma-Ray Analysis", Int. J. of Applied Radiation and Isotopes, Vol 19, pp 605-614 (1968)
- [G8] R. B. Galloway, "Criteria for Evaluating Background Suppression Techniques in Nuclear Spectroscopy based on Consideration of Statistical Accuracy", Nucl. Inst. and Meth. 55, pp 29-33 (1967)
- [H1] T. Harper, T. Inouye and N. C. Rasmussen, "GAMANL, A Computer Program Applying Fourier Transforms to the Analysis of Gamma Spectral Data", MITNE-97, Aug. 1968
- [H2] J. N. Hanson, "Investigation of High Resolution Gamma Ray Spectrometer", SM Thesis, Massachusetts Inst. of Tech. Dept of Nucl. Eng., Aug. 1965
- [H3] R. G. Helmer, R. L. Heath, M. Putnam and D. H. Gipson, "Photopeak Analysis Program for Photon Energy and

- Intensity Determinations", Nucl. Instr. and Meth. 57, pp 46-57 (1967)
- [H4] B. Hammermesh and V. Hummel, Phys. Rev. 88, p 916 (1952)
- [H5] H. C. Van de Hulst and J. J. M. Reesinck, "Line Breadths and Voigt Profiles", Astrophysics J. 106, pp 121-127 (1947)
- [H6] Bertram Hui, S.M. Thesis, MIT, Dept of Nucl. Eng., September 1969
- [H7] J. N. Hamawi and N. C. Rasmussen, " Neutron-Capture Gamma Rays of 75 Elements Listed in Terms of Increasing Gamma Ray Energy", MITNE-105, 1969 (prepublication)
- [H8] T. L. Harper, "Determination of Thermal Neutron Capture Gamma Yields", Ph.D. Thesis, MIT Dept. of Nucl. Eng., July 1969 (MITNE-104)
- [H9] Y. Hukai, Ph.D. Thesis, MIT Dept. of Nucl. Eng., in progress.
- [I1] T. L. Isenhour and G. H. Morrison, "Modulation Technique for Neutron Capture Gamma Ray Measurements in Activation Analysis", Anal. Chem 38, 2. pp 162-167 (Feb 1966)
- [I2(a)] T. Inouye and N. C. Rasmussen, "A Computer Method for the Analysis of Complex Gamma-Ray Spectra", Trans. Am. Nucl. Soc. 10, 1, p 38 (1967)
- [I2(b)] T. Inouye, T. Harper and N. C. Rasmussen, "Application of Fourier Transforms to the Analysis of Spectral Data", Nucl. Instr. and Meth. 67, pp 125-132 (1969)
- [L1] J. M. A. Leniham, "Trace Elements in Biomedical Research", Nucleonics 23, 1, p 50 (Jan 1965)
- [L2] H. R. Lukens, "Elemental Survey Analysis by Neutron Activation: Simplified Estimation of Upper Limits", Anal. Chim. Acta, pp 9-16 (1966)
- [L3] W. G. Lussie and J.L. Brownlee, Jr., "The Measurement and Utilization of Neutron-Capture Gamma Radiation", Proc. Modern Trends in Act. Anal., Int. Conf. College Station, Texas, pp 194-199 (1965)
- [L4] A. Liuzzi and B. S. Pasternack, "Analysis of Multi-Channel Gamma Ray Spectrometer Data with Adjustment for Gain and Baseline Discrepancies, Nucl. Instr. and Meth. 57, pp 229-236 (1967)

- [L5] S. M. Lombard, T. L. Isenhour, P. H. Heintz, G. L. Woodruff and W. E. Wilson, "Neutron-Capture Gamma-Ray Activation Analysis. Design of Apparatus for Trace Analysis", Int. J. Applied Radiation and Isotopes 19, pp 15-22 (1968)
- [M1] H. L. Malm, A. J. Tavendale and I. L. Fowler, Can. J. Physics 43, p7 (1965)
- [M2] T. C. Martin, S. C. Mathur and I. L. Morgan, "The application of Nuclear Techniques in Coal Analysis", Int. J. Applied Rad. and Isot. 15, 6, pp 331-338 (1964)
- [M3] J. W. Mandler, "Utilization of High-Yield Americium-Beryllium-Curium Neutron Source for in Situ Elemental Analysis", Trans. Am. Nucl. Soc. 10, 1, p 30 (1967)
- [M4] M. A. Mariscotti, "A Method for Automatic Identification of Peaks in the Presence of Background and its Application to Spectrum Analysis", Nucl. Instr. and Meth. 50, pp 309-320 (1967)
- [M5] H. T. Motz and E. Journey, Argonne Nat. Lab, Report WASH-1044(1963)40
- [O1(a)] V. J. Orphan and N. C. Rasmussen, "A Pair Spectrometer Using a Large Coaxial Lithium-Drifted Germanium Detector", Trans. Nucl. Science, IEEE, Vol. NS-14, No. 1, (Feb. 1967)
- [O1(b)] V. J. Orphan and N. C. Rasmussen, "Study of Thermal Neutron Capture Gamma Rays Using a Lithium Drifted Germanium Spectrometer", MITNE-80, Jan 1967
- [O2] V. J. Orphan and N. C. Rasmussen, "A Ge(Li) Spectrometer for Studying Neutron Capture Gamma Rays", Nucl. Instr. and Meth. 48, pp232-295 (1967)
- [P1] J. Pauly, G. Guzzi, F. Girardi and A. Borella, "Application of Gamma Ray Spectrometry and Computer Techniques to the Determination of the Minimum Detectable Content of Trace Elements in Neutron Activated Materials, Nucl. Instr. and Meth. 42, pp15-25 (1966)
- [P2] S. G. Pussin, J. A. Harris and J. M. Hollander, "Application of Lithium-drifted Germanium Gamma-Ray Detectors to Neutron Activation Analysis", Anal. Chem. 37, No. 9, p1127 (1965)
- [R1] W. C. Reinig, "Advantages and Applications of Cf^{252} as a Neutron Source", Nucl. Applications 5, No. 1, p 24 (1968)

- [R2] N. C. Rasmussen, Y. Hukai, T. Inouye and V. J. Orphan "Thermal Neutron Capture Gamma Ray Spectra of the Elements", MITNE-85, Jan 1969 (AFCRL-69-0071)
- [R3] N. C. Rasmussen and Y. Hukai, "The Prompt Activation Analysis of Coal Using Neutron Capture Gamma Rays", Trans. Am. Nucl. Soc. 10, 1, p 29 (1967)
- [S1] O. I. Sumbaev et al., "Investigation of the Excited States of Rh-104,104 by Observation of Gamma Rays from the (n, γ) Reaction", Izv. Akad. Nauk, SSSR, Ser. Fiz. 29, p 739-59 (1963)
- [S2] G. L. Schroeder, H. W. Kraner and R. D. Evans, "Lithium-drifted Germanium Detectors: Applications to Neutron Activation Analysis", Science 151, pp 815-817 (1966)
- [S3(a)] R. F. Stewart, "Nuclear Measurement of Carbon in Bulk Materials", Proc. Seventh Nat. ISA Conf. on Instrumentation for the Iron and Steel Industry, March 15-16, 1967, No. 2-1, and Trans. ISA vol. 6, No. 3, Sept 1967, pp 200-208
- [S3(b)] R. F. Stewart and W. L. Farrior, Jr., "Nuclear Measurement of Carbon in Fly Ash", Proc. Fly Ash Utilization Symposium. BuMines Inf. Circ. 8348, p 262 (1967)
- [S4] David P. Simonson, "Prompt Gamma Ray Spectra produced by Neutrons from a Pu-Be Source", SM Thesis, MIT Dept. of Nucl. Eng., August 1968
- [T1] A. J. Tavendale and G. T. Ewan, Nuclear Instr. and Meth. 25, p 185 (1963)
- [T2] J. I. Trombka, R. L. Schmadebeck, "A Method for the Analysis of Pulse-Height Spectra Containing Gain Shift and Zero-Drift Compensation", Trans. Am. Nucl. Soc. 10, 1, p 33 (1967) (also in Nucl. Instr. and Meths. 62, pp253-261, 1968)
- [T3] G. E. Thomas, D. E. Blatchley and L. M. Bollinger, "High-Intensity Neutron Capture Gamma-Ray Facility", Nucl. Instr. and Meth. 56, pp325-337 (1967)
- [V1] P. Van Assche et al., "Low-Energy Level Scheme of Sc-46 Deduced from the $^{45}\text{Sc}(n,\gamma)^{46}\text{Sc}$ Capture Gamma Rays", Nucl. Physics 84, pp 661-672 (1966)
- [W1] R. E. Wainerdi, "Activation Analysis Finds its Place in the Life Sciences", Nucleonics 22, No.2, p67 (1964)

- [W2] O. A. Wasson, K. J. Wetzel and C.K. Bockelman,
"Gamma Rays from Thermal Neutron Capture in Cl, V,
Mn and Co", Physical Rev. 136, No. 6B, p B1640 (1964)
- [W3] K. J. Wetzel, "Recoil Broadening of Secondary
Transitions in Neutron-Capture Gamma-Ray Cascades",
Argonne National Laboratory, prepublication.
- [W4] John R. Wolberg, "Prediction Analysis", Book,
D. Van Nostrand Co. Inc., Princeton, 1967
- [Y1] H. P. Yule, "Mathematical Smoothing of Gamma Ray
Spectra", Nucl. Inst. and Methods 54, pp61-65 (1967)